THE EXPRESSION OF TOLL-LIKE RECEPTORS-2 AND -4 BY HUMAN CRYPT INTESTINAL EPITHELIAL CELLS, INTESTINAL MYOFIBROBLASTS AND PUTATIVE INTESTINAL STEM CELLS IN INFLAMMATORY BOWEL DISEASE

DR MATTHEW RALPH LAVEN BROWN

BSC (HONS) MBCHB MRCP (UK)

Thesis submitted to the University of Nottingham

for the degree of Doctor of Philosophy

DECEMBER 2012

Dedicated to Eryn and Elijah Laven-Brown

Abstract

Host-microbial interactions are of major importance in the pathogenesis of inflammatory bowel disease (IBD). Toll-like receptors (TLR) are pattern recognition receptors which recognise conserved molecular patterns derived from micro-organisms. Crypt intestinal epithelial cells (IEC) were isolated form mucosal specimens of healthy controls and patients with IBD (ulcerative colitis, UC, and Crohn's disease). A population of IEC enriched for intestinal stem cells (ISC) were identified using Hoechst dye exclusion and by their adherence to cultured primary intestinal myofibroblast cell monolayers.

Compared to healthy control colon, TLR2 and TLR4 mRNA and surface protein were significantly up-regulated in crypt IEC isolated from the inflamed mucosa of UC and Crohn's colitis. Compared to healthy control ileum, TLR4 mRNA was significantly up-regulated in crypt epithelial cells isolated from the inflamed mucosa of Crohn's ileitis. TLR2 and TLR4 mRNA expression from histologically normal and inflamed colonic mucosa in UC did not significantly differ, and expression of TLR4 transcripts was significantly greater in crypt IEC isolated from histologically normal proximal colonic mucosal samples compared to healthy controls. Myofibroblast-adherent crypt cells expressed TLR2 and TLR4 protein to a greater level than the underlying myofibroblasts. Hoechst-effluxing putative intestinal stem cells expressed both TLR2 and TLR4 transcripts and protein, and TLR3 and TLR5 transcripts.

In conclusion, crypt intestinal epithelial cells up-regulated TLR2 and TLR4 expression in UC and Crohn's colitis and up-regulated TLR4 expression in Crohn's ileitis. TLR2 and TLR4 was expressed constitutively in crypt IEC from histologically normal mucosa, suggesting differential TLR expression may in part be a primary event in UC. This provides further insights into the pathogenesis of IBD. Putative intestinal stem cells expressed TLR2, TLR3, TLR4 and TLR5, suggesting that direct microbial sensing by ISC may be important in maintaining intestinal homeostasis and in regulating ISC function.

Acknowledgements

All laboratory work, data collection, image capture and statistical analyses were undertaken by Dr. Matthew Brown.

Dr. Brown is grateful to Mrs. Jacqueline Webb for her assistance in maintaining the myofibroblast cell cultures and for her technical support in the laboratory, and to Dr. Kevin Hughes for his introduction to basic laboratory skills. Thanks also to Dr. Paddy Tighe and Mr. Colin Nicholson for their technical assistance during the undertaking of the RNA micro array protocol. The assistance of Dr. Adrian Robins and Mrs. Nina Lane during flow cytometry and cell sorting was greatly appreciated, particularly during the work involving the side population of cells.

Dr. Brown would like to thank Prof. Mahida for his supervision and direction throughout the research project.

Finally Dr. Brown would like to thank the National Institute for Health Research for funding this project and those patients who kindly agreed to participate in this research project. Without the NIHR Clinical Research Fellowship funding and the donation of specimens by patients this work would not have been possible.

Contents

Abbreviations

αSMA	α-smooth muscle actin
ABCG2	ATP binding cassette transporter Bcrp1
APC	Allophycocyanin
aRNA	Anti-sense ribonucleic acid
Bp	Base pairs
BSA	Bovine serum albumin
CD	Crohn's disease
cDNA	Complimentary deoxyribonucleic acid
DAB	3,3'-diaminobenzidine
DC	Dendritic cell
DMEM	Dulbecco's modified Eagle's medium
dNTP	Deoxynucleoside triphosphate
DTT	Dithiothreitol
ECSIT	Evolutionary conserved signal intermediate in Toll pathways
EDTA	Ethylenediaminetetraacetic acid
FACS	Fluorescence-activated cell sorting
FFPE	Formalin-fixed, paraffin-embedded
FITC	Fluorescein isothiocyanate
FTC	Fumitremorgin C
GAPDH	Glyceraldehyde-3-phosphate dehydrogenase
gDNA	Genomic deoxyribonucleic acid
HBSS	Hanks' balanced salt solution
HPRT	Hypoxanthine guanine phosphoribosyl transferase
HRP	Horseradish peroxidase
IBD	Inflammatory bowel disease
ICC	Immunocytochemistry

IEC	Intestinal epithelial cell
IHC	Immunohistochemistry
IL	Interleukin
ISC	Intestinal stem cell
LPMC	Lamina propria mononuclear cell
LPS	Lipopolysaccharide
LTA	Lipoteichoic acid
MDR	Multi-drug resistance gene
MF	Myofibroblast
MFI	Median fluorescent intensity
mRNA	Message ribonucleic acid
MyD88	Myeloid primary response gene-88
NFκB	Nuclear factor κB
NOD	Nucleotide oligomerisation domain
PAMP	Pathogen-associated molecular pattern
PBMC	Peripheral blood mononuclear cell
PBS	Phosphate buffered saline
PRR	Pattern recognition receptor
P/S/G	Penicillin/Streptomycin/Gentamicin mixture
RIN	RNA integrity number
RT-PCR	Reverse transcription polymerase chain reaction
SDS-PAGE	Sodium dodecylsulphate polyacrylamide gel electrophoresis
SP	Side population
TAE	Tris, glacial acetic acid and EDTA
TLR	Toll-like receptor
TTBS	Tween2 Tris-buffered saline
UC	Ulcerative colitis
WB	Western blot

Chapter 1: Introduction

1.1 The gastrointestinal tract

The gastrointestinal tract is primarily an organ responsible for the digestion and absorption of nutrients, vitamins, minerals, electrolytes and water from the diet in a controlled and orderly manner as it passes from the mouth to the anus. It is responsible for the expulsion of faecal waste as a controlled and socially acceptable process and is controlled by a complex system involving neural, hormonal and nutrient (peptide and lipid)-mediated signals. Along its passage through the gastrointestinal tract the nutrient-containing fluid is mixed with digestive enzymes and other active secretions produced by various glands and structures, including the submandibular and parotid salivary glands, gastric glands, pancreas, liver and gallbladder, intestinal brush border cells and mucus-secreting colonic cells (1).

Nutrients are absorbed across the epithelial cells of the proximal small bowel. The distal ileum is responsible for the absorption of a small number of nutrients such as fat-soluble vitamins, bile acids and vitamin B12, with the colon responsible for the absorption of electrolytes and water. The gastrointestinal tract also provides an initial line of defence against enteric infection or harm by preventing access to the body by invading micro-organisms and toxins. This includes vomiting following the ingestion of harmful substances and the provision of a barrier to active and passive movement of substances and organisms across the epithelial layer.

It is becoming increasingly clear that the gut plays a key role in both the active immune response to infection and in the active maintenance of tolerance to antigens derived from beneficial, commensal micro-organisms resident in the intestinal tract and from food antigens. The gut is considered a secondary lymphoid organ, the so-called gut-associated lymphoid tissue (GALT), and plays a key role in the pathogenesis of inflammatory conditions

of the intestinal tract. The epithelial cells, once considered to be immunologically inactive, are increasingly being implicated in the pathogenesis of chronic inflammatory diseases of the bowel.

1.1.1 Anatomy

The digestive tract extends from the mouth to the anus and includes the pharynx, oesophagus, stomach, duodenum, small intestine (jejunum and ileum), colon, rectum and anus. The gastrointestinal tract (GIT) is lined with mucus membrane (mucosa), which is of stratified squamous type in the mouth, pharynx, oesophagus and anus (due to considerable mucosal abrasion at these sites) and columnar type in regions devoted to digestion and absorption. Muscle tissue in squamous mucosal regions of the GIT consists of striated muscle fibres, compared to the smooth muscle found throughout the rest of the gut. The absorptive surfaces in the small intestine are folded to reveal finger-like projections known as villi which increase surface area. Microscopically epithelial cells express microvilli which form the brush border, further increasing surface area and providing the site for small molecule transport. Between small bowel villi there are epithelial invaginations into the underlying layer (known as the lamina propria) called crypts of Lieberkühn. These contain the epithelial stem cells at their bases which replenish cells as they migrate from crypt to villus tip before being shed into the gut lumen.

The GIT is composed of a number of layers. The innermost layer is the mucosa, which consists of an intestinal epithelial cell (IEC) layer covering the underlying lamina propria (LP). The LP is rich in stromal cells like myofibroblasts, which secrete extra-cellular matrix and growth factors, and cells of the innate and adaptive immune system like dendritic cells (DC), macrophages and lymphocytes (which are also found situated between epithelial cells of the mucosa). The LP also contains blood vessels, nerves, lymphatics and more organised lymphoid structures including lymphoid follicles and Peyer's patches (PP).

The mucosa is separated from the underlying submucosa by a thin layer of smooth muscle known as the muscularis mucosae. Beneath the submucosa is the thicker muscle layer called the muscularis propria which comprises the inner circular and outer longitudinal layers of smooth muscle. These act to move intestinal contents along the GIT, a process termed peristalsis. The outer layer of the gut is known as the serosa.

The intrinsic nerves of the gut are known as the enteric nervous system and comprise of the myenteric (Auerbach's) plexus supplying the muscularis propria and the submucosal (Meissner's) plexus supplying the muscularis mucosae. These intrinsic nerve fibres convey excitatory and inhibitory signals to smooth muscle fibres. The input of these plexuses comes from the autonomic nervous system and from the intrinsic chemoreceptors and mechanoreceptors which have their sensory terminals in the epithelial sheet. Secreted peptides like gastrin, secretin, cholecystokinin, somatostatin, vasoactive intestinal peptide and glucagon-like peptide act as hormones in the regulation of gut function over longer time periods compared to the nervous control which acts rapidly. The pharynx, upper oesophagus and anus are under exclusive neuronal control, whereas hormonal control plays a greater role in gastric, pancreatic and biliary secretion (1).

1.1.2 Function

The digestive process starts with the grinding of food in the mouth and mixture with salivary enzymes from the salivary glands. After passage through the pharynx and oesophagus this material enters the stomach where it is acted upon by gastric acid and proteases. Digestion here is limited and the stomach functions partly as a storage structure for this material, known as chime, until it is passed steadily into the duodenum. Here it is mixed with biliary and pancreatic secretions which contain a high concentration of digestive enzymes, bile acids and phospholipids to aid digestion and absorption. The majority of the absorption occurs in the proximal small bowel although colonic bacteria provide critical nutritional

actions by fermenting dietary fibre and producing short chain fatty acids and vitamins (such as vitamin K).

As shall be discussed, beyond that of a simple barrier to the movement of large molecules and micro-organisms, the gut plays a key role in antigen recognition, generation of antigenic tolerance, initiation of innate immune responses and regulation of adaptive responses to a variety of antigens.

1.2 Inflammatory bowel disease

1.2.1 Clinical introduction

The inflammatory bowel diseases are a group of chronic conditions affecting the gastrointestinal tract characterised by a relapsing and remitting course. The two best characterised inflammatory bowel diseases (IBD) are Crohn's disease (CD) and ulcerative colitis (UC). Although CD and UC share a number of similar clinical features (such as symptoms, associated extra-intestinal manifestations and response to immunosuppressive therapies), clinical experience has led to wide acceptance that CD and UC are two separate conditions (2), as shown in table 1.1.

Table 1.1 Clinical features of Crohn's disease and ulcerative colitis

Feature	Crohn's disease	Ulcerative colitis
Distribution	Patchy and segmental	Continuous
Anatomical location	Mouth to anus	Rectum
	Predilection to terminal ileum and Peyer's patches	Proximal extension
Mural involvement	Transmural inflammation	Mucosal inflammation
Histological hallmarks	Macrophage infiltration and granulomas	Neutrophilic infiltration with crypt abscesses
Response to surgery	Non-curative with anastamotic recurrence	Curative
Cytokine profile	T_{H1}/T_{H17} cell cytokines	T_{H2} cell cytokines
Effect of smoking	Exacerbates	Protective

The United Kingdom, Northern Europe and North America have historically been considered the geographic regions associated with IBD, creating the so-called North-South divide. In Europe, the incidence of UC is 8.7-11.8 cases per 100,000 person-years and CD 3.9-7.0 cases per 100,000 person-years, with a prevalence of 21.4-243 and 8.3-214 cases per 100,000 persons, respectively. Thus, between 50,000 and 68,000 new cases of UC and 23,000 to 41,000 new cases of CD are diagnosed each year in Europe (3). IBD is more common in Western Europe, a phenomenon called the East-West divide.

IBD is rarer in other continents with the exceptions of Australia, Israel and South Africa, although the incidence is increasing in Japan, South East Asia, North India and Latin America. Although IBD has been considered a disease of the developed world, the incidence in developing worlds is increasing. In addition, Asian immigrants moving to the UK demonstrate a sharp rise in incidence of IBD and in some cases show higher incidence than the indigenous European population (4). This may in part represent diagnostic inaccuracies (dysentery and intestinal tuberculosis can mimic UC and CD respectively) but may suggest environmental factors. Indeed, the high prevalence of intestinal helminths in the developing world may play a role in modulating intestinal immune responses and protecting from IBD (5).

The peak age of onset of IBD is in persons aged 15 to 30 years, although a second peak in incidence in middle age is reported. There is a slight female preponderance to CD especially in late adolescence and adulthood, possible suggesting a hormonal influence, while the incidence of UC has a male preponderance. Men are particularly more likely to develop UC in the later decades (3, 6).

Crohn's disease generally affects the ileum and proximal colon although any part of the gastrointestinal tract from mouth to anus can be involved. Classically the intestinal involvement of CD is discontinuous, with so-called skip lesions identifiable with intervening regions of macroscopically normal bowel. The intestinal inflammation of CD is transmural, affecting all layers of the gut, and typified by granulomas (in up to 50% of cases), strictures and fistulae. Fistulae take the form of internal fistulae, for example enterocolic, or external, such as enterocutaneous and peri-anal fistulae.

By contrast, UC is a disease which always involves the rectum and extends proximally to a greater or lesser degree to involve the colon. The entire colon may be involved, a pan-colitis, and if this results in inflammation of the ileocaecal valve, incompetence of this valve can

result in back-wash ileitis. However, the small bowel is not inflamed in UC. The inflammation in UC is continuous and histologically confined to the mucosa. Strictures and fistulae are not seen in UC and granulomas are extremely uncommon, though have been reported in the peri-crypt location.

There are many extra-intestinal manifestations of IBD such as skin conditions (oral mucosal granulomas, erythema nodosum and pyoderma granulosum), ocular manifestations (episcleritis and uveitis), HLA-B27 positive arthropathy and oral aphthous ulceration. In addition, cholesterol gallstones and oxalate renal calculi are associated with terminal ileal CD, and both types of IBD are associated with anaemia, osteoporosis and a pro-coagulant state predisposing to venous thromboembolism. Primary sclerosing cholangitis (PSC) and autoimmune liver disease can progress to cirrhosis, cholangiocarcinoma and primary hepatoma (7). There are a number of recognised risk factors for the development of IBD (table 1.2) (8).

Table 1.2 Clinical risk factors for the development of inflammatory bowel disease

Risk factor	Crohn's disease	Ulcerative colitis
Smoking	Exacerbates	Protective
Appendicectomy	Future risk	Protective
Oestrogens	Possible	No
Peri-natal infection	Possible	No
Neonatal infection/antibiotics	Possible	No
Diet (sugars, fats)	Possible	Possible

Clinically, UC presents usually with bloody diarrhoea which is classically painless. Abdominal pain in the context of UC is suggestive of toxic colitis and impending perforation often localised over the caecum. The presentation of Crohn's disease depends on the disease location and phenotype. CD phenotype is generally classified as inflammatory, stricturing or fistulating (9). Pain is a prominent feature and often is accompanied by diarrhoea which may be secretory or steatorrhoea. Cutaneous or peri-anal fistulae are common to CD. Both conditions are associated with extra-intestinal manifestation which may

pre-date the intestinal symptoms and may be associated with constitutional symptoms such as weight loss and fatigue which may be related to systemic inflammation and anaemia.

In addition to the risk of cholangiocarcinoma and hepatocellular carcinoma in the context of IBD-associated chronic liver disease, patients with IBD have an association with other intestinal malignancy, notably colorectal carcinoma is those with extensive, active, pseudopolyp-forming disease, particularly in those who smoke or have a family history of colorectal carcinoma, and distal-predominant small bowel lymphoma in CD.

1.2.2 Pathogenesis

Despite extensive research over recent decades, the aetiology of “idiopathic IBD” remains incompletely understood. Granulomas (aggregations of immune cells with a centrally located core containing numerous macrophages surrounded by lymphocytes) are the hallmark of CD being present in 50-87% of intestinal biopsies and 20-38% of regional lymph nodes (10). Granulomas may represent a pathological extension of the normal function of the macrophage to defective intracellular killing by neutrophils and macrophages (11). More recently, the concept of defective immune responses in patients with CD were shown following trauma to the rectum, ileum and skin, resulting in reductions in neutrophil accumulation and pro-inflammatory cytokines interleukin (IL)-8 and IL-1β production (12). In addition, injection with heat-killed *Escherichia coli* resulted in reduced local inflammatory responses in CD (12). This suggests defective innate immune function results in accumulation of intracellular antigen leading to an over-active adaptive response attempting to clear foreign material.

A recent review suggests that IBD results from a number of pathological processes observed in clinical studies (13):

1) invasion of the intestine by pathogenic or commensal bacteria (including *Mycobacterium avium* subspecies *paratuberculosis* (MAP), adherent invasive *E. coli* (AIEC), *Bacteroides fragilis*);
2) alterations in the commensal flora of the gut (dysbiosis), resulting in higher bacterial numbers and reduced microbial diversity, with a predilection of sulphate-reducing species and loss of protective short chain fatty acid-producing species;
3) host genetic defects in containing commensal bacteria (defective microbial killing, reduced α-defensin 5 production, reduced nicotinamide adenine dinucleotide phosphate (NADPH)-dependent superoxide production); and
4) defective host immunoregulation (abnormal antigen processing and presentation, defective innate and adaptive immune regulation, overly aggressive T cell responses, host-microbial antigenic mimicry leading to autoimmune responses, mutations in pattern recognition receptor genes like nucleotide oligomerisation domain-2 (NOD2), autophagy and toll-like receptors).

In support of the role of commensal micro-organisms in the pathogenesis of IBD serological markers against various microbes have been reported. Anti-*Saccharomyces cerevisiae* antibody (ASCA) production is widely reported in Crohn's disease. ASCA levels have been associated with disease progression (14) and, in combination with other serological markers, associated with complicated disease and the requirement for surgery (15). IBD patients display serological responses to other bacterial antigens, such as *Escherichia coli* outer membrane porin C (Omp-C), *Pseudomonas fluorescens* (I2) and flagellin (CBir1), which may be associated with phenotype and severity of disease (16-18). For example, seropositivity for anti-CBir1 antibodies is associated with small bowel, internal penetrating and fibrostenotic CD (18). These antibodies are more common in patients with IBD-associated genetic mutations, such as NOD1 and NOD2 polymorphisms (19), hinting that these antibodies are produced following a loss of tolerance to commensal micro-organisms due to defects in the innate immune system.

Similarly, the atypical peri-nuclear anti-neutrophil cytoplasmic antibody (pANCA) has been shown to be positive in IBD, especially UC, and may represent cross reaction with a bacterial antigen rather than an auto-antigen (20). In support of this, atypical pANCA auto-antibodies react to human β-tubulin isotype 5 (TBB-5) and cross reacts with the microbial division protein FtsZ which shares high structural homology with TBB-5 (21).

During active IBD, macrophages, dendritic cells and mucosal B lymphocytes over-produce pro-inflammatory cytokines including IL-1, IL-6, IL-8, IL-12 and IL-23, leading to the recruitment of neutrophils, T cells and monocytes and subsequent stimulation of differentiation and proliferation of T cells. In Crohn's disease, T helper cell responses are polarised to type 1 (T_{H1}) and T_{H17} cells, leading to an up-regulation of IL-17, IL-23 and interferon gamma (IFN-γ) whereas in ulcerative colitis T_{H2} cells, IL-5 and transforming growth factor beta (TGF-β) predominate (2).

This loss of tolerance to intestinal flora and over-activation of adaptive immune responses result in chronic intestinal inflammation, the hallmark of the pathogenesis of IBD (22). It is interesting that IBD occurs in regions of the gut with the highest bacterial colonisation and that faecal diversion of intestinal contents away from inflamed bowel results in marked improvement of inflammation in Crohn's disease (23).

1.2.3 Genetics of inflammatory bowel disease

1.2.3.1 Innate immunity

The observation that CD and UC run in families speculated at a genetic aetiology to IBD. Historical reports of higher rates of concordance in monozygotic twins in CD rather than UC suggested a stronger genetic component to the former (24). Although 80% of families with IBD tend to a similar phenotype, the remaining family cohorts reveal mixed groups of relatives with some members having CD and others UC, meaning there must be common genes to both conditions (25).

Over the last decade there has been a wealth of interest and a vast expansion in the identification of genetic polymorphisms predisposing to or protecting from IBD. The first to be identified were three mutations in the NOD2 (Caspase recruitment domain-15, CARD15) gene (26, 27). These mutations (Arg702Trp, Gly908Arg and Leu1007fsinsC) are likely to affect ligand-receptor interaction and are highly associated with susceptibility to small bowel and stenosing Crohn's disease in a Caucasian (but not African or Oriental) population. Carriage of a heterozygous single nucleotide polymorphism (SNP) in the non-Jewish population equates to an odds ratio of 2.2-4.09 for developing CD; homozygosity or compound heterozygosity is associated with an odds ratio of 17.1 (28). Interestingly, NOD2 mutations affect disease phenotype independently of smoking status and do not influence extra-intestinal manifestations (29).

However, despite the clear relative risk of CD in NOD2 mutations, the absolute risk of IBD in carriers is small. Also, given that NOD2 mutations have a low penetrance and that these mutations are restricted to certain racial groups, NOD2 mutations cannot fully explain genetic predisposition to CD.

The other main association with CD in the innate immune system relates to the autophagy genes, ATG16L1 and IRGM (30-32). A SNP in the ATG16L1 gene (Ala281Thr) located near the N-terminus of the tryptophan-aspartate (WD) repeat domain of the protein results in loss of function affecting primarily intestinal epithelial cells (IEC), antigen presenting cells (APC) and CD4+ and CD8 + T cells. Autophagy is a cellular process responsible for removal of waste organelles and is involved in the starvation response, though more recently it has been implicated in removal of long-lived proteins, aggregated/misfolded proteins, apoptotic bodies (which are pro-inflammatory) and intracellular pathogens such as *Mycobacterium tuberculosis* and intracellular *Salmonella typhimurium* (33, 34).

The defects in NOD2, ATG16L1, and IRGM genes represent dysregulation of the innate immune system. Their association with CD (but not UC) may indicate that defects in intracellular killing of bacteria are key features of CD which may lead to the observed T_{H1} cell polarity.

As key pathogen sensors of the innate immune system, Toll-like receptor (TLR) genes play a role in IBD susceptibility. Two mis-sense mutations in the TLR4 gene, Asp299Gly and Thr399Ile, are associated with interrupted responses to lipopolysaccharide (LPS) in the human respiratory tract, with the former mutation interrupting TLR4 signalling (35). Both mutations are associated with CD (36) and the Asp299Gly mutation has been associated with both CD and UC, particularly in those with NOD2 mutations (37, 38). However, the association with UC is not a consistent finding (39). Association has also been made between the TLR signalling molecule TIRAP (Toll-IL-1 receptor domain containing adaptor protein) and CD susceptibility (39).

TLR5 recognises the ligand flagellin, a component of motile bacteria. Dominant negative mutations in the TLR5 gene are associated with reduced serological responses to flagellin and protection from the development of CD in the Jewish population (40). However, the prevalence of this mutation in the non-Jewish and UC populations were not different from healthy controls. Polymorphisms in the TLR9 promoter region (-1237 C/T) and the TLR9 gene coding region (2848 G/A) are associated with CD in a German cohort (41).

Other mutations to specific genes which logically link to the pathogenesis of IBD include: neutrophil cytosolic factor 4 (NCF4, involved in NADPH-dependent superoxide production in phagolysosomes) and CD (31); tumour necrosis super-family member 15 (TNFSF15) in Asians and Europeans and CD (42); TUNCAN (CARD8), a negative regulator of NF-κB signalling, and non-colonic CD (43); and E-cadherin (CDH1) polymorphisms (regulators of intestinal barrier function) and CD (44).

1.2.3.2 Adaptive immunity

Although genetic polymorphisms in the innate immune system are associated with primarily CD, genes responsible for adaptive immune response are associated with both CD and UC. CD4-positive T_H cells have traditionally been sub-divided into two main phenotypical groups: T_{H1} and T_{H2} cells. T_{H1} cells secrete IFNγ and are primarily responsible for facilitating cell-mediated immunity, including the activation of macrophages. By contrast T_{H2} cells secrete IL-4, -5, -6 and -10 and facilitate B cell-mediated antibody production (45). IL-4 is the key cytokine responsible for the differentiation of naïve T cells into the T_{H2} cell phenotype (via the transcription factors GATA-3 and STAT6), whereas IL-12 (a heterodimer comprising p35 and p40 subunits) drives T_{H1} cell differentiation (via the transcription factors STAT1, STAT4 and T-bet). For many years it was assumed that UC was mediated by T_{H2} cells and Crohn's disease by T_{H1} cells (46).

More recently a third phenotype of CD4-positive T_H cell has been described, the T_{H17} cell. Differentiation into the T_{H17} cell phenotype is driven by IL-23, TGF-β, IL-6 and the transcription factor RORc (46). Interestingly, IL-23 is a member of the IL-12 cytokine family and has a heterodimeric structure, comprising the p40 subunit (common to IL-12) and a unique subunit p19. T_{H17} cells secrete IL-17 and other pro-inflammatory cytokines and are responsible for the immune response against extracellular micro-organisms (47).

IL-17 is over-expressed in the LP of patients with IBD (48) and polymorphisms of the IL-23 receptor (IL-23R) are associated with both CD and UC (49). Although the IL-23R Arg381Gln mutation protects against CD (relative risk, RR=0.38) and UC (RR=0.73) there is no association with disease phenotype or with NOD2 mutations (50). Polymorphisms in key components of IL-23 signalling pathway, STAT3 and Janus kinase-2 (JAK2) genes, and in the IL-12B gene are associated with CD (51) and, with the exception of JAK2, with UC (52, 53). These "protective" mutations in the signalling pathway for IL-23 may reduce IL-23-mediated susceptibility to IBD and may further suggest a role for IL-17 in the pathogenesis of

IBD. Indeed, anti-p40 (54) and anti-p19 (55) antibodies which attenuate IL-17 signalling have shown promise in the treatment of IBD humans and mice respectively.

1.2.3.3 Disease phenotype

A group of genetic polymorphisms impact on disease phenotype rather than susceptibility per se. Individuals with fewer copies of the human β-defensin-2 gene have been associated with a predisposition to colonic CD (56). The TT polymorphism of the CD14 gene promoter is associated with a higher cumulative steroid doses in UC (57) and is seen more commonly in association with one or more NOD2 mutation in CD patients (58). In a Greek study, CD14 promoter polymorphisms were also associated with susceptibility (38).

The NOD1 deletion mutation, ND1 + 32656*1, is associated with early-onset CD and extra-intestinal manifestation of IBD (59). Mutations in the ATP binding cassette B1/multi-drug resistance gene ABCB1/MDR1 are associated with UC, particularly the extensive-disease phenotype (60). The Asp299Gly and Thr399Ile TLR4 gene mutations are associated with stricturing CD particularly in NOD2 wild types, whereas wild type TLR4 in combination with common NOD2 mutations predicted penetrating disease in this cohort (36). Finally, polymorphisms in TLR genes impact on phenotype. TLR1 Arg80Thr and TLR2 Arg753Gly mutations predispose to pancolitis in UC, while there are negative associations between TLR6 Ser249Pro and proctitis in UC and between TLR1 Ser602Ile and ileal disease in CD (61).

In addition to mutations associated with IBD in single genes, we see patterns of disease association extending over genomic regions containing several genes, such as the IBD5 locus on chromosome 5q31 and CD susceptibility (62). OCTN1/2 (SLC22A4/5 solute carrier genes) within the IBD5 locus have been associated with CD (63) and UC (64), possibly in early onset of disease in children with lower weight, height and body mass index (BMI) (65). Similarly, mutations in the 5q13.1 region of the 1.23Mb gene desert are associated with CD

and most likely relate to the prostaglandin receptor EP4 (PTGER4) that resides in the closest associated region (66).

1.2.3.4 Ulcerative colitis

The genetic basis contributing to the pathogenesis of ulcerative colitis has not always been studied alongside that of CD (67). However, with the emergence of large-scale genome-wide association studies (GWAS) several genetic mutations and single nuclear polymorphisms (SNP) have been described in patients with UC from the original CD cohorts. IL-23R (49) and IL-12B (52, 53) are important genes in UC pathogenesis. The HECT domain and RCC domain-2 (HERC2) and STAT3 have stronger association with UC than with CD (53).

The association with IL-10 is interesting in that mice deficient in IL-10 develop spontaneous enterocolitis, with associated crypt enlargement and branching, reduced goblet cells and loss of epithelial cells (68). Recovery and prevention of colitis was dependent on IL-10 production by CD4+CD25+ regulatory T cells and induction of the colitis was prevented by rearing mice in germ-free conditions, implicating microbial factors in the pathogenesis of this model (69). IL-10-knock out mice are deficient in TGF-β/Smad signalling and fail to inhibit pro-inflammatory gene expression in intestinal epithelial cells after colonisation with colitogenic bacteria, which are likely to prevent tissue healing and Treg cell generation and to exacerbate inflammation (70).

How IL-10 relates to the pathogenesis of human colitis remains unclear. Patients with UC show high rather than low levels of IL-10 mRNA expression in mucosal biopsies (71). The efficacy of human recombinant IL-10 in inducing remission or preventing post-operative recurrence of Crohn's disease has been disappointing (72, 73). Given that IL-10 may play a more pathogenic role in UC than CD, the benefits of IL-10 therapy in UC may warrant investigation.

Despite the significant advances in the understanding of the genetic basis of IBD, our current understanding incompletely explains the disease heritability. How far knowledge of the common mutations associated with small increases in disease risk will take us to understanding the pathogenesis of IBD and whether this will translate this into effective, safe therapies remains to be seen.

1.3 Immunology

The body is protected from infectious organisms and harmful external substances like toxins by a variety of physical, functional, chemical and cellular mechanisms. These make up the immune system and constitute varying levels of protection of the host from illness or harm (74).

When an individual first encounters a pathogenic organism or toxin, the first steps in the defence of the host are the physical and chemical barriers that prevent entry. These barriers include the epithelial layers of the skin and the mucosal linings of the intestinal, respiratory and urinary tracts and the eyes and nasal surfaces. Traditionally, these barriers are not considered parts of the immune response, but they do play a vital role in protecting the host from infection and, in essence, largely prevent the requirement for an active immune response in the majority of situations. It is only when the mucosal and epithelial barriers are breached that an active immune response is required (75).

Similarly, the functional role of certain components of barrier to infection, such as peristalsis and mucus production in the intestine or the action of cilia of the respiratory tract, play an important role in reducing the burden on the immune system to protect the host.

The immune system is broadly divided into two groups: innate and adaptive responses. The innate immune response recognises the presence of foreign, invading pathogens through a number of mechanisms and by a variety of white blood cells (leucocytes). This response is evolutionarily older and more primitive than the adaptive immune response, but reacts far more rapidly to invasion. Pathogens are recognised either through preformed, non-specific effector molecules resulting in the removal of the pathogen, or via activation of specific inherited receptors in the genome which remain evolutionarily conserved and which result in inflammation, recruitment and activation of effector cells to the site of invasion. Such

receptors are expressed by all cells of a particular type and trigger an immune response within hours of pathogenic invasion (76).

The innate immune system recognises components of a broad class of pathogen, such as a protein or polysaccharide component on bacterial cell walls. Although it can recognise subclasses of pathogen by their antigens (for example the Gram positive bacterial cell wall components, lipoteichoic acid or phosphocholine) and can discriminate host from pathogen, it cannot discriminate between more closely related molecular structures and cannot differentiate different micro-organisms expressing the same cell wall structures. In addition, there is no amplification of the innate immune response to repeated exposure to the pathogen (74).

By contrast, the adaptive immune system is a far more specific response to infection. Antigenic components of pathogens, following recognition by innate immune system cells, are transported to local lymphoid organs and presented to naïve B and T lymphocytes (45). This triggers clonal expansion and differentiation to effector cells and subsequent removal of the pathogen. Such adaptive immune system cells require receptors with unique specificity. These receptors are encoded in multiple gene segments, and require gene rearrangement and clonal expansion to provide a specific response (76). In addition, adaptive immune responses retain pathogen memory allowing a more rapid and effective adaptive response should that specific pathogenic antigen be encountered in the future. The trade off for such a complex and specific response is a delay of several days for the effectors of the adaptive response to become effective following antigen presentation to naïve lymphocytes. In many situations the innate immune response will clear pathogens successfully and the adaptive responses will remain primed for future encounter with the pathogen.

Recently, a group of cells known collectively as the innate lymphoid cells (ILC) have been described. These cells are present in the mucosal tissue of the gut and play a role in innate

immune responses to infectious micro-organisms, in lymphoid tissue formation, in tissue remodelling after damage inflicted by injury or infection and in the homeostasis of tissue stromal cells. This cell group includes natural killer cells, lymphoid tissue-inducer cells and related cells producing inflammatory cytokines traditionally associated with T_{H1}, T_{H2} and T_{H17} lymphocyte phenotypes of the adaptive immune system. These evolutionarily conserved cells are vital for protective immunity and their dysregulation can result in immune pathology (77).

Therefore the immune system is required to perform four main tasks to prevent harm. The first is immunological recognition whereby the infecting organism is detected by the immune system. The second is infection containment and elimination through effector functions, either humoral or cellular. However, the immune response must be kept under control, and therefore the third function is immune regulation. Failure of this function leads either to allergy and autoimmunity or the failure to mount an adequate immune response altogether. Fourthly, a unique feature of the adaptive immune response is memory, allowing the host a more rapid and stronger response to subsequent exposure (45).

1.3.1 Mucosal immunity

The gut-associated lymphoid tissue consists of lymphocytes at various sites throughout the gastrointestinal tract. Lymphocytes are found individually scattered between IEC and in ordered lymphoid aggregates (known as isolated lymphoid follicles, ILF) in the lamina propria (LP). In addition, lymphocytes aggregate in Peyer's patches (PP), sitting below the follicle-associated epithelium (FAE) and the dendritic cell-rich sub-epithelial dome (SED) in the LP, and are also found within mesenteric lymph nodes (MLN) (74).

The traditional pathway for antigen presentation in the gut was reviewed by Mowat (78). Luminal antigen is transported unprocessed across the IEC barrier to DC within the SED which migrate to PP. The activated DC expresses co-stimulatory molecules and secretes

cytokines and chemokines. In addition, DC undertake antigen processing, resulting in antigen presentation in class II MHC molecules to naïve CD4+ T cells in the PP. B cells interact with DC and T_H cells, resulting in differentiation and immunoglobulin (Ig) class switching to IgG.

Lymphocytes primed in the PP drain via afferent lymphatics to the MLN for further differentiation, resulting in loss of L-selectin expression and up-regulation of α4β7-integrin and CCR9, which orchestrate homing to the gut mucosa following their return to the circulation via thoracic duct via interaction with MAdCAM-1 and CC-chemokine ligand 25 (CCL25), respectively. This specific pattern of adhesion molecule and chemokine expression differs from other lymphocytes which express α4β1-integrin and CCR4 and which do not migrate to the gut mucosa (78).

Activated lymphocytes arriving in the mucosa distribute to various compartments. B cells mature into IgA-secreting plasma cells and CD4+ T cells distribute throughout the LP along the crypt-villus axis. About half of mucosal T cells are CD8+ and represent either true effector (cytotoxic) cells or “memory effector” cells. In addition, a proportion of CD4+ T cells in the LP are IL-10 and transforming growth factor (TGF)-β-secreting Treg cells which help maintain oral tolerance to food and commensal micro-organisms (79).

However, it is likely that antigen can take alternative routes leading to activation of naïve lymphocytes. Antigen can pass through or between IEC into the LP directly and bind to pattern recognition receptors (PRR) on DC. These APC may migrate directly to the MLN, bypassing the PP, and induce differentiation and migration of lymphocytes to the mucosa. The MLN would then be acting as a crossover point between peripheral and systemic immune systems and may explain the acquisition of systemic immunity to orally administered antigens. If in sufficiently high amounts, antigens may pass across the mucosal

barrier and enter either the lymphatic or venous systems directly and stimulate tolerogenic adaptive responses (78).

Upon recognition of an invading pathogen the mucosal immune system switches from a tolerogenic to an inflammatory phenotype, up-regulating pro-inflammatory cytokines (IL-1, IL-6, IL-8, IL-23, IL-12, IFN-γ and IL-4) and co-stimulatory molecules (CD80, CD86 and CD40). This results in the activation and recruitment of innate cells and differentiation of T cells into effector lineages (T_{H1}, T_{H17} and T_{H2} cells), clearing pathogenic organisms and acquiring immunological memory (45).

1.4 Pattern recognition receptors of the immune system

Pattern recognition receptors (PRR) are components of the innate immune system which detect highly conserved, invariant pathogen-associated molecular patterns (PAMP) found in most micro-organisms. However, these PAMP are not unique to pathogenic micro-organisms and can be found as cell wall components of many commensal gut bacteria. In addition, PRR have various endogenous (host-derived) ligands which are released during tissue destruction and apoptosis. These have been termed damage-associated molecular patterns (DAMP) and include heat shock proteins, β-defensins, fibronectin, hyaluronan fragments, heparin sulphate and extracellular fibrin.

PRR can be categorised into three main groups: (1) secreted PRR (including collectins, ficolins and pentraxins) which bind to microbial surfaces and activate the classical and lectin complement pathways; (2) transmembrane PRR (including Toll-like receptors and C-type lectins) expressed on either the plasma membrane or in endosome organelles, and (3) cytosolic PRR (including RIG-I-like receptors (RLR) and NOD-like receptors (NLR)) (80).

1.4.1 Toll-like receptors

The Toll-like receptors were discovered in 1991 following the description of a homology between Toll, a transmembrane protein involved in embryogenesis in the fruit fly *Drosophila*, and the human IL-1R protein (81). The TLR family is a group of receptors with a common cytoplasmic Toll/IL-1 receptor (TIR) domain. A total of thirteen mammalian TLR have been identified, though only ten are found in humans (TLR1-10) (82). Each TLR is responsible for the recognition of distinct invariant microbial structure across bacterial, viral, fungal and protozoal species and are widely distributed in many tissues, especially epithelium, endothelium and myeloid cells (table 1.3) (83).

Table 1.3 Cellular expression, recognised ligands and gastrointestinal disease associations of Toll-like receptors in humans

Toll-like receptor	**Intestinal location**	**Ligands**	**GI associations**
TLR1 (heterodimer with TLR2)	Ubiquitous	Tri-acyl lipopeptides	HCV
TLR2	Myeloid, mast, NK, mDC, T cells	Gram +ve bacteria LP, PGN, LTA, zymosan	IBD, *H. pylori*, CRC, HBV, HCV, PBC
TLR3 (intracellular)	mDC, NK	dsRNA	PBC
TLR4	Mono, mast, neutrophils, T cells, HSC	Gram –ve bacteria LPS, endogenous ligands	IBD, *H. pylori,* CRC, PBC, PSC, HBV, HCV, ALD, NASH, HCC, cirrhosis, fibrogenesis, post-OLT ACR
TLR5	Epithelial, NK, DC, mono	Bacterial monomeric flagellin	IBD, PBC
TLR6 (heterodimer with TLR2)	Myeloid, mast, B cells	Di-acyl lipopeptides	HCV
TLR7 (intracellular)	pDC, B cells, eosins	ssRNA	HCV
TLR8 (intracellular)	Myeloid, T cells, NK	ssRNA	
TLR9 (intracellular)	pDC, B cells, NK	Demethylated bacterial DNA CpG motifs	Colitis, HCV, PBC, PSC
TLR10	B cells, pDC	Unknown	

ACR Acute cellular rejection; ALD Alcoholic liver disease; CRC Colorectal cancer; DC Dendritic cell; DNA Deoxyribonucleic acid; dsRNA Double stranded RNA; Eosins Eosinophil; HBV Hepatitis B virus; HCC Hepatocellular carcinoma; HCV Hepatitis C virus; *H. pylori Helicobacter pylori*; HSC Hepatic stellate cell; IBD Inflammatory bowel disease; LPS Lipopolysaccharide; LTA Lipoteichoic acid; mDC Myeloid DC; Mono Monocyte; NASH Non-alcoholic steatohepatitis; NK Natural killer; OLT Orthotopic liver transplant; PBC Primary biliary cirrhosis; pDC Plasmacytoid DC; PGN peptidoglycan; PSC Primary sclerosing cholangitis; RNA Ribonucleic acid; ssRNA Single stranded RNA; TLR Toll-like receptor
Modified from Testro and Visvanathan (82)

TLR can be subdivided into two groups. TLR 1, 2, 4, 5 and 6 are expressed on the cell surface and recognise extracellular ligands, while TLR 3, 7, 8 and 9 are found within intracellular organelles. This intracellular location of the latter group means that their ligands, which closely resemble host endogenous ligands, require endosome-mediated internalisation and processing before TLR signalling is activated. Host nucleic acid is not accessible to these compartments so does not trigger TLR signalling.

TLR2 is generally regarded as the PRR for Gram positive bacteria and binds bacterial lipoproteins and peptidoglycan, though it also has a role in detecting *Mycobacteria*, spirochetes, fungi and hepatitis C, herpes simplex and cytomegalovirus. It also binds to endogenous DAMP ligands. TLR2 may heterodimerise with either TLR1 or TLR6 and the resulting complexes recognise bacterial triacylated and diacylated lipopeptides, respectively.

TLR4 is the main Gram negative bacterial sensing PPR and is best known as the LPS receptor, though it also detects a range of endogenous DAMP ligands. TLR5 recognises the constant domain D1 of flagellin, a component of bacterial outer membrane involved in motility.

TLR signal through one or both of two distinct pathways. The first requires the signalling molecule myeloid differentiation primary-response gene-88 (MyD88). Like the IL-1R and IL-18R, all TLR except TLR3 and some TLR4 signals require MyD88. In its simplest pathway MyD88 is recruited to the intracellular TIR domain and acts as a recruitment factor for the IL-1R-associated kinase 4 (IRAK4). This leads to attraction and binding of initially IRAK1 and subsequently two further molecules, tumour-necrosis-factor-receptor-associated factor 6 (TRAF6) and transforming-growth-factor-β-activated kinase 1 (TAK1). TRAF6 and TAK1 are activated by three ubiquitin factors, ubiquitin-conjugating enzyme E2 variant 1 (UEV1A), ubiquitin-conjugating enzyme 13 (UBC13) and evolutionarily conserved signal intermediate in Toll pathways (ECSIT) (84).

Activated TRAF6 and TAK1 bind to several TAK1-binding proteins (TAB1-3) and activate various pro-inflammatory transcription factors including NF-κB and the MAPK factors p38 and JUN N-terminal kinase (JNK). NF-κB is activated by phosphorylation and de-activation of its inhibitor protein, inhibitor of κB (IKB), by the protein complex inhibitor of κB kinases α/β/γ (IKKα, IKBβ and IKBγ). This releases NF-κB and allows its nuclear translocation. JNK and p38 are activated by MAPK kinases (MKK), including MKK7, MKK3, MKK4 and MKK6.

The activation of these transcription factors results in the production of IL-1, IL-6, IL-8, IL-12 and TNF-α. MyD88 can also couple to interferon-regulating factor 5 (IRF5) and, acting via TRAF6, represents a delayed source of TNF-α (figure 1.1) (85).

Figure 1.1 Intra-cellular signalling pathways of the Toll-like receptors

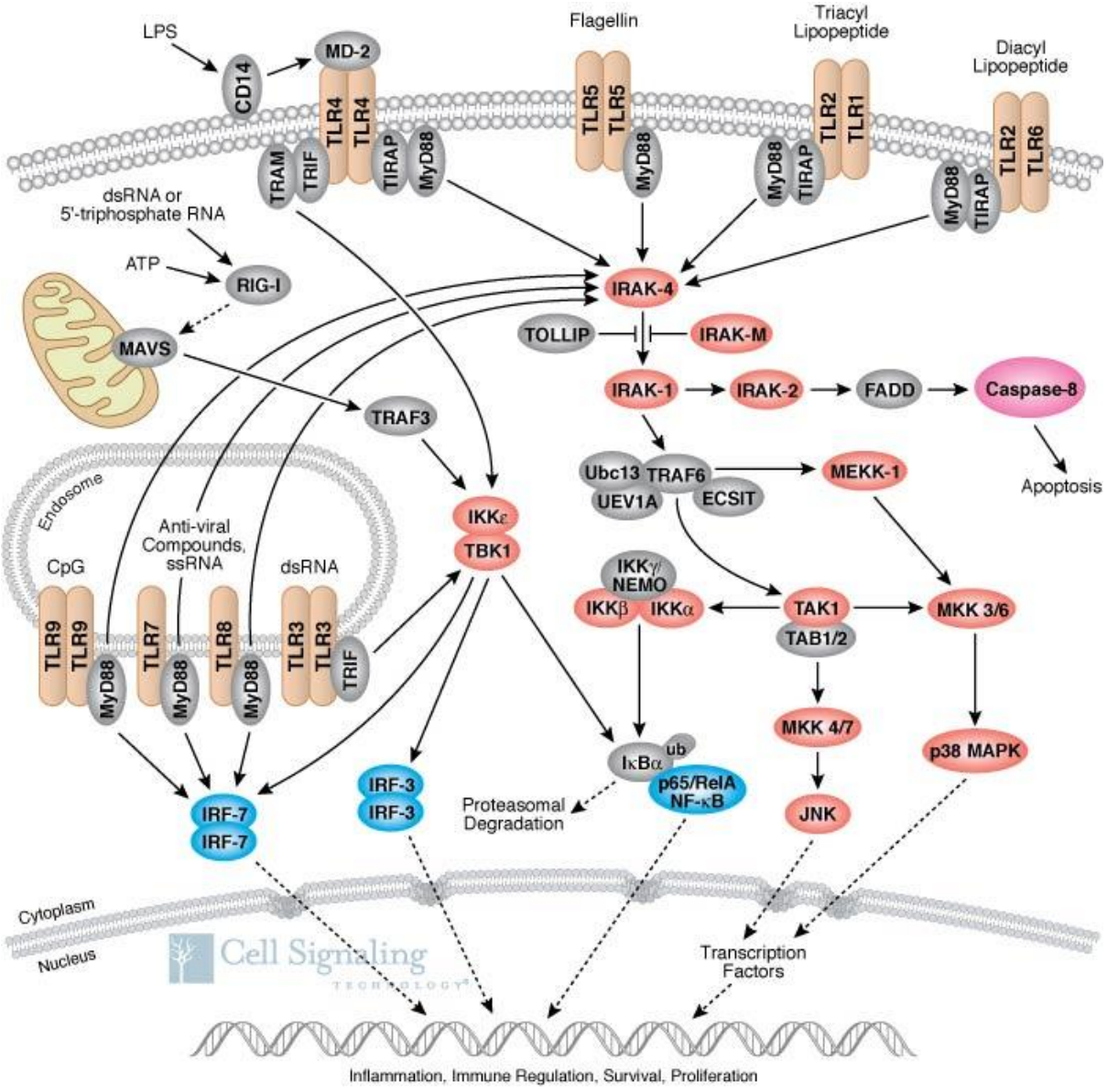

Courtesy of Cell Signaling Technology® reference signal pathways (86)

In the case of TLR7-9, the MyD88-IRAK4 pathways leads, through TRAF6 and TRAF3, to the activation of IRF7 (resulting in IFN-α production) and IRF5 activation (leading to delayed

TNF-α production). MyD88 can also directly translocate to the nucleus with IRF1 and produce IFN-β (85).

TLR2 and TLR4 require the bridging TIR adaptor protein TIRAP (also referred to as MyD88-adaptor-like protein, MAL) for MyD88 recruitment. In addition TLR4 is associated with the MD2 protein, which is critical for its function, and both TLR2 and TLR4 require expression of CD14 for respective ligand binding.

The second pathway for TLR signalling is known as the MyD88-independent pathway. TLR3 signals through the molecule known as Toll/IL-1 receptor-domain-containing adaptor protein inducing interferon-β (TRIF). This results in the attraction and activation of three pathways. Firstly TRAF3 acts through TRAF-family-member-associated-NF-κB-activator-binding kinase 1 (TBK1) to activate IRF3 and IRF7. Secondly, TRAF6 and receptor-interacting protein 1 (RIP1) activate NF-κB through IKB inactivation. Thirdly, RIP1 activates FAS-associated death domain (FADD) to induce apoptosis. TLR4 also signals through the TRIF pathway (in addition to its MyD88-dependent signalling), requiring the TRIF-related adaptor molecule (TRAM) to attract TRIF to the intracellular TIR domain of its receptor before subsequently inducing TRIF-associated pathways analogous to TLR3.

TLR signalling is subject to regulation at various levels (87). TIR-TIRAP binding requires Bruton's tyrosine kinase (BTK)-dependent phosphorylation and SOCS1-dependent degradation. A short form of MyD88 (MyD88s) and FADD interfere with IRAK4 attachment to MyD88, and IRAK-M inhibits signalling by preventing the release of IRAK1 and IRAK4 from MyD88 which is required for their downstream functions (though IRAK-M is found predominantly in peripheral blood leucocytes rather than mucosal tissues). In addition, TLR3 and TLR4 signalling is inhibited by sterile α- and armadillo-motif-containing protein (SARM) which prevents TRAF3, TRAF6 and RIP1 binding, and RIP3 is a negative regulator of RIP1 function (85).

Several other intracellular negative regulators at various stages of TLR signalling have been described, including phosphatidylinositol 3-kinase (PI3K), Toll-interacting protein (TOLLIP), IRAK2c, IRAK2d and the TRAF6 inhibiting cysteine protease de-ubiquitylating enzyme A20. The molecule TRIAD3A targets TLR4 and TLR9 for degradation through ubiquitylation (87).

In addition to the intra-cellular regulators, several transmembrane protein regulators of TLR signalling have been described. STL2 down-regulates NF-κB signalling and the tumour-necrosis-factor-related-apoptosis-inducing ligand receptor (TRAILR) stabilises IKBα to prevent nuclear translocation of NF-κB. The single immunoglobulin IL-1R-related molecule (SIGIRR) has also been shown to interfere with TLR signalling at the IRAK level and SIGIRR-deficient mice show enhanced inflammation and reduced threshold for lethal endotoxin challenge (88). Soluble forms of TLR2 and TLR4 (sTLR2 and sTLR4) have been described which may clear free PAMPs and prevent membrane-bound TLR signalling.

Finally, TLR can be down-regulated by anti-inflammatory cytokines like IL-10 and TGF-β and in the case of intestinal epithelial cells, TLR4 responses are abrogated by lack of expression of the LPS co-receptor MD-2 (89).

In summary, there has been great progression in the understanding of the mechanisms, actions, regulation and expression of the innate immune system pattern recognition receptors known as Toll-like receptors since their discovery two decades ago. TLR have emerged as the key receptors in the sensing of both pathogen- and damage-associated ligands and in the orchestration of the inflammatory response. However, TLR function has been shown to be for more complex and critical to the intestinal mucosa. Indeed, intestinal TLR play key roles in maintaining mucosal homeostasis and our understanding of their role in intestinal inflammatory diseases continues to expand.

1.5 Intestinal epithelial cells

One of the remarkable aspects of the intestinal epithelium lies in its role in the innate and adaptive immune responses. In the face of such massive antigenic challenge, both from commensal bacteria and food sources, the mucosa maintains a state of immunological hypo-responsiveness. However this is not an inactive state, but rather an active process of passivity to non-pathogenic antigens. In fact the epithelium remains primed to respond to pathogenic challenge.

1.5.1 Barrier function of intestinal epithelial cells

Although the skin is the most visible surface exposed to the external environment, the mucosal surfaces of the body have a much greater surface area, of which the intestinal mucosa comprises the majority. The intestinal mucosa is exposed to a vast array of dietary antigens in addition to the diverse micro-organisms of the intestinal flora. The adult human intestine is home to an estimated 10^{14} commensal bacteria (90) providing metabolic, nutritional and immunological benefits to the host (91).

In its simplest role, the epithelial cells lining the gastrointestinal tract form a physical barrier to the movement of nutrient molecules and luminal commensal bacteria. Unlike the leaky characteristic of many mucosal surfaces, the intestinal epithelium regulates molecular passage based on size with a progressive decrease in permeability to larger molecules from crypt to villus.

The mucosal surface is covered by a layer of mucus secreted from the gastric foveolar cells in the stomach and goblet cells in the intestine. Small molecules pass easily through this mucus layer whereas bulk fluid movement is limited, creating a thin unstirred layer adjacent to the mucosa protected from the mixing forces of luminal flow and peristalsis. This may aid nutrient absorption by preventing loss of the small nutrients released by the activity of brush

border enzymes (75). Defects in the mucus layer are implicated in the pathogenesis of murine models of intestinal inflammation as evident by the development of spontaneous colitis in Muc-2-deficient mice (92).

Barrier function is regulated in part by the action of inflammatory cytokines such as TNF-α and IFN-γ. The effects of TNF-α on barrier function have been demonstrated in inflammatory bowel disease and anti-TNF-α monoclonal antibody therapy restores barrier dysfunction in Crohn's disease (93). Likewise, myosin light chain kinase (MLCK) expression and MLC phosphorylation are increased in patients with active disease and appears to correlate with disease activity, further suggesting a role for cytokines in epithelial barrier dysfunction (94).

Interestingly, first degree relatives of patients with Crohn's disease have increased intestinal permeability despite being asymptomatic (95) and this may be related in part to the frame shift insertion at nucleotide 3020 of the NOD2 gene (96). Furthermore, during clinical remission in Crohn's disease, increased intestinal permeability predicts relapse using the lactulose-mannitol test (97).

1.5.2 The role of intestinal epithelial cells in the immune response

1.5.2.1 Recognition of commensal bacteria

Mammals are born with a sterile intestinal tract and rapidly acquire their commensal flora following birth. The diversity of the commensal bacterial within the GI tract is greatest in the colon where anaerobic species such as *Bacteriodes* spp, *Eubacterium* spp, *Bifidobacterium* spp, *Fusobacterium* spp and *Peptostreptococcus* spp predominate over aerobic species such as *Escherichia coli*, *Lactobacillus* spp and *Enterobacter* spp. It appears that there is no pre-determined pattern of commensal acquisition but rather these colonies appear as a result of random environmental encounters, possible starting with the mode of delivery at birth and the composition of the maternal flora. While there is a great variability amongst

individuals in terms of the composition of flora, intra-individual composition varies remarkable little over time (98).

Moreover, the presence of the flora is vital for normal GALT development. Mice reared in germ-free environments exhibit poorly formed Peyer's patches, altered composition of CD4+ T cells and IgA-secreting B cells in the lamina propria and reduced cellularity of mesenteric lymph nodes and splenic tissue (99). The experimental introduction of polysaccharide from the commensal *Bacteroides fragilis* corrects the defect in peripheral lymphoid organs through TLR2 and TLR4 activation and NF-κB signalling (100). Similarly, signalling through NF-κB via TLR is important in maintaining intestinal homeostasis. IEC-specific deletion of IKK results in increased expression of pro-inflammatory cytokines and susceptibility to intestinal inflammation in disease models of radiation-injury, ischaemic colitis and chronic inflammation (101-103). NOD2 plays a role in immune tolerance to bacteria by decreasing the production of inflammatory cytokines in response to TLR2 and TLR4 activation (104-106).

To contain the growth of commensal bacteria, IEC secrete a broad range of antimicrobial peptides in the gut lumen, including defensins, cathelicidins and calprotectins which damage bacterial cell walls and interfere with bacterial metabolism (107, 108). Reduced antimicrobial peptide production has been shown in colonic Crohn's disease (109) and intra-luminal processing of Paneth cell-derived pro-human defensin-5 (pro-HD5) into active HD5 is impaired in the small intestine of patients with Crohn's disease (110). Reduction in the production of α-defensins in the small bowel (111) and β-defensins in the colon (56) may be partly a result of NOD2 gene mutations (112), though reduced ileal α-defensin production may simply occur due to loss of absolute epithelial cell numbers (113).

Pathogenic bacteria adjacent to the epithelial layer are rapidly recognised, suggesting that a process of sampling of the luminal contents for foreign antigen occurs continuously. The

epithelium overlying Payer's patches and isolated lymphoid follicles contain specialised epithelial cells known as microfold (m) cells which lack villi but demonstrate a folded structure at electron microscopy. M-cells sample and deliver antigen to DC in the sub-epithelial dome (114) and this is enhanced by TLR2 and TLR4 activation (115).

IEC themselves express pattern recognition receptors such as TLR and NLR (116) and MHC class II molecules (117), but they lack lymphocyte co-stimulatory molecules (118). During intestinal inflammation IEC up-regulate co-stimulatory molecules (119) and induce *in vitro* production of IFN-γ when co-cultured with naïve CD4+ T cells (120).

One of the fascinating aspects of mucosal immunity is its ability to discriminate between commensal and pathogenic bacteria, both of which may express similar PAMP. A traditional explanation for this is that pathogenic bacteria have evolved mechanisms to invade the host epithelial cell barrier and survive within host tissues, and it is these factors that are recognised by the immune system. By contrast commensal bacteria lacking these virulence factors and pathogenicity genes do not survive in host cells or disseminate throughout tissue and fail to elicit an immune response.

Commensal bacteria can also produce anti-inflammatory molecules, such as the short-chain fatty acid butyrate, which inhibits pro-inflammatory cytokine expression and augments IL-10 production (121). Butyrate is reported to induce epithelial cell maturation along the crypt-villus axis and induces human epithelial cell line tolerance to LPS by down-regulating TLR4 expression in HT-29 cells (122).

Therefore in the normal state IEC possess the PRR to recognise bacterial PAMP and the intracellular signalling pathways to mount an innate immune response, but lack the co-stimulatory molecules to modulate an adaptive response. Concomitantly, commensal bacteria lack innate immune system-activating pathogenic factors and dampen inflammatory

responses in IEC. It is only during intestinal inflammation that IEC express the necessary proteins allowing them at act as antigen-presenting cells and play a pro-inflammatory role in the immune response.

1.5.2.2 Intestinal epithelial cell-dependent regulation of the mucosal immune response

In healthy conditions, dendritic cells are capable of sampling commensal bacterial antigen and transporting it to mesenteric lymph nodes (123). This is partly undertaken by extending cellular processes between epithelial cells and into the lumen to directly sample antigen, which requires expression of the CX3CR1 chemokine receptor (124, 125). These DC also express CD70, a co-stimulatory molecule that binds T cell surface CD27 (124). Moreover, CCR6 is highly expressed by Peyer's patch DC and may be important in generating an effective immune response at this site. However, despite possessing the molecular requirements for initiating inflammation, mucosal DC do not normally activate innate immune responses. This is due to adjacent IEC producing tolerogenic signals.

In vivo deletion of IEC-specific NF-κB signalling results in enhanced expression of DC-derived pro-inflammatory cytokines (IL-12/23 p40, TNF-α and IL-17), loss of T_{H2} cell phenotype, reduced thymic stromal lymphopoietin (TSLP) production and the development of intestinal inflammation in NF-κB knock-out mice exposed to *Trichuris* helminthic infection (126). This demonstrates that IEC-specific NF-κB activation is a critical step in maintaining intestinal homeostasis, directing T_H cell differentiation to the T_{H2} phenotype and mounting an appropriate immune response to *Trichuris* infection.

TSLP promotes positive selection of CD4+CD25+FoxP3+ regulatory T cells and expression of cytotoxic T-lymphocyte-associated protein-4 (CTLA-4), a negative regulator of CD4+ T cell activation (127, 128). TSLP receptor knock out mice express high levels of IL-12/23 p40 and IFN-γ and develop a more severe DSS-induced colitis than wild type mice, suggesting

an immunomodulatory role for TSLP in gut mucosa in preventing T_{H1}/T_{H17} cell-associated inflammation (129).

In human studies, mucosal TSLP levels are enhanced in patients with ulcerative colitis, a condition associated predominantly with a T_{H2} cell phenotype (130). Conversely, patients with Crohn's disease do not express TSLP, resulting in a T_{H1}/T_{H17} cell-associated pro-inflammatory response (131). Likewise, TSLP gene expression has been shown to be reduced in human colonic IEC in patients with Crohn's disease (132) resulting in a DC phenotype with up-regulated TLR2 and TLR4 expression and increased secretion of IL-6 and IL-12 (133).

IEC secrete other immunoregulatory cytokines which shape the immune response. TGF-β1 inhibits NF-κB-dependent gene expression and limits cytokine expression from human blood-derived intestinal macrophages (134) and murine tolerogenic "regulatory" DC (135). IEC induce CD103-positive DC through the production of TGF-β and retinoic acid (RA) which are capable of inducing de novo Treg cells with gut-homing properties that protect mice from experimental colitis and inhibit T_{H1}/T_{H17} cell development (136). Murine CD103-positive DC require tryptophan catabolism by the enzyme indoleamine-2,3-dioxygenase (IDO) to induce Treg differentiation (137). Furthermore, human IEC play a key role in modulating the differentiation of FoxP3+ Treg cell development *in vitro*, via CD103-positive CCR7-positive DC induction, a function lost in patients with Crohn's disease (132).

Retinoic acid imprints the gut-homing receptors CCR9 and $\alpha_4\beta_7$-integrin on T cells (138, 139) and favours a Treg cell phenotype (140, 141). When compared to healthy controls, IEC from patients with colonic Crohn's disease show reduced transcription of TGF-β and aldehyde dehydrogenase-1A1 and -1A2 (ALDH1A1/2), the enzymes converting retinal to RA, even from regions of macroscopically inactive disease (132).

Therefore, IEC-derived TGF-β, RA and TSLP play a key role in the differentiation of tolerogenic CD103-positive DC in the lamina propria of humans and mice. These DC express the MLN-homing CCR7 and drive tolerogenic FoxP3+ Treg cell differentiation. Patients with Crohn's disease appear unable to imprint DC with the ability to induce Treg cells. Interestingly, the probiotic commensal *Lactobacillus paracasei* increases levels of TGF-β and TSLP and protects mice from experimental DSS-induced colitis (142).

1.5.2.3 Intestinal epithelial cell-immune cell dysregulation in inflammatory bowel disease

In Crohn's disease, increased numbers of DC expressing the co-stimulatory molecule CD80 (143), TLR2, TLR4 and CD40 (133) are observed in the mucosa. These are a likely source of increased TNF-α in Crohn's disease (144), and this may be due to lack of TSLP expression and subsequent failure to control DC-mediated inflammation (131). Indeed, anti-TNF-α therapy is shown to reduce mucosal DC numbers (133). In patients with NOD2 gene mutations, DC show an impaired ability to induce TLR-mediated IL-17 expression in T cells, a process normally augmented by the NOD2 ligand muramyl dipeptide (MDP) (145).

The role of DC in ulcerative colitis is less clear, though CD80+ DC-like cells have been described in association with lymphocytes in the colonic mucosa lymphoid aggregates (146) and peripheral blood-derived DC show increased lymphocyte stimulatory capacity (147). Macrophage-enriched clusters and cells with DC-like morphology derived from inflamed small and large bowel induce resting T cell proliferation to a greater extent than those from healthy controls (148).

Whether the DC is a feasible target for therapeutic manipulation of the immune response remains to be seen. IL-10-treated DC, 1α,25-dihydroxyvitamin D, mycophenylate mofetil and various immunosuppressants (like corticosteroids, tacrolimus, sirolimus and chloroquine) are known to act in various ways to reduce pro-inflammatory DC maturation, reduce co-

stimulatory molecule expression and reduce IL-12 production (124). Indeed, IEC-derived DC tolerance may be an alternative approach to the treatment of IBD. Probiotics have an anti-inflammatory action on intestinal mucosal DC in mice, protecting against TNBS-induced colitis though TLR2 and NOD2 pathways and Treg generation (149).

Confluent cultured monolayers of the IEC line T84 express MHC class I and II molecules and can uptake and process antigen from the apical surface, suggesting that they can act as antigen presenting cells (150). However, their lack of or weak expression of co-stimulatory molecules suggests they cannot prime naïve T cells. In Crohn's disease, colonic IEC over-express MHC class II molecules and localise exogenous antigens to the late endosome on their basolateral surface (151). Alloreaction with human IEC results in the proliferation of CD8+CD28+ effector T cells and CD8+CD28- Tregs (152). These CD8+CD28- Tregs have suppressive function *in vitro*, appear to require direct contact with IEC (through interaction of the CD8 ligand pg180 on IEC) for generation, and express CD101 and CD103 (152). Furthermore, the regulatory CD8+CD28- Treg cell is defective and less abundant in Crohn's disease and ulcerative colitis patients (153).

In summary, it seems possible that gut-conditioned DC convert FoxP3- T cells into FoxP3+ T cells whereas IEC are important for expansion of pre-existing CD4+FoxP3+ T cells. IEC can modulate not just DC function but also regulate T cell function directly via MHC molecule expression. Altered IEC regulation of homeostatic balance between effector and regulatory cells may, in part, result in the inflammatory response seen in IBD.

1.6 The role of Toll-like receptors in inflammatory bowel diseases

1.6.1 Human inflammatory bowel disease

The altered expression of TLR in the mucosa of patients with IBD indicates a loss of tolerance to the luminal contents, though a primary causal link cannot made since TLR expression on IEC can be influenced by locally produced cytokines (154, 155). Therefore altered TLR expression may merely be a secondary phenomenon. Perhaps the most persuasive evidence for a direct role in human IBD is the association between genomic polymorphisms in TLR genes and susceptibility to or phenotype of IBD, as discussed in section 1.2.3.

The most exciting avenue for future work in IBD will centre on the modulation of TLR signalling in therapeutics. TLR agonists and antagonists are being developed as treatments of cancer, allergic diseases and viral infections, and as adjuvants for vaccines (83).

Given the differential expression of various TLR in intestinal inflammation, it would seem reasonable to investigate the therapeutic potential of blockage of the former and stimulation of the latter receptors in acute IBD. However, better characterisation of the expression of all TLR in active IBD, both CD and UC, is initially required.

1.6.2 Animal models of inflammatory bowel disease

Numerous experimental models of IBD have been used to further understand its pathogenesis and this has been extensively reviewed (156). Xavier and Podolsky suggest key lessons that have been learned from experimental models of IBD (157):

1. Compromise of the epithelial barrier is sufficient to result in intestinal inflammation
2. T cells have been implicated in many models and presumably promote inappropriate inflammatory responses

3. Haematopoietic cells mediate or regulate intestinal inflammation
4. Various cytokines play key roles in certain models and chemokines may have a unique role in IBD
5. The resident flora seems necessary for colitis induction (in most cases).

The experimental induction of intestinal inflammation occurs through a number of mechanisms. The earliest models of colitis involved sensitisation to an antigen (such as OVA) followed by epithelial disruption with an agent like formalin and, finally, local or systemic re-administration of the antigen. Subsequent models involve primary defects in barrier function following administration of toxins like dextran sulphate sodium (DSS), acetic acid and carageenan. In time a number of murine gene knockout models have been developed which target specific genes like epithelial cell depletion of NEMO, multidrugresistant-1α-depletion (MDR-1α$^{-/-}$), Muc2$^{-/-}$ and N-cadherin$^{-/-}$. Other models involve depletion of regulatory T cells, including IL-10$^{-/-}$, IL-2$^{-/-}$, IL-2Rα$^{-/-}$, TGFβ1$^{-/-}$, TGFβR2$^{-/-}$, CD45BR^{high} transfer and SMAD3$^{-/-}$ mice. Finally models can induce inflammation by: increasing LPS responsiveness (macrophage and bone marrow STAT3$^{-/-}$ and A20$^{-/-}$ mice); impairing TLR responses (Cdcs$^{C3H/HeJBir}$ mutant mice); increasing migration of T cells to the intestine (CD40L transgenic and SAMP1/Yit mutant mice), or T cell transfer into knock out mice (CD4+ CD62L+ T cell transfer from wild type into RAG$^{-/-}$ mice) (156).

The flora has been shown to play a conflicting role in experimental colitis. Germ-free reared IL-10-deficient mice develop colitis only with the introduction of *Escherichia faecalis*. Likewise, TLR4-, TLR9- and MyD88-knockout mice are resistant to T cell-mediated and chronic DSS-induced colitis when reared in germ-free conditions (156). Conversely, the development of colitis in the acute DSS model is worsened in germ-free environments and in TLR4-, TLR9- and MyD88-deficient mice (158). Indeed, NF-κB activation in IEC has been shown to protect the intestinal mucosa from inflammation via production of type I interferons

(IFN-α/β) and TSLP which reduce IL-12/23 p40-induced T_{H1}/T_{H17} cell responses, implicating TLR signalling as protective in some models of experimental colitis (156).

Interestingly, the role of TLR signalling in experimental colitis has been investigated using various models. $TLR9^{-/-}$ mice are protected from developing chronic DSS colitis, as are mice subjected to chronic T-cell mediated models such as $TLR4^{-/-}$ mice in TNBS colitis and dual knock out $MyD88^{-/-}$ $IL\text{-}10^{-/-}$ mice (159).

The most compelling evidence supporting a role for TLR signalling in the pathogenesis of IBD is derived from work investigating the effects of TLR agonists and antagonists on established murine models of colitis. Indeed, TLR ligands have been used in both prophylaxis and treatment of experimental colitis. Oral TLR2 and TLR4 ligands, and parenteral TLR3 and TLR9 ligands, prevent acute DSS colitis, while a TLR9 agonist has been shown to prevent chronic DSS colitis (159). Similarly, TLR4 (160) and TLR5 (161) agonists have been shown to protection against radiation-induced enteritis.

However, TLR agonists administered during established colitis have very different effects. Rectal TLR5 and systemic TLR9 agonists aggravate established acute and chronic DSS-induced colitis (159). Only the oral TLR2 agonist PCSK ($Pam_3CysSK4$) has been shown to ameliorate established acute DSS colitis by enhancing epithelial barrier integrity (162, 163). By contrast TLR antagonists appear more effective in treating established colitis. Systemic administration of the TLR4 antagonist CRX-526 (a lipid A-mimetic) attenuated disease in the acute DSS colitis and spontaneous chronic $MDR\text{-}1\alpha^{-/-}$ colitis models (164). Recently, a blocking monoclonal antibody against TLR4 improved acute DSS colitis but impaired mucosal healing (165).

It would appear that TLR agonists and antagonists play a complex and variable role in the evolution of experimental colitis and have the potential for significant side effects. It is likely

that ligation of TLR in the absence of colitis protects against the development of inflammation, whereas once colitis is established, TLR agonists exacerbate while TLR antagonists ameliorate inflammation. The role of these and future TLR-manipulating agents in the management of acute and chronic IBD in humans is eagerly awaited. Perhaps TLR agonists may play a therapeutic role in preventing relapse in quiescent IBD, whereas TLR antagonists may be of benefit in reducing inflammation in acute exacerbations of IBD.

1.6.3 Toll-like receptors-2 and -4 in human inflammatory bowel disease

The main Gram-positive and Gram-negative bacterial-sensing pattern recognition receptors of the innate immune system are TLR2 and TLR4, respectively (82, 83). Inflammatory bowel diseases are widely regarded to result from an abnormal immune response to microbial components of the intestine. This results in the observed changes to the flora in IBD including increased bacterial numbers, reduced bacterial diversity, alterations in bacterial genus towards sulphate-reducing species at the expense of short chain fatty acid-producing species, and bacteria persistence/invasion of the mucosa and mesenteric lymph nodes (13).

Genetic polymorphisms in the TLR2 receptor complex have been reported to significantly influence the phenotype of IBD (61). Similarly, polymorphisms in the TLR4 gene predispose to the development of colitis in both UC and Crohn's disease (36-38). Animal studies have shown that the presence of a bacterial flora is an important requirement in the development of experimental colitis (156, 157). TLR4- and MyD88-knock out mice are resistant to several types of experiments colitis such as chronic DSS-induced, TNBS-induced and IL-10-deficient models (159). These suggest altered TLR2 and TLR4 expression or function may be important events in the primary pathogenesis in IBD.

The observation that TLR2 and TLR4 agonists prevent the induction of experimental colitis (159), and that a TLR4 antagonist (164) and an anti-TLR4 monoclonal antibody (165)

significantly reduce inflammation in established experimental colitis, suggest manipulation of TLR function and signalling may have therapeutic implications for human IBD.

As will be discussed in chapter 4, TLRs have been reported to be expressed by human epithelial cancer cell lines, though the expression of TLR in primary human epithelial cells is less extensively reported. Given that the main cell type shown to have direct contact with the contents of the intestinal lumen (including the bacterial flora) is the intestinal epithelial cell, it seems reasonable to investigate the expression of TLR2 and TLR4 in primary human intestinal epithelial cells and to characterise any differential expression of TLR2 and TLR4 by these cells in IBD compared to normal epithelium.

1.7 Intestinal myofibroblasts, inflammation and the intestinal stem cell niche

Myofibroblasts (MF) are mesenchymal cells responsible for the secretion of structural proteins, including the basement membrane fibrils, providing a supportive matrix in which the epithelial cells and gut immune cells reside. A sub-population of intestinal MF located in the peri-crypt region of the lamina propria, beneath the overlying epithelial cells, is referred to as the sub-epithelial MF (SEMF). These cells have a spindle shape when located around the crypt base and a more stellate appearance when located in the upper crypt and around the villi (166). In addition to their striking morphological appearance, SEMF are characterised by the expression of the cellular markers α-smooth muscle actin (αSMA) and vimentin, markers associated with smooth muscle cells and fibroblasts respectively (167). However, MF have been phenotypically classified by their expression of cytoskeletal fibril proteins into several types including those which also co-express desmin (168).

Electron microscopically the 18Co cell MF cell line demonstrate abundant, dilated rough endoplasmic reticulum, numerous Golgi, mitochondria, lysosomes and multivescicular bodies, and many caveolae occupying the sub-plasma membrane cytoplasm which may play a role in endocytosis (169).

Myofibroblasts have a broad range of functions including but not limited to the secretion of extra-cellular matrix (ECM) proteins. The ECM is crucial as a provider of structural support to organs and tissues, and for cell layers to form such as the epithelium overlying the basement membrane. Cells attach to the ECM through a variety of receptors, including members of the integrin superfamily, and the ECM can transmit signals which alter cell behaviour and function. As a result, ECM proteins are key messengers in controlling cell differentiation, proliferation, survival, polarity and migration through their highly conserved structures and multiple distinct domains. Furthermore, many growth factors, for example fibroblast growth

factor (FGF) and vascular endothelial growth factor (VEGF), bind to ECM proteins to act as a growth factor reservoir; while other growth factors, like transforming growth factor (TGF)-β, are actually presented to their receptor following binding to ECM proteoglycans (170).

Myofibroblasts secrete collagen types I, III, IV and VIII and numerous glycoproteins such as the basement membrane constituent laminin-β1, laminin-γ1 and fibronectin. In addition, MF secrete type I-III matrix metalloproteases (MMP), which degrade and remodel the ECM, and specific tissue inhibitors of MMP (TIMP) which regulate this process (167).

The basement membrane has been shown to contain numerous pores. These are in continuity with tunnels within the ECM and it is through these pores that mononuclear cells and MF have been observed to migrate, following removal of the epithelial cell layer (171).

The sub-epithelial MF is located immediately adjacent to the basement membrane and contributes to the stromal aspect of the region of the mucosa referred to as the stem cell niche. Its position around the crypt base places the SEMF in an ideal location to interact with the putative stem cell population (section 1.8). The interaction between the overlying IEC and the MF-derived ECM proteins is a key factor in maintaining IEC survival. Epithelial cells undergo rapid apoptosis within hours when removed from the underlying basement membrane, a process termed anoikis. This process can be either attenuated by exposing the cells to collagen I-coated membranes or when whole crypts are embedded in a collagen gel, or can be accelerated by pre-incubating cells with a β1-integrin blocking antibody (172). Interestingly, the crypt base appears particularly susceptible to apoptosis.

A number of key signalling molecules are involved in the regulation of the stem cell population (173). Wnt signalling is perhaps the most widely characterised ISC signalling molecule. Upon ligation by a Wnt ligand, the Wnt receptors Fzd (Frizzled) and LRP (low density lipoprotein-related protein co-receptor) inactivate the destruction complex comprising

APC (adenomatous polyposis coli) and Axin, via a protein called Disheveled. This prevents the destruction of a molecule called β-Catenin, resulting in its translocation to the nucleus and activation of the transcription factors LEF (lymphoid enhancing factor) and TCF (T cell factor). The result of this cascade is the maintenance of the ISC in an un-differentiated state, and promotion of self renewal and proliferation within stem cells and progenitors, respectively. Defects in APC and β-Catenin, resulting in over-expression of Wnt signalling, are associated with hereditary colorectal carcinoma syndromes. Wnt ligands are expressed in a gradient such that expression is greatest at the crypt and declines along the crypt-villus axis. Wnt also plays a role in compartmentalising Paneth and stem cells to the crypt base and is involved in specifying a secretory lineage of IEC (173).

The PI3K/Akt signalling pathway plays a role in anti-apoptotic mechanisms, cell cycle progression and augmentation of the Wnt pathway, and disorders of this pathway result in intestinal hamartomatous polyp formation (including Cowden's syndrome) and neoplastic conditions. Moreover, Notch signals result in stem cell proliferation and favour absorptive cell lineage differentiation (174). Conversely, bone morphogenetic protein (BMP) signalling suppresses cellular proliferation and induces differentiation towards a secretory lineage. BMP expression is greatest at the villus tip and decreases along the villus-crypt axis (the exact opposite of Wnt ligand expression). BMP signalling requires the SMAD4 protein and may inhibit PI3K/Akt signalling by enhancing the function of the PI3K inhibitor protein PTEN. Mutations in either SMAD4 or BMP receptor 1A (BMPR1A) result in the juvenile polyposis syndrome of the distal intestine (173).

BMP antagonists are secreted only at the base of the crypt to prevent BMP-mediated differentiation. Importantly, BMP antagonists such as Noggin in mice (175) and Gremlin-1 and -2 in humans (176) are expressed by SEMF. Murine SEMF have been reported to express mRNA for several Wnt ligands (such as Wnt2, 3, 4, 5A and 5B) while mRNA transcripts for Wnt receptors (Fzd1-7) were detected in SEMF and IEC (177). Similar mRNA

expression profiles have been reported in cultured human MF for Wnt ligands (Wnt2, 5A and 5B) and Wnt receptors (Fzd1, 2, 4, 6, 7, 8 and LRP6), whereas human IEC express Wnt ligand receptors (Fzd1, 5, 7 and 8 and LRP6) but not Wnt ligands (178).

These data suggest that MF residing within the stem cell niche play a vital role in maintain stem cells in an un-differentiated and proliferating state by secreting stem cell signalling factors which act in a paracrine effect on both ISC and local SEMF. This regulation acts through the BMP and Wnt pathways and is likely to regulate other pathways including PI3K/Akt signalling. These cells may also play a role in neoplastic conditions on the intestine.

The role of MF proliferation and differentiation in intestinal fibrosis has recently been reviewed (179). Fibroblasts have been observed to contribute to the development of intestinal fibrosis via a number of pathways. Local proliferation of fibroblasts, fibroblast migration into regions of inflammation and myofibroblast differentiation from intestinal stellate cells all result in the expansion of the fibroblast population. In addition, bone marrow-derived MF are detected both in regions of inflammation/repair and normal mucosa in mice receiving gender-mismatched bone marrow stem cell transplantation and subject to TNBS-induced colitis (180). It is likely that a number of mechanisms exist which result in migration, proliferation and differentiation of fibroblasts in the intestinal mucosa, and these contribute to the processes of healing and fibrosis. These may be particularly relevant in fibrostenotic conditions such as Crohn's disease.

The regulation of MF proliferation and differentiation is complex. Many growth factors including FGF-2, TGF-β, platelet-derived growth factor, keratinocyte growth factor, insulin-like growth factor and epidermal growth factor, are reported to play roles in the proliferation and activation of MF (179). It is noteworthy that pro-inflammatory cytokines known to be expressed in high levels in the mucosa of patients with IBD such as IL-1, IL-17 and TNF-α

are also implicated in the activation and proliferation of MF (177). This implies a possible MF-dependent mechanism for the development of fibrosis and stricturing in IBD and may partly explain the progressive phenotypical changes seen in Crohn's disease over time (181).

In addition to the regulation of MF function by humoral factors of the immune system, there is an increasing body of evidence to suggest that MF play an active role in the immune response. The location of MF immediately below the antigen-sampling epithelial cells (including the microfold M-cells) and surrounded by antigen-responsive immune cells (including lymphocytes) provides the MF with an ideal environment in which to interact with these cellular compartments. Human cell lines of intestinal MF (CCD-18) and lung MF (CCD-37), and cultured primary human intestinal MF have been shown to express mRNA for TLR1-9, NOD1 and NOD2, and to express protein for TLR2, TLR4 and several TLR-associated signalling molecules (182). Although this has not been a consistently finding in all publications (183), these data suggest a role for MF in innate immune responses via recognition of specific PAMP epitopes.

Myofibroblasts constitutively express both cyclo-oxygenase (COX)-1 and -2 enzyme isoforms (167). While COX-1 is constitutively expressed in many tissues and has a role in maintaining tissue homeostasis, COX-2 is the inducible isoform which is involved in the inflammatory response. In response to IL-17 and LPS, primary cultured colonic MF up-regulate COX-2 mRNA and protein and PGE2 protein synthesis, implicating MF in the pathogenesis of gut inflammation (183). Myofibroblasts also constitutively secrete VEGF, which is over-expressed in active IBD and may play a role in the angiogenesis seen in the repair phase of the inflamed mucosa (184).

Furthermore, MF may well partake in shaping specific adaptive immune responses to infection. Human myofibroblasts have been reported to up-regulate IL-23 p19 subunit mRNA

expression in response to incubation with IL-1β and TNF-α through NF-κB signalling (185). IL-23 p19 is a critical cytokine responsible for the differentiation of naïve CD4-positive T cells into the IL-17-secreting T_{H17} cell lineage in conjunction with TGF-β and IL-6. Moreover, T_{H17} cells are heavily implicated in the pathogenesis of Crohn's disease (46). Interleukin-17 in turn has been shown to act directly on cultured MF and induce rapid secretion of IL-6 and the chemokines IL-8 and monocyte chemoattractive protein (MCP) -1 (186). Subsequently, a large number of cytokine and chemokine genes have been shown to up-regulate in cultured MF in response to IL-17 (166).

Therefore, the intestinal MF is an important mucosal stromal cell for a number of reasons. MF secrete stem cell regulating factors and secrete components of the extracellular matrix, which is vital in providing structure to the intestinal wall, regulating the movement and attachment of cells, and binding inflammatory and growth factors. The interaction between the ECM and the overlying epithelial cells is crucial for their survival. Myofibroblast function is, in part, regulated by mucosal inflammatory mediators and may play an important role in regulating the immune response. Furthermore, the MF plays a pathological role in the formation of intestinal fibrosis in conditions such an inflammatory bowel disease.

Although cultured intestinal MF have been reported to respond to a number of intercellular messenger molecules, including cytokines, the possible mechanisms by which the MF senses microbial antigens directly is not well investigated. Therefore the differential expression of TLR2 and TLR4 by primary cultured intestinal myofibroblasts from healthy controls and patients with IBD was investigated.

1.8 Putative intestinal stem cells

The function of the intestinal stem cell is to maintain the integrity, and therefore functionality, of the intestinal epithelium. To achieve this, the stem cell must self-renew, proliferate and differentiate. Intestinal stem cells are located in a niche; comprising not only the proliferating epithelial cells but also mesenchymal cells such as myofibroblasts, enteric neurons, blood vessels and intra-epithelial lymphocytes, and extra-cellular matrix. Although the epithelial cells are separated from these cells by the basement membrane, epithelial-mesenchymal cross-talk is key to the maintenance and function of this niche (187).

Schofield originally described haematopoietic stem cells as an essentially fixed tissue cell. Its maturation is prevented by its location in the stem niche and its progeny, unless able to occupy a similar location within the niche, will differentiate and proliferate into first-generation colony-forming cells (188). The intestine is interesting in that the epithelium can be separated into two compartments: functional and proliferative. The functional compartment comprises of cells unable to further proliferate, but rather contains predominantly mature absorptive columnar cells which populate the small bowel villi and luminal epithelium of the colon. The proliferative compartment is known as the crypt of Lieberkühn and contains the rapidly dividing cells which populate the functional compartment. Cells migrate from crypt to villus and are shed from the villus tip over a time course of approximately five days. The villi are polyclonal, potentially receiving cells from several adjacent crypts (187).

Intestinal crypt cells differentiate into one of four mature lineages; columnar cells (known as enterocytes or colonocytes in the small and large bowel respectively), mucin-secreting goblet cells, hormone-secreting enteroendocrine cells and Paneth cells which secrete anti-microbial peptides. The latter are noteworthy in that they are located deep in the crypts, in a region otherwise populated with undifferentiated stem cells, and that Paneth cells are only located in the small bowel and occasionally the proximal colon (108). Beneath the basement

membrane lie myofibroblasts. These cells maintain gut homeostasis through the secretion of a number of mediations including COX-2 and can regulate the immune response by secretion of signalling molecules such as TGF-β, IL-8, VEGF and chemokines and the expression of innate immune receptors (189).

In 1990, Potten and Loeffler suggested that the “stemness” in the intestine is not a single property but rather a number of properties that a cell is capable of performing. Stem cells must be undifferentiated and capable of self-renewal and proliferation. Between the stem cells of the crypt (which divide but do not mature) and the mature lineage cells (which do not divide but are functionally competent) is a region of the crypt termed the transit amplifying region. This region contains cells which “can under certain circumstances behave like actual stem cells while they undergo maturation under other conditions” and which shows rapid cell division and differentiation into functional cell lineages (190).

Bjerknes and Cheng described the stems cell location as being at positions 1-4 in the crypt (labelling the most basal crypt cell as occupying position 1 and counting cells in an upwards direction from crypt to villus), with cells occupying position 5 or above being induced into differentiation (191, 192). Stem cells have been reported to number from between four and twenty cells per crypt.

There are two current models of stem cell division in the intestine, deterministic and stochastic (187). The deterministic (or immortal) model describes a situation in which each stem cell divides into exactly one stem cell which remains within the niche and one daughter cell which leaves the niche; a process termed asymmetrical cell division. Under this model the stem cell is immortal and its genome is well protected from replication error because the stem cell retains the original template DNA strand whereas the daughter cell acquires the non-template strand. This has been demonstrated by Potten’s group using the labelling of stem cell DNA with tritiated thymidine (^{3}HTdR) following radiation injury and by labelling

newly synthesised DNA strands with bromodeoxyuridine (BrdU). Template strands retain ^{3}HTdR in the stem cell zone (label-retaining cells) whereas newly synthesised BrdU-labelled strands are seen to migrate up the crypt (193). This work on label-retaining cells demonstrated that the dual ^{3}HTdR- and BrDU-labelled cells (putative stem cells) on average reside at the “+4” position of the crypt base (193).

The stochastic (or niche) model describes the result of stem cells division in terms of one of three outcomes: two stems cells (no daughter cell), one stem cell (and one daughter cell) or two daughter cells (no stem cell). This leads to “drift” in the number of descendent of each stem cell over time such that all stem cells within a given crypt are derived from a single common ancestral stem cell. Studies characterising the methylation patterns of CpG sites of non-expressed gene regions of stem cell DNA support this model and suggest that one stem cell has the potential to expand and replace the whole stem cell population stochastically (194).

The issue of stem cell location within the crypt has led to differing reports in the literature regarding stem cell location. In particular, the character of the +4 position cells and the crypt-based columnar cells (CBC), the latter originally described by Cheng and Leblond in 1974 (195), is debated. Dekaney’s group have taken to using the terms upper and lower stem cell zones (USZ and LSZ, respectively) (196) and suggest that the USZ may represent a quiescent reserve population whereas the LSZ contains cells which are active and more rapidly cycling (174).

Identifying stem cells by the expression of a unique combination of markers has been a challenging area of intestinal stem cell research, though a number of intestinal stem cell markers have recently been described. The first was Musashi-1 (Msi-1) which is expressed in stem cells of the USZ and LSZ. Msi-1 is involved in asymmetrical cell division in neural stem cells of Drosophila (197) and acts as an RNA-binding protein in mammalian cells to

augment Notch signalling (198). Subsequently, Msi-1 has been reported as a stem cell marker in murine small and large intestine (199). Notch signalling up-regulates the expression of a transcription factor from the basic helix-loop-helix family, known as hairy and enhancer of split-1 (Hes-1). Hes-1 expression in the intestine commits cells to differentiate in to the columnar cell phenotype at the expense of secretory cell lineages. This occurs by the repression of math-1 expression, a key transcription factor for the secretory cell lineages (200). Both Msi-1 and Hes-1 co-localise to cells in the stem cell zone and are best described as surrogate stem cell markers.

A number of markers have been described which label the CBC cells of the LSZ specifically, such as: leucine-rich-repeat-containing G-protein-coupled receptor 5 (LGR5), CD133 (prominin-1), β-catenin, Ascl2 and SRY-box containing gene 9 (Sox9) (174). Conversely, B lymphoma Mo-MLV insertion region 1 homolog (Bmi1) and Doublecortin and CaM kinase-like-1 (DCAMKL-1) mark the USZ, though Bmi1 is limited to the proximal small intestine and DCAMKL-1 may be a marker more of stem cell response to injury (196). Recently, a fraction of epithelial cells from mouse small intestine with stem cell properties have been reported to express the CD24(lo) and CD45-negative phenotype. These cells were enriched for LGR5 and Bmi1 transcripts and generated organoid structures, including all four cell lineages, using Matrigel culture (201). However, approximately 30% of these cells express Paneth cell-associated lysozyme mRNA and protein, suggesting this sub-population of cells may not be homogeneous.

Despite these advances in intestinal stem cell marker identification, these markers all represent intracellular proteins and are generally identified by immunostaining fixed histological tissue sections. An ideal combination of surface markers allowing positive cytological sorting of an enriched ISC population remains elusive. However, an alternative technique for isolating ISC has been described and uses the efflux properties on stem cells for the DNA-binding bis-benzimide blue fluorescent dye Hoechst 33342.

In 1996 Goodell *et al.* described a sub-population of murine bone marrow-derived haematopoietic cells which efflux Hoechst 33342 (202). When emission signal from live bone marrow-derived haematopoietic cells were viewed simultaneously following Hoechst 33342 staining using the blue and red lasers on a linear scale of a flow cytometer, a population of cells with low signal in both emission wavelength channels and with a phenotype consistent with multipotent haematopoietic stems cells (HSC) was observed. These cells were subsequently shown to contain the vast majority of the HSC activity from murine bone marrow and to protect mice from lethal irradiation, even at low transplant cell numbers, by contributing to both the myeloid and lymphoid lineages (202). These cells are referred to as side population (SP) cells.

SP cells with stem cell properties have been described in human breast (203), human prostate (204), murine liver (205) and murine skeletal muscle cells (206, 207). In 2005 Dekaney *et al* described the isolation of murine SP cells from the jejunum of C57B1/6J mice using EDTA and dispase treatment followed by Hoechst 33342 staining (208). This yielded a mixed population of SP cells which were both CD45-positive and CD45-negative, and accounted for about 3% of the isolated epithelial cells. The CD45-negative SP cells were subsequently shown to stain negatively for common haematopoietic markers (Sca-1, Thy-1.2, c-kit and CD34), negatively for the mesenchymal marker α smooth muscle actin, but positively for β1-integrin and the epithelial marker cytokeratin. These CD45-negative SP cells were enriched for Msi-1 mRNA expression, de-enriched for various mature epithelial lineage markers (intestinal trefoil factor, lysozyme and sucrase-isomaltase) and stained negatively for mesenchymal collagen IV mRNA expression (208).

Subsequent work on isolated mouse jejunal IEC characterised a list of genes with enriched and de-enriched mRNA expression in CD45-positive SP compared to non-SP (NSP) cells in using micro array technology. Notch1 and fibroblast growth factor receptor-3 (Fgfr3, another

putative ISC marker) were shown to be enriched by four-fold and localise to the intestinal crypt base using immunohistochemistry (209).

Most recently, SP cells of the human colon have been shown to express the epithelial-specific marker BerEP4, CD133 and β1-integrin, but not the haematopoietic stem cell marker CD34 (210). Moreover, these cells preferentially adhere to confluent myofibroblast monolayers for up to 5 days in a β1-integrin-independent manner and were demonstrated to be Msi-1 positive using immunocytochemistry.

The key feature in the identification of the SP is the ability of isolated cells to efflux the fluorescent dye Hoechst 33342. Hoechst 33342 readily binds to AT-rich regions of the minor groove of the DNA double helix and is used in cell cycle analyses (211). The efflux of Hoechst 33342 from the SP cells was initially thought to be a result of MDR-like pump action, however, bone marrow-derived cells from mice deficient in the MDR1a/1b gene were subsequently shown to efflux Hoechst 33342 and to demonstrate a side population of cells (212). Zhou *et al.* characterised the ATP binding cassette (ABC) transporter Bcrp1 (ABCG2) as being widely expressed in a variety of stem cell populations and identified ABCG2 as the molecular determinant of the side population (212). ATP depletion using 2-deoxyglucose with sodium azide, or reserpine, resulted in the abolishment of the SP. In addition, fumitremorgin C (FTC) (210, 213) and verapamil, a non-specific dihydropyridine calcium channel blocking agent (202, 204, 210), have been shown to block the ABCG2 pump and abolish the side population. These ABCG2-blocking agents allow identification of the side population and facilitate accurate SP cell sorting.

Although the expression of ABCG2 is required to demonstrate a SP, mice deficient in both Mdr1a/b and Bcrp1 genes develop normal numbers of peripheral blood cells and demonstrate normal haematopoietic development (214). However, these bone marrow cells are more sensitive to the cytotoxic agent mitoxantrone *in vitro* than cells from mice

expressing either one of these genes, suggesting that these transporters play a role in providing environmental protection for the stem cell rather than being necessary for HSC development. Therefore, the SP likely represents a population of cells enriched with stem cell properties rather than representing a homogenous population of stem cells *per se*.

Current evidence suggests that host-microbial interactions are important in the pathogenesis of IBD (13). Importantly, intra-epithelial neutrophil infiltration (cryptitis) and neutrophil crypt abscess formation are key histological features in IBD which result in epithelial cell loss and subsequent exposure of the underlying lamina propria to bacterial antigens (215). Regeneration of the epithelial barrier requires expansion and differentiation of the intestinal stem cell population. It is possible that the stem cell population, located in the base of the crypt, plays an important role in the pathogenesis of IBD through innate immune receptor-mediated bacterial sensing. Therefore, the ability of this side population of cells (enriched for intestinal stem cells) to sense bacterial antigens by the expression of TLR2 and TLR4 was investigated.

1.9 Hypothesis

Current evidence implicates epithelial cells in playing a key role in shaping the innate and adaptive immune responses of the intestinal mucosa. Toll-like receptors are important pattern recognition receptors which are indispensable in the developing gut-associated lymphoid tissue in early life and in maintaining intestinal homeostasis throughout life. Differential signalling through Toll-like receptors has been shown to prevent intestinal injury in a number of models of intestinal inflammation and to ameliorate established inflammation in models of colitis. Furthermore, Toll-like receptor expression has been demonstrated on human intestinal epithelial cells and differential expression of Toll-like receptors may contribute to the pathogenesis of human inflammatory bowel diseases.

Recently, there has been interest in the role of intestinal myofibroblasts in mediating mucosal inflammation through the expression of innate immune system receptors, such as Toll-like receptors, and by the secretion of pro-inflammatory cytokines. Myofibroblasts also play a role in the pathogenesis of intestinal fibrosis in chronic inflammatory bowel diseases. Mediation of myofibroblast-induced intestinal fibrosis may, in part, be a result of toll-like receptor expression.

Mucosal inflammation in inflammatory bowel disease results from abnormal immune responses to the intestinal flora. It is histologically identified by changes to epithelial crypt architecture and by inflammatory cell infiltration of the (usually sterile) crypts, forming crypt abscesses and cryptitis. Intestinal stem cells reside at the base of these crypts and are responsible for replenishing the epithelium following epithelial cell damage. These intestinal stem cells are surrounded and regulated by a variety of stromal cells, including intestinal myofibroblasts. It is unknown if intestinal stem cells directly recognise bacterial antigens through the expression of innate immune receptors, but their location at the crypt base places them in a prime position to response to bacterial antigens. Direct stem cell-mediated

bacterial antigen sensing may have key implications for mucosal homeostasis and inflammation.

The hypotheses of this study are: (i) crypt intestinal epithelial cells and intestinal myofibroblasts in patients with inflammatory bowel disease differentially express Toll-like receptors-2 and -4 compared to healthy control subjects, and (ii) intestinal stem cells have the ability to directly sense bacteria through the expression of Toll-like receptors-2 and -4.

1.10 Aims

The aims of this study are to characterise the expression of Toll-like receptors-2 and -4 in isolated crypt epithelial cells and primary intestinal myofibroblasts from patients with inflammatory bowel disease and to compare expression to healthy control subjects. Furthermore, this study will aim to isolate a sub-population of putative colonic intestinal stem cells based on their fluorescent dye efflux properties and characterise their expression of Toll-like receptors-2 and -4 in healthy control subjects.

Chapter 2: General methods and materials

This chapter describes the methods and materials used in routine laboratory techniques. Specific techniques relevant to certain chapters will be described in detail in the relevant chapter.

2.1 Cell counting and assessment of cell viability

Cell counting and viability assessments were undertaken using a haemocytometer. Twenty microlitres (µl) of suspended cells were mixed with 0.4% trypan blue (Sigma-Aldrich Company Ltd, UK) in a 1:1 ratio. Two 12.5µl aliquots were added to the haemocytometer and the number of viable (unstained) and dead (stained) cells within the 25x25 square grid counted by light microscopy. Mean cell numbers were multiplied by the dilution factor (DF, in this 1:1 example the dilution factor is x2) to determine the concentration of cells per millilitre (ml) by the following formula:

Cell concentration ($x10^4$/mL) = [(total cell count in grid 1) + (total cell count in grid 2)] x DF / 2

2.2 RNA isolation

Total RNA was isolated from cellular samples using the Qiagen RNeasy Plus Mini Kit (74134, Qiagen, Germany) as per the manufacturer's instructions. Briefly, $5x10^6$ cells were collected per tube. Cell membranes were disrupted by adding 600µl of Buffer RLT with 1% 2-mercaptoethanol (M7522, Sigma) and mixing by pipette. The cellular lysate was homogenised using a Qiashredder spin column (79654, Qiagen, Germany) and centrifugation at 13,000 rpm for 2 minutes until all the lysate has passed through the column. The homogenised lysate was transferred to a genomic DNA (gDNA) Eliminator spin column® and centrifuged for 30 seconds at 13,000 rpm (>10,000g) to remove any contaminating gDNA. Genomic DNA binds to the column membrane whereas total RNA

passes through the membrane and into the flow-through. By discarding the gDNA column, contaminating gDNA is removed and total RNA is retained.

Next, 600µl of 70% ethanol was added to the flow-through and mixed. This was transferred to an RNeasy spin column® and centrifuged for 15 seconds at 13,000 rpm (>10,000g). At this stage total RNA was bound ionically to the spin column membrane and required a number of subsequent wash steps for purification. Thus, 700µl of Buffer RW1® was added to the column and spun for 15 seconds at 13,000 rpm (>10,000g), followed by two further 13,000 rpm (>10,000g) centrifugation steps using 500µl of Buffer RPE® each, for 15 and 120 seconds respectively. The flow-through was discarded after each spin step.

The spin column membrane containing bound total RNA was centrifuged dry for 1 minute at 13,000 rpm (>10,000g) to minimise ethanol transfer from the Buffer RPE® wash steps. Finally, two elution steps each using 30µl of RNase-free water applied to the column and spun at 13,000 rpm for 1 minute were undertaken. Samples of total RNA were labelled and stored at -80^{o}C in 20µl aliquots.

2.3 Assessment of RNA quality

2.3.1 Spectrophotometric analysis using Nanodrop®

To assess protein and organic acid contamination of total RNA samples, spectrophotometric analysis was undertaken using the Nanodrop® spectrophotometer (Thermo Scientific, Loughborough, UK). A sample of total RNA was thawed at room temperature and a 1µl aliquot stored on ice for analysis. The absorbance of electromagnetic radiation (EMR) of 260nm wave length is directly proportional to the concentration of the nucleic acid in solution and can be measured to calculate actual RNA concentration using the Beer-Lambert equation (216):

Absorbance = [Wavelength dependent coefficient] x [Path length] x [Solute concentration]
(AU) (cm) (g/L)

Similarly protein absorbs EMR at 280nm and organic acids, such as phenolate and thiocyanates, absorb EMR at 230nm. By measuring the ratio of absorption at these wavelengths it is possible to quantify contamination by the corresponding organic compound. The Nanodrop® is also able to quantify accurately total RNA concentration in the sample. All total RNA samples were analysed by the Nanodrop® spectrophotometer prior to further experimentation using nucleic acid. 260:280 and 260:230 ratios of greater than 1.8 were considered suitable for down-stream experimentation (217).

A typical spectrophotometric trace using the Nanodrop® is shown. This trace provides a quantitative value for RNA concentration in addition to the indices of RNA purity, namely 260:280 and 260:230 absorbance ratios (figure 2.1)

Figure 2.1 Spectrophotometric trace using the Nanodrop® spectrophotometer

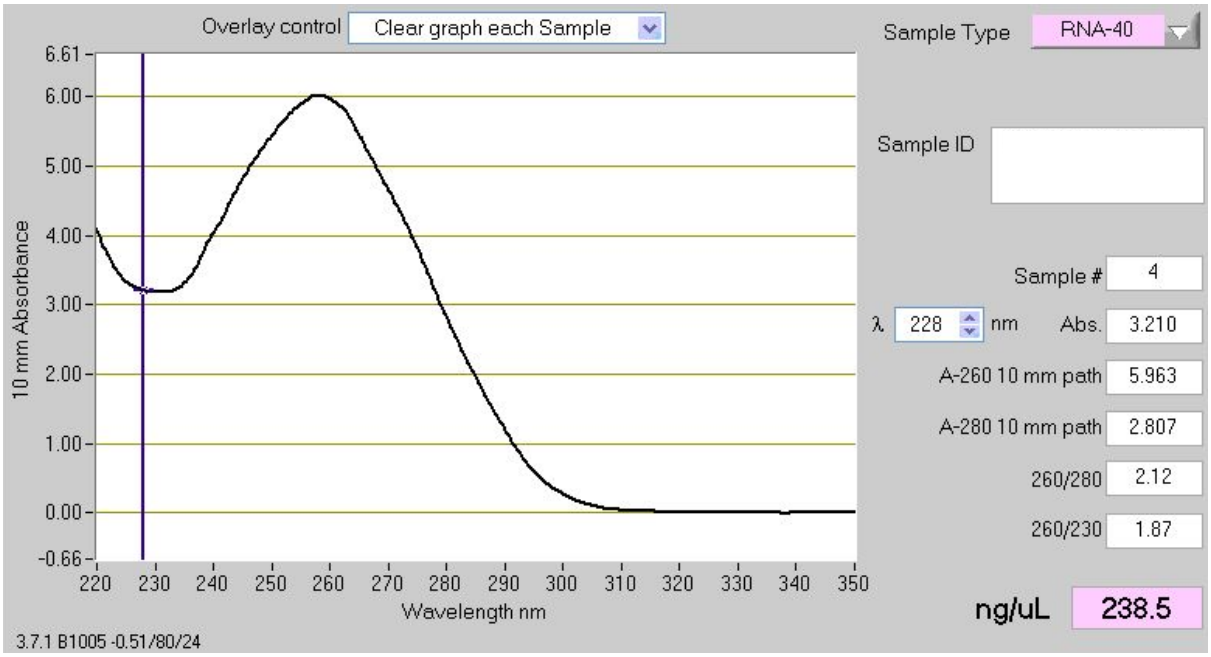

Nanodrop® trace representing total RNA spectrophotometric properties. The absorbance at 260nm (A-260), A-280, absorbance ratios and total RNA concentration are shown on the right of the panel.

2.3.2 Analysis of RNA integrity using Agilent 2100 Bioanalyser®

In addition to spectrophotometric ratios, RNA quality has been historically assessed electrophoretically using an agarose gel and a fluorescent probe such as ethidium bromide. Typically two bands corresponding to the 28S and 18S ribosomal RNA (rRNA) species are analysed visually. High RNA quality is defined as a 28S:18S ratio greater than 2.0. However, it has been suggested that both spectrophotometric analysis (using a Nanodrop®) and electrophoretic analysis to calculate rRNA ratios are not sensitive enough to detect slight RNA degradation which may impact on the quality of down-stream applications (217).

Micro-fluid capillary electrophoresis using the Agilent 2100 Bioanalyser® (Agilent Technologies, USA) assesses the quality of total RNA samples by creating an electrophoretic strip (figure 2.2).

Figure 2.2 Micro-fluid capillary electrophoresis gel using the Agilent 2100 Bioanalyser®

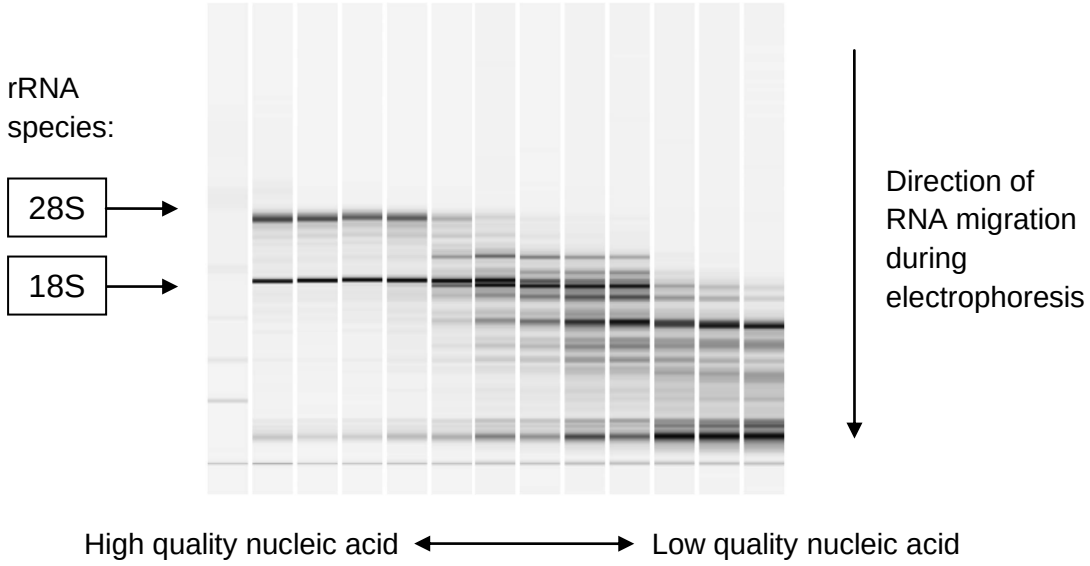

Micro-fluid capillary electrophoresis gel of a range of RNA samples, from high quality (vertical lanes to the left of the panel) to low quality (vertical lanes to the right of the panel). Ribosomal 18S and 28S are shown for size comparison. Reproduced from Mueller *et al.* 2004 (218).

Subsequently, the software assigns the RNA sample a RNA Integrity Number (RIN) ranging from 0 to 10, which represents low to high quality RNA, based on analysis of several aspects of the electrophoretic trace (figure 2.3).

Figure 2.3 Agilent 2100 Bioanalyser® fluorescent trace using micro-fluid capillary electrophoresis

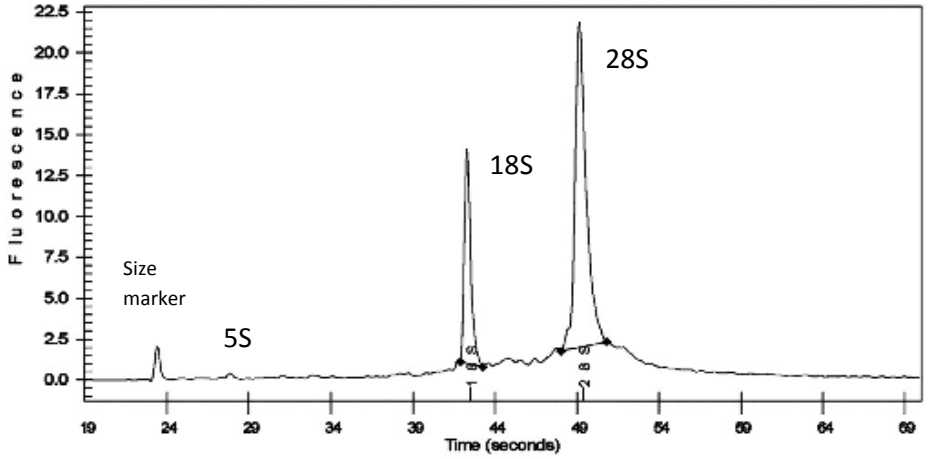

Agilent 2100 Bioanalyser® trace showing measured fluorescence of the RNA-binding Nano dye along the micro-fluid capillary electrophoresis gel during RIN calculation. The size marker, 5S, 18S and 28S peaks are shown. Modified from Imbeau *et al.* 2005 (217).

The RNA electrophoretic parameters analysed by the Agilent 2100 Bioanalyser® are: ratios of the area of the 28S and 18S peaks to the total curve area; 28S peak height; 'fast' region analysis (assessing the region between the 5S and 18S peaks for degradation products), and heights of a small size marker (219). This technique has been shown to demonstrate less inter-measurement variability and greater correlate with RNA quality and gene expression than other techniques using both cell lines and human tissue (217, 220).

Therefore, prior to down-stream nucleic acid experimentation all total RNA samples were analysed using the Agilent 2100 Bioanalyser according to the manufacturer's instructions and the Agilent RNA 6000 Nano Kit. Briefly, a light-sensitive Nano Dye Concentrate was mixed with a gel matrix and added to a 12-sample chip. A 1µl aliquot of either a fixed-size ladder marker or a sample of template RNA was loaded into a chip well following heating at 70^{o}C for 2 minutes to minimise secondary structure. Up to twelve samples could be analysed on a single chip. The chip was vortex mixed (IKA - Model MS2-S8/MS2-S9) for 1 minute at 2,400rpm and then inserted into the analyser. Acquisition of data was obtained

within 30 minutes of analysis. Samples of RIN >6.5 were considered suitable for down-stream experimentation.

2.4 Conventional reverse transcriptase polymerase chain reaction

2.4.1 Reverse transcription using Qiagen QuantiTect RT kit

Synthesis of complementary DNA (cDNA) from message RNA was undertaken using the Qiagen QuantiTect RT kit (205311, Qiagen, Germany) according to the manufacturer's instructions. This protocol involved a further gDNA elimination step prior to reverse transcription and to ensure complete removal of genomic DNA from the sample. The gDNA elimination reaction involved adding up to 1µg RNA to 2µL gDNA Wipeout Buffer x7® and making the solution up to a volume of 14µL with RNase-free water. This was heated to 42^{o}C for 3 minutes to eliminate residual gDNA through its DNase activity.

Samples were then placed on ice and added to the reverse-transcription (RT) reaction components: Quantiscript reverse transcriptase® with RNase inhibitor (1µL); Quantiscript RT Buffer x5® including magnesium and deoxynucleotide triphosphates (dNTP) (4µL), and an RT Primer mix® (1µL). The final volume of 20µL was incubated at 42^{o}C for 15 minutes before being placed at 95^{o}C for 3 minutes to inactivate the RT. The 20µL samples were made up to 50µL with RNase-free water, pipette mixed and placed on ice for down-stream experimentation or stored at -80^{o}C.

The Quantiscript reverse transcriptase® has desirable enzymatic properties including functions such as a RNA-dependent DNA polymerase, hybrid-dependent exoribonuclease (RNase H) and DNA-dependent DNA polymerase. The first property allows cDNA transcription from the RNA template strand, while the second property subsequently degrades the RNA component of the newly synthesised RNA-DNA hybrid (but not the pure

un-hybridised RNA strands) to release cDNA. This avoids the need for a separate RNase H step prior to PCR (221).

2.4.2 Primer design for RT-PCR

In order to design reliable and specific primers for accurate PCR reactions, a number of rules were followed whenever possible. The proportion of guanine (G) and cytosine (C) bases was kept to between 40 and 60% of the sequence. If possible, positioning G/C bases at the 3' end of the sequence was avoided to reduce the chances of primer-dimer formation. Self-annealing regions within each primer were avoided. Primers were designed to be intron-spanning whenever possible. The melting temperature (T_M) in ^oC was calculated using the following equation:

$$T_M = 4(G + C) + 2(A + T)$$

where A and T represent adenine and thymine bases, respectively. Annealing temperatures (T_A) were calculated as follows:

$$T_A = T_M - 5$$

The annealing temperature of a primer pair was taken as the T_A of the primer with the lowest value. The target T_A range was 54-62^oC.

However, the equations above are only an approximation to the melting and annealing temperatures and, on occasion, manufacturers of oligonucleotides supply specifically measured melting temperatures with their synthesised primers. In such cases, if there was a discrepancy between the estimated and manufacturer's calculated T_M then the higher of the two was used. In some cases, primers were selected from published scientific articles. If the published primer pairs fulfilled many of the above criteria, and were cited in at least one

quality scientific publication, they were considered for use. In this case the author's protocol was initially followed and subsequently modified (if necessary) to optimise the PCR efficiency.

Finally, primers were run through the National Institute for Health (NIH) PubMed Basic Local Alignment Search Tool (BLAST) to ensure accurate homology to the target sequence and confirm primer-sequence specificity (222).

2.4.3 Conventional polymerase chain reaction

2.4.3.1 Introduction to RT-PCR

Polymerase chain reaction (PCR) is a process whereby segments of DNA (amplicons) are copied exponentially by a process of cycling reactions of different temperatures. This allows detection of the sequence from an initially small amount of template nucleic acid. During each cycle of the PCR protocol each double strand of DNA is separated (denatured) and a complimentary strand synthesised, resulting in a doubling of the amount of nucleic acid. Over a reaction of 35 cycles, the end amount of DNA is a 2^{35}-fold multiple of the starting amount of template.

This process required primers, short sequences of DNA (oligonucleotides) which are designed to have complete homology with a specific DNA sequence of interest. Two primers are required which will anneal to each end of the region of interest, spanning the amplicon, and are of the correct orientation such that, when extension by the DNA polymerase enzyme occurs, the gene region of interest is copied. DNA polymerases always extend DNA in the 5' to 3' direction.

Each cycle has three steps. The first step is denaturation where the double-stranded DNA (dsDNA) melts and separates into two single-stranded (ssDNA) molecules. This occurs at approximately 94^{o}C and at this temperature all enzymatic reaction (including polymerisation)

ceases. It is often referred to as the denaturation temperature (T_D). The second step is the annealing step. The mixture is cooled to a predetermined temperature (T_A), usually between 54 and 60^oC, in order that primers and DNA collide and hydrogen bonds between the stands are formed and quickly broken repetitively. When the primer collides with its homologous region of interest, the hydrogen bonds formed are stronger that those formed between non-homologous interactions. This allows the primer to remain annealed to the DNA sequence long enough for the polymerase to attach and begin to copy the DNA strand. Once the sequence begins to elongate, the hydrogen bonds are so strong that the template and elongating copy strand will not denature at this temperature. Annealing takes only a few seconds and the annealing step need only last 15-30 seconds to avoid spurious primer annealing (216).

Finally the target region of DNA is copied during the extension step. This occurs at 72^oC and involves extension of the copied strand in the 5' to 3' direction with coupled deoxynucleoside triphosphate (dNTP) molecules attached to the growing 3' end of the complimentary strand. DNA polymerases generally have a base insertion rate of 50 bases per second and the duration of the elongation step is usually only required to be 15-30 seconds, though longer times are required for longer amplicons. This three step cycle is repeated 35-45 times to exponentially amplify the template sequence.

During RT-PCR reactions primers were used in the concentration of 1-2µM. Similarly, dNTPs were used at a concentration of 200µM. Magnesium ions (Mg^{2+}) are critical for optimal PCR reactions. Mg^{2+} ions bind to template DNA, dNTPs and primers, and the *Thermus aquaticus* (Taq) polymerase requires free Mg^{2+} ions to function. Mg^{2+} ion concentration influences primer annealing, T_M and product specificity with high concentrations leading to reductions in stringency (specificity) (216). For each RT-PCR reaction an Mg^{2+} ion dilution experiment was undertaken to identify optimal Mg^{2+} ions concentration for the reaction. This was usually within the range 1.5-3.5mM.

2.4.3.2 RT-PCR protocols

Conventional RT-PCR was undertaken using the AmpliTaq Gold® DNA polymerase with GeneAmp® 10x PCR Gold Buffer kit (4311816, Applied Biosciences). Components of the RT-PCR reaction were added sequentially, for example nuclease-free water 16.25µl, 25mM $MgCl_2$ 2.5µl, 10x PCR Buffer 2.5µl, 10mM dNTP 0.5µl, 100µM sense primer 0.5µl, 100µM anti-sense primer 0.5µl, 5U/µl Taq polymerase 0.25µl and template cDNA 2.0µl to give a final volume of 25µl (for HPRT amplification).

The volume of $MgCl_2$ and nuclease-free water was dependent on the $MgCl_2$ dilution test. This involves running parallel samples of cDNA for amplification with increasing concentration of $MgCl_2$ in the buffer solution. The concentration of $MgCl_2$ which resulted in the brightest band following electrophoresis was selected for future PCR reactions.

All samples were run with a “no RT” negative control. This is a sample where no RT enzyme was added to the mRNA sample during cDNA synthesis, theoretically resulting in the absence of cDNA synthesis. In such a sample, any detectable PCR product would indicate gDNA contamination. In addition, some samples were run with a “no template control”. In these samples no cDNA sample was added to the PCR master mix. Again, any detectable product on the gel would indicate gDNA contamination as some stage of the protocol.

Table 2.1 lists the RT-PCR protocol cycling conditions and the denaturing, annealing and elongation temperatures for all the primers used for conventional RT-PCR. The primer sequences used during conventional RT-PCR are shown in table 2.2.

Table 2.1 Cycling protocols for conventional RT-PCR primers

Primer	Stage 1	Stage 2: denaturation	Stage 2: annealing	Stage 2: elongation	No. of cycles	Stage 3
HPRT	95°C 10 min	95°C 15 sec	60°C 30 sec	72°C 30 sec	40	72°C 20 min
TLR2	95°C 10 min	94°C 15 sec	60°C 30 sec	72°C 30 sec	40	72°C 20 min
TLR4	95°C 1 min	95°C 45 sec	54°C 45 sec	72°C 1 min	38	72°C 20 min

HPRT, Hypoxanthine-guanine phosphoribosyltransferase; TLR, Toll-like receptor

Table 2.2 Conventional RT-PCR primer sequences

Gene	Primer sequence	Melting temperature (T_M)	Amplicon size
HPRT	GAC CAG TCA ACA GGG GAC AT (sense) CGA CCT TGA CCA TCT TTG GA (anti-sense)	59.4°C 57.3°C	160bp
TLR2	AGT TGA TGA CTC TAC CAG ATG (sense) GTC AAT GAT CCA CTT GCC AG (anti-sense)	55.9°C 57.3°C	599bp
TLR4	TGG ATA CGT TTC CTT ATA AG (sense) GAA ATG GAG GCA CCC CTT C (anti-sense)	51.2°C 58.8°C	507bp

bp, base pairs; HPRT, Hypoxanthine-guanine phosphoribosyltransferase; TLR, Toll-like receptor

2.4.3.3 Separation of PCR products using agarose gel electrophoresis

Following RT-PCR, nucleic acid amplicons were separated by agarose gel electrophoresis and visualised by the use of the fluorescent molecule ethidium bromide. Nucleic acids are negatively charged and will migrate towards the anode following the application of an electric field, with the rate of migration being proportional to the applied field strength. The shorter the nucleic acid sequence, the faster it migrates through the sieve-like agarose gel. Moreover, higher concentration agarose gels restrict the movement of larger nucleic acids to a greater degree and allow separation of shorter sequences, while lower concentration gels allow separation of longer sequences (216).

In order to make a 1% agarose solution, 1g agarose (A9539, Sigma) was dissolved in 100mL TAE solution (Tris, glacial acetic acid and EDTA, pH 8.0). This was heated for 2 minutes on full power in an 800W microwave oven to fully dissolve the agarose. This was added to a gel cast and 10µL of 0.5mg/ml ethidium bromide added to the solution. This was

left for 30 minutes to set. The gel was submerged in the running tank with further TAE solution.

To each 10µL PCR samples was added 2µL of anionic loading dye (161-0767, Bio-Rad Laboratories, California, US). These samples were transferred to consecutive wells in the agarose gel and run for 60-90 minutes with an applied electric field of 120V. The first well of each gel contained a 100 base pair ladder to allow sizing of amplified products. Bands were visualised using an ultraviolet (UV) trans-illuminator with appropriate eye protection.

2.5 DNA sequencing using ABI PRISM BigDye Terminator® protocol

Following agarose gel electrophoresis, PCR product bands were visualised under UV trans-illumination. Using a scalpel blade, the band was cut from the gel and stored at 4^{o}C until required. To extract the PCR product and dissolve the agarose gel the Qiagen MinElute Gel Extraction kit (28604, Qiagen, Germany) was used as per the manufacturer's instructions. The gel slice was weighed and 300µL of Buffer QG added per 100mg of gel. This was incubated at 50^{o}C for 10 minutes until the gel had dissolved, with vortex mixing every 2-3 minutes during the incubation. The Buffer GQ contains a pH indicator to ensure the solution remains below pH 7.5. Should the pH of the dissolved gel rise above this value, the buffer undergoes a colour change from yellow to orange/purple and the addition of 10µL of 3M sodium acetate is required to return the pH to its optimal level.

Next, 100µL of isopropanol was added per 100mg of initial gel weight and this mixture transferred to a MinElute® spin column for centrifugation at 13,000 rpm for 1 minute. This column binds the DNA to the membrane and allows through passage of the dissolved gel. The membrane was washed with a further 500µL of Buffer GQ® spun at 13,000 rpm (>10,000g) for 1 minute, and then left to stand for 2-5 minutes with 750µL of Buffer PE® applied to the membrane before being spun at 13,000 rpm (>10,000g) for a further 1 minute.

To elute the DNA, 10µL of Buffer EB® (10mM Tris·Cl, pH 8.5) was added to the centre of the membrane and left to stand for 1 minute before centrifugation at 13,000 rpm (>10,000g) for 1 minute. The average eluate volume was 9µL. The DNA eluate was used immediately for sequencing or stored at -20^{o}C.

Sequencing was undertaken using the BigDye Terminator® protocol (Applied Biosystems, US). Following DNA extraction from the agarose gel, the following were mixed:

DNA eluate	0.5µL
BigDye Ready Reaction Mixture®	0.5 µL
1µM sense primer	1.5µL
Better Buffer®	3.5µL
Nuclease-free water	4µL
Total	10µL

The following PCR reaction was subsequently performed: 25 cycles of 96^{o}C for 30 seconds, 50^{o}C for 15 seconds and 60^{o}C for 4 minutes, followed by a single cycle of 28^{o}C for 1 minute. Following this PCR reaction, the following were added to the 10µL PCR mixture:

125mM EDTA	2µL
3M sodium acetate	2µL
100% ethanol	50µL
Nuclease-free water	10µL
Total	74µL

This was vortex-mixed and incubated at room temperature for 15 minutes. Next, the solution was centrifuged at 13,000 rpm (>10,000g) for 20 minutes at 4^{o}C (30 minutes for sequences over 600 bases). The supernatant was carefully aspirated and 70µL of 70% ethanol added

followed by centrifugation at 13,000 rpm (>10,000g) for 10 minutes at 4°C (15 minutes for sequences over 600 bases). The supernatant was carefully aspirated and a further ethanol wash and centrifugation was performed, as above, for sequences over 600 bases in length. Following aspiration of the ethanol, the pellet was dried with the tube lid open at 50°C for 10 minutes.

The pellet was stored at -20°C and transferred to the Post-Genomic Technologies Facility, University of Nottingham, for production of the BigDye® gel and subsequent reading of the sequence. Following sequencing analysis, a report is generated which provides the nucleotide sequence and allows assessment of the quality of the sequencing reaction. An example of the sequencing report for the HPRT housekeeping gene is shown, using Chromas 2 software (figure 2.4).

Figure 2.4 HPRT gene sequencing using the BigDye Terminator® protocol technology and Chromas2 software

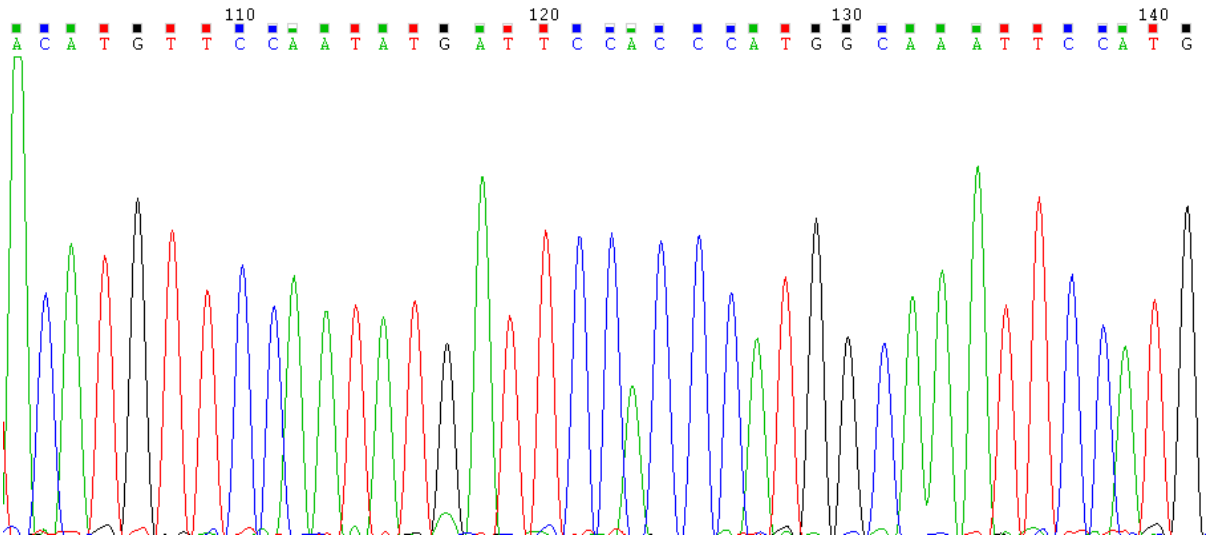

A Chromas2 software readout of a section of the hypoxanthine guanine phosphoribosyltransferase (HPRT) sequence using BigDye® gel. Peaks represent individual nucleobases; A (adenine, green), C (cytosine, blue), G (guanine, black) and T (thymine, red). Successful sequencing reactions show clean sequences with discrete ordered peaks corresponding to the nucleotide sequence of the amplified product, as shown above.

In some cases rather than being sequenced from the gel, the PCR product was sequenced directly from the initial RT-PCR reaction mixture. In this case, the 10µL PCR product was mixed with 4µL of ExoSAP-IT (Exonuclease I and Shrimp Alkaline Phosphatase, GE Healthcare, UK) and incubated at 37^{o}C for 30 minutes followed by 80^{o}C for 15 minutes. At this stage 0.5µL of this mixture is added to the BigDye Ready Reaction mixture, 1µM sense primer, Better Buffer and Water and the protocol completed as above.

2.6 Haematoxylin and eosin staining of cytospins and tissue sections

Cytospin slides, stored at -20^{o}C, were thawed for 30 minutes still wrapped in foil. They were then transferred to a metal slide rack and hydrated in running tap water for 5 minutes. The slides were transferred to pre-filtered haematoxylin for 15 minutes before being returned to a running water wash. The slides were then transferred to 1% acid alcohol for 10 seconds and 0.5% ammoniated water for 30 seconds with a running water wash after each step.

Finally, slides were transferred to eosin for 3 minutes, washed and then dehydrated in graded alcohols (50%, 70%, 80%, 90% and 100%) followed by three 1 minute treatments in xylene to make the slide hydrophobic so that a cover slip may be applied with resin. The specimens were covered by the drop of DPX (44581-500ML, Sigma) resin followed by a cover slip and allowed to dry overnight in a fume hood before being stored at room temperature.

For whole bowel tissue sections, formalin-fixed, paraffin-embedded tissue sections, stored at room temperature, were placed into a metal rack and de-waxed by three treatments using xylene for 1 minute each. Tissue sections were then hydrated by sequential incubation in graded alcohols of reducing concentration (100%, 90%, 80%, 70% and 50%) for 1 minute each. Finally the slides were placed in distilled water for 5 minutes before staining with

haematoxylin and eosin, as described for cytospins. Tissue sections were covered using DPX mount and a coverslip.

2.7 Immunocytochemistry

Immunocytochemical (ICC) staining was undertaken using the avidin/biotin system. Avidin is a 68kDa glycoprotein with a very high affinity ($10^{15}M^{-1}$) for the small molecular weight vitamin biotin. This high affinity essentially produces irreversible binding of avidin to biotin, and this can be exploited by using biotin-conjugated (biotinlyated) enzymes such as horseradish peroxidase (HRP). In addition, avidin has four binding sites for biotin molecules (223).

Monoclonal or species-specific polyclonal primary antibodies bind to a specific epitopes on target antigens (such as the extra-cellular domain of a toll-like receptor protein). These were applied to the tissue or cytological specimen following sequential blocking with hydrogen peroxide, normal serum, avidin and biotin solutions (to prevent non-specific staining by the secondary antibody or avidin/biotin complex). Following primary antibody incubation, a biotinylated secondary antibody reared in another species (for example horse) was applied. This binds to the primary antibody-antigen complex. The avidin/biotinylated-HRP complex was subsequently added to the specimen to bind to the secondary antibody. The detection of antibody binding was visualised by adding 3,3'-diaminobenzidine (DAB), which turns brown in the presence of the antibody-bound horseradish peroxidise. The specimen was counter stained and viewed with the light microscope (figure 2.5).

Figure 2.5 Schematic of the immunoperoxidase staining technique

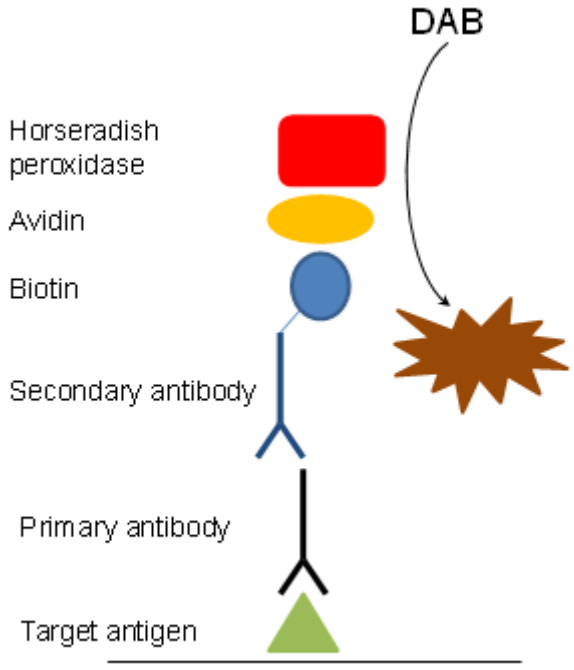

Schematic diagram of immunoperoxidase staining using a primary unconjugated monoclonal antibody (black), a biotinylated secondary antibody (blue), the avidin/biotin (yellow)-horse radish peroxidase (HRP) complex (red) and the colorimetric reagent 3,3'-diaminobenzidine (DAB). In the presence of HRP, DAB turns a brown colour, allowing indirect visualisation of primary antibody-antigen binding.

To perform ICC, slides stored at -20^{o}C were thawed for 30 minutes (still wrapped in foil) and then transferred to a metal slide rack and hydrated in phosphate buffered saline (PBS) for 20 minutes. To prevent slides drying out, slides were laid in a slide incubation chamber surrounded by PBS-soaked paper towel. The area of the slide containing the adhered cells was highlighted with a wax pencil and then slides were blocked with 200µL neat avidin and biotin blocking solutions (SP-2001, Vector Labs) separately for 30 minutes each, and then wash in PBS twice for 5 minutes. Thereafter 200µL of blocking serum (5% horse serum in PBS) was applied to the cells at room temperature for 30 minutes and washed with PBS twice for 5 minutes.

The primary antibody was prepared from stock as shown in the following table. The normal serum block was removed and replaced with 200µL of primary antibody in PBS and incubated for 1 hour at room temperature. Negative control slides were also made by omitting the primary antibody and applying only PBS at this stage (table 2.3).

Table 2.3 Working dilutions and DAB reagent detection times for the primary antibodies using in immunoperoxidase staining

Primary antibody	Dilution of stock antibody	Duration of DAB detection
Cytokeratin (Abcam)	1:400	2 minutes
BerEP4 (Dako)	1:400	2 minutes
α-smooth muscle actin (Abcam)	1:500*	2 minutes
Vimentin (Abcam)	1:40*	2 minutes
Desmin (Abcam)	1:20*	2 minutes
TLR2 (eBioscience)	1:50	4 minutes
TLR4 (eBioscience)	1:50	4 minutes
Lysozyme (Thermo Scientific)	1:100	2 minutes

DAB, 3,3'-diaminobenzidine; PBS Phosphate buffered saline; TLR, Toll-like receptor
* Initially stock antibody was diluted to 1:5 with PBS and 1% BSA before storage at -80^{o}C

Following incubation the slides were transferred back to the metal slide rack and washed twice for 5 minutes in PBS to remove unbound primary antibody. Next, peroxidise activity was blocked by incubating the slides in 0.3% hydrogen peroxide in methanol (2mL hydrogen peroxide and 198mL methanol) for 30 minutes. Thereafter slides were again washed twice for 5 minutes in PBS.

The biotinylated secondary antibody (PK-6200 Vectastain ABC Universal kit, Vector Labs) was prepared in a 1:100 dilution in PBS with 5% blocking serum. This was added to the slides following their transfer back to the incubator chamber and left for 30 minutes at room temperature. The avidin/biotin-HRP complex (ABC) was prepared at the same time by adding 100µL each of reagents A and B to 5mL PBS and leaving for 30 minutes, as per the manufacturer's instructions.

After the secondary antibody incubation step, the slides were washed twice for 5 minutes in PBS. The avidin/biotin complex was added to the slides and incubated for 30 minutes at room temperature followed by two 5-minute washes in PBS.

To detect HRP activity, a solution of DAB was prepared (SK-4100 Vector peroxidise substrate kit, Vector Labs) by adding 100µL of Buffer pH 7.5, 200µL DAB stock solution and 100µL hydrogen peroxide solution to 5mL distilled water. The DAB solution was applied to the slides and left for the indicated time (table) before rinsing under running tap water for 5 minutes.

The slides were counter-stained sequentially in Coles' haematoxylin for 2 minutes, 1% hydrochloric acid for 10 seconds and ammoniated water for 45 seconds, with a tap water wash step between each stain. Specimens were then dehydrated by passage through graded alcohol solutions (50%, 70%, 80%, 90% and 100%) and through xylene three times for 1 minute each. Finally, samples were mounted with DPX and a cover slip, and left to dry in a fume hood overnight.

2.8 Statistical analysis

Continuous quantitative data were analysed for Gaussian distribution using a Kolmogorov-Smirnov test and by plotting data on a frequency-density histogram. Normally-distributed data were analysed using a paired or un-paired student t-test, as appropriate. Non-normal data were analysed using non-parametric testing, either a Wilcoxon or Mann Whitney U test. Any categorical data were analysed using a Fisher's exact test.

Statistical analyses were undertaken using two statistical software packages, SPSS (version 19) and Graphpad Prism (version 5). All graphs were produced in Graphpad Prism except those relating to correlation calculations which were produced in SPSS. All statistical tests

were two-tailed and statistically significant results were those with p-values less than 0.05 (5%).

Chapter 3: Isolation and characterisation of human crypt intestinal epithelial cells

3.1 Introduction

Intestinal epithelial cells form the largest area of any body surface. They function to provide key roles in the digestion and absorption of nutrients vital for host organism survival as well as providing a barrier to the migration of micro-organisms or toxins into the underlying host tissue (1). Recent work has demonstrated that the roles of the IEC go beyond these functions alone. IEC are now regarded to provide key roles in the immune response, modulating the adaptive immune response to tolerate commensal and food antigens and acting as innate immune system cells in times of inflammation (98).

As will be further discussed in chapters 6 and 7, the mature functional epithelial cells are progeny of stem cells which reside in the base of the crypts of Lieberkühn (224). These stem cells have the capacity to populate the crypts of the intestine and the villi of the small intestine through rapid recycling and subsequent differentiation. Critically these stem cells can differentiate into all four mature lineages of IEC, namely columnar cells, Paneth cells (in the small intestine only), mucus-secreting goblet cells and enteroentocrine cells. This is a tightly regulated process which involves the secretion of various factors which regulate cell turnover and differentiation (174). The location of the stem cells within a niche is crucial to the stem cell response to injury and inflammation and plays a role in the pathogenesis of conditions such as inflammatory bowel disease (187). The niche is the term used to describe a functional location in which stem cells are surrounded by mesenchymal and vascular cells, extra-cellular matrix and numerous factors which regulate growth and differentiation.

One challenging area of IEC research has been the difficulty in producing epithelial cell cultures. Numerous immortalised human cancer cell lines have been developed which

potentially can be maintained in culture indefinitely. However, these cell lines tend to proliferate independently of their surroundings, as is typical of neoplastic cells, and bear only modest relation to the original cell phenotype (225). In contrast, IEC *in vivo* differentiate and mature as a result of their interactions with surrounding cells and structures as they migrate from crypt to villus over the course of a few days. Therefore, the use of cell lines in the study of IEC physiology has its clear limitations.

There have been several attempts to culture primary IEC over the last two decades. Whitehead *et al.* described the use of a collagen gel over a feeder layer of bovine aortic endothelial cells and demonstrated cell division at 7 days and survival to at least 16 days following isolation of human crypt cells (226). Collagen-coated surfaces have also been shown to facilitate murine colonic IEC proliferation for 10 days and survival for up to 35 days (227). The challenge has always been to isolate pure IEC from intestinal mucosa without mesenchymal or haematopoietic cell contamination, and to maintain viable and proliferating IEC in culture.

This chapter describes the *ex vivo* method for isolating human small and large intestinal crypts and the disaggregation of these crypt cells into single cells. Unlike methods which isolate and culture whole crypts, the current technique isolates individual cells, allowing further study of these cells using techniques such as flow cytometry and fluorescence-activated cell sorting (FACS). The protocol is a modified version of the method described by Bjerknes and Cheng in 1981 using murine small intestine (228) and later using human colon by Whitehead *et al.* in 1999 (229). More recently our laboratory has demonstrated isolation of individual human colonic IEC and with sufficient viability to allow subsequent flow cytometric analysis (210, 230).

3.2 Methods

Primary human intestinal crypt epithelial cells were isolated from fresh full thickness small and large bowel resection specimens, as previously reported (210). Informed consent was obtained from patients prior to surgery to allow tissue samples to be included in the current study as part of the School of Clinical Sciences Tissue Bank, University of Nottingham. All patients received an information sheet prior to consent and were required to provide written consent for inclusion in the study. Permission to use tissue samples from the Tissue Bank was obtained following approval of the research project by the Research Ethics Committee. All patient data were pseudo-anonymised by entering data onto a secure database and assigning each case a unique, non-identifiable numerical code.

3.2.1 Case selection

All patients with inflammatory bowel disease (IBD), either ulcerative colitis or Crohn's disease, undergoing operative bowel resection were considered for entry into the study. Data were collected on patient demographics (age, disease location and activity, current medical therapy, relevant past medical history, previous endoscopic evaluation of disease extend and activity, previous histological assessment for disease activity and exclusion of dysplasia, previous surgical interventions and proposed operative procedure). All patients were over 16 years of age. There was no upper limit of inclusion based on age.

To act as controls, patients undergoing bowel resection for colorectal cancer were included. Macroscopically normal-looking tissue was taken at least 5cm from the margin of the cancer lesion. Similar demographic data were collected for control patients and those with a history of inflammatory bowel conditions (e.g. diverticular disease) were excluded. In addition, patients who had received pre-operative chemotherapy or radiotherapy of any type or duration were excluded to avoid any potential confounding factors, such as changes in gene and protein expression.

The anatomical location of specimen acquisition was recorded for every specimen. The post-operative histopathology report was obtained to ensure the absence of dysplasia in either group (IBD or control). Any sample subsequently found to show features consistent with dysplasia was excluded from analysis.

3.2.2 Tissue acquisition

Full thickness fresh, unfixed specimens of small and large bowel were collected from the operating theatres of the Queen's Medical Centre, Nottingham University Hospitals NHS Trust, Nottingham UK. In the category III room in the Department of Histopathology 2cm x 2cm square full thickness sections of bowel were cut from the specimen. This tissue was washed three times by gentle shaking in 20mL Hanks' Balanced Salt Solution (HBSS) without magnesium or calcium (Mg/Ca) (14180-46, Gibco, Invitrogen). Samples were then stored in 40mL F-12 with glutamine (21765, Gibco, Invitrogen) at 4^{o}C. All collected specimens were stored at identical conditions for 12-14 hours until the intestinal epithelial cell isolation protocol (section 3.2.4) was undertaken.

3.2.3 Tissue embedding in paraffin

Prior to commencing the IEC isolation protocol, a small section of whole bowel 2mm x 2mm was cut and stored in 3.7% formaldehyde neutral buffer solution overnight (formalin, Sigma-Aldrich) and then transferred to 70% ethanol. This was taken to the Department of Histopathology for paraffin embedding. The formalin-fixed, paraffin-embedded (FFPE) samples were stored in a dry location at room temperature until required. In some cases, strips of primary mucosal tissue were collected after each of the three EDTA/DTT protocol steps (see section 3.2.4). These were formalin-fixed and paraffin-embedded in preparation for later examination.

3.2.4 Intestinal epithelial cell isolation

Strips of intestinal mucosa were cut from the remaining whole bowel specimen and washed gently five times in cold HBSS (without Mg/Ca) and then weighed. The mucosal strips were subsequently incubated in 40mL 1mM ethylenediaminetetraacetic acid (EDTA, Sigma-Aldrich) and 0.05mM dithiothreitol (DTT, Acros Organics, New Jersey, US) (EDTA/DTT) at 37^{o}C in a shaking water bath for 30 minutes. EDTA/DTT solution was made freshly by adding 20mL of filter-sterilised stock 10mM EDTA (1.86g EDTA in 500mL HBSS without Mg/Ca, pH 7.0) and adding 2mL of fresh DTT (38.6mg DTT in 50mL HBSS without Mg/Ca) to 178mL HBSS (without Mg/Ca) and subsequent filter sterilisation through a 0.2µm filter.

After 30 minutes incubation, the mucosal strips were shaken vigorously for 1 minute in cold HBSS (without Mg/Ca). The detached cells were retained in fluid suspension and the mucosal strips transferred to fresh HBSS (without Mg/Ca) for repeat vigorous shaking. The process of shaking in fresh media was repeated to a total of five times to ensure detachment of all loose epithelial crypt cells. This yield of suspended epithelial cells (still anatomically identifiable together in a crypt structure) was termed E1.

The mucosal strips were returned to fresh EDTA/DTT for a further 30 minutes, after which the process of epithelial cell detachment by shaking was repeated, yielding an isolation of E2 epithelial cells. This EDTA/DTT treatment with cell detachment was repeated for a third and final time, yielding E3 epithelial cells.

Suspended crypts were transferred into 50mL falcon tubes and centrifuged at 1,000 rpm (800g) for 5 minutes. The supernatant was discarded and the pellet of cells re-suspended in 40mL of filter-sterilised 0.25% pancreatin (0.1g porcine pancreatin, P-1500 Sigma, in 40ml HBSS with Mg/Ca). This was incubated at 37^{o}C for 90 minutes with occasional mixing. This resulted in the disaggregation of crypt cells into individually isolated cells.

Following pancreatin treatment, samples were diluted two-fold with an equal volume (40mL) of cold HBSS (without Mg/Ca) and centrifuged at 1,000 rpm (800g) for 5 minutes. The supernatant was discarded and the cells re-suspended in 20mL EDTA/DTT solution and centrifuged at 1,000 rpm (800g) for 5 minutes. Again the supernatant was removed and the cells re-suspended in 20mL cold HBSS (without Mg/Ca) and centrifuged at 1,000 rpm (800g) for 5 minutes. Finally, the supernatant was removed and the pellet re-suspended in 5mL HBSS (without Mg/Ca) for cell counting using trypan blue exclusion. Cell suspensions were stored on ice for further down-stream experimentation.

For E2 and E3 yields, after the shaking/detachment step and prior to the first centrifugation step, the suspension of cells was examined at x4 magnification under a light microscope to ensure continued crypt detachment. If intact crypts were visualised, the suspended cells were centrifuged and the protocol completed as described. If no crypts were identified, the sample was discarded.

3.2.5 Cell counting

Cell counting and viability was undertaken using a haemocytometer and 0.4% trypan blue exclusion, as described in section 2.1. On occasion, pancreatin-treated cells were observed to clump together, forming cellular aggregates. In these circumstances the suspended cells were passed through a 21 gauge needle several times before counting.

3.2.6 Cytospin preparation

Freshly isolated IEC and peripheral blood mononuclear cells, and cultured human epithelial cell lines, were suspended in HBSS (with Mg/Ca) medium to a concentration of $2.5x10^5$ cells/mL and adhered to glass slides using the Shandon Cytospin® 2 cytocentrifuge (Wolf Laboratories). SuperFrost plus® slides (Thermo Scientific) were labelled, covered in filter card and positioned in the metal grip, ensuring the hole in the card was aligned with the hole in the plastic cup. Two hundred microlitres of cell solution was transferred to each cup and

centrifuged at 800rpm (22.4g) for 10 minutes. The slides were removed and allowed to dry at room temperature. A diamond pencil was used to draw around the circle of attached cells. The slides were fixed in acetone for 5 minutes and allowed to dry at room temperature. Slides were wrapped in foil and stored at -20^{o}C until further use.

3.2.7 Immunocytochemistry

Immunocytochemical staining was undertaken using the avidin/biotin system. The general protocol for immunocytochemical staining is described in chapter 2.7. In brief, frozen cytospin slides were thawed and hydrated in PBS. Endogenous peroxidase activity was quenched using 0.3% hydrogen peroxide in methanol and non-specific protein binding blocked using 5% normal horse serum in PBS. Cells were labelled with the murine anti-human primary antibody at its optimal concentration as described in chapter 2.7 (determined initially by using serial dilutions of primary antibody) for 1 hour at room temperature. Biotinylated horse anti-mouse secondary antibody was applied followed by incubation with the avidin/biotin complex. Colour was developed using the Vector DAB peroxidise substrate before counter-staining with haematoxylin. Finally slides were dehydrated in graded ethanol, dipped in xylene and mounted using DPX mounting medium overnight.

3.2.8 Cell viability analysis

To assess the duration of cell viability, primary human crypt IECs were isolated and suspended in culture medium (HBSS (without Mg/Ca) with 10% FCS, 5ml of 200mM L-glutamine, 50,000 units of penicillin G (Britannia Pharmaceuticals Ltd, Surrey, UK), 50mg streptomycin sulphate (Sigma-Aldrich Company Ltd, Dorset, UK) and 24mg gentamicin (Roussel Laboratories, Uxbridge, UK) (P/S/G)). Cell suspensions were stored at 37^{o}C and 5% CO_2 and viability by trypan blue exclusion was assessed daily over a period of up to 4 days.

3.2.9 HT-29 and T84 human intestinal epithelial cell line culture

HT-29 cells are a human colon adenocarcinoma grade II cell line. They are frequently used *in vitro* as a model representing luminal surface colonic epithelial cells in humans. By contrast, T84 cells are a human colonic adenocarcinoma cell line used *in vitro* to represent colonic epithelial cells derived from the crypt of the large bowel epithelium (89, 154, 231-233).

Cryovials of HT-29 or T84 cells of various passages were preserved in the liquid nitrogen store. As required, a cryovial was removed and rapidly thawed in a 37^{o}C water bath. Cells were transferred to a T75 flask containing 20mL of media. The flask was incubated at 37^{o}C and 5% CO_2 overnight and media replaced with 14mL fresh media (500mL Dulbecco's Modified Eagles Media (DMEM) with 10% fetal calf serum, 5mL of 200mM glutamine and 1 ampoule of Penicillin/Streptomycin/Gentamicin mixture) the following day, following confirmation that the revived cells had adhered to the flask using a light microscope. Media was changed three times weekly for the duration of the cell culture experiments with 14mL fresh media pre-warmed to 37^{o}C. T84 cell culture medium was identical except 500mL DMEM Nutrient Mixture F-12 (DMEM/F-12) (1:1) (x1) (21331-020, Invitrogen) was used.

Prior to media changes, HT-29 and T84 cells were examined under the light microscope. Cells were split prior to fully confluent growth, which was usually within 3-5 days. To split cells, medium was aspirated and the cells washed with 2mL 0.25% trypsin (Sigma-Aldrich) in Versine (0.02% EDTA in PBS, pH7.2). This was removed and replaced with a further 3mL of fresh 0.25% trypsin and incubated for 10 minutes at 37^{o}C. Light microscopy was used to confirm cell detachment. Next 3mL of media was added to neutralise the trypsin and the 6mL of cell suspension was collected and split equally (2mL) into three new T75 flasks each containing 13mL of fresh media. Alternatively, cells were counted and used immediately for further experimentation or centrifuged to adhere to cytospin slides.

For long-term storage, freezing mixture was prepared by mixing 550µL of dimethyl sulphoxide (DMSO) (Sigma-Aldrich) in 5mL FCS (Invitrogen). Cells were trypsinised, as described above, and the 6mL cell suspension centrifuged at 1,000rpm for 5 minutes. The supernatant was removed and the pellet re-suspended in 1mL of freezing mixture in a 1mL cryovial (Camlab). The cryovial was stored at -80^{o}C overnight in a cardboard box filled with tissue paper and transferred to the nitrogen freezer the following day for permanent storage.

3.2.10 Peripheral blood mononuclear cell isolation

Peripheral blood mononuclear cells (PBMC) were used as positive controls for TLR2 and TLR4 expression. To isolate PBMC, whole blood was collected in sodium heparin tubes (10µL heparin per tube), transferred to a 50mL Falcon tube and diluted 1:1 with HBSS (with Ca/Mg) at room temperature. Next 5mL of Histopaque-1077 (H8889-100ML, Sigma) was added to a fresh 15mL Falcon tube and 10mL of diluted whole blood gently layered on top using a sterile Pasteur pipette. This was centrifuged at 2,000rpm (800g) for 20 minutes and the PBMC-containing white buffy layer (between the plasma, above, and the Histopaque, below) was transferred to a fresh Falcon tube.

The PBMC were suspended in 5mL cold HBSS (with Ca/Mg) and centrifuged for 10 minutes at 1,800rpm (700g). The supernatant was removed and the PBMC re-suspended in 5mL cold HBSS (with Ca/Mg) and centrifuged at 1,600rpm (600g) for 10 minutes. The supernatant was removed and the cells finally re-suspended in 5mL cold HBSS (with Ca/Mg) and kept on ice until required or were centrifuged to adhere to cytospin slides.

3.2.11 THP-1 human monocyte cell line culture

THP-1 cells are a monocyte cell line (234). Cryovials of THP-1 cells of various passages were preserved in the liquid nitrogen store. As required, a cryovial was removed and rapidly thawed in a 37^{o}C water bath and transferred to a Falcon tube containing 5mL medium (500mL RPMI 1640, 10% fetal calf serum, 5mL of 200mM glutamine, 1 ampoule of P/S/G

and 20µmol/L β-mercaptoethanol). The tube was centrifuged at 800rpm (300g) for 5 minutes and the supernatant removed. The pellet was re-suspended in 15mL fresh medium and added to a T75 flask. The flask was incubated at 37^{o}C and 5% CO_2 overnight and medium replaced the following day.

THP-1 cells do not adhere to the T75 flask wall but remain in suspension during incubation. To replace the medium, the cell suspension was centrifuged in a falcon tube at 800rpm (300g) for 5 minutes. The supernatant was removed and the pellet re-suspended in 14mL of fresh medium in a fresh T75 flask. Media was changed three times weekly for the duration of the cell culture experiments with 14mL fresh medium pre-warmed to 37^{o}C.

Cells were split when the cell concentration reached 8x10^{5} cells/mL using trypan blue exclusion. Cells were diluted to a concentration of 2-4x10^{4} cells/mL (approximately 1:30 dilution) and transferred to a fresh T75 flask. Alternatively, cells were counted and used immediately for further experimentation or centrifuged to adhere to cytospin slides.

For long-term storage, freezing mixture was prepared by mixing 250µL of DMSO with 5mL THP-1 medium. Cells were centrifuged at 800rpm for 5 minutes and the supernatant removed. The cells were re-suspended in 1mL freezing mixture and transferred to a 1mL cryovial. The cryovial was stored at -80^{o}C overnight in a cardboard box filled with tissue paper and transferred to the nitrogen freezer the following day for permanent storage.

3.3 Results

3.3.1 Treatment with ETDA releases intestinal epithelial crypts

On incubation of intestinal mucosa from the small and large bowel with EDTA, disruption to the IEC-lamina propria interface resulting in the release of IEC crypts into solution was evident (figure 3.1). Following the first 30-minute incubation the majority of cells (E1 cells) visible in solution using light microscopy were derived from the villus or luminal surface. There were very few crypts visible in suspension. In general these cells were discarded unless, as was occasionally seen, significant numbers of crypts were present in suspension. The majority of crypts were isolated following the second 30-minute EDTA incubation (E2 cells) and could easily be seen in suspension in the mucosal tissue wash solution (figures 3.1A and 3.1B). Following the third 30-minute incubation (E3 cells) washings were almost universally devoid of all cells and crypts, and were therefore discarded.

Following pancreatin treatment crypt epithelial cells were seen to disaggregate into individual cells (figure 3.2). Mucosal strips cut from the whole bowel specimen were formalin-fixed and paraffin-embedded prior to treatment and after each 30-minute EDTA/DTT incubation step. These were sectioned and stained with haematoxylin and eosin. Figure 3.3A shows the appearance of the intact mucosa before EDTA incubation, with crypts visible as invaginations of IEC into the underlying lamina propria. Following EDTA treatment, loss of the crypts is clearly identified. The appearance of empty “spaces” in the underlying LP corresponds with regions in which the crypts previously resided (figure 3.3B). Similar appearances could be seen after EDTA treatment of the small intestinal mucosa (figure 3.4).

3.3.2 Isolated and disaggregated cells stain positively for intestinal epithelial markers

Isolated and disaggregated epithelial cells were centrifuged onto cytospin slides. The cells were labelled with murine anti-human antibodies to the epithelial markers: pan-cytokeratin (CK, P2871 Sigma Aldrich) and epithelial antigen (BerEP4, M0804 Dako). In addition, to

investigate the number of haematopoietic, non-epithelial (contaminating) cells isolated from mucosal preparations, cytospin slides were incubated with an anti-CD45 antibody (14-0459-82, eBioscience). Furthermore, to confirm the reactivity of the antibodies, cytospin slides with the T84 human intestinal epithelial cell line and the THP-1 haematopoietic monocyte cell line were labelled. Additional slides without a primary antibody label were included with each experiment to act as negative controls.

Primary isolated epithelial cells expressed the epithelial marker BerEP4 (figure 3.5A). Isolated cells were largely CD45-negative however the occasional CD45-positive cell was identified (figure 3.5B). To confirm the reactivity and specificity of the epithelial and haematopoietic antibodies, cytospin slides containing T84 epithelial cells and THP-1 monocyte cells were made. T84 cells stained positively for CK (figure 3.6A) and BerEP4 (figure 3.6B), but not for CD45 (figure 3.6C). By contrast, THP-1 cells stained negatively for BerEP4 (figure 3.7A) but positively for CD45 (figure 3.7B). A similar pattern of CD45-positive, BerEP4-negative staining cells was seen for cytospin slides of primary PBMC (data not shown).

To quantify the number of CD45-positive cells in the primary preparations, cytospin slides were blinded and the number of CD45-positive cells per 100 isolated cells was calculated. Cells were counted under a light microscope in replicates of ten high powered fields per slide and the average CD45-positive cell count calculated. This was repeated for ten sample slides for each of the following groups: healthy controls, ulcerative colitis and Crohn's disease (figure 3.8). The proportion of CD45-positive cells (mean $\pm$ SEM) was not significantly different between healthy controls (2.2% $\pm$0.25) and either patients with UC (1.9% $\pm$0.20, P=0.41) or patients with CD (2.2% $\pm$0.49, P=0.96). There was no difference between UC and CD patients (P=0.58).

Similarly, the number of BerEP4-positive cells per 100 isolated cells was calculated (figure 3.9). Again there was no significant difference in the number of BerEP4-positive cells between healthy control subjects (97.4% ±0.28) and either UC (97.8% ±0.23, P=0.38) or CD (97.2% ±0.47, P=0.62), or between patients with UC and CD (P=0.27).

3.3.3 Disaggregated cells show a linear decline in viability following isolation

To assess the viability of isolated and disaggregated cells in culture medium, cells were suspended in culture medium (HBSS (without Mg/Ca) with 10% FCS, 5ml of 200mM L-glutamine, 50,000 units of penicillin G) and stored in an incubator at 37^{o}C 5% CO_2. Cell viability using trypan blue exclusion was assessed at 24 hour intervals. There was an observed decline in cell viability with time, from 58.5%±2.0 (mean±SEM) immediately following isolation to 33.8%±7.6 at 24 hours and 9.6%±3.7 at 48 hours (figure 3.10). Regression analysis showed a linear relationship between decline in viability and time since cell isolation (slope -24.46, R^2=0.9944 and P=0.003).

3.3.4 Viability of disaggregated cells is not influenced by patient demographics, tissue sample site, underlying diagnosis or severity of intestinal inflammation

The viability of isolated cells was distributed normally (figure 3.11, Kolmogorov-Smirnov test for normality p=0.165). To assess the influence of cellular and subject demographic factors on the intestinal epithelial cell viability (at the time of isolation) a number of analyses were undertaken. Firstly, cell viability assessed by trypan blue exclusion was plotted against subject age. There was no relation between increasing age and cell viability (figure 3.12, R^2=0.003, p=0.626). Similarly, cell viability did not correlate with either the total weight of the mucosal tissue removed from the whole bowel specimen prior to crypt IEC isolation (R^2=0.005, p=0.52) or the cell count of isolated IEC in suspension following pancreatin treatment (R^2=0.0002, p=0.973).

The viability of isolated intestinal epithelial cells was not significantly different between healthy control subjects (57.8%±1.53) and patients with either Crohn's disease (60.6%±2.15, p=0.3) or ulcerative colitis (57.2%±1.82, p=0.785). Likewise, samples from CD or UC did not significantly differ significantly from each other (p=0.268). The cell viability was not different when cells derived from un-inflamed and inflamed tissue were compared (57.95%±1.36 versus 59.42%±1.79 respectively, p=0.508), and this observation persisted when the viability of cells derived from colonic inflamed tissue was sub-divided using the histological system described by Riley *et al* (235). Using this grading system, inflammation was assessed on the basis of six factors: acute inflammatory cell (neutrophil) infiltrate, crypt abscess formation, mucin depletion, surface epithelial integrity, chronic inflammatory cell infiltrate and crypt architectural irregularities. The severity of acute inflammation was then graded as follows: none, mild, moderate or severe. To avoid having group of small numbers, samples were grouped into either mild/moderately inflamed or severely inflamed and compared to cells from normal tissue samples. No significant difference in cell viability was noted (ANOVA p=0.308). Furthermore, the cell viability of IEC isolated from the small bowel (59.15%±2.23) was not significantly different from cells isolated from the large bowel (58.54%±2.23, p=0.814).

The viability of isolated IEC was not related to the following demographic features of the subject: hypertension (p=0.693), ischaemic heart disease (p=0.109), cerebrovascular disease (p=0.240), diabetes mellitus (p=0.566), obesity (p=0.666), peripheral vascular disease (p=0.768), osteoporosis (p=0.363), prior intestinal surgery (p=0.87), or use of the following medications at the time of surgery: 5-amino salicylic acid (p=0.541), thiopurines (p=0.349), corticosteroids (p=0.961), cyclosporine (p=0.353), methotrexate (p=0.129), anti-TNFα monoclonal antibody therapy (p=0.842) and antibiotic therapy (p=0.886).

3.3.5 Paneth cells are present in isolated epithelial cell preparations from the small intestine

Cytospin slides from isolated crypt cells were stained for the Paneth cell marker lysozyme. Initially, cells isolated from small intestine preparations were labelled with a rabbit polyclonal antibody to lysozyme at a dilution of 1:200 (Thermo Scientific, RB-372-A) and developed using the Vector DAB system. Cytospin slides of isolated crypt cells derived from healthy small intestine revealed a minority sub-population of lysozyme-positive cells (figure 3.13). Lysozyme-positive cells were similarly observed on cytospin slides from patients with Crohn's ileitis. Lysozyme-positive cells were not identified on cytospin slides of isolated crypt cells from the large intestine of healthy controls or patients with UC or Crohn's colitis.

Paneth cell metaplasia in the colon is a recognised histological feature of inflammatory bowel disease, although its diagnostic value is unclear (215). Paneth cells were identified histologically as lysozyme-positive cells with a granular appearance located predominantly in the crypt base. To investigate the number of lysozyme-positive staining epithelial cells in the small and large bowel, whole bowel tissue sections from healthy controls and patients with inflammatory bowel disease were formalin-fixed and paraffin-embedded, sectioned and mounted onto glass histology slides before being stained with the anti-lysozyme antibody. Blinded sections were viewed at high power and the number of lysozyme-positive cells per crypt was calculated over at least five high power fields per section for at least two cases per disease group.

Lysozyme-positive cells with secretory granules morphologically consistent with being Paneth cells were detected in the epithelial crypts of the small intestine of healthy controls and patients with Crohn's colitis (figure 3.14). The number of lysozyme-positive epithelial cells per crypt in healthy control small bowel epithelium (2.2 ± 0.2) was similar to the number of positive cells in inflamed Crohn's disease subjects (2.2 ± 0.2, $p=0.95$), figure 3.15.

Lysozyme-positive cells with Paneth cell morphology were not detected in the bases of the crypts of the large intestine of healthy controls or patients with IBD (figure 3.16). Lysozyme-positive cells were detected in the lamina propria of the small and large intestine sections from healthy controls and patients with IBD, and are likely to represent haematopoietic mononuclear cells. Rarely, lysozyme-positive cells were detected in the large intestine crypt of healthy controls and patients with IBD (less than one positively-staining cell per 20 crypts). These cells did not have Paneth cell morphological features, such as containing secretory granules, and likely represent intra-epithelial lymphocytes (figure 3.17). Furthermore, the number of these lysozyme-positive colonic crypt epithelial cells did not differ between healthy controls and patients with IBD-associated colitis of any degree of histological inflammation (Kruskal-Wallis test $p=0.536$).

3.4 Figures

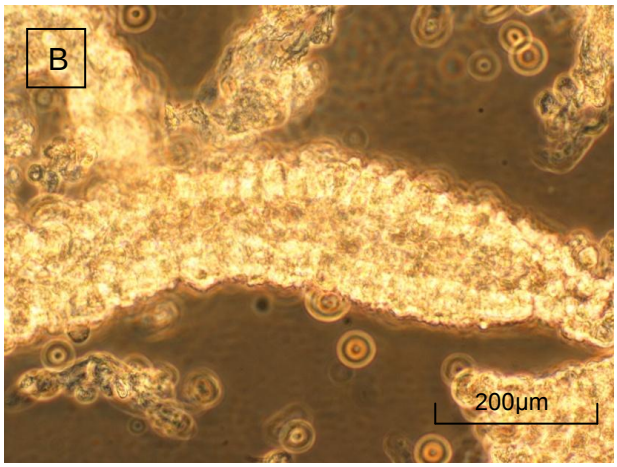

Figure 3.1 EDTA/DTT treatment releases epithelial cell crypts from the underlying lamina propria. Mucosal samples were treated with EDTA/DTT in a shaking water bath for 30 minutes at 37^{o}C. Following vigorous shaking, intact epithelial crypts were released from the underlying mucosa and visible in solution using light microscopy at low power (X10, A) and high power (X40, B) magnification.

DDT, dithiothreitol; EDTA, ethylenediaminetetraacetic acid.

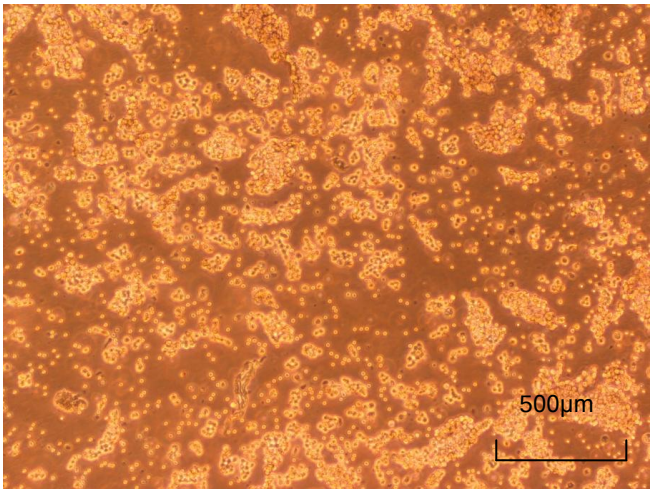

Figure 3.2 Isolated intestinal crypt cells disaggregate into individual cells following pancreatin treatment. Isolated intestinal epithelial crypts were treated with pancreatin for 90 minutes following whole crypt isolation, and viewed under light microscopy. Cells were seen either individually or in small clumps. Clumped cells were further disaggregated by passing the cell suspension through a 21-gauge needing using a 10mL syringe.

DDT, dithiothreitol; EDTA, ethylenediaminetetraacetic acid.

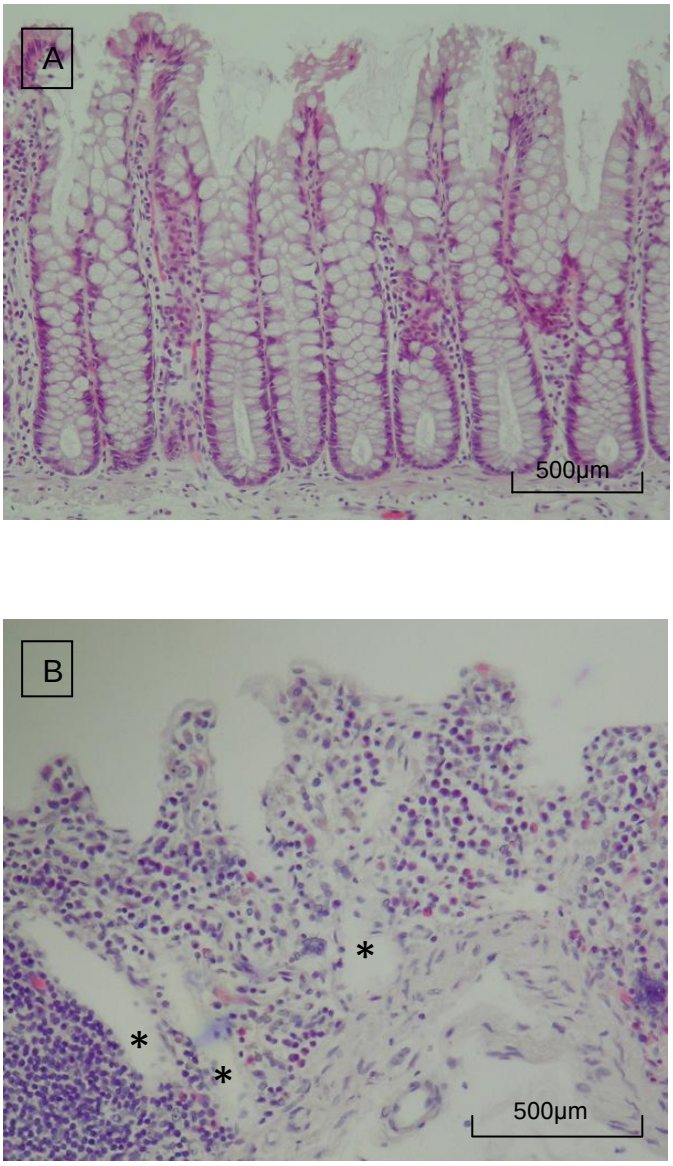

Figure 3.3 EDTA/DTT treatment results in the loss of surface epithelial crypts from large intestine mucosal tissue. Colonic mucosal samples before and following EDTA/DTT treatment were formal-fixed and paraffin-embedded before cutting into 5µm thick sections and mounting on glass microscopy slides at low power (x10). Slides were stained with haematoxylin and eosin. Untreated colonic mucosa (A) shows an intact epithelium with visible crypt epithelial cells. Following EDTA/DTT treatment (B) there is loss of epithelial crypt cells from the underlying lamina propria. Empty structures previously containing crypts were identified (*).

DDT, dithiothreitol; EDTA, ethylenediaminetetraacetic acid.

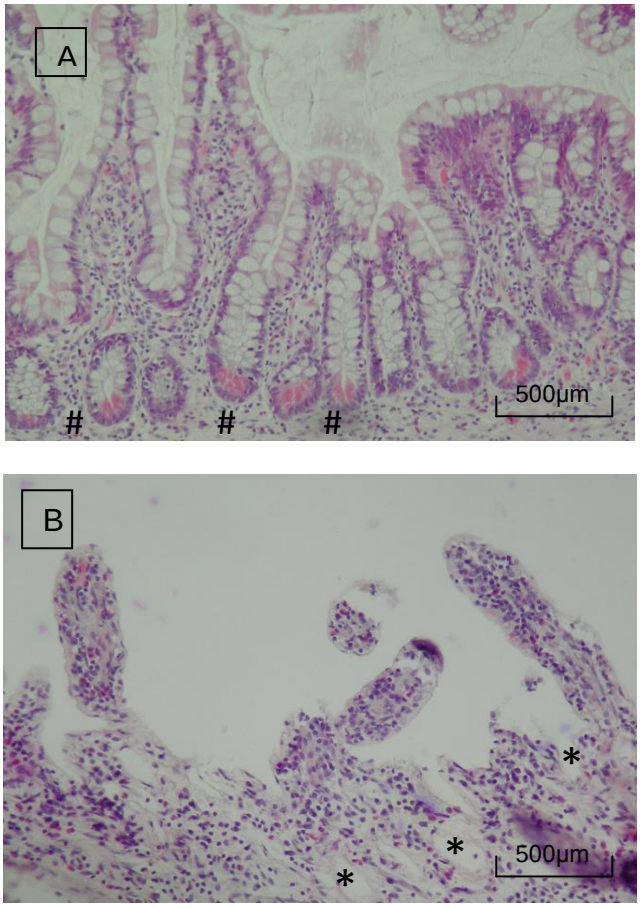

Figure 3.4 EDTA/DTT treatment results in the loss of surface epithelial crypts from small intestine mucosal tissue. Mucosal samples from the small intestine before and following EDTA/DTT treatment (three 30 minute incubations) were formal-fixed and paraffin-embedded before cutting into 5µm thick sections and mounting on glass microscopy slides at low power (x10). Slides were stained with haematoxylin and eosin. Untreated colonic mucosa (A) shows an intact epithelium with visible crypt epithelial cells. Following EDTA/DTT treatment (B) there is loss of epithelial crypt cells from the underlying lamina propria. Empty structures previously containing crypts were identified (*). In untreated samples, eosin-staining Paneth cells are seen at the base of the small intestinal crypts (#).

DDT, dithiothreitol; EDTA, ethylenediaminetetraacetic acid.

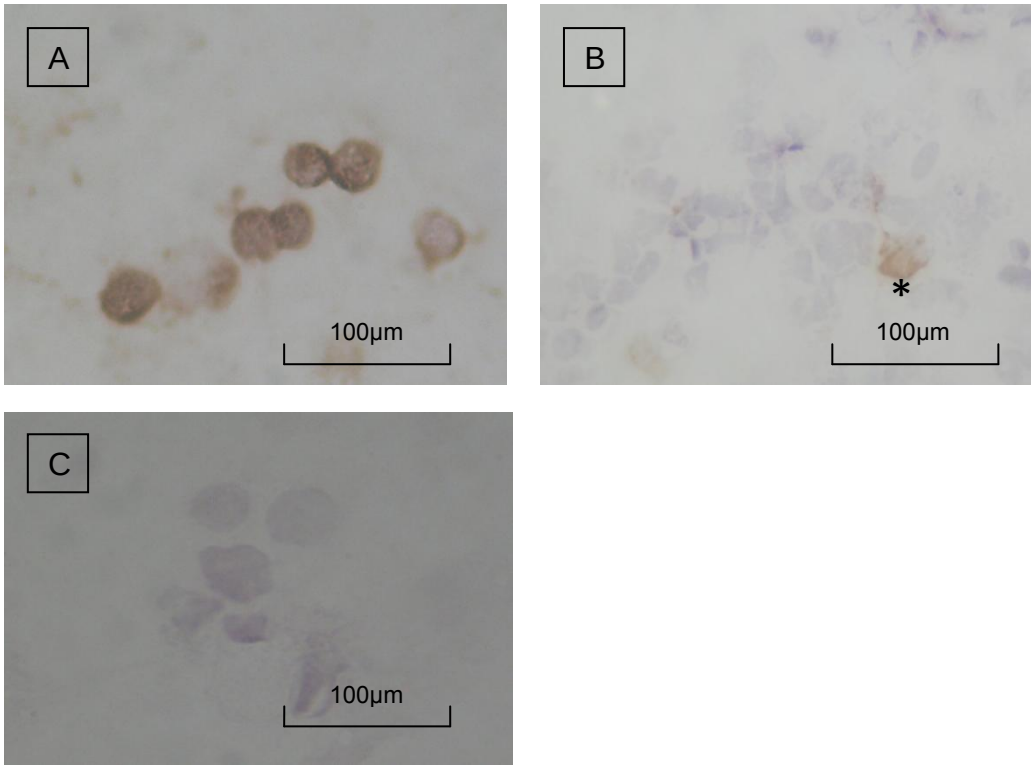

Figure 3.5 Isolated crypt cells express the epithelial-specific marker BerEP4, but not the haematopoietic marker CD45. Isolated intestinal epithelial cells were centrifuged onto cytospin slides and labelled with (A) anti-BerEP4 monoclonal antibody, (B) anti-CD45 monoclonal antibody or (C) negative control (no primary antibody). Primary antibody colorimetric detection was undertaken using 3,3'-diaminobenzidine (DAB) substrate followed by haematoxylin counter-staining. Isolated crypt cells were strongly positive for the epithelial-specific BerEP4, but negative for the haematopoietic marker CD45. However, the occasional CD45 positive staining crypt cell was noted (*, panel B). The absence of staining on the negative control slides excluded non-specific binding of the secondary antibody or avidin/biotin-conjugated horseradish peroxidise enzyme complex.

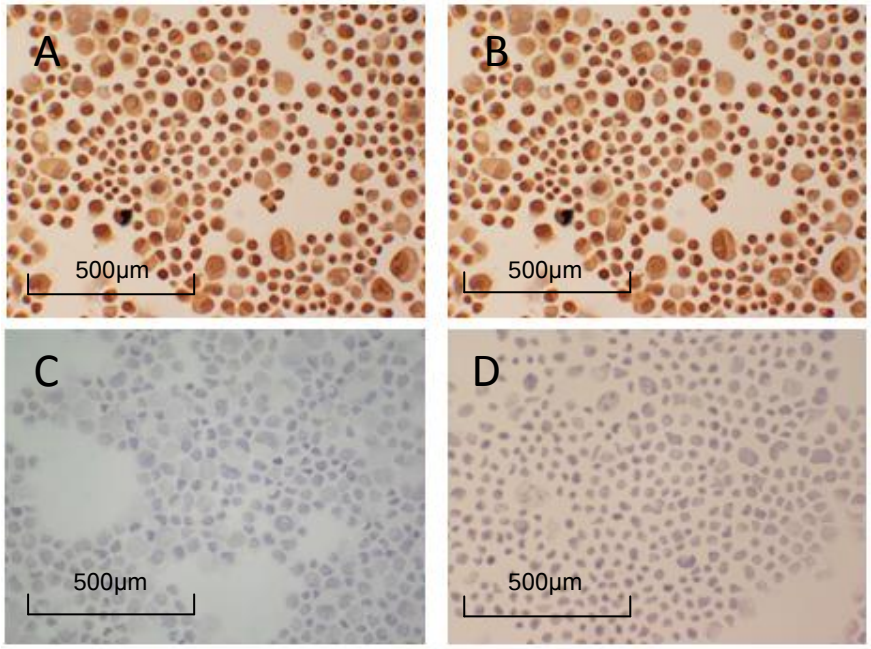

Figure 3.6 T84 cells express the epithelial-specific markers pan-cytokeratin and BerEP4, but not the haematopoietic marker CD45. Cells from the T84 intestinal epithelial cancer cell line were centrifuged onto cytospin slides and labelled with monoclonal antibodies to (A) human pan-cytokeratin, (B) BerEP4, (C) CD45, or (D) negative control (no primary antibody). Primary antibody detection required the 3,3'-diaminobenzidine substrate and haematoxylin counter-staining.

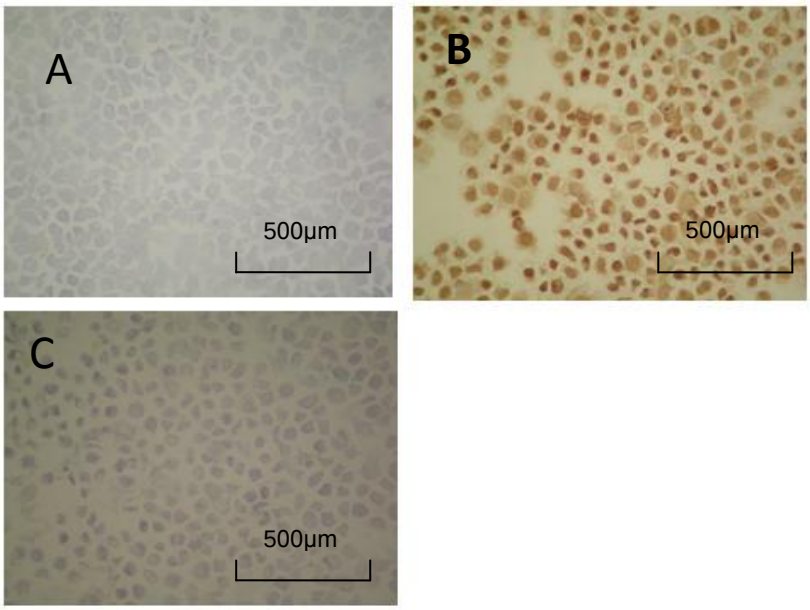

Figure 3.7 THP-1 cells express the haematopoietic marker CD45, but not the epithelial-specific marker BerEP4. Cells from the THP-1 monocyte cell line were centrifuged onto cytospin slides and labelled with monoclonal antibodies to (A) BerEP4, (B) CD45 or (C) negative control (no primary antibody). Primary antibody detection required the 3,3'-diaminobenzidine substrate followed by haematoxylin counter-staining. THP-1 cells were positive for the haematopoietic marker CD45, but negative for the epithelial-specific marker BerEP4.

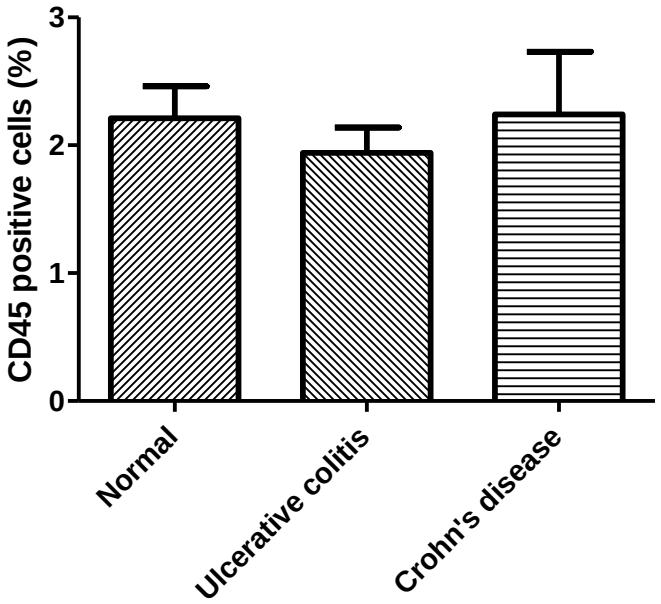

Figure 3.8 Isolated crypt cells from healthy controls and patients with inflammatory bowel disease include similar proportions of CD45-positive cells. Mucosal samples from healthy controls and patients with inflammatory bowel disease were treated with EDTA/DTT to release epithelial crypts which were subsequently disaggregated into individual cells using pancreatin. Isolated cells were centrifuged onto cytospin slides and stained with an anti-CD45 monoclonal antibody, before detection using 3,3'-diaminobenzidine substrate. Cells were counter-stained with haematoxylin. CD45-positive-staining cells were counted per hundred cells using light microscopy.

DTT, dithiothreitol; EDTA, ethylenediaminetetraacetic acid

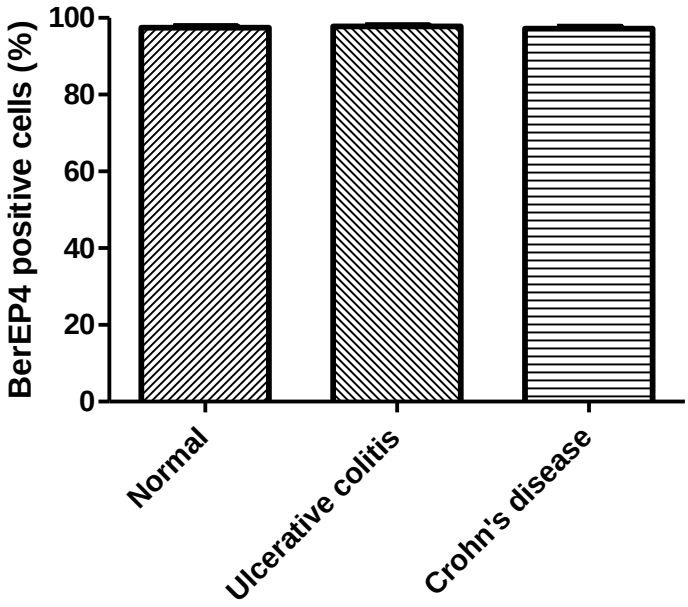

Figure 3.9 Isolated crypt cells from healthy controls and patients with inflammatory bowel disease include similar proportions of BerEP4-positive epithelial cells.
Mucosal samples from healthy controls and patients with inflammatory bowel disease were treated with EDTA/DTT to release epithelial crypts which were subsequently disaggregated into individual cells using pancreatin. Isolated cells were centrifuged onto cytospin slides and stained with an anti-BerEP4 antibody, before detection using 3,3'-diaminobenzidine substrate. Cells were counter-stained with haematoxylin. BerEP4-positive cells were counted per hundred cells using light microscopy.

DTT, dithiothreitol; EDTA, ethylenediaminetetraacetic acid

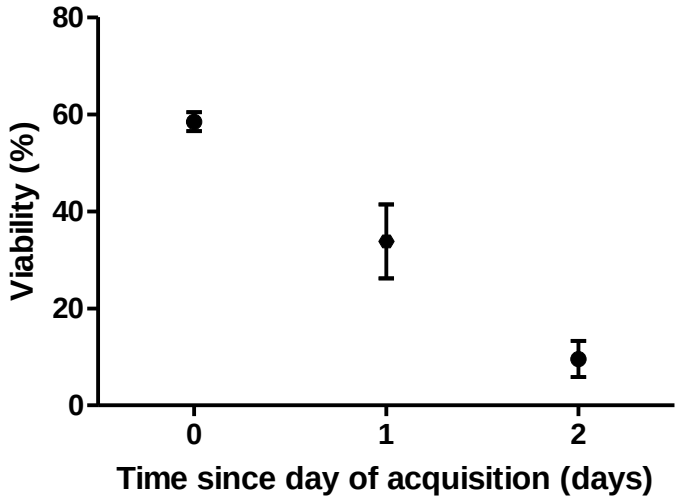

Figure 3.10 Intestinal crypt cell viability declines linearly with time following isolation from the underlying lamina propria. Intestinal crypt cells were isolated and suspended in cell culture medium for up to 48 hours. Cell viability was assessed by percentage trypan blue exclusion daily for 48 hours. A strong linear relationship between time since isolation and percentage cell viability was observed (R^2=0.9944, p=0.0033). Dots represent mean cell viability and bars represent standard error.

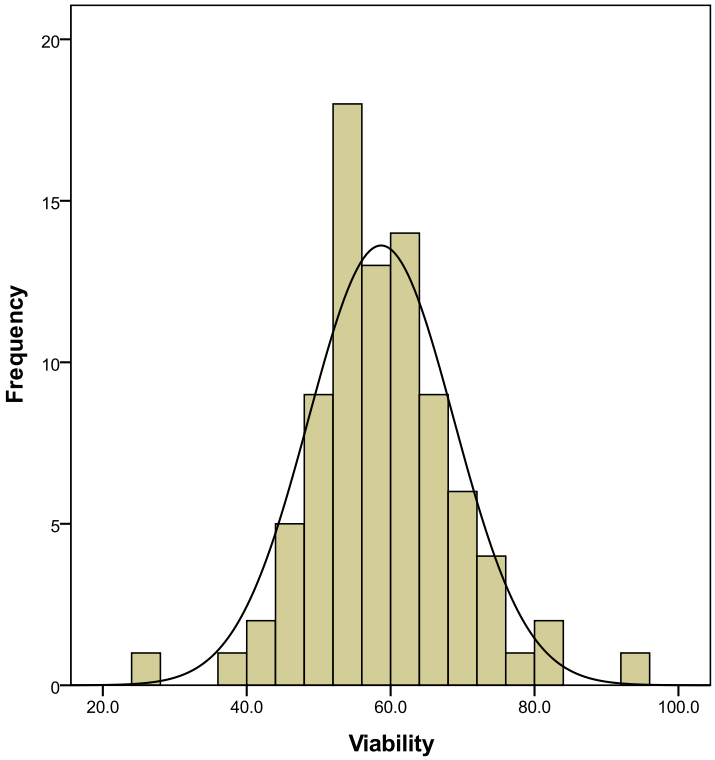

Figure 3.11 Isolated crypt cell viability following acquisition is normally distributed. Intestinal epithelial cells were isolated and disaggregated before analysis of cell viability using trypan blue exclusion. Cell viability at the time of isolation was plotted on a frequency-distribution histogram and shown to be normally distributed (Kolmogorov-Smirnov test p=0.165). The normal curve is shown as a black line against the frequency distribution bars.

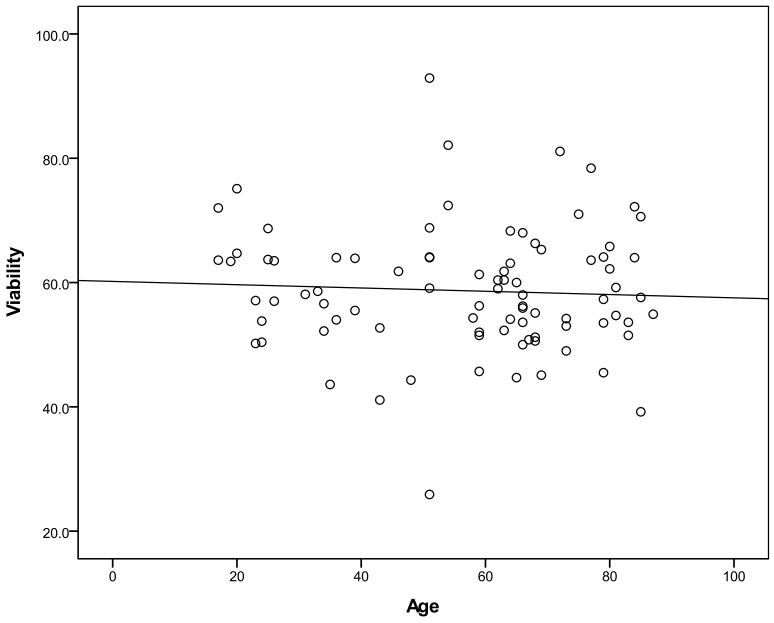

Figure 3.12 Initial intestinal crypt cell viability is independent of sample subject age. Intestinal epithelial cells were isolated and disaggregated before being suspended in medium. Cell viability assessed using trypan blue exclusion at the time of acquisition and plotted against subject age. Age did not determine initial cell viability (R^2=0.003, p=0.626).

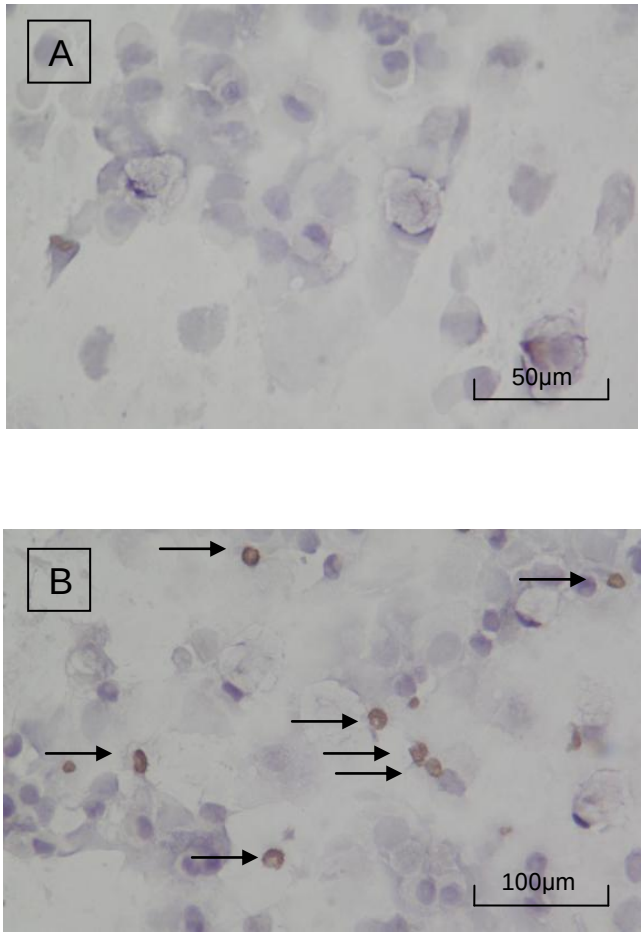

Figure 3.13 A sub-population of isolated normal small intestinal crypt cells are lysozyme-positive. Cytospin slides of freshly isolated and disaggregated small intestinal cells were labelled with (A) no-antibody control serum or (B) a polyclonal antibody to lysozyme. Slides were sequentially incubated with a biotinylated secondary antibody, an avidin/biotin-conjugated horseradish peroxidise enzyme complex and the 3,3'-diaminobenzidine (DAB) substrate. Slides were counter-stained with haematoxylin. Occasional brown-staining lysozyme-positive Paneth cells were seen at low power light microscopy (arrows, B).

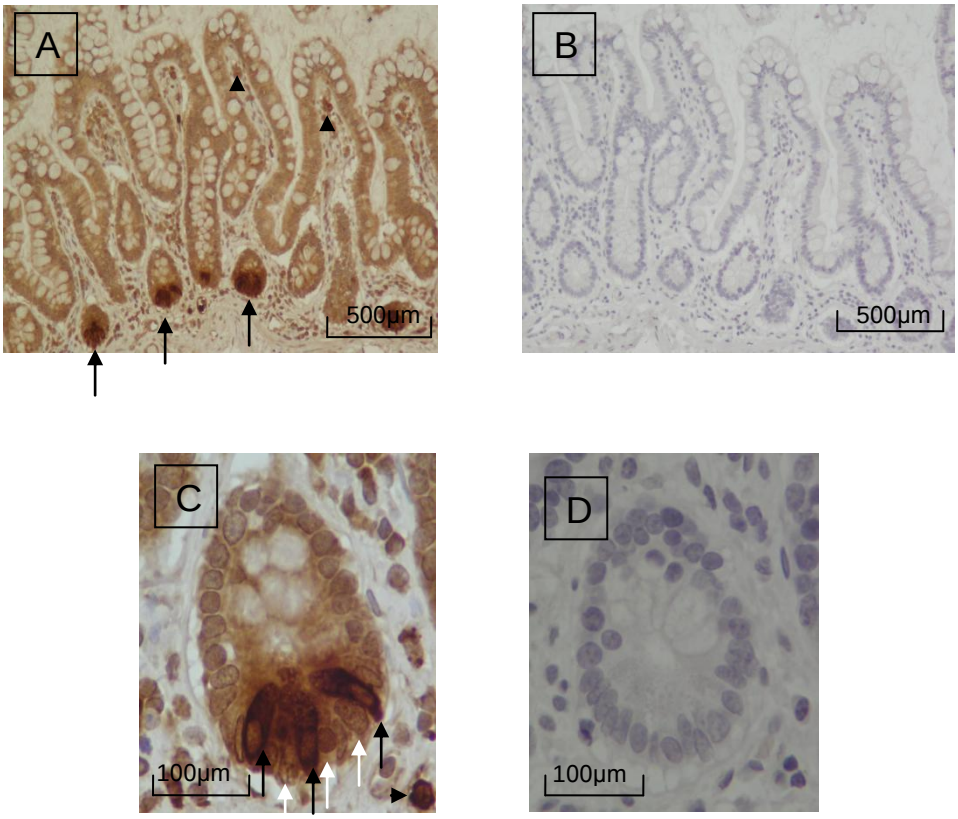

Figure 3.14 Normal small intestinal crypt base epithelial cells express intracellular lysozyme. Whole bowel sections from the small intestine were formalin-fixed and paraffin-embedded before being sectioned and stained with (A and C) an anti-lysozyme antibody or (B and D) no-antibody control serum, and subsequently developed using 3,3'-diaminobenzidine (DAB) substrate and counter-staining with haematoxylin. Dark brown-staining lysozyme-positive cells were observed in both the base of the crypts (arrow) and in scattered cells of the lamina propria (arrowhead) (A, x10 magnification), but not on the no-antibody control slide (B). Weaker, non-specific staining of epithelial cells was noted (A and C). At a higher magnification (x40), dense lysozyme-staining crypt base cells (with cytoplasmic secretory granules, black arrow) were identified, interspersed between lysozyme-negative crypt base cells (white arrow, C). Lysozyme-positive lamina propria cells were also identified (arrowhead). A high power negative-control slide demonstrated no staining (D).

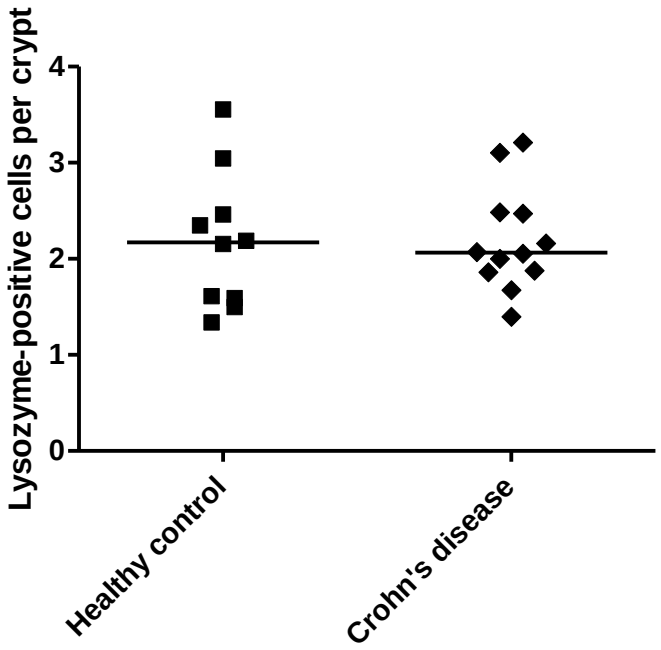

Figure 3.15 The number of lysozyme-positive crypt epithelial cells in small intestine crypts from healthy controls and patients with Crohn's ileitis is similar. Whole bowel sections from the small intestine of healthy controls and patients with Crohn's ileitis were formalin-fixed and paraffin-embedded, before 5µm sectioning and staining with an anti-lysozyme antibody. The number of lysozyme-positive cells per crypt was counted by light microscopy on at least five high powered fields per slide.

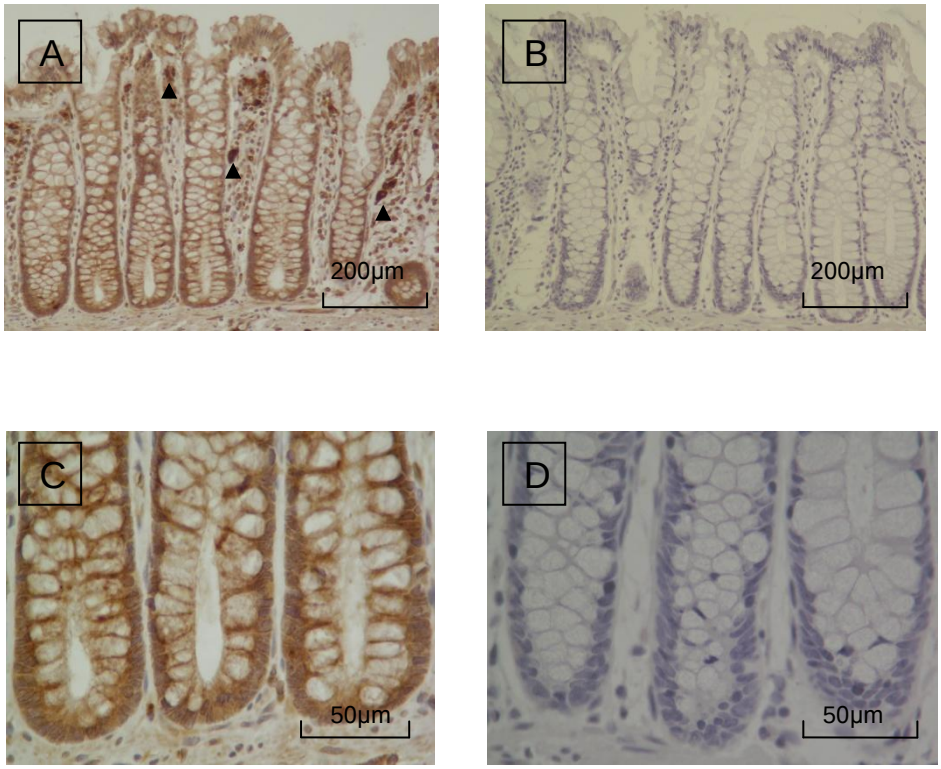

Figure 3.16 Normal large intestinal crypt base epithelial cells do not express lysozyme. Whole bowel sections from the large intestine were formalin-fixed and paraffin-embedded before being sectioned and stained with (A and C) anti-lysozyme antibody or (B and D) no-antibody control serum, and subsequently developed using 3,3'-diaminobenzidine (DAB) substrate and counter-staining with haematoxylin. Lysozyme-positive cells were not observed in the epithelium, but scattered lysozyme-positive cells were observed in the lamina propria (arrowheads) (A, x10 magnification). Weak, non-specific brown staining of epithelial cells is noted (A and C). At a higher magnification (x40), crypt base cells are lysozyme-negative (C). Low and high power negative-control slides demonstrated no lysozyme staining (B and D).

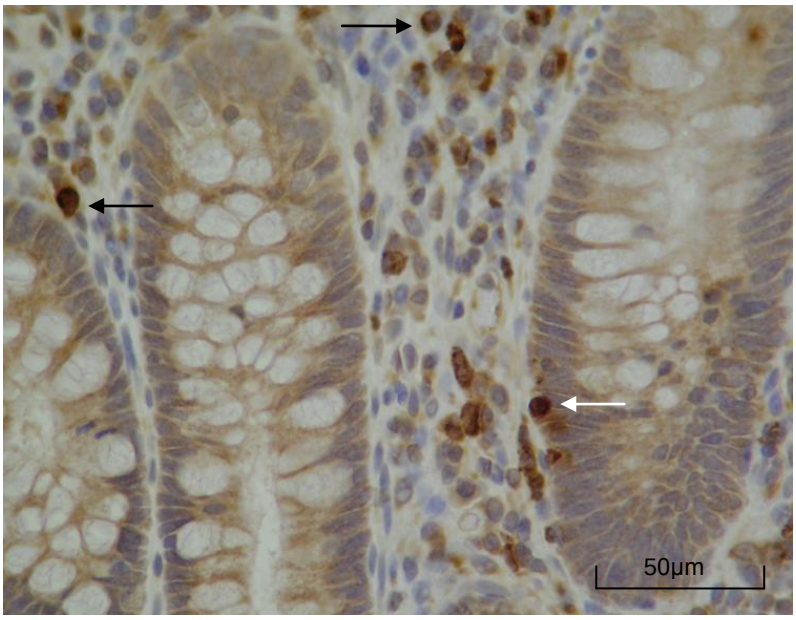

Figure 3.17 Colonic crypt base epithelial cells from inflamed ulcerative colitis contain lysozyme-positive cells without Paneth cell morphology. Whole bowel sections from the large intestine were formalin-fixed and paraffin-embedded before being sectioned and stained with anti-lysozyme antibody, and subsequently developed using 3,3'-diaminobenzidine (DAB) substrate and counter-staining with haematoxylin. Occasional (less than one cell per 20 crypts) lysozyme-positive cells were observed in the epithelium (white arrow) at high power. These did not contain secretory granules and morphologically resembled lamina propria mononuclear cells (black arrow).

3.5 Discussion

The epithelium of the intestine has the fascinating ability to rapidly replenish itself over a period of five days due to the population of stem cell which reside at the base of the crypts of Lieberkühn (174). A key to the survival of intestinal epithelial cells is their interaction with the underlying basement membrane, which comprises structural proteins and growth factors. Attachment to this basement membrane is vital for cell viability and IEC rapidly undergo apoptosis when detached from this underlying structure (172). There is a need to advance our understanding of the biology of the ISC if the therapeutic potential of stem cell treatment in the intestinal tract is to be realised.

Attempts at long term *in vitro* culture of intestinal epithelial cells have proved challenging (226, 227). However, the long term culture of murine intestinal epithelial organoids has recently been reported using techniques which are both dependent (236) and independent (237) of stromal niche cells. Such long term cultures may well lead to expansion in our understanding of stem cell biology, but it is unclear if they will be useful in experimentation into the functional state of epithelial cells in conditions such as inflammatory bowel disease. To understand the functional role of IEC in gut inflammation, primary cells from patients with IBD are required to be isolated and characterised rapidly *ex vivo*.

In this chapter, primary crypt intestinal epithelial cells were isolated using a technique described by Whitehead *et al.* (229) and modified for use in our laboratory (210). During this technique, treatment with EDTA/DTT results in the detachment and isolation of intact epithelial crypts in solution. Thereafter, crypt cells are disaggregated into individual cells using porcine pancreatin. This results in a high crypt yield due to complete loss of crypt cells from the underlying lamina propria. Moreover, villus/luminal IEC could be largely discarded, allowing the crypt cells to be the main isolated cell type.

Consistent with previous reports demonstrating that IEC undergo rapid apoptosis following removal from the underlying basement membrane, it was shown that isolated crypt cell viability declines linearly with time. Almost all cells were non-viable within 48 hours of isolation and maintenance in cell culture medium. The mean viability of isolated epithelial cells was 58.5% as assessed immediately after isolation. To ensure consistency of results, all specimens were processed identically and all down-stream experiments were performed immediately following crypt cell isolation.

Interestingly, the viability of isolated crypt cells was not dependent on patient baseline demographics, such as age, medical history or drug treatment using regression analysis. Likewise cell viability was not influenced by acquired mucosal tissue weight, underlying diagnosis (healthy control, CD or UC), severity of inflammation using the scoring system reported by Riley *et al.* (235) or whether the sample was of small or large bowel origin. It is unknown if the rates of apoptosis following isolation differ amongst specimens from patients with different baseline demographics, diagnoses or severity of underlying inflammation. There was no significant difference in cell viability (using trypan blue exclusion) amongst the groups studied.

It was important to confirm that the isolated crypt cells represented a population of epithelial cells without significant numbers of contaminating non-epithelial cells. In normal healthy mucosa, intra-epithelial lymphocytes are visualised between epithelial cells at a frequency of up to 5 lymphocytes per 100 epithelial cells (215). Therefore, using EDTA/DTT treatment to isolate whole crypts, it would seem unlikely that this technique would yield a population of pure epithelial cells, but rather it would isolate a cell population containing a small proportion of non-epithelial cells. Moreover, neutrophil infiltration of the epithelium (cryptitis) and of the crypt lumen (crypt abscess) are characteristic features in the mucosa of patients with IBD and commonly observed in addition to the increased numbers of these cells present in the underlying lamina propria (215). Since both lymphocytes and neutrophils are known to

express TLR, it was crucial to investigate if the EDTA/DTT treatment resulted in the isolation of large numbers of these cells in addition to the epithelial cells isolated from inflamed mucosa. If this were the case, any differential expression of TLR in the isolated cells as a whole could be the result of non-epithelial (haematopoietic) cell contamination rather than differential expression in the epithelial cell population itself.

To address this question, monoclonal antibodies directed against epithelial (BerEP4) and haematopoietic (CD45) markers were chosen and target specificity tested using human cell lines of epithelial (T84) and haematopoietic (THP-1) origin. Thereafter, cytospin slides prepared form healthy controls and patients with IBD were shown to comprise statistically similar numbers of CD45-positive cells (1.9-2.2%). Notably, this was at the reported frequency of less than 5 CD45-positive cells per 100 epithelial cells in healthy mucosa. Likewise, the numbers of BerEP4-positive (epithelial) cells were statistically similar on cytospin slides from healthy controls and patients with IBD (97.2-97.8%). This suggests that the current crypt cell isolation technique using EDTA/DTT yields a population of almost exclusively epithelial cells and which includes approximately two haematopoietic cells per 100 isolated cells. More importantly, cellular isolates from patients with active IBD are not abundant with haematopoietic cells and, therefore, samples from healthy controls and IBD patient groups are comparable.

Paneth cells are found in the base of the crypts of the small bowel and secrete the antimicrobial peptide lysozyme (108). Although their expression is almost universal in the bases of the crypts of the small bowel, Paneth cells are rarely present in the normal large intestine. However, Paneth cell metaplasia is a recognised consequence of chronic epithelial cell damage and is occasionally observed in the epithelium of the large intestine in IBD (215). Crucially, Paneth cells have been reported to sense bacteria via toll-like receptor signalling (238). Therefore, it was possible that Paneth cell metaplasia in the large intestine,

or Paneth cell expansion in the small intestine, could account for differential expression of TLR in isolated crypt cell preparations.

To address this issue, cytospin slides of disaggregated crypt cells and slides of FFPE whole bowel sections were stained with a polyclonal antibody to lysozyme. Staining of cytospin slides from healthy small intestine and Crohn's ileitis demonstrated lysozyme-positive cells which are likely to represent Paneth cells. However, due to the method of cytospin slide preparation (i.e. adherence of isolated cells into a glass slide by high speed centrifugation) the cellular morphology can be disturbed and it was not possible to definitively characterise the lysozyme-positive cells as Paneth cells on morphology alone. Importantly, cytospin slides from healthy large intestine and patients with IBD-associated colitis did not demonstrate lysozyme-positive cells.

Immunohistochemical staining of FFPE whole bowel sections resulted in weak non-specific staining of epithelial cells despite numerous attempts to optimise the protocol and minimise this staining, including the use of longer serum, avidin and biotin blocking steps, and a shorter DAB substrate development step. Despite this weak staining, intense staining of cells with a typical granular Paneth cell appearance was demonstrated. These lysozyme-positive Paneth cells were easily identifiable and located exclusively in the bases of the small intestine crypts. These cells were also strongly eosin-staining on H&E slides, another feature of Paneth cells. When the numbers of positive-staining cells were counted in the normal small intestine epithelium, approximately 2 lysozyme-positive cells per crypt were identified. Statistically similar numbers of lysozyme-positive cells were identified in the crypts of samples from patients with inflamed small intestinal Crohn's disease. This suggests that there is no significant expansion in the number of Paneth cells in the mucosa of Crohn's ileitis that would account for any differential TLR expression.

Lysozyme-positive cells with typical Paneth cell morphology were not observed in whole bowel sections of colonic tissue. Lysozyme-positive cells without secretory granules were rarely observed in the crypts of the large intestinal epithelium of healthy controls and patients with IBD at a frequency of less than one lysozyme-positive cell per twenty crypts. The number of these intra-epithelial lysozyme-positive cells was statistically similar in sections from patients with colitis compared to healthy controls. It is likely that these cells represent intra-epithelial lymphocytes, which are reported to express lysozyme (239). Indeed, lysozyme-positive mononuclear cells were present in the lamina propria of the small and large intestine regardless of the degree of inflammation, and had similar morphological appearance to intra-epithelial lysozyme-positive mononuclear cells in the lamina propria. In many specimens, no lysozyme-positive cells were identified in entire colonic tissue sections, both for healthy controls and patients with IBD.

These data suggests that the reported occurrence of Paneth cells in the inflamed epithelium of patients with colonic IBD is unlikely to significantly contribute to changes in TLR expression in colonic crypt epithelial cell isolates from patients with inflammatory bowel disease.

In summary, treatment of mucosal specimens with ETDA/DTT and pancreatin results in the isolation and disaggregation of crypt intestinal epithelial cells which contain minimal numbers of non-epithelial cells and which can be identified by their lack of expression of the epithelial marker BerEP4. The viability of the isolated cells was approximately 60%. The number of CD45-positive haematopoietic cells was not increased in crypt cells isolated from inflamed specimens compared to healthy control specimens and the number of epithelial Paneth cells was not significantly increased as a result if mucosal inflammation. Therefore, ETDA/DTT and pancreatin treatment of mucosal samples is an effective method of isolating a population of crypt intestinal epithelial cells suitable for down-stream comparative analysis.

Chapter 4: Expression of toll-like receptors-2 and -4 mRNA in crypt intestinal epithelial cells in health and inflammatory bowel disease

4.1 Introduction

4.1.1 The expression of Toll-like receptors on human intestinal epithelial cell lines

The expression of Toll-like receptors in human IEC has been studied in both intestinal cancer cell lines and primary intestinal epithelial cells, although the majority of studies have characterised expression in the former. TLR4 has been the most extensively investigated TLR given its role in recognising LPS, the endotoxin associated with septic shock. Abreu reported Caco-2 HT-29 and T84 human cancer cell lines to be unresponsive to LPS (lack of IL-8 secretion and NF-κB luciferase activation) due to low TLR4 messenger RNA (mRNA) and protein expression and absence of the TLR4 accessory molecule MD-2 (89).

Conversely, the HT-29 and T84 cell lines have been reported to actively express TLR2/3/4 mRNA and surface TLR2 and TLR4 protein, though not CD14 mRNA or protein. TLR4 ligation results in activation of different components of the MAP kinase pathway in different cell lines, namely p42/44 in T84 and p38 in HT-29 cells suggesting functional receptors in these cell lines (232). A foetal small bowel cell line (H4 cells) has also been shown to express TLR2 and TLR4 at both the mRNA and protein level (240).

The cellular location of TLR expression has also been investigated. Flagellin has been demonstrated to stimulate TLR5-induced IL-8 production from confluent cultured and polarised T84 cells when applied to the basolateral membrane but not the apical membrane. Subsequently, TLR5 protein was demonstrated to reside only on the basolateral membrane (241). Following ligation, TLR2 and TLR4 receptors on confluent T84 cell cultures undergo basolateral scattering which results in apical hypo-responsiveness to subsequent apical stimulation (242). This may form part of the pathway for apical tolerance to bacterial antigens

in the gut. Intracellular cytoplasmic scattering of TLR2 and TLR4 following ligation has also been observed in SW480 cells (243).

The expression of TLR2 and TLR4 in particular depend on a number of factors in cultured cell lines. Firstly the cell line phenotype is a key factor in receptor expression. The colonic SW480 line expresses TLR4 mRNA and protein to a greater level than HT-29 and T84 cells lines, which in turn have greater expression than Caco2 and HCT116 lines. This was reported to be due to variations in TLR4 promoter regulation by DNA methylation and histone deacetylation in these cell lines (233). This may explain differential responses of these cell lines to TLR ligands (122). TLR expression in SW480 and Colo205 lines has been suggested to most closely resemble expression in primary human colonic IEC at the genomic level, although TLR expression is still variable and no similar study has compared luminal surface versus crypt cell position or investigated optimal cell line models for small bowel IEC (243).

It is generally accepted that TLR2 and TLR4 respond to extracellular ligands in humans, and that a cytoplasmic TLR2 or TLR4 location indicates cell immaturity. However it has been reported by Hornef *et al.* that a murine crypt cell line m-IC_{cl2} expresses peri-nuclear, cytoplasmic TLR4 and MD-2 proteins, and that co-localisation of LPS and TLR4 occurs adjacent to the Golgi organ (244) following clarithrin-mediated internalisation (245). Suzuki *et al.* report cytoplasmic staining of up-taken LPS in the human colonic epithelial cancer cell lines Colo205, HT-29 and SW480 with surface expression of TLR4 protein only observed in SW480 cells (246). *In vitro* IFN-γ was shown to augment LPS responsiveness and increase total TLR4 protein levels in Colo205 and HT-27 cells, but not to increase their surface TLR4 expression. This may suggest that Colo205 and HT-27 cells express intracellular TLR4 which responds to LPS only after IFN-γ-facilitated LPS uptake. By contrast, SW480 cells are primed to respond to extracellular LPS even in un-primed conditions (246).

To further investigate the role of TLR4 expression in differential cellular compartments, Latz *et al.* used the kidney cell line HEK293, which does not express TLR4, MD-2 or CD14, and transfected cells with fluorescently tagged TLR4, MD-2 and CD14 (247). Experiments showed continuous, rapid tracking of TLR4, MD-2 and CD14 to and from the plasma membrane and Golgi. Critically, MD-2 but not CD14 was shown to be required for LPS-mediated signal transduction and this pathway also required translocation of MyD88 to the plasma membrane rather than the Golgi. Both the use of a non-internalisable stimulatory monoclonal anti-TLR4 antibody and the Golgi disrupting agent Brefeldin A did not reduce LPS-mediated signal transduction intensity, suggesting that it is the plasma membrane-bound TLR4 that is site of inflammatory signal transduction whereas the Golgi directs TLR4 cellular trafficking (247). Whether this is true for primary IEC remains unclear.

In support of the more conventional view of surface TLR2 and TLR4 expression, surface TLR4 protein was reported by Takahashi *et al.* in SW480, T84 and HT-29 cells (233) and by Otte *et al.* in SW480 cells (243). Likewise surface TLR2 protein has been reported in low levels by Melmed *et al.* in Caco2 and T84 cells (231) and by Otte *et al.* in SW480 cells (243). Intracellular TLR4 has not been reported in primary human epithelial cells and it is unclear if the observations by Hornef *et al.* and Suzuki *et al.* bear any resemblance to human crypt IEC.

Secondly, the maturation of the cell lines is critical in TLR expression. Cario showed that mature T84 cells express surface TLR2 and TLR4 protein while immature cells retain these in the cytoplasm (242). Butyrate (a short chain fatty acid produced in the human gut by the epithelial-adjacent commensal flora) induces maturation and differentiation of epithelial cells and results in loss of LPS responsiveness (122). Similarly prior treatment of HT-29 cells with butyrate results in loss of LPS-mediated, TLR4-dependent IL-8 production due to down-regulation of TLR4 mRNA and protein expression (248). Interestingly, the harvesting of sub-confluent cultures of HT-29 cells resulted in maintenance of LPS responsiveness whereas

culture to full confluence led to a loss of TLR4 signalling by similar mechanisms (248). It is possible that similar processes occur in the human gut as cells differentiate and migrate along the small bowel crypt-villous and large bowel crypt-luminal axes.

Thirdly, cellular location along the crypt-villous axis influences TLR expression. Crypt IEC internalise peptidoglycan (PGN) which co-localises with PGN recognition protein-3 (PGLYRP-3) and is held within an intracellular compartment before being subsequently exocytosed along the basolateral membrane. This was not observed in non-crypt IEC (249). The enhanced expression of TLR4 in crypt cells versus luminal cells would further support the concept of down-regulation of extracellular TLR with maturation (246). TLR4 and MD-2 protein has been shown to be localised to the crypt IECs in mice (250) and a murine crypt cell line responds to LPS (244, 245).

Fourthly, the expression of TLR may be mediated by the abundance of certain ligands, leading to receptor down-regulation and tolerance. Otte *et al.* showed that SW480, Colo205 and T84 cells were responsive (by the production of IL-8) to exposure to lipoteichoic acid (LTA), LPS and Gram positive (*Staphylococcus aureus*) and Gram negative (*Escherichia coli*) bacteria. Pre-incubation with these ligands blunted subsequent TLR- and IL-1-mediated responses which both signal through the common TIR domain, but not TNF-α-mediated responses which have a different signalling cascade (243). Hypo-responsiveness was shown to be due to increased cytosolic expression of TLR2 and TLR4 protein and up-regulation of TOLLIP mRNA and protein rather than by altered expression of total TLR2, TLR4, MyD88, IRAK molecules or TRAF6 (243). To the contrary, it has been reported that pre-incubation with LPS and IL-1 does not tolerise responsiveness to either ligand in HT-29 or Caco-2 cells (122). Apical pre-stimulation of polarised HCA-7 cells with CpG-ODN, a TLR9 ligand, resulted in loss of subsequent response to TLR3, 5 and 9 ligands, whereas apical pre-stimulation with TLR3 and 5 ligands did not induce this loss of response (251).

This may be a contributory mechanism responsible for IEC tolerance to antigens expressed by the intestinal flora.

Furrie *et al.* showed a rather variable response in differing cell lines to various TLR ligands and bacterial co-cultures. Caco-2 cell TLR expression was uninfluenced by bacterial flora co-culture. However, HT-29 cells show increased TLR2 and TLR3 mRNA expression in response to Gram positive organisms but not individual TLR ligands, whereas TLR4 was up-regulated by *Enterococcus faecalis* and lipid A but down-regulated by *Escherichia coli*. TLR1 was up-regulated only by poly I:C (252). Nandakumar *et al.* showed that HT-29 and T84 cells produce mRNA for TLR4 in response to *Vibrio cholerae* and *Salmonella typhi* and down-regulated TLR5 in response to *Vibrio cholerae* and *enterohaemorrhagic Escherichia coli*, with micro-organism also reducing TLR9 expression (253). How these *in vitro* observations relate to the *in vivo* state in humans is unclear.

Finally, cytokine exposure influences expression of TLR. TNF-α, IFN-γ and IFN-α up-regulate TLR4 and MD-2 mRNA to a variable degree, especially in HT-29 more than T84 cells (154). Mueller *et al.* reported that the T_{H2} cell cytokines IL-4 and IL-13 down-regulate TLR3, TLR4 and MD-2 mRNA, whereas TLR2 and TLR5 mRNA were unaffected in a variety of human cell lines. In contrast, the T_{H1} cell cytokine IFN-γ up-regulates TLR2-5 and MD-2 mRNA and TLR4 protein (155).

In summary, it is clear that the use of human cell lines can yield a significant amount of data regarding the expression, location and function nature of TLR in IEC. However, the variability of differentiation, anatomical origin and extracellular environment during *in vitro* studies, in addition to the fact that these cells are cancer cell lines, limits the applicability of experimentation in these circumstances to cellular behaviour in human inflammatory disease. This has led to work on primary epithelial cells.

4.1.2 The expression of Toll-like receptors on human primary intestinal epithelial cells

The literature on the expression of TLR in primary IEC is sparse. EDTA-isolated primary human colonic IEC have been shown to express mRNA for TLR1-9 but not TLR10 and with variable TLR7 expression (243). Böcker *et al.* investigated dispase-isolated primary epithelial cells and reported consistent expression of TLR4 and MD-2 mRNA with more variable TLR2 mRNA expression (122). Conversely, Abreu *et al.* found low expression of TLR4 mRNA and no MD-2 mRNA in healthy subjects using laser capture microdissection (154).

Immunohistochemical analysis of colonic biopsy samples from healthy subjects revealed expression of TLR2 and TLR4 protein mainly in the crypt IEC with gradual loss of expression along the crypt-luminal axis, whereas TLR3 protein was expressed mainly in the sub-apical cytoplasmic region in mature (luminal) colonocytes (252). Of note mononuclear lymphoid cells also stained for TLR2-4 protein and were localised to the peri-crypt region of the lamina propria.

Additionally, TLR1/2 and TLR1/4 heterodimers, but not TLR3 or TLR5, have been shown to be expressed in the crypts of healthy small and large bowel, and these cells display an enteroendocrine phenotype (254). Conversely, isolated specimens of primary colonic mucosa were shown to respond to the TLR5 ligand flagellin only when applied to the basolateral but not the apical surface using an Ussing chamber (255) which is similar to that seen in equivalent experiments of cultured IEC lines (241). Primary IEC have been shown to express TLR8 mRNA and protein particularly at the luminal surface (256), and TLR9 mRNA but not protein (257).

TLR2 and TLR4 proteins are expressed in the basolateral compartment of IEC from foetal small bowel, particularly in the crypt rather than villous region (240). Wolfs *et al.* report the intracellular expression of the TLR4 accessory protein MD-2 in Paneth cells of small bowel crypts in term infants and adults and it was postulated that this represented a role as a

locally secreted anti-LPS peptide (258). The observation that MD-2 is not expressed in premature infants implies that the immature bowel lacks the ability to sense colonic bacteria which may predispose to neonatal conditions like necrotising enterocolitis (NEC) which is thought to be an abnormal TLR-driven inflammatory response to the intestinal flora (259).

4.1.3 The expression of Toll-like receptors in inflammatory bowel disease

The epithelial cell expression of various TLR has been studied in the context of IBD. Cario and Podolsky showed immunohistochemically that TLR2 and TLR4 are minimally expressed in health and, although active ulcerative colitis and Crohn's disease did not influence TLR2 expression, TLR4 was significantly up-regulated in both diseases regardless of disease activity. Interestingly, TLR4 was located basolaterally in UC and apically in CD. TLR3 was expressed in healthy controls and significantly down-regulated in CD but not UC. Finally, TLR5 was expressed throughout the small bowel villous and large bowel luminal cells (but not in the crypt cells) and expression did not differ from controls in any disease state (260). To the contrary, in active UC Stanislawowski *et al.* report reduced *mucosal* TLR5 mRNA, by quantitative RT-PCR, and reduced cytoplasmic and basolateral TLR5 protein in epithelial cells by qualitative immunohistochemical staining (261).

Hausmann *et al.* did not detect TLR2 or TLR4 protein in epithelial cells of colonic resection specimens using immunohistochemistry and, although they report a small number of TLR2 and TLR4 protein positive cells in active IBD, these were identified as macrophages restricted to the peri-crypt region of the LP which were absent in healthy tissue (262). In a smaller study involving genomic expression Naik *et al.* showed qualitative, detectable TLR2 expression regardless of disease state or activity but failed to detect TLR4 mRNA in healthy or diseased IEC, though TLR4 mRNA was detectable in LPMC in active colonic IBD (263). However, the small bowel lamina propria was not examined and therefore conclusions about LPMC in the small intestinal cannot be made. Furthermore this study did not assess TLR protein expression in any cell type. Melmed *et al.* demonstrated TLR1, TLR2 and TLR6

mRNA expression in laser capture microdissected IEC of healthy subjects using quantitative PCR and noted a reduction in mRNA expression in TLR1 but not TLR2 or TLR6 in active UC (231).

TLR8 mRNA is more highly expressed in EDTA-isolated IEC samples from active colonic IBD than inactive colonic IBD which in turn was greater than healthy epithelium (256). Interestingly TLR8 protein was only expressed in inflamed luminal IEC but not crypt cells and not in un-inflamed or healthy epithelium. Immunofluorescent staining for TLR8 varied between CD and UC, which a more diffuse intense staining in the former and more focal in UC. Sporadic cytoplasmic staining for TLR8 was only seen in inactive disease with the use of immuno-electron microscopy. Interestingly, TOLLIP mRNA expression was independent of intestinal inflammation (256).

Pedersen *et al.* demonstrated expression of TLR9 mRNA in EDTA-isolated colonic IEC samples from healthy controls and IBD patients using quantitative PCR, and although TLR9 protein was not detectable in healthy IEC using Western blotting, IEC from inflamed were not assessed for TLR9 protein (257). The authors suggested that TLR9 mRNA is down-regulated in active versus inactive colonic IBD, though this comparison was made using whole mucosal tissue rather than isolated epithelial cells, thus any changes in TLR9 expression may be explained by expression changes in resident LPMCs (shown in this study to express TLR9 mRNA).

Therefore the current evidence on the expression of TLR in epithelial cells in IBD remains conflicting and controversial. Specifically, both TLR2 and TLR4 have been shown to be up-regulated, unchanged and not expressed in epithelial cells in IBD. TLR3 and TLR5 are reported to be either unchanged or down-regulated depending on disease phenotype or publishing group. TLR1, TLR8 and TLR9 have single publications in this field and TLR7 has not been investigated in human IBD to date.

One of the interesting features of the current literature is that TLR2 and TLR4 appear to be expressed primarily in the crypt of the epithelium, with loss of TLR expression observed as cells migrate up the crypt towards the villi of the small intestine and luminal epithelium of the colon (240, 252). As discussed in sections 1.7 and 1.8, intestinal stem cells reside in the bases of these crypts of the small and large intestine. This region is referred to as the stem cell niche and comprises a variety of mesenchymal cells, including intestinal myofibroblasts, which regulation intestinal stem cell function through the secretion of intercellular messenger molecules (187). During intestinal inflammation, such as that seen in inflammatory bowel disease, there is often observed a dense inflammatory cell infiltrate surrounding the crypt bases, with further infiltration into the epithelium resulting in the formation of crypt abscesses and the distortion of the crypt architecture (215). Therefore, the epithelial crypt may play a key role in the pathogenesis of mucosal inflammation and for this reason intestinal epithelial cells of the crypt specifically were chosen to be studied.

The aim of this chapter was to characterise the expression of TLR2 and TLR4 mRNA from isolated primary crypt intestinal epithelial cells and to quantitatively investigate for any differential expression in IBD compared to healthy controls.

4.2 Methods

4.2.1 Gene expression profiling micro array using Ambion MessageAmp II® kit

4.2.1.1 Introduction

To further characterise the expression of toll-like receptors in the crypt epithelial cells of control subjects and to compare this to the expression in patients with inflammatory bowel disease, an initial RNA gene expression micro array was undertaken. This technique allows rapid qualitative confirmation regarding the expression of TLR1-10 messenger RNA in primary crypt epithelial samples derived from small and large bowel tissue samples. In addition, semi-quantitative assessment of gene expression in IBD patients relative to the expression in healthy controls is possible. Finally, the differential expression of intracellular molecules known to be important in the TLR signalling pathway can be analysed in control and IBD samples using this method.

4.2.1.2 Methodological overview

A two dimensional micro array is a solid material which assays a large amount of biological material. It requires a glass, plastic or silicon slide (the biochip) to which the nucleic acid probes are bound. It differs from a macro array, which binds the probe to a membrane not a solid material. A micro array consists of thousands of oligonucleotide probes (also called reporters), each corresponding to a different gene in the genome or genomic region of interest. The probes are arranged on a grid in columns and rows as known as spots (or features) and can easily be located by their unique grid reference location.

The probes are used to hybridise to target nucleic acid sample, either to complementary DNA (cDNA) or complimentary RNA (cRNA, also known as antisense RNA, aRNA), on the basis of their sequence homology. Detection of the probe-target hybridisation is achieved using fluorescent-, silver- or chemiluminescent-labelling of the target sequence to determine the relative abundance of the target molecule. DNA micro arrays can be used to measure

changes in expression levels, to detect single nuclear polymorphisms, or to genotype or re-sequence mutant genomes.

Micro array technology makes use of the binding of complementary nucleic acid sequences through the formation of hydrogen bonds between nucleotide base pairs (264). In a phenomenon similar to the binding of a primer to its DNA target sequence during PCR, the greater the sequence homology between the probe and the target sequence, the stronger the probe-target interaction between the two strands. Following this hybridisation process, non-bound and weakly bound targets can be easily washed away, leaving only complementary sequences bound to the probe and, therefore, bound to the micro array slide itself. Each gene feature on the slide consists of thousands of copies of the same identical probe and therefore the abundance of the labelled target sequence can be indirectly measured by quantifying the intensity of the signal from the labelling molecule.

The most common measurement of target abundance is relative gene expression, whereby the expression of cDNA or cRNA is compared under various experimental conditions (for example, by comparing absolute gene expression in manipulated cells to expression in control cells) or by comparing samples from patients with a particular disease with those of healthy control cases. It is possible to quantitatively measure absolute target sequence expression levels obtained using chips with inbuilt control spots with standardised signal intensity, although this method is less commonly used (264).

There are broadly two sub-types of micro array; spotted and oligonucleotide. In spotted micro arrays, the utilised probes are one of a number of possible molecules, such as oligonucleotides, cDNA molecules or small fragments of PCR products that correspond to specific mRNA sequences. The probes are synthesised prior to their deposition on the array surface and are then "spotted" onto the glass chip. This approach requires an array of fine needles controlled by a robotic arm that dips into wells containing DNA probes and then

deposits each probe at designated locations on the array surface. The resulting grid of probes represents the nucleic acid profiles of the prepared probes and is ready to receive complementary cDNA or cRNA targets derived from experimental or clinical samples. This technique can be produced in-house and customised for each experiment and is more cost effective.

By contrast, oligonucleotide micro arrays are produced by a manufacturing technique where the oligonucleotide sequence is built and printed directly onto the micro array surface, rather than depositing the pre-synthesised intact probe onto the chip. One example of such a micro array is the Affymatrix GeneChip^{TM} which uses photo-labile blocking groups attached to nucleotide triphosphate molecules, masking filters and lasers to synthesise (nucleotide by nucleotide) the required probes directly onto the chip surface (264) . Oligonucleotide micro arrays are usually commercially produced and are often more expensive than spotted micro arrays.

Micro array analysis can be undertaken using either a single- or two-channel protocol. In the single-channel method, target cDNA/cRNA is labelled with a single fluorophore and passed across the gene chip surface. The intensity of fluorescence at each spot relates to the relative expression of the corresponding gene. In this way, relative expression of several samples can be compared for differential gene expression or technique reproducibility.

Two-channel protocols involve labelling two samples with different fluorophores initially and then mixing the samples together prior to their passage across the gene chip surface. Specific computer software measures the intensity of each fluorophore at each spot and calculates the relative expression of each gene on the micro array chip. Two samples expressing a gene equally would be expected to show a relative expression of 1, and values greater or lesser than this would indicate differential expression. In practice there is a certain

amount of noise in the system and relative expressions of 0.5 to 2 are taken as representing the boundaries of equivalent gene expression (264).

The advantages of single-channel micro arrays are that an aberrant sample cannot affect the raw data derived from the other sample (as is the case with two-channel micro arrays) and it is easier for samples from different experiments to be compared, so long as all other experimental variables have been controlled. However, single-channel micro arrays require a single gene chip per sample so twice as many are required for comparison. Two-channel micro arrays are generally cheaper and allow a larger number of samples to be run on fewer gene chips.

The major advantage of DNA micro array technology is the sheer number of genes that can be examined in a single experiment. Potentially the entire genome, whether it is of a bacteria or a human, can be analysed. Similarly this technique can be used to identify genomic regions of altered expression which are of potential interest for further (perhaps more robust and fully quantitative) characterisation, or be used in patients with a particular disease to identify abnormal sequences in genetic regions which potentially contain pathogenic mutations.

4.2.1.3 Micro array RNA sample suitability and selection

Gene micro array chips were produced in the Post-Genomic Technologies Facility of the University of Nottingham. Primary whole bowel samples were obtained during surgical resections and intestinal crypt cell samples were isolated using ETDA/DTT (section 3.2.4). Total RNA was isolated and its quality analysed using the Nanodrop® spectrophotometer and Agilent 2100 Bioanalyser (section 2.3). RNA samples of good quality (RNA 260:280 ratio $\geq$1.8 and RIN $\geq$6.5) were considered suitable for micro array analysis.

Thirteen healthy control RNA samples (8 male (62%), mean age 72.8 years [SEM 2.16]) of good quality were pooled to form the “pooled control sample”. Samples of 1µg RNA from each case were pooled together to form the “pooled control sample”. The pooled control sample had an RNA concentration of 356.6ng/µL and a RIN of 8.2. The rationale of using a pooled control sample of this size as a control was to reduce the random variation in gene expression that may be present had a smaller numbers of control samples been used. The pooled control sample could be compared to individual healthy control samples (to ensure gene expression was similar) and to IBD patients (to characterise changes in TLR gene expression and identify other differential gene expression).

Three individual control cases (2 male (67%), age 71.3 [7.42] years) and three cases from patients with ulcerative colitis (2 male (67%), age 34.3 [5.17] years) were initially chosen. These six samples were referred to as the “test samples”. Amino allyl RNA was synthesised for each test sample and equal amounts of aaRNA from each test samples was mixed with aaRNA from the pooled control sample. Absolute values of gene expression were normalised to the three housekeeping genes HPRT, GAPDH and β-actin. Gene expression in the UC patients was compared to expression in healthy controls.

4.2.1.4 Protocol

The Ambion MessageAmp II® aRNA amplification kit (265) uses a micro array protocol to amplify RNA based on the method devised in the Eberwine laboratory (266). The template RNA sample is hybridised to an oligo (dT) primer bearing a T7 promoter region. Subsequently, the ArrayScript™ reverse transcriptase enzyme catalyses the first strand synthesis of full-length antisense cDNA. Next, RNA strand degradation (RNase H activity), second strand cDNA synthesis (DNA polymerase activity) and clean-up steps are undertaken to produce double-stranded cDNA. This cDNA is the template for linear amplification using a T7 RNA polymerase which binds to the T7 promoter region at the 5’-end of the antisense cDNA strand. Importantly, this amplification process transcribes

hundreds of thousands of copies of the antisense cDNA strand, producing antisense RNA (aRNA). From as little as 1µg of template RNA, 120µg of aRNA can be synthesised (figure 4.1).

During the aRNA synthesis stage, amino allyl uridine triphosphate (aaUTP) is included in the reaction mixture along with the T7 RNA polymerase and the regular (unmodified) nucleoside triphosphates (NTP). The amino allyl UTP molecule comprises a UTP molecule with an amino allyl side chain to which fluorescent molecules can be bound. During aRNA elongation, aaUTP molecules are randomly incorporated into the growing aRNA molecule in place of unmodified UTP.

A further purification step is performed and, following completion of the amplification of the aRNA molecule, an N-hydroxysuccinimide (NHS) ester moiety conjugated to a fluorescent molecule (such as cyanine-3 or Alexa Fluor^{TM} 488 (AF488)) is bound to the aaUTP via the amino allyl side chain. The efficiency of NHS-dye conjugate inclusion in the aRNA molecule is determined using a frequency on incorporation (FOI) calculation derived from a spectrophotometric trace. For example, using cyanine-3:

$$FOI = 58.5 \times \frac{\text{Absorbance at 550nm}}{\text{Absorbance at 260nm}}$$

FOI for AF488 was acquired from the online Invitrogen base:dye ratio calculator after calibration for background absorbance at the appropriate wavelengths (http://probes.invitrogen.com/resources/calc/basedyeratio.html). A target of 30-50 aaUTP molecules per 1000 nucleotides is desirable for cyanine-3, and >80 molecules per 1000 nucleotides for AF488. At this stage the aRNA sample is ready for hybridisation to the micro array gene chip. From this stage, the hybridisation procedure was undertaken by the Post-Genomic Technologies Facility, University of Nottingham. The Post-Genomic Technologies

Facility produce to order spotted oligonucleotide array chips with over 30,000 spots, each corresponding to a different gene of interest.

For analysis of TLR mRNA expression, a two-channel micro array protocol was undertaken. Each individual test sample, whether from a control sample or an IBD patient, was labelled with the green cyanine-3 (Cy3)-conjugated NHS moiety. The pooled control sample was labelled with blue AF488-conjugated NHS moiety. Five hundred nanograms of aaRNA from each of the test sample were mixed with 500ng of aaRNA from the pooled controls sample and analysed on a gene chip. Therefore each individual gene chip would compare a test sample (either a control or IBD case) with the pooled control sample. Furthermore, the gene chips from control cases could be compared with the gene chips from individual IBD cases.

The processing and data acquisition from the micro array chips following hybridisation requires the use of three software packages. Initially the arrayer produces a file containing information on each spot on the chip. This information includes a chip grid reference as to the location of each spot relative to a reference spot and other key information such as the corresponding gene name and accession number. There is also data on the average spot size (approximately 8µm) and spot spacing (approximately 165µm). This file is known as the gal file and requires Genepix Pro software v6.1 4200 (www.moleculardevices.com) for interpretation. Following hybridisation Genepix Pro® produces a file known as the gpr file, an adjusted gal file, containing data on location of the centre of each gene spot and actual spot diameters.

In order to analyse specific fluorescent intensity at each and every spot, a second software package is required called J-express® (www.molmine.com). This filters the signal intensity data to allow exclusion of poorly hybridised spots and ensure all data analysis is performed on spots of good size, rounded shape and in which the majority of pixels within the included spots are above a given threshold.

Each spot contains a number of pixels which represent fluorescent intensity data. Thus each spot contains many pixels of information. The signal intensity of each spot is calculated individually as a median, rather than a sum or mean, of all the pixels contained within the spot. The software locates each spot by recognising the transition from the lower background signal intensity (between spots) to the higher signal intensity within a given spot. A circular boundary is marked around the spot and the mean (and standard deviation) of background signal intensity between spots is measured. A spot is only included in data analysis if >80% of its pixels are above the mean plus two standard deviations of the background signal intensity.

The J-express® software also avoids the exclusion of a given spot should a signal be absent on one chip but present on another. This prevents the loss of data should there be no expression of the gene in only one sample, thus avoiding falsely excluding relevant data.

The final software package required for micro array data analysis is the Ingenuity Pathways Analysis® programme (www.ingenuity.com). This can overlay expression data from the micro array to a continually updated database of signalling pathway molecules and gene function. It allows assessment of differential expression of key components of the signalling cascade.

4.2.2 Conventional reverse transcriptase polymerase chain reaction

Isolated and disaggregated IEC were collected using EDTA/DTT and pancreatin (section 3.2.4). Isolated cells were suspended in HBSS (without Ca/Mg) medium and cell concentration calculated using trypan blue exclusion. Aliquots of $5x10^6$ cells were collected for RNA isolation from each tissue specimen and RNA isolated immediately. After confirmation that the RNA quality was suitable for down-stream analysis (RNA 260:280 ratio $\geq$1.8 and RIN $\geq$6.5) cDNA was synthesised and amplified using conventional RT-PCR techniques, run on an agarose gel and identified bands were cut and sequenced.

4.2.3 Quantitative real-time reverse transcriptase polymerase chain reaction

4.2.3.1 Introduction

The molecular technique of polymerase chain reaction allows the exponential amplification of DNA for a variety of techniques such as gene sequencing and mutation analysis. The development of reverse transcription (RT)-PCR allows RNA material to be reverse-transcribed into complementary DNA (cDNA) and provides a method for assessing gene expression.

Traditional methods for the detection of RT-PCR amplicon sequences involve electrophoresis of the PCR product through an agarose gel and visualisation, or densitometry analysis, of the resulting band using ethidium bromide, an intercalating molecule which fluoresces after irradiation with UV light primarily when bound to nucleic acids. Southern blotting is an alternative technique for detecting DNA which suffers from the fact that it is time consuming and requires multiple handling steps, increasing the likelihood of contamination. In addition, PCR-enzyme-linked immunosorbent assay (ELISA) may be used to capture amplicon onto a solid phase and detected using the avidin/biotin or anti-digoxigenin reported molecules (267).

By contrast, real-time RT-PCR allows the detection of the fluorescent signal during the amplification process, in so-called “real time”. This has allowed quantification of nucleic acid concentration and has been largely due to the advances made in the chemistry of fluorogenic molecules, which have benefits over radiogenic oligoprobes in the avoidance of radioactive emission, ease of disposal and extended shelf life. In addition, the rapid speed of real-time RT-PCR analysis is largely the result of reduced cycle times, removal of post-PCR detection procedures and the use of sensitive methods to detect fluorogenic label emissions.

In a similar principle to conventional RT-PCR, real-time RT-PCR depends upon the use of specific oligonucleotide probes (primers) which anneal to either end of the target sequence

to be amplified. In general the amplicon is shorter in base pair length that conventional primers and this increases efficiency of DNA synthesis during the rapid cycling steps.

The most commonly used fluorogenic oligoprobes rely upon fluorescence resonance energy transfer (FRET), a spectroscopic process where energy is passed between molecules separated by a distance of 10-100 Ángstrom (Å). Some molecules act as non-fluorescent quenchers, preventing the emission of FRET if located in close enough proximity the fluorogenic molecule. In such cases, once the fluorophore and quencher are sufficiently separated the fluorophore will produce a detectable emission. There are several different types of fluorogenic probes used in real-time PCR (267).

The earliest and simplest fluorophores are the non-specific DNA-binding molecules including ethidium bromide, YO-PRO-1 and SYBR Green 1. These probes will fluoresce when in contact with and bound to the minor groove of the dsDNA strand (in the case of SYBR Green 1) upon exposure to a suitable wavelength of light. These probes bind to any dsDNA molecule present in the reaction solution and have the advantage that they require less specialist knowledge of fluorogenic probe design, are less expensive and do not need to be specifically matched to a sequence in the target nucleic acid.

However there are certain disadvantages to non-specific fluorophores. Primers can self-anneal and produce a dsDNA molecule known as a primer-dimer. Non-specific fluorophores will therefore also bind to primer-dimers in addition to amplified dsDNA, and emit a fluorescent signal which can cause difficulty in data interpretation. This is particularly troublesome with templates of low initial concentrations. To overcome this problem, use is made of the observation that the denaturing temperature of the primer-dimer is lower that of the complimentary primer-template melting temperature (T_M). The addition of a short, higher temperature detection step, after the elongation step of the PCR cycle, can overcome this issue by measuring fluorescence when primer-dimer bonds have dissociated. Of additional

note, SYBR Green 1 fluorescence has been observed to increase non-specifically in the later cycles of no template controls (267).

To overcome these non-specific probe-related problems a number of alternative probes can be designed. These include linear (adjacent), 5' nuclease, hairpin, sunrise and scorpion oligoprobes and have been reviewed by Mackay *et al.* and Giuliette *et al.* (267, 268). These probes are specific DNA-binding probes. They contain a fluorescent molecule with a closely positioned non-fluorescent quencher molecule, which prevents the emission of FRET. These probes also contain a sequence of nucleic acid which is specific for a region of the gene of interest. During the PCR reaction, the probe anneals to its target gene and the fluorophore and quencher become separated sufficiently that FRET emission is possible.

One advantage of specific primers is that the concern of spurious primer-dimer fluorescent signal using non-specific probes is not an issue because these probes will not anneal to primer-dimers. Additionally, the sequence specificity to the complimentary gene sequence prevents the probes annealing to contaminating and/or non-amplified nucleic acid. However, these probes are expensive and much more challenging to design and manufacture.

During real-time RT-PCR a thermal cycler is used to rapidly cycle the sample through pre-specific and optimised denaturing, annealing and elongation temperatures, in much the same way as is undertaken for conventional RT-PCR. This allows separation of dsDNA strands, annealing of primers to complimentary gene regions and complimentary DNA strand synthesis, respectively. During this process, SYBR Green 1 fluorescent probe in the reaction mixture binds to the dsDNA as it is synthesised, resulting in a fluorescent emission. As the PCR process enters the linear phase of replication, the fluorescent intensity increased in direct proportion to the amount of synthesised dsDNA.

The point at which a given threshold value is reached is known as the threshold cycle (C_t) and each sample is assigned a C_t value. The more abundant the initial target cDNA concentration in the original sample, the earlier in the cycling reaction it will reach the threshold value and, therefore, the lower the measured C_t value. The threshold value is taken as ten standard deviations above the baseline fluorescence calculated during cycles 3 to 15 and is, therefore, calculated for each experimental run. Thus, the relative amount of synthesised dsDNA is measured in "real time", rather than being measured at the end of the reaction when exhaustion of reaction components (such as dNTP) can influence final dsDNA calculation value.

4.2.3.2 Quantification of relative gene expression using the Pfaffl method

To investigate changes in gene expression, two quantification techniques are available. The first is relative expression, where the expression of the target gene is expressed relative to the expression of a reference gene, usually a ubiquitously expressed housekeeping gene such as HPRT or GAPDH. The second technique is absolute quantification and is based on an internal or external calibration curve to allow exact measurement of nucleic acid concentration. The latter method requires identical cycling efficiencies for target and standard cDNA samples and is a time-consuming and expensive method. However, it is necessary when calculating, for example, viral loads in virology (267). For most purposes, the first method of calculating relative gene expression (normalised to a housekeeping gene) is sufficient. It must be born in mind however that housekeeping gene expression may vary under experimental conditions (269, 270) although this is unlikely to be significant if all samples are treated in the same way using identical experimental methodologies.

To calculate the PCR reaction efficiency, a standard curve is plotted during each real-time RT-PCR run to ensure efficient cDNA replication. An aliquot of high quality RNA is reverse transcribed into cDNA and serially diluted two-fold to obtain 1/2, 1/4, 1/8, 1/16 and 1/32 dilutions of the original sample. Each serial dilution is run in triplicate alongside two negative

controls (“no reverse transcriptase” and “no template” control samples) for each primer pair on every run to exclude DNA contamination or non-specific amplification.

Following amplification, the C_t values for each serially diluted sample are plotted against the logarithm of the dilution fraction to produce the “standard curve”. Since the dilution fraction is a logarithmic plot, the standard curve plot produces a straight line, the slope of which is related to the efficiency of the PCR reaction. The efficiency of the PCR run can be calculated by the following equation (271):

$$\text{Efficiency (E)} = [10^{(-1/\text{slope})}] - 1$$

By plotting a standard curve with each experimental run, the efficiency of each reaction could be measured to act as an internal inter-run control. Thereafter, samples were run in triplicate from cases with IBD and healthy controls to calculate the relative expression of the target genes, TLR2 and TLR4, to the housekeeping gene, HPRT. To calculate the relative expression of each target gene the following formula described by Pfaffl is used (272):

$$\text{Ratio(R)} = \frac{(E_{\text{target}})^{\Delta C_t (\text{control} - \text{sample})}}{(E_{\text{reference}})^{\Delta C_t (\text{control} - \text{sample})}}$$

where target is the target gene; reference is the housekeeping gene; sample is the disease sample of interest, and control is the control sample.

Using this equation, two difference R values can be calculated for a given sample. In the first instance, all samples from the disease group, for example active ulcerative colitis, are pooled to give a single group C_t value, and this normalised to a C_t from a pooled sample of healthy control cases. This gives a single relative expression of the target gene in diseases cases relative to controls but gives no measure of variability within the sample groups.

In the second calculation, a mean of the three triplicate samples for each diseased case (giving a mean C_t per case) is compared to a mean C_t value for the three triplicate samples for each control case. Thus, variation of target gene expression within each disease group is characterised.

Finally, to investigate for the occurrence of primer-dimer formation, a melting curve analysis is undertaken for each set of primer pairs. Following the 40 cycles of cDNA amplification, the reaction mixture is cooled to 55^{o}C and sequentially heated to 95^{o}C at a rate of 0.5^{o}C per second. At each 0.5^{o}C increment, fluorescence is measured and plotted against temperature. In the ideal situation, there is a single peak at the dissociation temperature (T_D) of the primer-template complex. Should primer-dimers occur, a smaller second peak at a lower temperature is seen, corresponding to the melting temperature of the primer-dimer complex (T_M).

If primer-dimer occurrence is detected on melting (dissociation) curve analysis, it can be negated by the inclusion of a fourth step in the real-time RT-PCR cycling protocol. Following the three traditional dissociation, annealing and elongation steps, an acquisition step is included which is set at a temperature above that required to dissociate the primer-dimers (i.e. above the T_M) but below the dissociation temperature (T_D) of the dsDNA molecule. At this temperature, the primer-dimer-SYBR Green 1 complex will dissociate (resulting in prevention of aberrant fluorescent signal from this complex) but the SYBR Green 1 molecule will remain bound to the synthesised dsDNA molecule and continue to produce a fluorescent signal (which thus reflects only the total dsDNA content). In such cases, fluorescence is measured at the end of this fourth (acquisition) step.

4.2.3.3 Protocol for quantitative real-time RT-PCR

For quantitative real-time RT-PCR, different primers were designed to those used in conventional PCR. Real-Time RT-PCR was undertaken using QuantiTect SYBR Green I®

technology (204141, Qiagen). Primers were designed to similar standards as conventional RT-PCR primers except that the amplicon length was kept shorter than 200 base pairs due to the rapid cycling step in real-time RT-PCR protocols. The Basic Local Alignment Search Tool was used to confirm primer specificity (222).

For each primer pair, samples were initially run using the conventional RT-PCR protocol, described in section 2.4.3, and using cDNA from a TLR2- and TLR4-expressing cell line (T84 and THP-1 cells) as template to optimise annealing temperature conditions. Samples were run on a 1% agarose gel to confirm a single band of anticipated base length was visible, suggesting specific amplification of a single DNA sequence. Bands were cut and sequenced (section 2.5) to further ensure primer specificity for the gene of interest. Once the real-time primer specificity was confirmed and optimal cycling conditions characterised, samples were analysed on a Stratagene MX4000P real-time PCR cycler to undertake standard curve and melting (dissociation) curve analyses.

For each real-time RT-PCR reaction, 12.5µL of QuantiTect SYBR Green PCR Master Mix (providing a final concentration of 2.5mM $MgCl_2$) was added to 2.0µL of cDNA, 0.1µL of 100µM sense primer, 0.1µL of 100µM anti-sense primer and 10.3µL nuclease-free water, to make a final volume of 25µL. This gave a final primer concentration of 0.4µM. The sample was thoroughly mixed and kept on ice until analysis.

Samples were transferred to the Stratagene MX4000 real-time PCR cycler. The cycling conditions are shown in the table below for the respective real-time primers. A melting curve analysis and standard curve of serially diluted samples were performed for every real-time RT-PCR run (table 4.1). The sequences of the real-time RT-PCT primers are shown in table 4.2. Real-time RT-PCR data were analysed using MxPro Mx3000P v4.01 software (Stratagene). The demographic data for the subjects included in the real-time RT-PCR analyses are shown in table 4.3.

Table 4.1 Cycling protocols for real-time RT-PCR primers

Gene	Stage 1	Stage 2: Denature	Stage 2: Annealing	Stage 2: Elongation	Stage2: Acquisition step*	No. of cycles	Stage 3
HPRT	95°C 15m	95°C 15s	60°C 30s	72°C 30s	NR	40	95°C 1m
TLR2	95°C 15m	95°C 15s	58°C 30s	72°C 30s	78°C 30s	40	95°C 1m
TLR4	95°C 15m	95°C 15s	58°C 30s	72°C 30s	NR	40	95°C 1m

HPRT, hypoxanthine-guanine phosphoribosyltransferase; m, minute; NR, not required; s, second; TLR, Toll-like receptor

* Only required when using TLR2 primers. Fluorescent measurement was taken at the end of this step (in other cases fluorescent measurement was taken at the end of the elongation step)

Table 4.2 Real-time RT-PCR primer sequences

Gene	Primer Sequence	Melting temperature (T_M)	Amplicon size (base pairs)
HPRT	GAC CAG TCA ACA GGG GAC AT (sense) CGA CCT TGA CCA TCT TTG GA (anti-sense)	59.4°C 57.3°C	160bp
TLR2	GGG TTG AAG CAC TGG ACA AT (sense) CTG CCC TTG CAG ATA CCA TT(anti-sense)	57.3°C 57.3°C	134BP
TLR4	CGG AGG CCA TTA TGC TAT GT (sense) TCC CTT CCT CCT TTT CCC TA (anti-sense)	57.3°C 57.3°C	141BP

Bp, base pairs; HPRT, hypoxanthine-guanine phosphoribosyltransferase; TLR, Toll-like receptor

Table 4.3 Demographic data for study subjects

Demographic variable	Large intestine			Small intestine	
	Healthy control	Ulcerative colitis	Crohn's colitis	Healthy control	Crohn's ileitis
Number	11	18	11	7	7
Age mean (SEM) years	70.5 (4.15)	51.5 (4.75)**	48.9 (4.10)**	74.1 (3.36)	44.3 (7.18)**
Sex male/female (% male)	7/4 (64)	9/9 (50)	2/9 (18)	5/2 (71)	2/5 (29)
Medications					
• 5ASA	0	11 **	3	0	0
• Thiopurine	0	8 *	3	0	4
• Corticosteroid	0	3	4	0	1
• MTX	0	2	2	0	0
• Anti-TNFα	0	0	6 *	0	2
• Cyclosporine	0	1	0	0	0
• Metronidazole	0	1	0	0	0
Medical History					
• PSC	0	0	1	0	0
• DM	2	1	1	2	0
• NAFLD	0	0	1	0	0
• Obesity	1	1	0	0	0
• Osteoporosis	2	2	0	0	0
• IHD	2	3	0	2	0
• CVD	0	2	0	1	0
• PVD	1	0	0	0	1
• MS	0	1	0	0	0
• IgA deficiency	0	0	1	0	0
• Hyperchol	0	0	2	0	0
• Hypothyroidism	0	0	1	0	1
• Pernicious anaemia	0	0	1	0	1
• Schizophrenia	0	0	1	0	1
• Interstitial nephritis	0	0	0	0	1
• Atrial fibrillation	1	0	0	1	0
• COPD	1	0	0	0	0

5ASA, 5-aminosalicylic acid (mesalazine); COPD, chronic obstructive pulmonary disease; CVD, cerebrovascular disease; DM, diabetes mellitus; Hyperchol, hypercholesterolaemia; IHD, ischaemic heart disease; MS, multiple sclerosis; MTX, methotrexate; NAFLD, non-alcoholic fatty liver disease; PSC, primary sclerosing cholangitis; PVD, peripheral vascular disease; TNFα, tumour necrosis factor-α.
* $p<0.05$; ** $p<0.01$ versus healthy controls (Student t-test for continuous variables and Fisher's exact test for ordinal variables)

4.3 Results

4.3.1 Isolated intestinal crypt cells contain RNA of high quality which is not influenced by patient demographics, tissue sample site, underlying diagnosis or severity of intestinal inflammation

RNA was isolated from 109 intestinal epithelial cell samples. The RNA 260:280 absorbance ratio was measured using the Nanodrop® spectrophotometer. This ratio is a measure of protein contamination of nucleic acid samples, with a higher the ratio indicating a purer RNA sample. RNA solutions of ratio $\geq$1.8 were considered suitable for down stream analysis. The mean 260:280 ratio was 2.1 with a standard error of 0.004. A histogram of the 260:280 ratio was plotted and showed an approximately normal (Gaussian) distribution (mean $\pm$SEM 2.11$\pm$0.01; Kolmogorov-Smirnov test p=0.072).

To further measure the quality of the isolated RNA samples from primary epithelial cells, samples were analysed using the Agilent 2100 Bioanalyser®. The Agilent 2100 Bioanalyser® uses micro-fluid capillary electrophoresis to measuring a number of key aspects of the electrophoretic strip. Higher values indicate less degraded (higher quality) RNA samples and values $\geq$6.5 are considered suitable for downstream analysis (220). The RIN values were normally distributed (mean $\pm$SEM 7.69$\pm$0.11; Kolmogorov-Smirnov test p=0.548). When samples with a RIN <6.5 were excluded (n=12), the distribution of the 97 remaining samples remained approximately normal (8.01$\pm$0.08; Kolmogorov-Smirnov p=0.357).

To investigate the influence of various sample demographic factors on RNA quality, the RIN value and 260:280 ratio were compared to corresponding values including subject age, mucosal sample weight, isolated IEC concentration in suspension, cell viability using trypan blue exclusion, diagnosis, severity of tissue inflammation, medication use and concurrent medical conditions.

There was no correlation between the RIN and the age of the participant (figure 4.2, R^2=0.011, p=0.27). Similarly, RIN was also not associated with mucosal tissue weight (R^2=0.001, p=0.90) or cell viability (R^2=0.021, p=0.125).

Tissue sections of 5μm in thickness were formalin-fixed and paraffin-embedded, and subsequently stained with haematoxylin and eosin. The severity of inflammation of colonic specimens from patients with UC was assessed using the system described by Riley *et al* and graded as none, mild, moderate or severe (235). Small intestinal samples were graded as either un-inflamed (normal) or inflamed since a validated scoring system for the severity of small intestinal inflammation has not been reported. RIN values of isolated crypt IEC samples from histologically un-inflamed bowel (7.88±0.14) were similar to samples from inflamed bowel (7.46±0.17, p=0.058). Furthermore, if inflamed samples were sub-divided following histological assessment of the severity of inflammation into either mild/moderately inflamed (7.31±0.19) or severely inflamed (7.78±0.37), comparison with samples from un-inflamed bowel revealed no significant difference of the RIN amongst these three groups (ANOVA test p=0.087).

Sample RIN values of isolated crypt IEC samples from healthy controls (7.65±0.17) did not differ significantly from patients with Crohn's disease (7.67±0.20, p=0.928) or UC (7.78±0.20, p=0.663). Likewise RIN values of isolated crypt IEC samples did not differ between Crohn's disease and UC (p=0.745). With regard to the anatomical site of the tissue, RIN values of isolated crypt IEC samples from the small and large bowel were similar (7.44±0.22 and 7.75±0.13, respectively, which were not significantly different, p=0.267).

To compare the reliability of the Agilent 2100 Bioanalyser® measurements, RIN values were plotted against the corresponding 28S:18S ribosomal RNA ratios for each case. A higher RIN values should be associated with higher 28S:18S ribosomal RNA ratio. Indeed these variables were shown to highly correlate (figure 4.3, R^2=0.448, p<0.001).

The RIN value was not influenced by a number of demographic variables, including a history of hypertension (p=0.953), ischaemic heart disease (p=0.823), cerebrovascular disease (p=0.399), diabetes mellitus (p=0.061), obesity (p=0.32), peripheral vascular disease (p=0.371), osteoporosis (p=0.287), prior surgery (p=0.881), or use of the following medications: aminosalicylic acid preparations (p=0.96), thiopurines (p=0.675), corticosteroids (p=0.177), cyclosporine (p=0.086), methotrexate (p=0.908), anti-TNFα monoclonal antibody therapy (p=0.87) or systemic antibacterial therapy (p=0.247).

4.3.2 Conventional and real-time RT-PCR primers are specific for human TLR2 and TLR4

To ensure primer specificity and to optimise RT-PCR reaction conditions, human intestinal epithelial cells lines (HT-29 and T84 cells) were obtained which are reported in the literature to express both TLR2 and TLR4 transcripts (154, 231, 232, 252). The human monocyte cell line THP-1 was also used as a non-intestinal, TLR2- and TLR4-expressing cell control (233, 240, 246, 248).

T84 and HT-29 cells were cultured and RNA isolated using the Qiagen RNeasy Mini Elute Kit. RNA quality was analysed using the Nanodrop® spectrophotometer and Agilent 2100 Bioanalyser®. Suitable samples were reverse transcribed into cDNA and subjected to conventional PCR amplification. Following agarose gel electrophoreses, bands were viewed using a UV-transilluminator and cut using a scalpel. Bands were sequenced using the ABI Prism BigDye Terminator® protocol.

Agarose gel electrophoresis of cDNA samples from T84 cells revealed well demarcated amplicon bands for TLR2, TLR4 and HPRT at the expected base pair sizes (figure 4.4). Similar results were observed with the THP-1 monocyte cell line. However, these results could not be replicated with HT-29 cells, which showed variable and low level TLR2 and TLR4 transcript expression.

The bands at approximately 599bp, 507bp and 160bp were cut and sequenced. These sequences were confirmed as human TLR2, TLR4 and HPRT, respectively, using the National Centre for Biotechnology Information Basic Local Alignment Search Tool (BLAST) (222). Identical bands were observed when cDNA from primary human peripheral blood mononuclear cells (PBMC) was used as template (data not shown).

Real-time RT-PCR requires the synthesis of shorter cDNA amplicons compared to conventional RT-PCT. Ideally amplicon length should be less than 200bp. Therefore, the primers used for conventional RT-PCR were unsuitable for real-time RT-PCR and alternative primers were designed. Following primers design, cDNA samples were amplified for TLR2 and TLR4 using T84 cells and THP-1 cells as templates. Again PCR amplicons were run on a 1% agarose gel and bands were detected at the appropriate nucleotide sizes. Bands were cut and subsequent DNA sequencing confirmed specificity for human TLR2 and TLR4 mRNA.

4.3.3 Isolated intestinal crypt cells express TLR2 and TLR4 mRNA using RNA micro array

To assess the efficiency of inclusion of the NHS-dye conjugate in the aRNA molecule during the RNA micro array protocol, a measurement known as the frequency of incorporation (FOI) was calculated. A target of 30-50 aaUTP molecules per 1000 nucleotides is desirable for cyanine-3 and >80 molecules per 1000 nucleotides for AF488 to indicate adequate dye inclusion. FOI for AF488 was assessed on the pooled samples and found to be satisfactory (116 dye molecules per 1000 nucleotide bases). The FOI values for the RNA micro array suggested adequate NHS-dye inclusion (table 4.4).

Table 4.4 RNA micro array frequency of NHS-dye incorporation

Sample	FOI of Cyanin-3
Control 1	30.52
Control 2	51.53
Control 3	50.66
Ulcerative colitis 1	54.04
Ulcerative colitis 2	51.86
Ulcerative colitis 3	50.00

Analysis of the RNA micro array data confirmed the expression of RNA transcript for human TLR1-10 in the majority of 6 cases (three controls and three patients with ulcerative colitis). TLR7 mRNA was not detected in control cases and TLR1 and TLR10 transcripts were detected in only one UC patient. Several TLR gene transcripts were expressed in only two control or UC subjects, including TLR1, TLR3, TLR5 and TLR7. However TLR2 and TLR4 transcripts were detected in all healthy control (C1-3) and UC (UC1-3) subjects (table 4.5).

Table 4.5 Expression of TLR1-10 mRNA in primary crypt intestinal epithelial cells using micro assay technology

Sample	Toll-like Receptor									
Control	1	2	3	4	5	6	7	8	9	10
C1	0.066465	0.111782	0.187311	0.465257	0.084592	0.10574	0	0	0.259819	0.042296
C2	0.037915	0.057601	0	0.032082	0	0.054685	0	0.021145	0.022603	0.183011
C3	0	0.013059	0.034154	0.029131	0.004018	0.025113	0	0	0.099424	0.009041
Ulcerative colitis										
UC1	0	0.046819	0.159845	0.046819	0.042748	0.198473	0	0.079389	0.554707	0
UC2	0	0.047976	0.031484	0.031484	0.013493	0.086957	0.046477	0.017991	0.302849	0.013493
UC3	0.138127	0.784621	0.108936	0.045568	0.030616	0.007832	0.037736	0.04272	0.104664	0

RNA expression is given in fluorescent units per fluorescent unit of the housekeeping gene HPRT. Zero values indicate a gene-spot fluorescent intensity of equal to or less than the background (inter-spot) chip intensity; implying non-expression of the corresponding gene.

The fluorescent intensity, and therefore RNA expression, of each micro array gene-spot (feature) can be normalised to the fluorescent intensity of one of several housekeeping genes. Using this method, TLR1-10 RNA expression relative to HPRT, GAPDH and β-actin was calculated. A similar pattern of expression was observed regardless of the chosen housekeeping gene. Therefore HPRT was chosen for all further micro array analyses.
The median relative expression of TLR2 and TLR4, adjusted for HPRT expression, between healthy controls and patients with UC were compared (figure 4.5). There was no significant difference between healthy controls and UC subjects for either TLR2 (median [range] of relative expression 0.058 [0.013-0.111] versus 0.048 [0.047-0.785], respectively, p=0.45) or TLR4 (relative expression 0.032 [0.029-0.465] versus 0.046 [0.031-0.047], respectively, p=0.45).

A “comparison analysis” using the Ingenuity Pathway Analysis® (IPA) software was undertaken to investigate the differential expression of multiple signalling molecules within the TLR signalling pathway at the RNA level. This analysis compares the expression of a given set of intracellular signalling molecules in the UC group relative to the healthy control group. Using this analysis the following molecules were shown to be up-regulated in the UC group: SITPEC (signalling intermediate in Toll pathway, evolutionarily conserved; also known as ECSIT, evolutionary conserved signalling intermediate in toll pathways) (relative expression 1.072), c-Jun (relative expression 1.113) and c-Fos (relative expression 1.269). In addition, IκKβ (relative expression 0.946) and Iκβα (relative expression 0.957) were significantly down-regulated in the UC group compared to the healthy control group ($p<0.05$ for all). The location of these signalling molecules in the TLR signalling pathway is shown graphically in figure 4.6.

4.3.4 Isolated intestinal crypt cells express TLR2 and TLR4 mRNA using conventional RT-PCR

To confirm the micro array findings in a larger cohort of subjects, and to investigate the expression of TLR2 and TLR4 mRNA in subjects with Crohn's disease, primary intestinal epithelial cells were isolated from colonic and small intestine specimens of healthy control subjects and patients with Crohn's disease and ulcerative colitis. Crypt epithelial cells were isolated and disaggregated, total RNA purified and complimentary DNA synthesised. Following amplification using conventional RT-PCR protocols, the PCR products were run on an agarose gel and visualised using a UV trans-illuminator.

Primary intestinal epithelial cells from small and large bowel specimens were shown to express TLR2, TLR4 and HPRT transcripts (figure 4.7). This included small bowel samples from healthy controls and Crohn's disease patients, and colonic samples from healthy controls and patients with both Crohn's disease and ulcerative colitis (n=5 for all groups).

4.3.5 Patients with inflammatory bowel disease up-regulate TLR2 and TLR4 mRNA expression in intestinal crypt cells

To determine whether the expression of TLR2 and TLR4 mRNA levels differ in subjects with inflammatory bowel disease compared to healthy control subjects, real-time RT-PCR analysis was undertaken. cDNA samples were analysed using the DNA-binding molecule SYBR Green as the fluorescent probe following amplification with specifically designed primers. cDNA samples from each subject (healthy controls and patients with IBD) were run in triplicate and the mean cycle threshold value for each case was calculated. Each mean value was compared to the pooled mean cycle threshold value for all healthy control samples. This allowed each case to be assigned a value corresponding to the gene transcript expression relative to the mean healthy control expression.

Initially, several quality control tests were undertaken. To investigate the efficiency of the PCR reaction, standard dilutions of pooled cDNA samples from primary crypt intestinal epithelial cells were plotted against cycle threshold on a logarithmic scale. This allowed derivation of the efficiency (E) of the PCR reaction from the slope of the plotted line using the equation: $E=10^{(-1/slope)}$. A typical standard curve for TLR2 is shown in figure 4.8. Similar standard curve analyses were obtained for TLR4 and HPRT primer pairs. Real-time RT-PCR runs were only considered suitable for analysis if the efficiency of the amplification was equal to 100% $\pm$10% (figure 4.8).

To exclude the presence of undesirable oligonucleotide annealing and primer-dimer formation, a dissociation curve analysis was undertaken for each real-time RT-PCR run. Samples were healed from 55^{o}C to 95^{o}C in 0.5^{o}C increments and the fluorescent intensity measured at every step. A typical dissociation curve for TLR4 PCR product is shown in figure 4.9, demonstrating optimal primer-template annealing and no primer-dimer formation (illustrated by the absence of a fluorescent peak at annealing temperatures lower that the main PCR product dissociation peak).

Similar results were demonstrated with primers for HPRT (data not shown). However, the TLR2 primer pairs demonstrated evidence of primer-dimer formation at lower annealing temperatures (between 70^{o}C and 77^{o}C). This was mainly observed in standard samples of high dilution (i.e. low cDNA concentration) or in primary epithelial cell samples with low cDNA concentration (i.e. high cycle threshold values), as shown in figure 4.10.

Primer-dimer oligonucleotide formation during real-time RT-PCR measurement steps is undesirable because SYBR Green fluorophore molecules can bind non-specifically to these dimers, resulting in measurement of erroneous fluorescent signal. To overcome this eventuality, a fourth (acquisition) step at 78^{o}C was introduced to the cycling protocol following the three standard denature, annealing and elongation steps for the TLR2 primer

pairs. Fluorescent intensity was measured at the end of this fourth step. Repeat dissociation curve analysis using the modified four-step protocol resulted in the abolition of the primer-dimer formation, as shown in figure 4.11.

To exclude the possibility of non-specific cDNA amplification causing erroneous fluorescent signal during the PCR cycling protocol, wells with no nucleic acid (no template controls, NTC) and no cDNA (no reverse transcriptase controls, no RT) were included in all real-time RT-PCR runs. Control wells failed to show significant fluorescent signal, as shown for TLR2 primers in figure 4.12. Similar results were obtained for HPRT and TLR4 primers.

Following optimisation of real-time RT-PCR conditions, primary intestinal epithelial cell samples from healthy controls and patients with inflammatory bowel disease were examined. TLR2 and TLR4 expression levels were normalised to the expression of HPRT transcript in the corresponding sample. Thereafter all transcript levels were calculated as the expression level relative to the mean expression level from the pooled healthy control samples.

In patients with ulcerative colitis (n=18, 9 males (50%), mean (SEM) age 51.5 (4.76) years), IEC from regions of histologically inflamed colon expressed significantly more transcripts for TLR2 (median relative expression [inter-quartile range] 3.18 [1.03-10.4], p=0.003) and TLR4 (2.33 [1.15-4.45], p=0.024) compared to healthy controls (n=10, 6 males (60%), age 70.5 (4.15) years). In regions of histologically normal (un-inflamed) colon, expression of TLR4 mRNA transcripts was also higher compared to healthy controls (1.9 [1.69-4.31], p=0.017), but TLR2 mRNA transcripts were not significantly up-regulated (1.36 [0.75-5.77], p=0.254) (figure 4.13).

Subsequently, inflamed samples were sub-classified by the severity of inflammation using the scoring system described by Riley *et al.* (235). For convenience and to avoid groups with small numbers, samples of either mild or moderate histological severity were combined to

form a single group. Severely inflamed UC samples showed significantly greater expression of TLR2 (10.4 [5.35-255.91], p=0.0002) and TLR4 (4.45 [1.75-7.56], p=0.031) transcripts compared to healthy controls. However, UC samples from mild/moderate histological inflammation did not show greater TLR2 transcript expression compared to healthy controls (1.06 [0.99-1.56], p=0.088) and, although there was a trend towards up-regulation of TLR4 transcript, it did not reach statistical significance (2.12 [1.15-2.56], p=0.124) (figure 4.14).

In patients with Crohn's colitis (n=11, 2 males (18%), age 48.9 (4.10) years), IEC from regions of histologically inflamed colon expressed significantly more transcripts for TLR2 (3.45 [0.8-5.4], p=0.012) and TLR4 (1.71 [1.0-4.32], p=0.042) compared to healthy controls (figure 4.15).

Intestinal epithelial cells were also obtained from the small bowel of patients with Crohn's ileitis (n=7, 2 males (29%), age 44.3 (7.18) years) and healthy controls (n=7, 5 males (71%), age 74.1 (3.36) years). All small bowel tissue samples isolated from patients with Crohn's disease were histologically and macroscopically inflamed. IEC from patients with Crohn's ileitis expressed significantly greater TLR4 transcripts compared to healthy controls (1.84 [1.43-4.66], p=0.030) and, although there was a trend towards up-regulation of TLR2 mRNA, this did not reach statistical significance (1.72 [0.52-2.74], p=0.208) (figure 4.16).

These data are summarised in the following table demonstrating the median expression of TLR2 and TLR4 mRNA in patients groups relative to healthy controls (table 4.6).

Table 4.6 Expression of TLR2 and TLR4 mRNA in patients with inflammatory bowel disease relative to expression in healthy control subjects

Sample location	Sample group	N	Relative TLR2 mRNA expression		Relative TLR4 mRNA expression	
			Median [IQR]	p-value	Median [IQR]	p-value
Large bowel	Healthy control	11	1.0 [0.59-1.42]	-	1.0 [0.82-1.37]	-
	UC normal (UI)	5	1.36 [0.75-5.77]	0.254	1.90 [1.69-4.31]	0.017
	UC mild/mod inflamed	7	1.06 [0.99-1.56]	0.088	2.12 [1.15-2.56]	0.124
	UC severely inflamed	6	10.4 [5.35-255.9]	0.0002	4.45 [1.75-7.56]	0.031
	UC inflamed #	13	3.18 [1.03-10.4]	0.003	2.33 [1.15-4.45]	0.024
	CD inflamed	11	3.45 [0.8-5.4]	0.012	1.71 [1.0-4.32]	0.042
Small bowel	Healthy control	7	1.0 [0.77-1.22]	-	1.0 [0.72-1.89]	-
	CD inflamed	7	1.72 [0.52-2.74]	0.208	1.84 [1.43-4.66]	0.030

CD, Crohn's disease; IQR, inter-quartile range; Mod, moderate; N, number of cases; UC, ulcerative colitis; UI, un-inflamed (normal)

UC inflamed group is an amalgamation of the mild/moderate and severely inflamed UC groups (see text)

P-values are calculated by Mann-Whitney test and compared to healthy control group

It was noteworthy that colonic samples taken from healthy controls were collected from statistically older subjects (mean (SEM) age 70.5 (4.15) years) than the colonic samples from patients with either UC (51.5 (4.76) years, p=0.009) or Crohn's colitis (48.9 (4.10) years, p=0.001). A similar observation was made when comparing the ages of small intestine healthy controls (74.1 (3.36) years) to patients with Crohn's ileitis (44.3 (7.18) years, p=0.003).

It is not known if TLR2 and TLR4 expression changes with age. If the expression of TLR2 and TLR4 mRNA transcripts were to decline with age, this may explain the observed differences between (statistically younger) IBD patients and (statistically older) healthy controls. To investigate this possibility, the healthy control group was divided by age into two groups of equal size, "younger" and "older" controls. The mean age of subjects in the

younger control group (n=5, age 61.2 (6.18) years) was statistically similar in age to patients with both UC (p=0.296) and Crohn's disease (p=0.108). When the relative expression of transcript between the younger and older healthy control groups was compared, there was no statistical difference in the expression of TLR2 mRNA (mean (SEM) relative expression 1.21 (0.35) versus 0.83 (0.05), p=0.343, respectively) or TLR4 mRNA (0.98 (0.14) versus 1.36 (0.36), p=0.384, respectively). Therefore, no change in TLR2 or TLR4 mRNA expression by age was observed.

Within the group of patients with severely inflamed ulcerative colitis (n=6) there appeared to be a polarity in the group, with crypt cells from three patients expressing higher transcripts for TLR2 and, to a lesser extent, TLR4 mRNA than the remaining three subjects. However, when the absolute transcript expression values were tested there was no significant difference between the higher and lower expressing cases for TLR2 (p=0.1) or TLR4 (p=0.1) mRNA. Furthermore, although the higher expressing subjects were taking more thiopurine, methotrexate, corticosteroid and antibiotic therapy at the time of surgery than the lower expressing subjects, none of these differences were statistically significant (p>0.05 for all Fisher's exact tests).

4.3.6 Patients with isolated left-sided ulcerative colitis express similar levels of TLR2 and TLR4 mRNA in un-inflamed and inflamed colon

In a sub-group of patients with ulcerative colitis, five patients were identified with endoscopically and histologically isolated left sided colitis (Montreal classification E2 (9)). Two patients were receiving mesalazine, two were receiving mesalazine in combination with azathioprine, one was receiving corticosteroids and one patient was not receiving any pharmacological therapy at the time of surgery. Intestinal epithelial samples from histologically normal (right-sided) and inflamed (left-sided) regions of the colon were obtained and RNA isolated as described. Relative TLR2 and TLR4 mRNA expression from these paired samples was compared to the pooled sample of healthy control cases using

real-time RT-PCR. A Wilcoxon test was used to analyse these paired data, comparing normal (un-inflamed) to inflamed regions for each case.

Relative TLR2 expression was similar in histologically normal and inflamed tissue (p=1.0). Likewise, there was no significant difference between TLR4 mRNA expression in histologically normal and inflamed, paired samples (p=0.625, figure 4.17).

4.3.7 TLR2 mRNA expression is greater in the distal small intestinal and TLR4 mRNA expression is greater in the colon in healthy subjects

Expression of Toll-like receptors has been reported to vary along the gastrointestinal tract. TLR2 mRNA is reported to be highest in the distal small bowel and TLR4 mRNA highest in the distal colon and stomach in mice (250). In a sub-group of small and large intestinal samples from healthy controls, real-time RT-PCR analysis was undertaken to compare TLR2 and TLR4 mRNA expression in the small intestine compared to expression in the colon. Median [inter-quartile range] TLR2 mRNA expression was significantly higher in healthy small bowel (17.52 [12.52-19.70]) relative to healthy large bowel (1.0 [0.74-1.35], p=0.004). Conversely, TLR4 mRNA expression was significantly lower in healthy small bowel (0.20 [0.08-0.38]) relative to healthy large bowel (1.0 [0.86-1.69], p=0.004), figure 4.18.

4.4 Figures

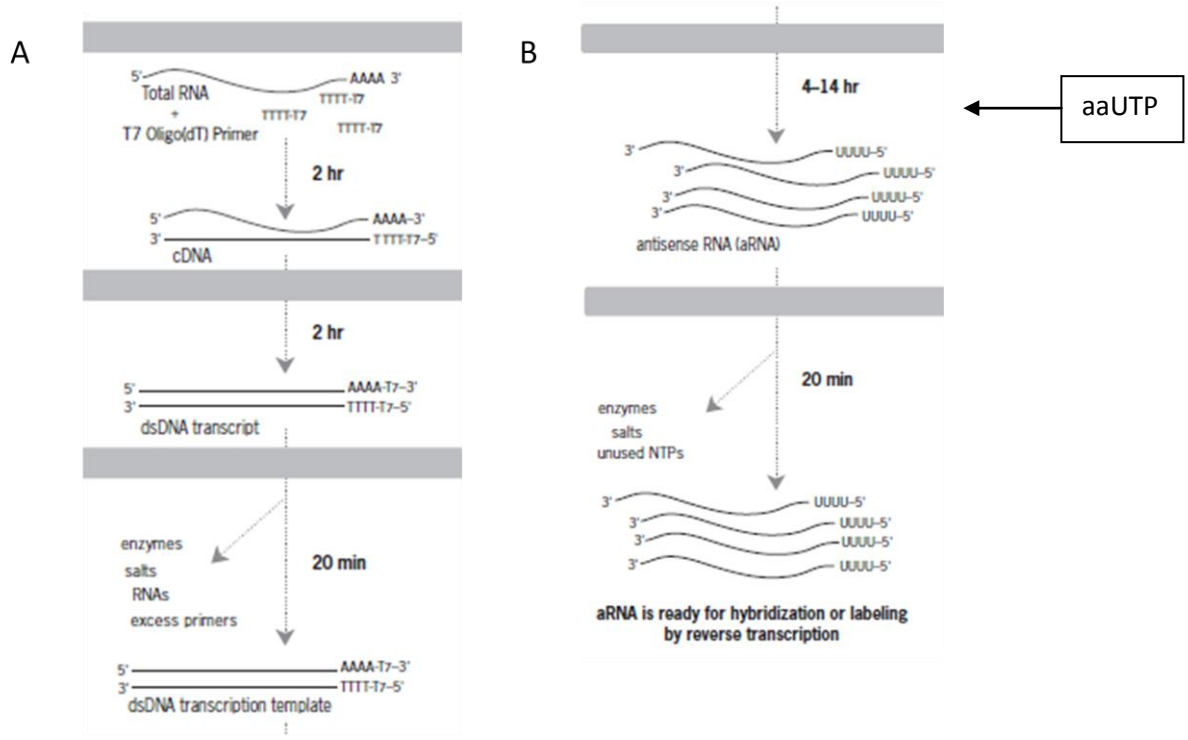

Figure 4.1 Synthesis of anti-sense RNA using the Ambion MessageAmp II® aRNA amplification kit. (A) cDNA is synthesised from total RNA and cleaned, leaving dsDNA. (B) A T7 RNA polymerase synthesises anti-sense RNA (aRNA) from the anti-sense cDNA strand. The use of amino allyl UTP (aaUTP) at this step allows incorporation of aaUTP molecules into the elongating aRNA strand which is necessary for the subsequent conjugation of fluorescent dye to its aa side chain (265).

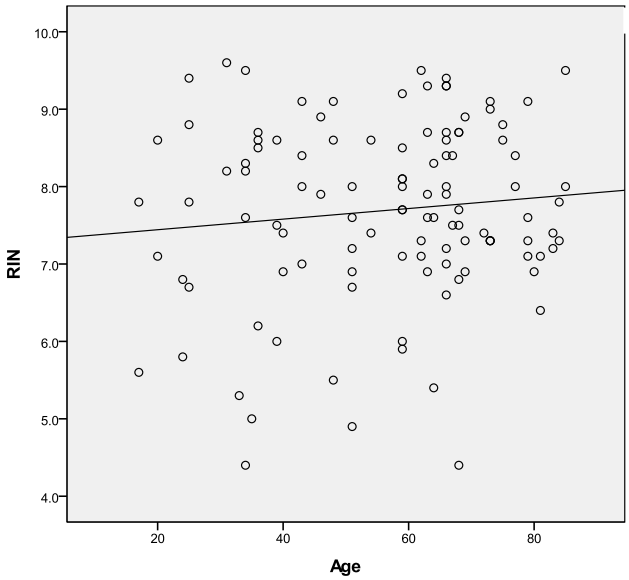

Figure 4.2 The RNA Integrity Number values for mRNA samples isolated from intestinal crypt cells is independent of sample subject age. Intestinal crypt cells were isolated from mucosal samples. The Agilent 2100 Bioanalyser® was used to assess mRNA quality by ascribing a RNA Integrity Number (RIN) value to each sample. Thereafter, RIN values were plotted against patient age (years) for each sample case. Age did not influence the quality of the RNA sample as measured by the RIN (R^2=0.011, p=0.27).

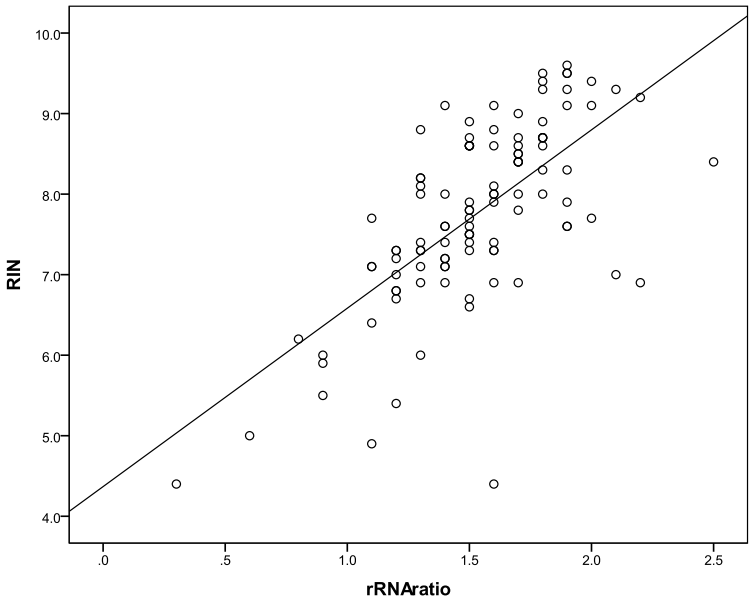

Figure 4.3 RNA Integrity Number and ribosomal RNA 28S:16S ratio values from intestinal crypt cell RNA samples show high correlation. Intestinal crypt cells were isolated and mRNA analysed using the Agilent 2100 Bioanalyser®. For each sample the RNA Integrity Number (RIN) and 28S:18S ribosomal RNA ratio (rRNAratio) was calculated and shown to highly correlate (R^2=0.448, p<0.001).

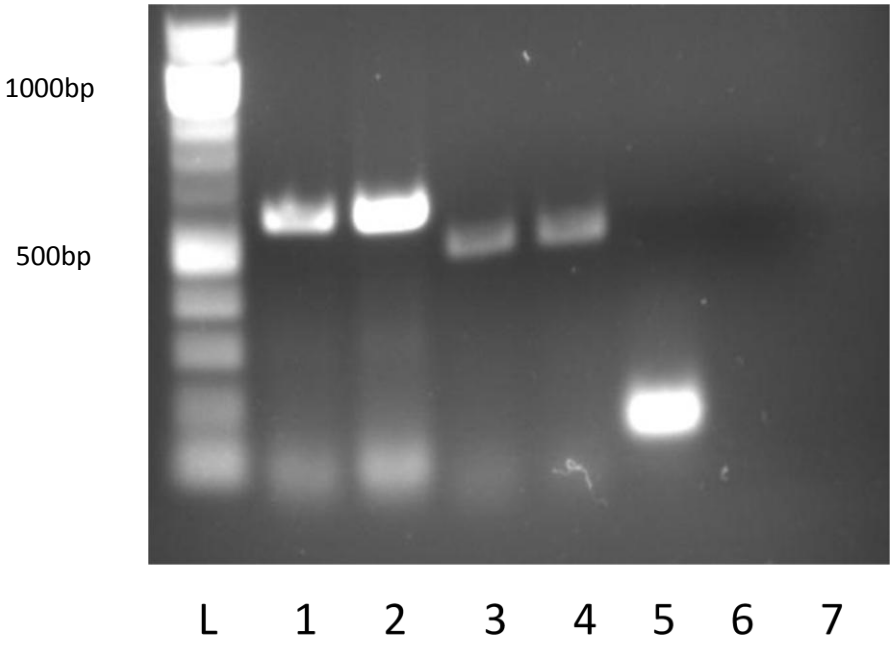

Figure 4.4 T84 cells express TLR2 and TLR4 mRNA. T84 epithelial cancer line cells were cultured to act as positive TLR2 and TLR4 mRNA controls. Isolated mRNA from T84 cells was amplified using RT-PCR. Amplicon products were run on a 1% agarose gel and visualised with an UV-transilluminator. A 100 base pair (bp) nucleotide size ladder is shown (L). Samples examined for TLR2 and TLR4 were run in duplicate with appropriate internal and negative controls.

Lanes 1 and 2: TLR2 (size 599bp)
Lanes 3 and 4: TLR4 (size 507bp)
Lane 5: HPRT (size 160bp)
Lane 6: No RT control
Lane 7: NTC

HPRT, Hypoxanthine guanine phosphoribosyltransferase; No RT, No reverse transcriptase; NTC, No template control; TLR, Toll-like receptor

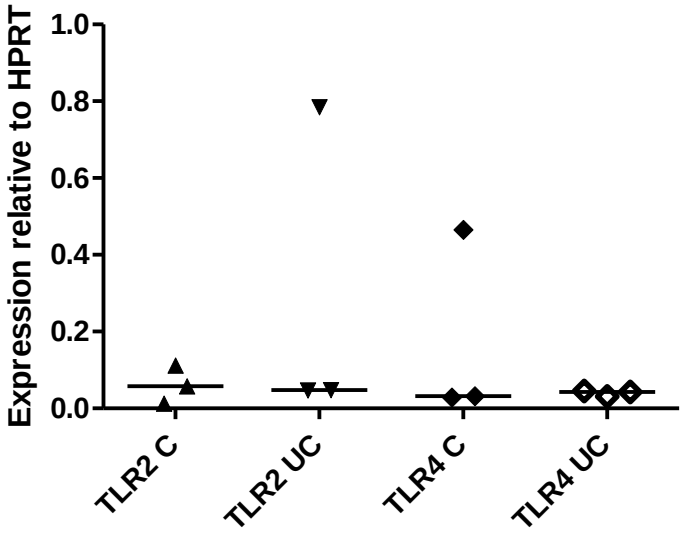

Figure 4.5 Intestinal crypt epithelial cells from patients with ulcerative colitis express similar levels of TLR2 and TLR4 mRNA compared to healthy controls. The expression of TLR2 and TLR4 RNA in large intestinal epithelial cells from healthy control subjects (C) and patients with ulcerative colitis (UC) were analysed using an RNA micro array. RNA samples were analysed using the Ambion MessageAmp II® RNA micro array kit. Absolute fluorescent intensity of gene spots was expressed relative to absolute expression of the housekeeping gene hypoxanthine-guanine phosphoribosyltransferase (HPRT).

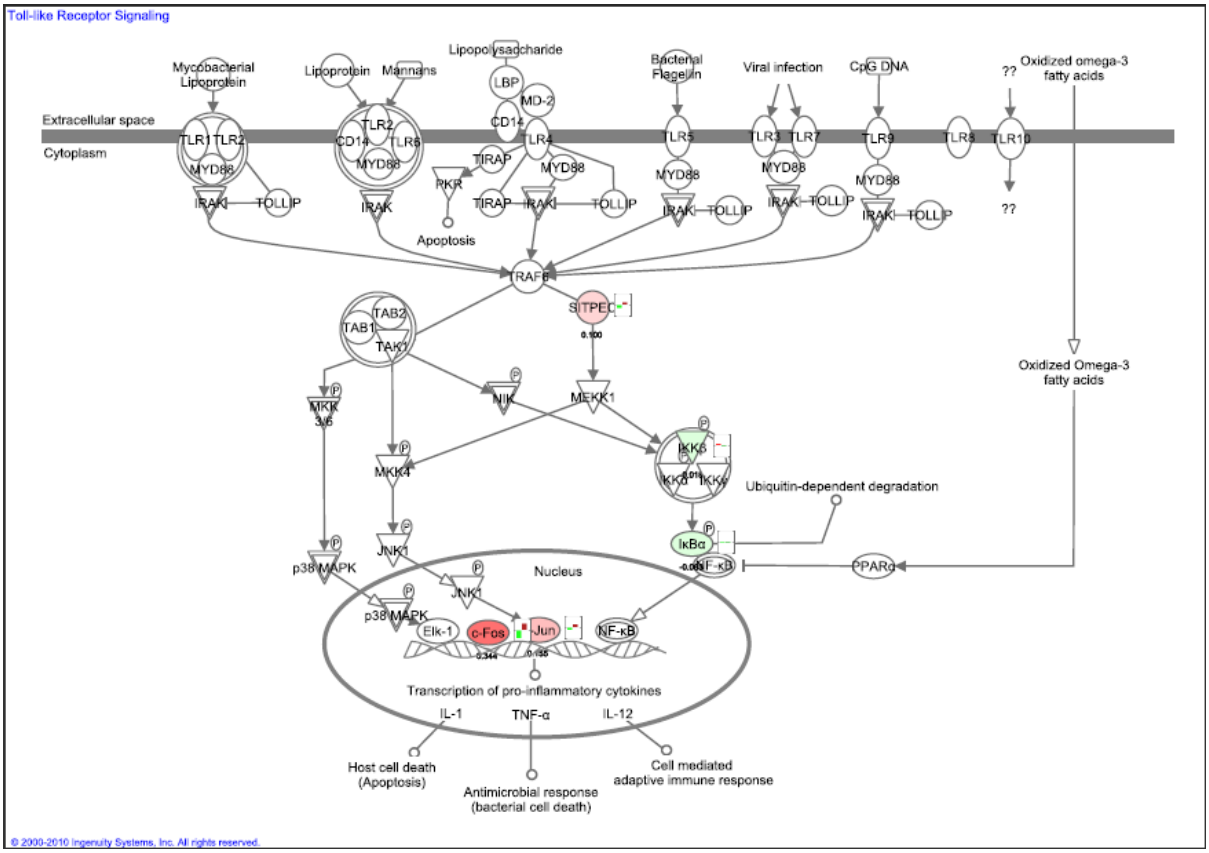

Figure 4.6 Intestinal epithelial cells from patients with ulcerative colitis show up-regulation of SITPEC, c-Fos and c-Jun, and down-regulation of IκBα and IκKβ mRNA expression using a micro array pathway analysis. The Toll-like receptor signalling pathway is shown following overlay of relative RNA expression levels from controls and ulcerative colitis patients using a "comparison analysis" in the Ingenuity Pathway Analysis® (IPA) software. Up-regulated signalling molecules in UC patients versus healthy controls are shown in red and down-regulated molecule are shown in green. This figure is derived from the IPA® software canonical pathway building function and unique to the overlaid data. SITPEC, c-Fos and c-Jun are up-regulated in UC, whereas IκBα and IκKβ are down-regulated in UC compared to control subjects ($p<0.05$ for all).

IκBα, Inhibitor of kappa B-alpha; IκKβ, Inhibitor of kappa B kinase-beta; SITPEC, signalling intermediate in Toll pathway, evolutionarily conserved.

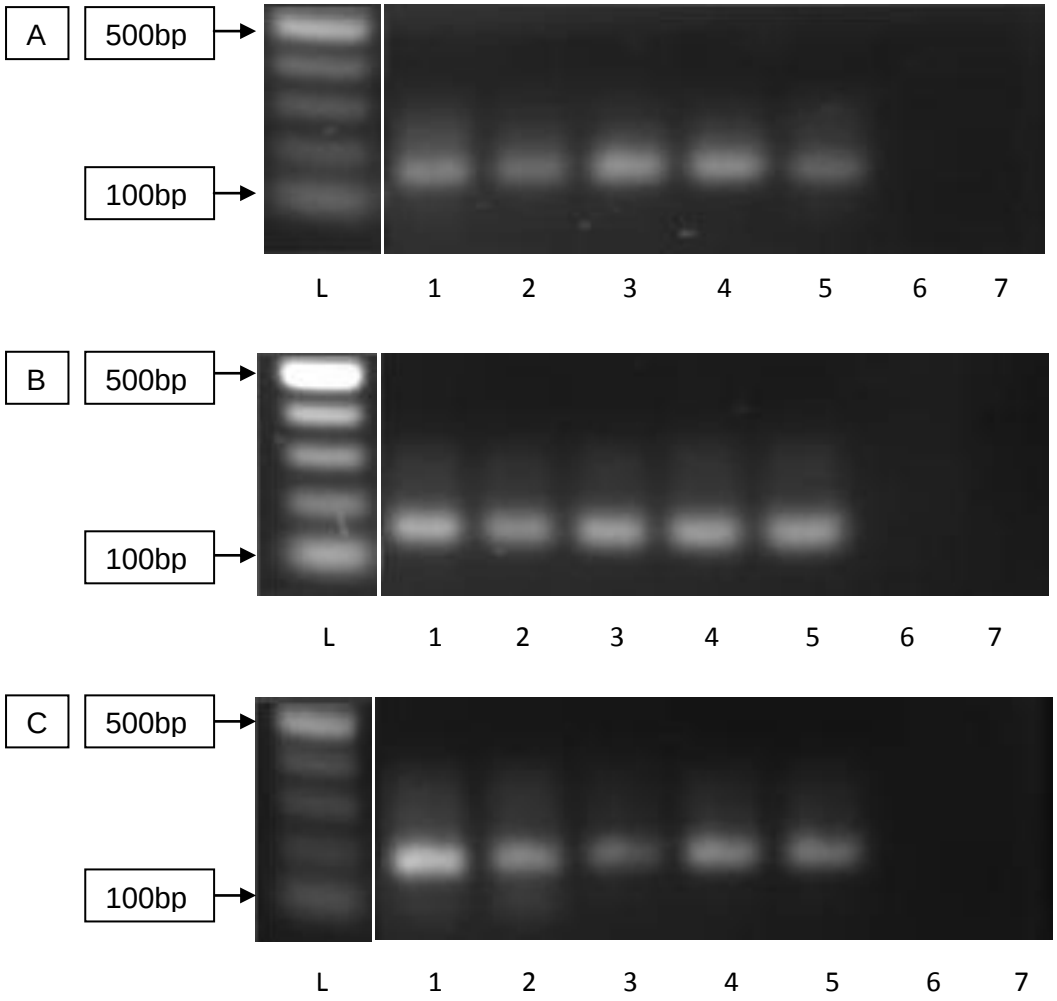

Figure 4.7 Isolated primary intestinal epithelial cells express TLR2 and TLR4 mRNA. The expression of (A) TLR2, (B) TLR4 and (C) HPRT mRNA in isolated primary intestinal epithelial cells was examined using conventional RT-PCR with bespoke real-time PCR primers. The ladder marks (L) correspond to 100bp increments and demonstrates PCR bands at the expected sizes (TLR2 134bp; TLR4 141bp; and HPRT 160bp). Subsequent DNA sequencing confirmed specificity for human TLR2, TLR4 and HPRT respectively.

Lane 1: Healthy control small bowel
Lane 2: Crohn's disease inflamed small bowel
Lane 3: Healthy control colon
Lane 4: Crohn's disease inflamed colon
Lane 5: Ulcerative colitis inflamed colon
Lane 6: No reverse transcriptase (negative) control
Lane 7: No cDNA template (negative) control.

Bp, base pairs; HPRT, Hypoxanthine guanine phosphoribosyltransferase; TLR, Toll-like receptor

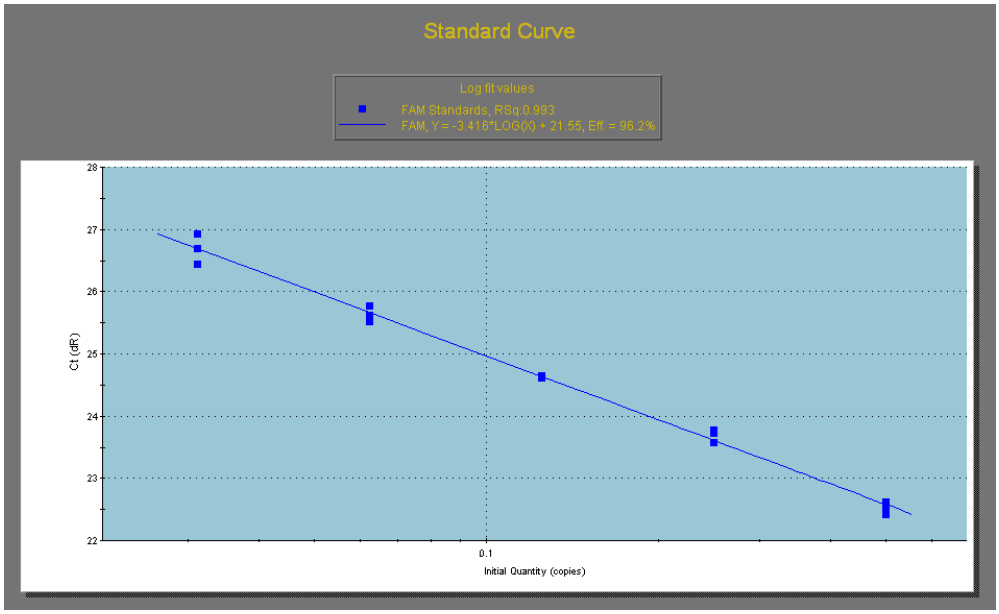

Figure 4.8 Standard curve analysis of TLR2 mRNA amplification using real-time RT-PCR and SYBR Green technology on serially diluted template mRNA from pooled primary crypt intestinal epithelial cells. To investigate the efficiency of the PCR reaction, standard dilutions (X-axis) of pooled cDNA samples from primary crypt intestinal epithelial cells were plotted against cycle threshold (Y-axis) on a logarithmic scale. This allowed derivation of the efficiency (E) of the PCR reaction from the slope of the plotted line using the equation: $E=10^{(-1/slope)}$.

TLR, Toll-like receptor

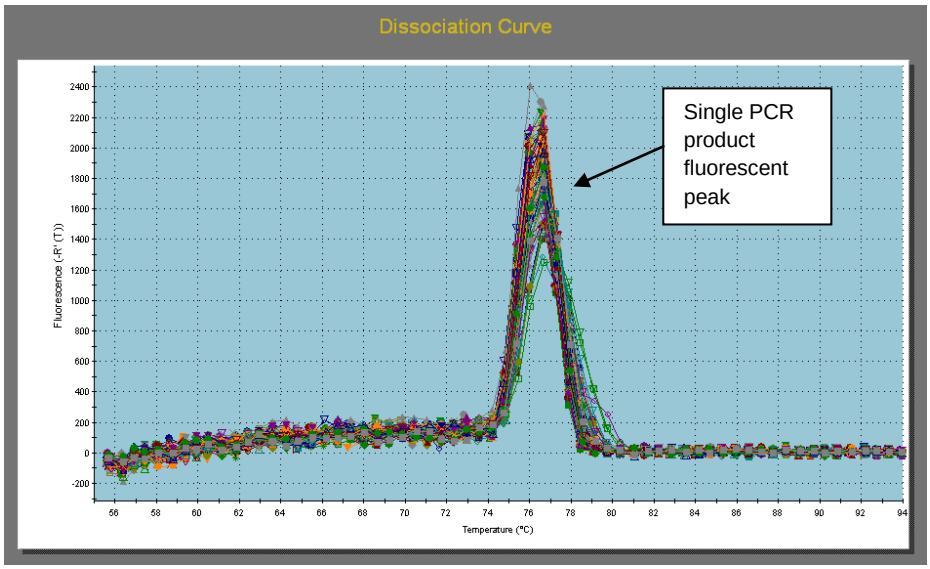

Figure 4.9 Dissociation curve analysis of TLR4 mRNA expression by primary crypt intestinal epithelial cells using real-time RT-PCR. To exclude the presence of undesirable oligonucleotide annealing and primer-dimer formation, a dissociation curve analysis was undertaken for each real-time RT-PCR run. Samples were healed from 55^{o}C to 95^{o}C (X-axis) in 0.5^{o}C increments and the fluorescent intensity (Y-axis) measured at every step. A dissociation curve with a single peak was observed in the absence of primer-dimer formation (illustrated by the absence of a fluorescent peak at annealing temperatures lower that the main PCR product dissociation peak).

RT-PCR, Reverse transcription polymerase chain reaction; TLR, Toll-like receptor

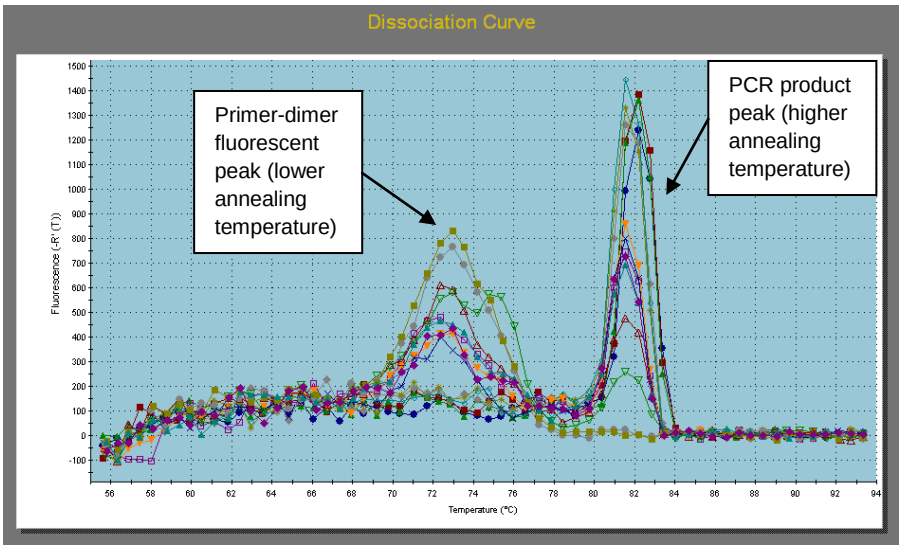

Figure 4.10 Dissociation curve analysis of TLR2 mRNA expression by primary crypt intestinal epithelial cells using real-time RT-PCR. During dissociation curve analysis, amplified cDNA samples using TLR2 primers were healed from 55^{o}C to 95^{o}C (X-axis) in 0.5^{o}C increments and the fluorescent intensity (Y-axis) measured at every step. A second fluorescent peak (at a lower annealing temperature that the main PCR product) was observed in cycling protocols generating primer-dimers.

RT-PCR, Reverse transcription polymerase chain reaction; TLR, Toll-like receptor

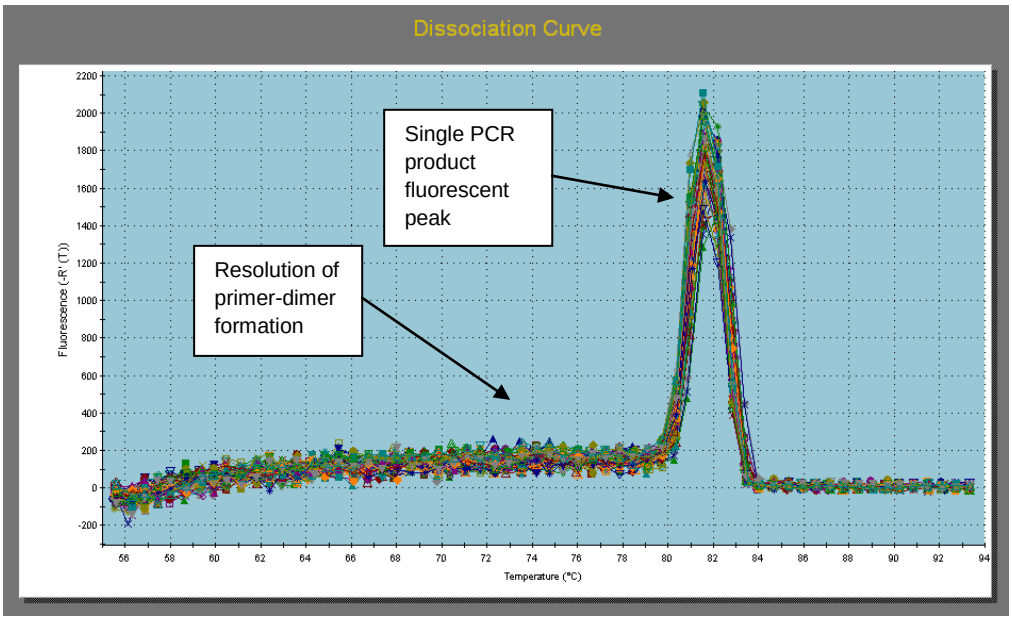

Figure 4.11 Dissociation curve analysis of TLR2 mRNA expression by primary crypt intestinal epithelial cells using real-time RT-PCR with the inclusion of a fourth (acquisition) step in the real-time RT-PCR protocol. During dissociation curve analysis, amplified cDNA samples using TLR2 primers with a modified protocol, which included a fourth (acquisition) step, were healed from 55^{o}C to 95^{o}C (X-axis) in 0.5^{o}C increments and the fluorescent intensity (Y-axis) measured at every step. A dissociation curve with a single peak was observed in the absence of primer-dimer formation (illustrated by the absence of a fluorescent peak at annealing temperatures lower that the main PCR product dissociation peak).

RT-PCR, Reverse transcription polymerase chain reaction; TLR, Toll-like receptor

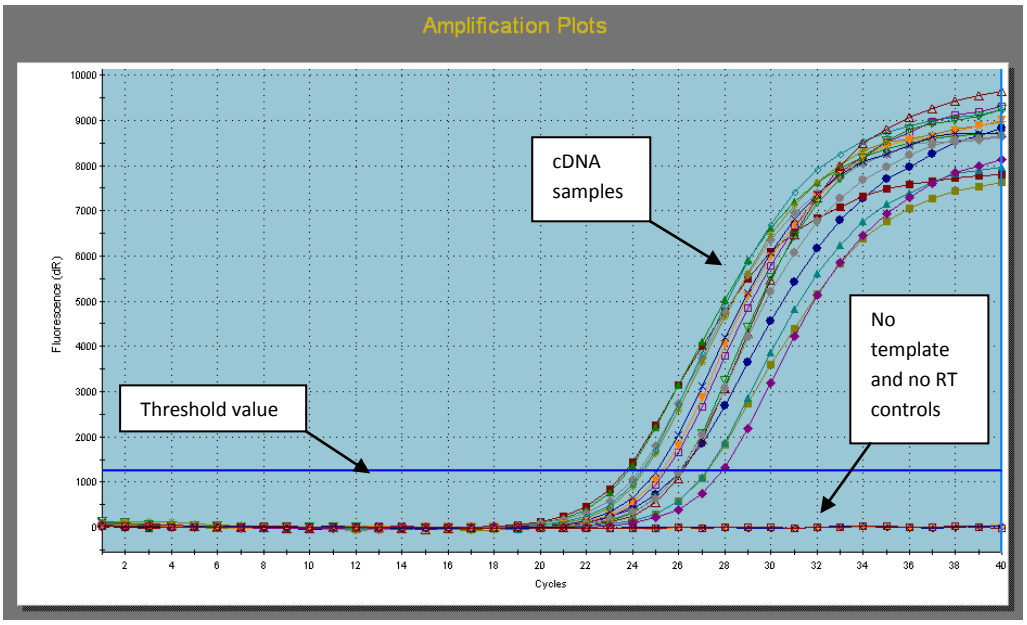

Figure 4.12 Amplification plot of TLR2 mRNA expression by primary crypt intestinal epithelial cells using real-time RT-PCR. To exclude the possibility of non-specific cDNA amplification causing erroneous fluorescent signal during the PCR cycling protocol, wells with no nucleic acid (no template controls, NTC) and no cDNA (no reverse transcriptase controls, no RT) were included in all real-time RT-PCR runs in addition to wells containing cDNA from sample cases. The absence of fluorescent signal (Y-axis) in control wells indicated absence of non-specific cDNA amplification.

NTC, No template control; RT, Reverse transcription; TLR, Toll-like receptor

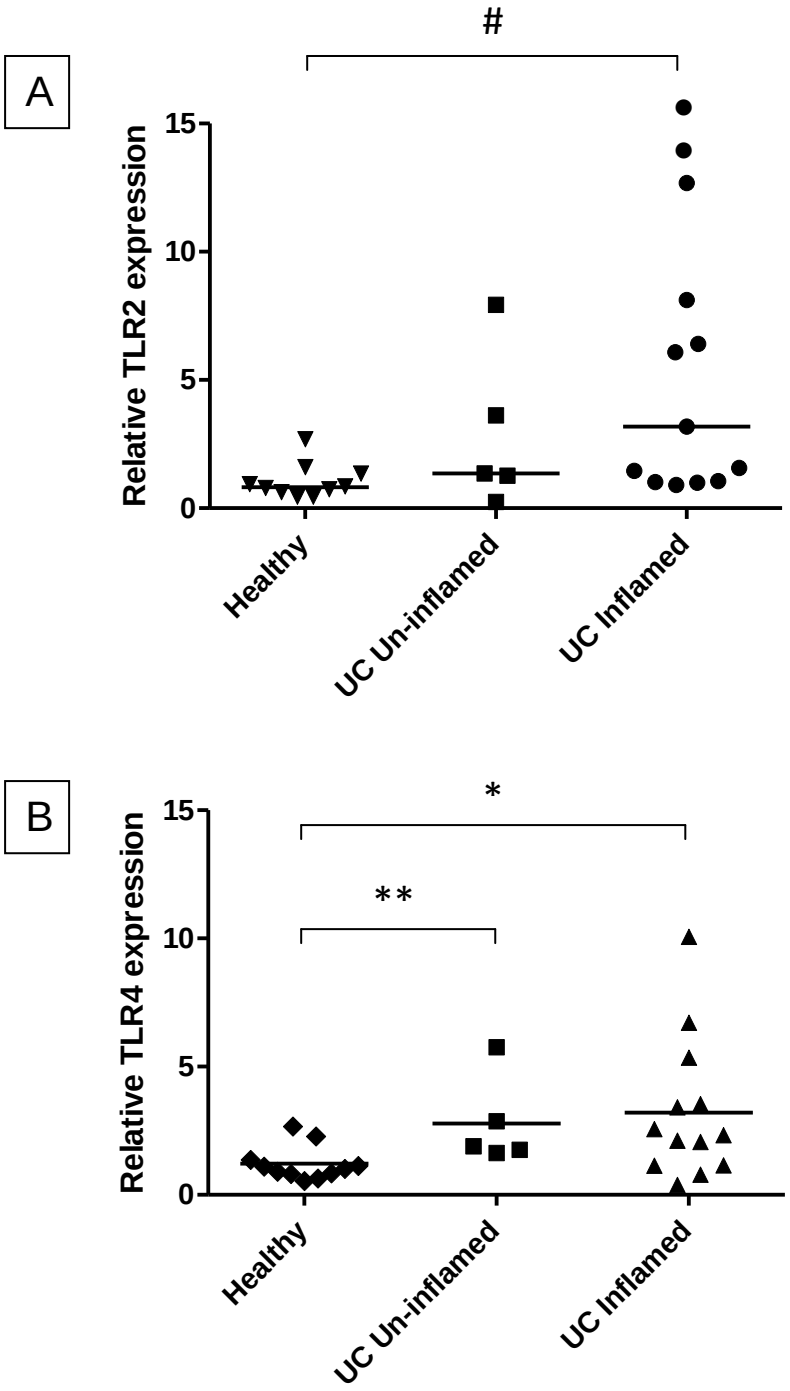

Figure 4.13 TLR2 and TLR4 mRNA expression is up-regulated in colonic epithelial cells from patients with inflamed ulcerative colitis, and TLR4 mRNA is up-regulated in normal (un-inflamed) ulcerative colitis. The relative expression of (A) TLR2 and (B) TLR4 mRNA in isolated colonic intestinal epithelial cells from patients with ulcerative colitis (UC) was compared to healthy controls. UC samples were graded as un-inflamed (normal) or inflamed by histological assessment. Each data point represents the mean TLR2 or TLR4 mRNA expression of three samples per patient, expressed relative to a pooled sample of healthy controls using real-time RT-PCR. Horizontal bars represent median expression.
p=0.003; * p=0.024; ** p=0.017

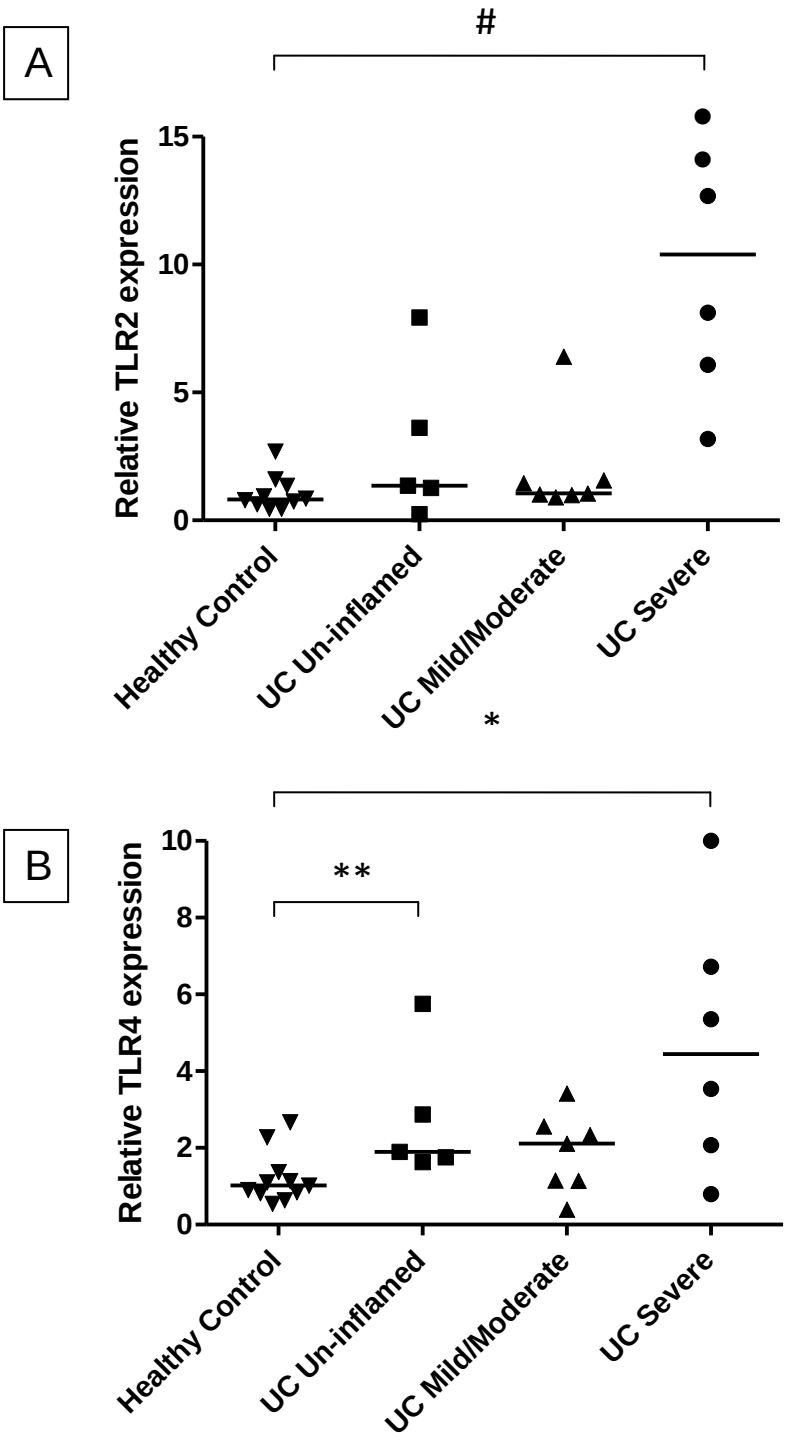

Figure 4.14 Observed up-regulation of TLR2 and TLR4 mRNA expression in colonic epithelial cells from patients with inflamed ulcerative colitis is predominantly seen in samples from histologically severe disease. The relative expression of (A) TLR2 and (B) TLR4 mRNA in isolated colonic intestinal epithelial cells from patients with ulcerative colitis (UC), graded by severity of histological inflammation, was compared to healthy controls. UC samples were graded using the method described by Riley *et al.* (235). Samples of mild or moderate severity were combined to form a single group (Mild/Moderate). Each data point represents the mean TLR2 or TLR4 mRNA expression of three samples per patient, expressed relative to a pooled sample of healthy controls using real-time RT-PCR. Horizontal bars represent median expression.
# $p<0.001$; * $p=0.031$; ** $p=0.017$

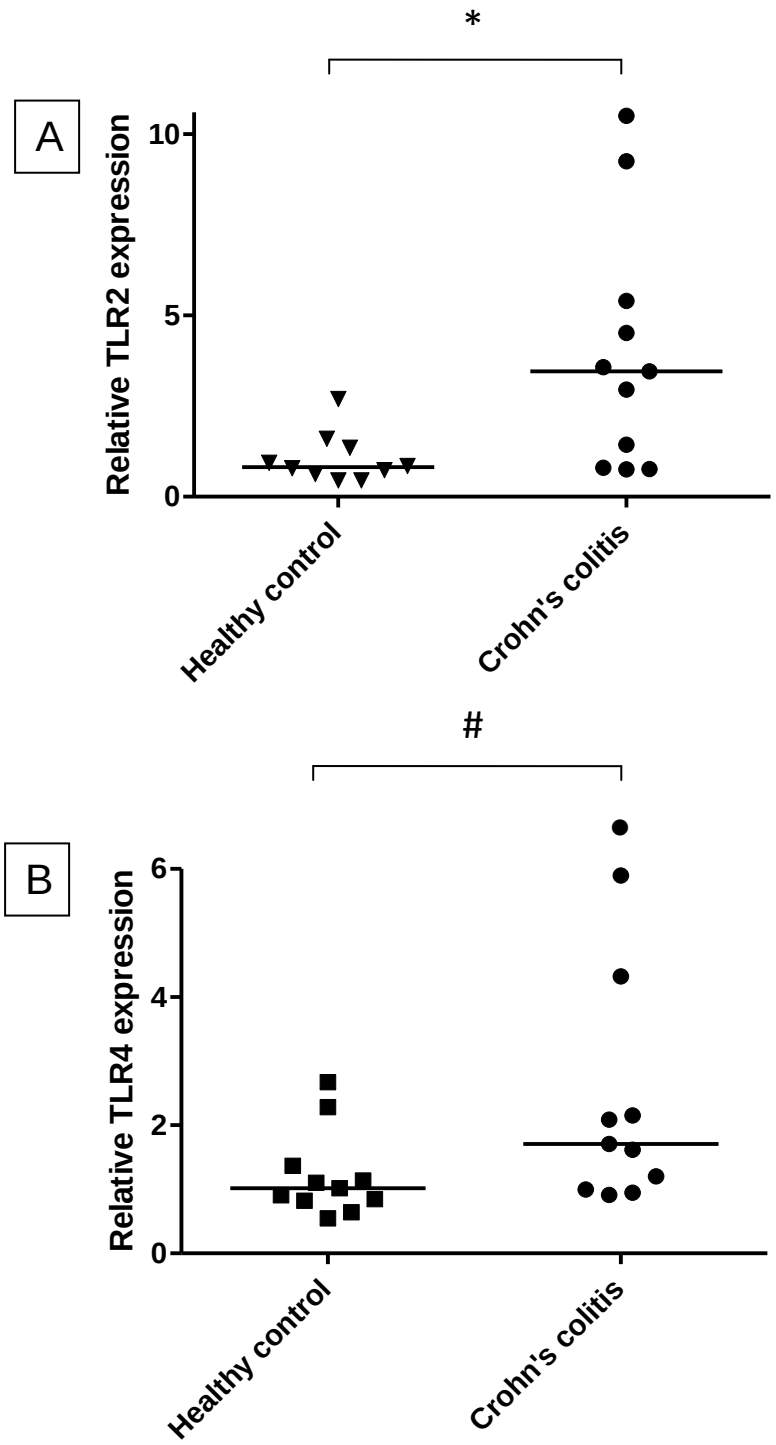

Figure 4.15 TLR2 and TLR4 mRNA expression is up-regulated in colonic epithelial cells from patients with inflamed Crohn's colitis. The relative expression of (A) TLR2 and (B) TLR4 mRNA in isolated colonic intestinal epithelial cells from patients with Crohn's disease (CD) was compared to healthy controls. Each data point represents the mean TLR2 or TLR4 mRNA expression of three samples per patient, expressed relative to a pooled sample of healthy controls using real-time RT-PCR. Horizontal bars represent median expression.
* p=0.012; # p=0.042

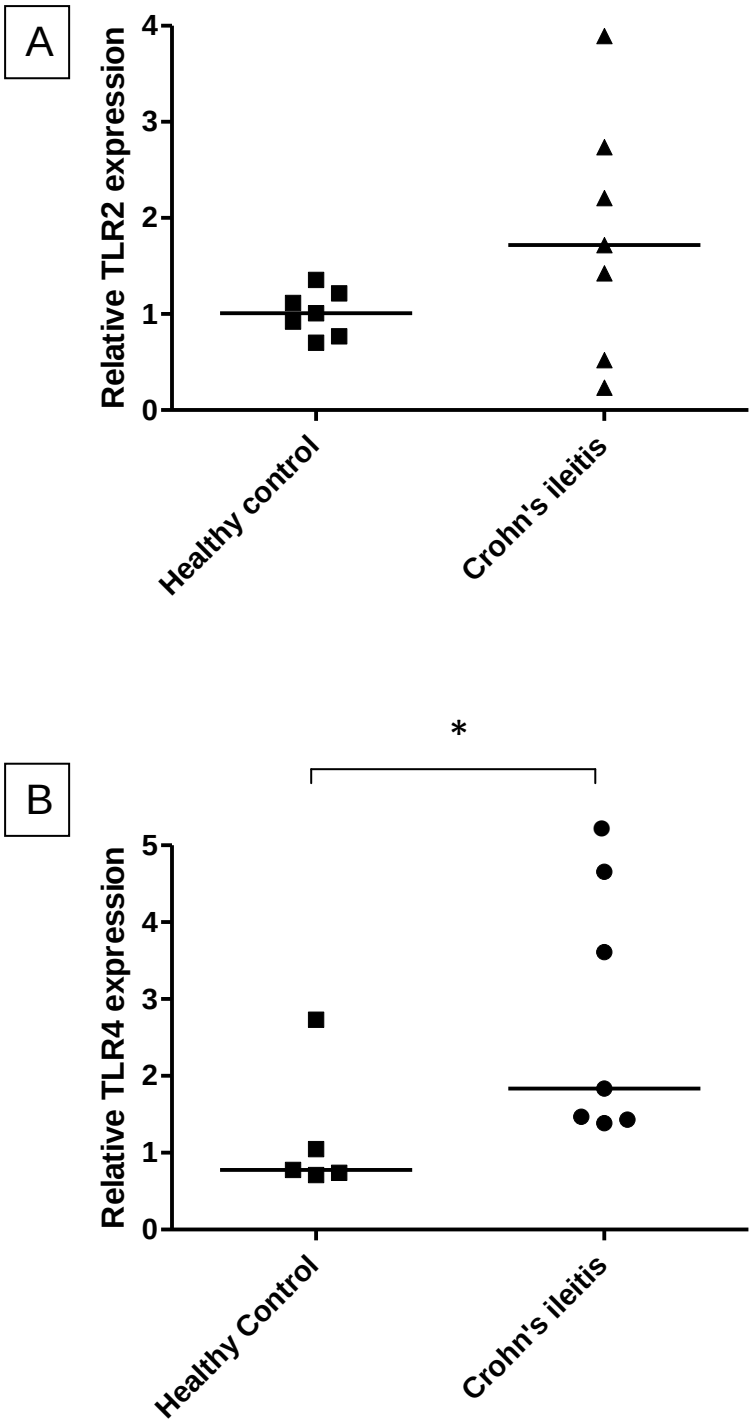

Figure 4.16 TLR4 mRNA expression is up-regulated in small intestinal epithelial cells from patients with Crohn's ileitis. The relative expression of (A) TLR2 and (B) TLR4 mRNA in isolated small intestinal epithelial cells from patients with Crohn's disease was compared to the expression in healthy controls. Each data point represents the mean TLR2 or TLR4 mRNA expression of three samples per patient, expressed relative to a pooled sample of healthy controls using real-time RT-PCR. Horizontal bars represent median expression.
* p=0.030

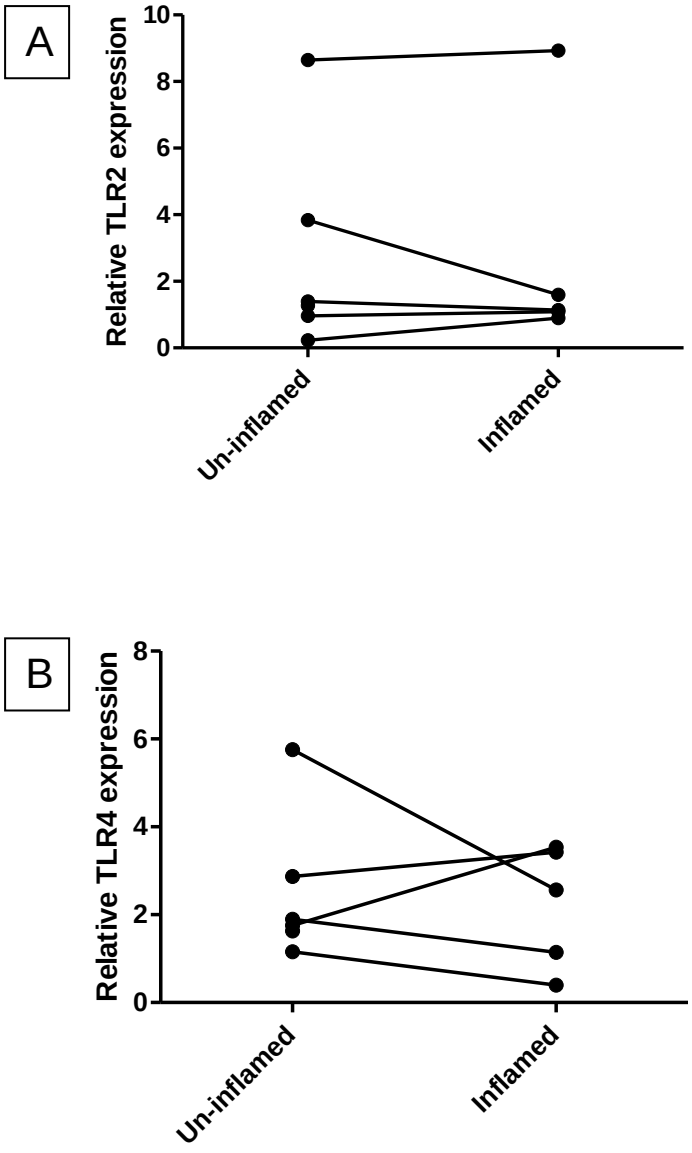

Figure 4.17 Intestinal crypt epithelial cells from histologically normal and inflamed regions of large bowel express similar levels of TLR2 and TLR4 mRNA in patients with isolated left-sided ulcerative colitis. Intestinal crypt epithelial cells were isolated from region of un-inflamed (right-sided) and inflamed (left-sided) colon in patients with endoscopically and histologically confirmed left-sided ulcerative colitis (Montreal classification E2). The expression of (A) TLR2 and (B) TLR4 mRNA was calculated relative to expression from a pooled sample of healthy controls using real-time RT-PCR. Each data point represents the mean TLR2 or TLR4 mRNA expression of three samples per patient.

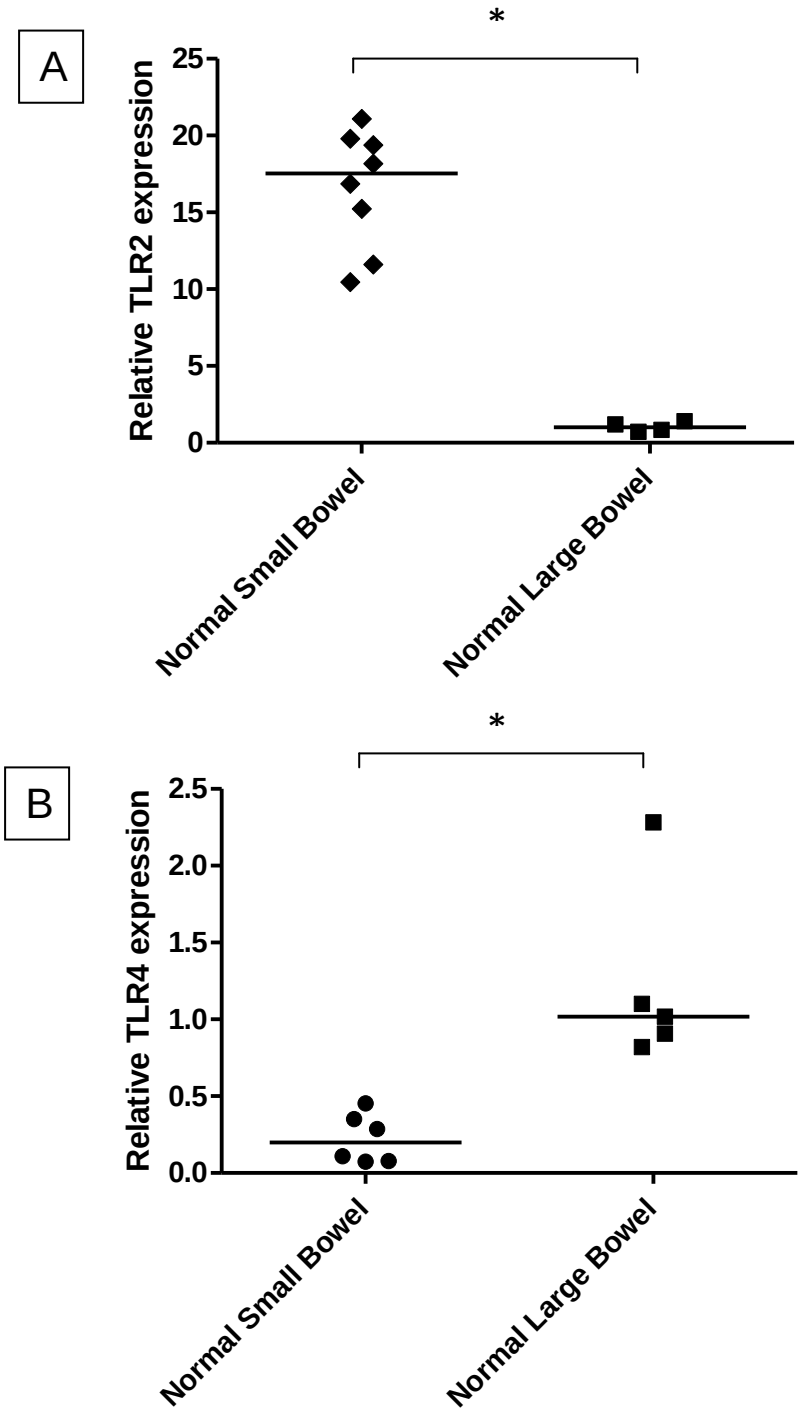

Figure 4.18 Healthy small bowel intestinal crypt epithelial cells express greater TLR2 mRNA but less TLR4 mRNA than healthy colonic intestinal crypt epithelial cells. The relative expression of (A) TLR2 and (B) TLR4 mRNA in isolated small intestinal epithelial cells from healthy controls was compared to their expression in colonic IEC from healthy controls. Each data point represents the mean TLR2 or TLR4 mRNA expression of three samples per subject, expressed relative to a pooled sample of healthy large bowel control subjects using real-time RT-PCR. Horizontal bars represent median expression.
* p=0.004

4.5 Discussion

In order to accurately and meaningfully assess the expression of any gene at the mRNA level it is important to obtain nucleic acid samples of high quality. Examination of the 18S and 28S ribosomal RNA species following electrophoresis and spectrophotometric analysis have historically been the two main methods used for assessing RNA qualitatively and quantitatively, respectively (216). Micro-fluid capillary electrophoresis is a recent technique that quantifies RNA quality and assigns a RNA Integrity Number (RIN) (218). RNA samples with a RIN above between 6 and 7 have been reported as being of suitable quality for down-stream applications regardless of the length of storage at -80^{o}C (220). Critically it has been demonstrated that relative gene expression declines with declining RIN values, whereas samples of similar RIN demonstrate comparable gene expression (217).

With this in mind, primary IEC samples with a RIN $\geq$6.5 were considered suitable for down-stream applications. RIN values were not significantly different amongst the healthy control, UC and Crohn's disease groups. Furthermore, RIN values were similar regardless of the degree of inflammation, small or large intestine origin, or various demographics including patient age, medical history, concurrent medication use, tissue sample weight or isolated IEC viability. Therefore, it was concluded that all isolated IEC RNA samples were of comparable quality and were suitable for subsequent qualitative and quantitative analysis.

Several human intestinal cancer cell lines were used as positive controls for TLR2 and TLR4 transcript expression, as reported in the literature. The human colon cancer cell line T84 and the human monocyte cell line THP-1 demonstrated high TLR2 and TLR4 mRNA expression using both conventional RT-PCR and real-time RT-PCR primer pairs. Subsequent sequencing confirmed primer pair specificity. Of interest, the colon cancer cell line HT-29 demonstrated variable and inconsistent TLR2 and TLR4 expression. This observation has been previously reported (122) and may be due to a number of factors, including DNA methylation (233), its luminal rather than crypt origin (246, 249, 250), or due to confluent cell

monolayer culture growth (248). Indeed, down-regulation of TLR2 and TL4 expression by IEC as they differentiate and migrate along the crypt-villus axis may be one mechanism for the observed epithelial tolerance to commensal bacteria in the intestinal lumen.

It was initially important to determine TLR2 and TLR4 mRNA expression by crypt IEC isolated from patients in this cohort. Therefore a spotted RNA micro array was undertaken using samples from healthy controls and patients with UC. A two-channel RNA micro array was chosen because it allows relative gene expression to be investigated between two sample groups using the minimal number of chips, thus minimising cost. Micro arrays have the advantage of allowing the analysis of a large number of genes during a single experimental run. Moreover, the gene-specific features on the micro array chip itself can be produced in a bespoke fashion to suit the specific interests of the researcher. Finally, it is possible to use the intensity of the fluorescent signal at the gene of interest to semi-quantitatively characterise relative gene expression between two groups, a process which would generally require subsequent confirmation with fully quantitative methods such as real-time RT-PCR.

To limit cost, three healthy controls and three patients with inflammatory UC were chosen for the micro array experiment. Expression of mRNA for TLR1-10 and several intracellular TLR-associated signalling molecules was demonstrated. From this data further analysis using quantitative methods was deemed suitable and subsequently undertaken.

To further investigate and verify the micro array data for TLR2 and TLR4 mRNA expression, conventional RT-PCR analysis on a larger number of crypt IEC samples from healthy controls and patients with IBD was undertaken, both on samples from the small and large intestine. This confirmed transcript expression of TLR2 and TLR4 in these patient groups. The expression of TLR2 and TLR4 mRNA in primary human IEC has previously been reported in a small number of publications. Otte *et al.* described EDTA-isolated colonic crypt

IEC expression of TLR1-9 transcripts, with variable expression of TLR7 and non-expression of TLR10 mRNA (243). Abreu *et al.* and Wolfs *et al.* used laser capture microdissection to demonstrate TLR4 mRNA expression in primary IEC, the former reporting expression in colonic IEC, and the latter demonstrating that TLR4 mRNA expression was limited to the crypts rather than the villi of the small intestine (154, 258). Bocker *et al.* used dispase to demonstrate TLR4 and variable TLR2 transcripts expression in isolated colonic crypt IEC from healthy mucosa (122).

Therefore these data confirm previous reports in the literature and add to the current body of evidence on qualitative TLR2 and TLR4 mRNA expression in human primary IEC. It can be concluded that crypt intestinal epithelial cells of the small and large intestine express TLR2 and TLR4 and have the potential to sense Gram-positive and Gram-negative bacterial cell wall components of the intestinal flora.

To investigate differential expression of TLR2 and TLR4 transcript in crypt IEC in patients with UC compared to healthy controls, a semi-quantitative analysis using the RNA micro array data was undertaken. Expression of TLR2 and TLR4 mRNA was normalised to the housekeeping gene HPRT and compared between the UC and healthy control groups. No statistical difference in expression was detected between the two groups. There are a number of possible reasons to explain this observation. Firstly, TLR2 and TLR4 mRNA may not be differentially expressed in active UC. Secondly, the sample size (three samples per group) may have been too small to detect any differences in transcript expression at a statistically significant level. Thirdly, semi-quantitative analysis of relative gene expression using RNA micro array technology may be less accurate than fully quantitative methods, such as real-time RT-PCR, particularly when using mRNA samples from primary biological samples compared to cultured cell lines. Fourthly, mRNA samples from two of the three UC patients were from regions of only mild to moderate inflammation, as assessed by the Riley score (235). It is possible that differential expression of TLR2 and TLR4 mRNA is related to

the degree of inflammation such that a significant change in transcript expression is detectable only in the most severely inflamed tissue. Indeed, the relative expression in the patient with severely inflamed UC was greater than the expression in either of the mild to moderately inflamed patient samples.

Therefore the analysis of a larger number of samples from a variety of disease activities was undertaken using real-time RT-PCR. Notably TLR2 and TLR4 mRNA was shown to be significantly up-regulated both in colonic crypt IEC from patients with inflamed UC and inflamed Crohn's colitis. Critically, the expression of TLR2 and TLR4 transcripts in crypt IEC isolated from regions of severely active UC were up-regulated to a greater degree (10.4- and 4.45-fold, respectively) than in crypt IEC from patients with mild to moderately inflamed UC (1.06- and 2.12-fold, respectively), suggesting gene expression of TLR2 and TLR4 was related, in part, to the severity of disease activity.

Even more intriguing is the observation that TLR4 mRNA was up-regulated in crypt IEC derived from regions of histologically normal (un-inflamed) colon in UC. If TLR4 up-regulation was purely a secondary phenomenon occurring in response to local mucosal tissue inflammation, relative TLR4 expression in normal UC tissue would be expected to be similar to TLR4 expression in healthy controls. The observation in this study that TLR4 was up-regulated in crypt IEC from normal (un-inflamed) UC mucosa suggests constitutive TLR4 transcript expression in these patients.

Furthermore, a sub-group of five UC patients with histologically and macroscopically left-sided UC was collected. Paired samples of isolated crypt IEC mRNA expression for TLR2 and TLR4 were analysed, comparing histologically normal (un-inflamed) right-sided samples with inflamed left-sided samples. Despite crypt IEC TLR2 and TLR4 mRNA expression in this sub-group being significantly up-regulated compared to healthy controls, there was no difference in expression between left- and right-sided samples for either TLR2 and TLR4,

suggesting similar expression of these genes in crypt IEC derived from normal and inflamed UC mucosa. This further suggests that TLR2 and TLR4 mRNA expression is constitutively expressed in colonic crypt IEC in patients with UC, and may be a primary event in the pathogenesis of ulcerative colitis. Interestingly, epithelial TLR4 over-expressing mice develop more severe experimental DSS-induced colitis than wild type mice, implying constitutive (pre-induction) TLR4 expression plays a role in colitis susceptibility (273), supporting the observation in this study that IEC from patients with UC expressed higher levels of TLR4 mRNA in regions of histologically normal colon.

In support of TLR2 and TLR4 mRNA up-regulation being a secondary event in IEC, *in vitro* data has reported up-regulation of TLR2 and TLR4 mRNA in intestinal epithelial cell lines in response to pro-inflammatory cytokines. Differential expression of TLR2, TLR3 and TLR4 mRNA has been reported in HT-29 and T84 cell monolayers in response to co-culture with various intestinal bacteria (252, 253). TNFα and IFNγ are reported to up-regulate TLR4 mRNA in HT-29 and T84 cell lines (154) and IFNγ up-regulates TLR2 to TLR5 mRNA and TLR4 protein in a variety of human IEC lines (155).

Moreover, patients with active inflammatory bowel disease demonstrate higher levels of both peripheral blood and gut mucosal tissue pro-inflammatory cytokines (274). This observed systemic inflammatory response, which may result in elevated cytokine levels in the intestinal mucosa of un-inflamed bowel, may explain the up-regulation of TLR2 and TLR4 mRNA in primary IEC isolated from histologically normal mucosa in patients with left-sided UC.

It would seem conceivable that high levels of *in vivo* pro-inflammatory cytokines in the mucosa of patients with IBD could result in up-regulation of TLR2 and TLR4 expression. This may explain the greater up-regulation of TLR2 and TLR4 in crypt IEC derived from severely inflamed compared to mild or moderately inflamed mucosa observed in this study. It would

be interesting to investigate if TLR2 and TLR4 expression could be suppressed with successful immunosuppressive treatment for IBD, particularly following biological anti-TNFα therapy, and to investigate whether there is a difference in the magnitude of suppression of TLR2 and TLR4 expression in patients who clinically respond to immunosuppressive treatment compared to the so-called non-responders.

Toll-like receptors are reported to play a complex role in maintaining intestinal gut homeostasis. On one hand, TLR-mediated bacterial sensing is vital to the development of mature mucosal associated lymphoid tissue (99, 100) and TLR signalling protects mice against radiation-induced enteropathy (101), ischaemic-reperfusion injury (102) and chronic inflammation (103). TLR signalling facilitates bacterial sensing by intestinal epithelial m-cells which play a role in maintaining tolerance to intestinal luminal bacteria (115). Furthermore, oral TLR2 and TLR4 ligands and parenteral TLR3 and TLR9 ligands protect mice against DSS-induced colitis (159), and both TLR4 (160) and TLR5 (161) ligands protect against radiation-induced enteritis.

On the other hand, intestinal inflammation has been shown to be in part mediated by enhanced IEC-associated TLR signalling. TLR-expressing IEC up-regulate their expression of T cell-associated co-stimulation molecules (119) and can induce naïve T cells to differentiate into a pro-inflammatory, IFNγ-secreting T_{H1} cell phenotype (120). Over-expression of TLR2- and TLR4-positive DC is reported in the lamina propria in Crohn's disease (133). TLR-knock out mice have been shown to be protected against various experimental models of colitis, while TLR5 and TLR9 ligands exacerbate established chronic DSS-induced experimental colitis (159). Furthermore, both a TLR4 antagonist (164) and an anti-TLR4 monoclonal antibody (165) are reported to improve inflammation in established acute DSS-induced colitis.

Therefore current literature suggests that epithelial TLR signalling maintains intestinal homeostasis and induces a tolerogenic state to luminal antigens in the healthy state, whereas TLR signalling exacerbates inflammation in the situation of established colitis. Given the observation in this study that TLR4 is constitutively expressed in crypt IEC in the colon of histologically normal UC patients, it is possible that TLR4 ligation may provide a therapeutic option in maintaining remission in quiescent disease. Conversely, the finding of marked up-regulation of TLR2 and TLR4 in crypt IEC of patients with both UC and Crohn's colitis, particularly in IEC derived from regions of severely inflamed mucosa, may suggest that blockade of TLR2 and TLR4 signalling could improve intestinal inflammation in active disease.

Regarding the small intestine, quantitative real-time RT-PCR data demonstrated approximately two-fold up-regulation of TLR4 mRNA in the inflamed ileum of patients with Crohn's ileitis. Although up-regulation of TLR2 mRNA was of a similar magnitude, it did not reach statistical significance. Up-regulation of both TLR2 and TLR4 transcripts in Crohn's ileitis was less marked than in Crohn's colitis or UC. One possible explanation is that many of the patients included in this study required small intestinal resection for chronic stricturing Crohn's disease rather than for treatment-refractory inflammatory disease. Indeed, epidemiological data suggests that most patients with ileal Crohn's disease progress initially from an inflammatory phenotype to either a fistulating or a stenosing phenotype over the disease course (181). Chronic stricturing Crohn's disease tends not to respond to immunosuppressive or biological treatment, and symptoms from this disease phenotype are usually secondary to mechanical bowel obstruction rather than inflammation per se. Therefore, this group of patients with Crohn's disease may not be the most suitable for investigating TLR2 and TLR4 expression. Another explanation is that TLR2 and TLR4 over-expression is less important in the pathogenesis of Crohn's ileitis and other pathways play a more crucial role.

Crohn's disease is characterised by so-called skip lesion, regions of transmural inflammation interspersed between regions of normal (un-inflamed) mucosa (2). Mucosal samples from regions of inflamed Crohn's colitis could easily be identified macroscopically and subsequently confirmed histologically. However, obtaining normal (un-inflamed) samples from patients with Crohn's colitis is more challenging. Normal-appearing tissue can turn out to be microscopically inflamed. In addition, due to the intermittent nature of the disease, it was not possible to be certain that samples taken from a reportedly un-inflamed specimen were not actually taken from adjacent regions of inflamed mucosa. Therefore it was not possible to obtain a reliable group of colonic crypt IEC from normal Crohn's colitis and the evaluation of the expression of TLR2 and TLR4 in normal Crohn's colitis was not possible.

The healthy control groups in this study were derived from patients undergoing surgical resection for colon cancer. Inflammatory bowel disease affects younger persons and it was not surprising that the IBD patient population was significantly younger than the healthy control population. Comparing non-age matched groups raises the possibility that inter-group differences are a result of age rather than disease process. To address this, two age groups of healthy control subjects were analysed. Younger controls (statistically similar in age to the IBD patients) expressed similar levels of TLR2 and TLR4 transcripts compared to statistically older controls. This suggests the expression TLR2 and TLR4 transcripts did not vary with age. Therefore it was concluded that the observed differences in expression were not age-related.

The data reported in this study are new in that quantitative expression of TLR2 and TLR4 mRNA in a wide range of IBD patient groups has not been published. Naik *et al.* reported similar levels of TLR2 mRNA expression in two paediatric patients with Crohn's ileocolitis compared to healthy controls, but mRNA expression was analysed by visually examining electrophoresis gel band width following conventional RT-PCR rather than using a fully quantitative method (263). Melmed *et al.* reported down-regulation of TLR1 mRNA, but no

differential expression of TLR2 or TLR6 mRNA, between paired un-inflamed and inflamed colonic IEC, isolated by laser capture micro-dissection, from two patients with UC (231). However, no healthy controls were used for comparison and the sample size was small in this study. Interestingly, mRNA for both TLR2 and TLR4 are reported to up-regulate in IEC in mice following induction of DSS colitis (250, 275).

The final aspect of the characterisation of TLR2 and TLR4 mRNA expression in UC samples related to the comparison analysis in the IPA software using the RNA micro array data. Pathway analysis of the three cases of UC compared to the three healthy controls demonstrated up-regulation of two MAP kinase-associated signalling molecules, c-Jun and c-Fos, and up-regulation of the signalling molecule ECSIT (SITPEC) in the crypt IEC derived from the UC patients. Moreover, transcripts for the NF-κB-regulating molecule IκBα was down-regulated in UC patients. Although differential expression of signalling molecules in the MAP kinase and NFκB pathways are not unique to TLR signalling, the up-regulation of ECSIT is intriguing. ECSIT is an intracellular signalling molecule of the TLR/IL-1 pathway (84) and has been implicated in TLR-dependent macrophage killing of bacteria via mitochondria-derived reactive oxygen species (276). These data suggest that the TLR signalling pathway is up-regulated in crypt IEC derived from patients with UC, though further investigation into the regulation and functional state of signalling molecules in the TLR pathway is clearly required.

It has been reported in mice that TLR2 mRNA is predominantly expressed in the distal small intestine and the proximal colon, with TLR4 mRNA predominantly expressed in the distal colon (250). Although compartmental expression of TLR2 and TLR4 has not been reported in the human intestine, Bocker *et al.* reported predominant expression of TLR4 mRNA in the colon, with TLR2 mRNA expression being weaker and more variable (122). To address this question, samples of mRNA from normal distal small intestine and colon were analysed using real-time RT-PCR. The data showed that TLR2 mRNA is more than ten-fold higher in

the small intestine compared to the colon, whereas colonic TLR4 transcript expression is five-fold that of the small intestine. This is consistent with the mouse data suggesting compartmental TLR2 and TLR4 expression in the intestine with a shift from TLR2 to TLR4 in the distal large bowel (250).

It is unclear why this pattern of TLR2 and TLR4 expression should be the case. The greatest burden of bacteria is found in the colon and it may be functionally more critical for the host to sense Gram-negative bacteria in this region to maintain homeostasis. Interestingly, the survival of Gram-negative bacteria in the ileal mucosa and their translocation to the mesenteric lymph nodes is well described in Crohn's ileitis (13). The relatively lower expression of TLR4 in the distal small bowel may increase the likelihood of mucosal invasion and immune system evasion by Gram negative bacteria, such as adherent invasive *E coli*, in individuals predisposed to developing Crohn's disease (277, 278). A higher baseline ileal TLR2 expression may also explain why the data in this study detected up-regulation only of TLR4 in Crohn's ileitis.

The compartmentalisation of TLR4 to the colon is also interesting. Murine DSS-induced colitis results in predominantly distal colonic inflammation, the region of the colon with the highest expression of TLR4 mRNA and protein, and DCC colitis resembles UC more closely (250). The observation that a TLR4 antagonist (164) and an anti-TLR4 monoclonal antibody (165) improve inflammation in this experimental model support the concept that TLR4 plays a role in the pathogenesis of DSS colitis. In this study, the observed up-regulation of TLR4 mRNA in crypt IEC from both normal and inflamed mucosal specimens in UC in this study provides further evidence to suggest that UC is in part mediated by TLR4-induced inflammation.

In summary, EDTA-isolated crypt IEC from the small and large bowel contains high quality mRNA and expresses TLR2 and TLR4 transcripts. Quantitative real-time RT-PCR analysis

demonstrates significant up-regulation of TLR2 and TLR4 mRNA expression in inflamed UC and Crohn's colitis, particularly in IEC derived from mucosal regions with histologically severe disease activity. Similarly, TLR4 mRNA expression is up-regulated in crypt IEC derived from patients with Crohn's ileitis. Interestingly, compared to healthy controls TLR4 mRNA is up-regulated in crypt IEC isolated from normal (un-inflamed) mucosa in patients with UC, suggesting constitutive TLR4 mRNA expression. Moreover, TLR2 and TLR4 mRNA is similarly expressed in paired crypt IEC samples isolated from histologically normal and inflamed mucosa in patients with left-sided UC, further suggesting constitutive TLR expression in UC patients. TLR2 mRNA is expressed to a greater level that TLR4 mRNA in crypt cells of the normal small intestine and this pattern is reversed in crypt cells of the normal colon. This may in part explain the distal anatomical distribution of colitis in UC. These data provide further insight into the role of TLR2 and TLR4 in the pathogenesis of IBD.

Chapter 5: Expression of Toll-like receptors-2 and -4 protein in crypt intestinal epithelial cells in health and inflammatory bowel disease

5.1 Introduction

The expression of Toll-like receptors in human epithelial cell lines and primary human intestinal epithelial cells at the genomic level has been discussed in chapter 4. However, to fully understand their roles in intestinal homeostasis and intestinal inflammation, TLR expression must also be analysed at the protein level.

Regarding human cell lines, surface TLR4 protein expression has been reported in Caco-2, HT-29, T84 and SW480 cells (89, 231, 232, 243), though the TLR4-associated molecule MD-2 was inconsistently detected (89). TLR4 expression is reported to be dependent on the particular cell line studied, with greatest expression by SW480, lesser expression by HT-29 and T84, and least expression by Caco-2 and HCT116 cells. This differential expression may be due to changes in TLR gene promoter methylation and histone deacetylation (233). TLR2 and TLR4 protein has also been reported in a foetal small intestine cell line (240).

Functional TLR2 and TLR4 protein has been demonstrated in T84 and HT-29 cells. These cells were responsive to LPS as demonstrated by up-regulation of p42/44 (T84) and p38 components of the MAPK pathway (HT-29), even in the absence of the TLR4-associated molecule CD14 (232). Functional TLR2 and TLR4 signalling has also been reported in T84, SW480, caco2 and Colo205 cells by demonstrating up-regulation of p-ERK1/2, down-regulation of IκBα, ligand uptake assays and/or production of IL-8 (122, 162, 242, 243, 246, 248, 249); although non-responsiveness in cell lines has also been reported (89).

In primary intestinal tissue, TLR2 and TLR4 protein have been demonstrated to be expressed predominantly in the crypt cells of the colon using immunohistochemistry, with TLR3 protein expressed mainly on the luminal surface (252). TLR1/2 and TLR1/4 heterodimers have been reported in small and large bowel epithelial cells, and their immunofluorescent co-localisation with serotonin-staining cells suggested an enteroendocrine phenotype to these TLR-expressing IEC (254). Immunohistochemical staining has demonstrated TLR2 and TLR4 protein expression in primary foetal small bowel, especially in the crypts (240).

There are no functional studies investigating the response of primary intestinal epithelial cells to TLR2 and TLR4 ligands. Primary IEC have been reported to up-regulate DMBT1 mRNA expression (a putative anti-microbial peptide) in response to TNF-α (279) and to respond to a TLR8 ligand by secreting IL-8 (256), and primary mucosal samples respond to the TLR5 ligand flagellin when applied to the basolateral, but not apical surface (255). Despite the reporting of functional intracellular TLR4 protein in murine intestinal cell lines (m-IC_{cl2} cells) (244, 245), primary IEC have not been reported to express intracellular TLR4 protein. Indeed it is likely that surface rather than intracellular TLR4 protein is the key cellular location for LPS recognition (247).

Regarding expression during intestinal inflammation, TLR2 and TLR4 protein has been reported to be expressed at low level in healthy colonic tissue, with TLR4 but not TLR2 up-regulated in both ulcerative colitis and Crohn's disease, regardless of disease activity (260). However this is not been a universal observation (262). In another study, although both TLR2 and TLR4 protein were reported to be up-regulated in the mucosa of children with IBD using western blot analysis, the potential confounding contribution of lamina propria immune cells could not be excluded which prevents conclusions regarding the role TLR2 and TLR4 in IEC specifically from being made (280).

In summary, functional TLR2 and TLR4 protein has been demonstrated to varying degrees in human cells intestinal epithelial lines. Qualitative immunostaining has demonstrated TLR2 and TLR4 protein to be expressed primarily in the crypt cells, though expression throughout all epithelial cells has also been reported. There is a paucity of data regarding the differential expression of these receptors in active IBD and to date there are no publications in this area using quantitative methods. The aim of this chapter was to investigate the expression of TLR2 and TLR4 protein in isolated crypt IEC and to quantitatively characterise their expression in IBD and healthy controls.

5.2 Methods

5.2.1 Protein isolation and Bradford protein assay

Following isolation of primary epithelial cells or cultured cell lines, cells were lysed and protein isolated for subsequent analysis using CelLytic M cell lysis buffer (C2978, Sigma) following the manufacturer's instructions. 10^6 cells were collected in solution and centrifuged for 3 minutes at 450g. The supernatant was removed and the cells washed three times in PBS. Following centrifugation, 125µL of CelLytic M was added to the pellet along with 1.25µL of Phosphatase inhibitor cocktail 2 (P5726, Sigma) and 1.25µL of Protease inhibitor cocktail (P8340, Sigma) and the cells re-suspended.

This cellular suspension was incubated for 15 minutes, followed by a centrifugation step at 13,000 rpm (>10,000g) for 15 minutes to pellet the cellular debris. The protein-containing supernatant was removed and stored undiluted at -80^{o}C until required.

To measure the concentration of total protein in the lysate solution, a protein assay based on the Bradford method was used (216). A stock solution of 2mg/mL bovine serum albumin (BSA) was serially diluted into the following concentrations: 200µg/mL, 100µg/mL, 50µg/mL, 25µg/mL, 10µg/mL and 5µg/mL in PBS. Pure PBS was used as a negative control. 10µL aliquots of each diluted sample and 300µL of Coomassie Blue reagent (Biorad) were added to wells in a 96-well plate in duplicate. Coomassie Blue reagent is a triphenylmethane dye which actively binds to protein. Unbound Coomassie Blue reagent has a brown colour which changes to blue on protein binding. Of importance, the absorbance of light at 595nm (A_{595}) of protein-bound Coomassie Blue reagent is linearly related to the protein concentration, within the range 0µg/mL to 200µg/mL of protein. With protein concentrations greater than 200µg/mL the relationship becomes non-linear and therefore less accurate.

Using the Coomassie Blue reagent and serially diluted BSA samples it was possible to demonstrate this linear relationship between A_{595} and protein concentration (figure 5.1).

Using this “standard curve”, the total protein concentration in primary IEC and cell line lysates could be directly derived from their individual A_{595} reading. Primary IEC and cell line lysates were analysed using this method. If the total protein concentration was greater than 200µg/mL the assay was repeated following sample dilution with PBS until the measured A_{595} fell within the linear range. In such cases, calculation of the actual protein concentration was made multiplying the measured concentration by the dilution factor.

5.2.2 Polyacrylamide gel electrophoresis and Western blotting

Western blotting (WB) was undertaken following sodium dodecyl sulphate polyacrylamide gel electrophoresis (SDS-PAGE). Reagents for SDS-PAGE and Western blotting were made in stock solution prior to use and stored at room temperature. The following three stock solutions were required:

- 4x Resolving gel stock solution (containing 1.5M Tris and 0.4% SDS at pH 8.8): 18.2g Tris-Cl (T3253, Sigma) and 4mL of 10% SDS (L4522, Sigma) were added to 96mL dH_2O and pH balanced to 8.8 using concentrated NaOH solution.

- 4x Stacking gel stock solution (containing 0.5M Tris and 0.4% SDS at pH 6.8): 6.05g Tris-Cl and 4mL of 10% SDS were added to 100mL dH_2O and pH balanced to 6.8 using concentrated NaOH solution.

- 5x SDS running buffer stock solution (containing 0.5% SDS): 1.5g Tris-Cl, 72g glycine and 50mL of 10% SDS solution made up to 1L with dH_2O.

In addition, the following three reagents were made fresh for each run:

- Transfer buffer (containing 48mM Tris, 39mM glycine, 0.05% SDS and 20% methanol at pH 9.2): 5.82g Tris-base (T6066, Sigma), 2.93g glycine (BP 381-1, Fisher), 0.5mL SDS and 200mL of methanol were made up to 1L with dH_2O and pH balanced to 9.2 using concentrated NaOH solution.

- Tween 20/Tris-buffered saline wash solution (TTBS, containing 100mM Tris, 150mM NaCl and 0.1% SDS): 12.1g Tris-Cl, 8.7g NaCl (S/3160/63, Fisher) and 1mL Tween 20 (P1379, Sigma) were made up to 1L with dH_2O and pH balanced to 7.5 using concentrated NaOH solution.

- 10% ammonium persulphate solution: 22.5µg ammonium persulphate (161-0700, Biorad) in 225µl dH_2O.

To perform SDS-PAGE, glass plates and spacers were cleaned with 70% ethanol and assembled in the rack. A 10% resolving gel was made up by mixing the following: 5mL 30% acrylamide/0.8% bisacrylamide (161-0156, Biorad), 3.75mL 4x resolving gel stock solution, 6.25mL dH_2O, 50µL 10% ammonium persulphate and 14µL TEMED (NNN'N'-tetramethylethylenediamine, T9281, Sigma). This was immediately poured between the glass plates to a mark 2cm below the top of the plates. Isopropanol (propan-2-ol, P/7507/PB17, Fisher) was layered on top of this, to a mark 1cm from the top of the glass plates. This was left to polymerise for 30 minutes at which point the isopropanol was removed with filter paper.

A 5% stacking solution was mixed as follows: 0.65mL 30% acrylamide/0.8% bisacrylamide, 1.25mL 4x stacking gel stock solution, 3.05mL dH_2O, 25µL 10% ammonium persulphate and

5µL TEMED. This was immediately layered on top of the set gel and allowed to polymerise following insertion of a Teflon comb.

During this step, 40µg of total protein from each sample was mixed with Laemmli buffer (161-0737, Bio-Rad, UK) in a 1:1 ratio and heated for 5 minutes at 100^{o}C for soluble intracellular proteins (e.g. β-actin) or 37^{o}C for 10 minutes for hydrophobic transmembrane proteins (e.g. TLR2 or TLR4). The gels were placed facing in a tank of dilute 1x running buffer solution and the combs were removed. Protein samples were loaded into the wells and the gel run at 120-140V for 90-150 minutes depending on the molecular size of the protein.

To perform the Western blot, two filters and one polyvinylidene difluoride (PVDF) membrane (RPN303F, GE Healthcare) were cut to the size of the gel. The gel was removed from the tank and glass plates, and soaked in SDS running buffer for 15 minutes. During this time the PVDF membrane was soaked in 100% methanol for 15 seconds and rinsed in dH_2O for 2 minutes before being soaked in transfer buffer for 10 minutes. Similarly, the filters and sponges were soaked in transfer buffer.

Next the sponges, filters, gel and membrane were assembled, placed in a tank and filled with transfer buffer before undertaking electrophoresis at 90V, 0.2A for 50 minutes (figure 5.2).

To prevent non-specific antibody-protein binding, a 5% protein blocking solution was made by adding 2.5g Marvel to 50mL TTBS. The PVDF membrane was removed from the tank apparatus and incubated in this blocking solution for 30 minutes on a rocking platform at room temperature. Primary antibody solutions were made to the working concentrations and incubated as shown in table 5.1.

Table 5.1 Working dilutions and incubation protocols for primary antibodies used in Western blotting

Antibody	Dilution factor	Incubation protocol
β-Actin (A5060, Sigma)	1:1,000	1 hour at room temperature
TLR2 (14-9922, eBioscience)	1:250	18 hours at 4^{o}C
TLR4 (ab22048, Abcam)	1:250	18 hours at 4^{o}C

TLR, Toll-like receptor

Following primary antibody incubation, the membrane underwent three 5-minute washes in TTBS. The biotinylated secondary horse anti-mouse/anti-rabbit antibody (Vectastain ABC Universal kit PK-6200, Vector Labs) was diluted to 1:100 in 5mL of 5% Marvel, and applied to the membrane for 30 minutes on a rocking platform at room temperature. During this incubation the avidin/biotin-HRP complex was prepared by adding 100µL each of reagents A and B to 5mL PBS and leaving for 30 minutes, as per the manufacturer's instructions (Vectastain ABC Universal kit PK-6200, Vector Labs).

After the secondary antibody incubation step, the membrane was washed three times for 5 minutes in TTBS. The avidin/biotin-HRP complex was added to the membrane and incubated for 30 minutes at room temperature on a rocking platform followed by three 5-minute washes in TTBS.

To detect HRP activity, a solution of VIP reagent (Vector peroxidise substrate kit SK-4600, Vector Labs) was prepared by adding 150µL of each of reagents 1, 2 and 3 and 150µL of hydrogen peroxide solution to 15mL PBS. The membrane was immersed in the VIP solution for 1-5 minutes before quenching in dH_2O for 5 minutes. The membrane was allowed to air dry before scanning.

5.2.3 Immunofluorescent staining

Formalin-fixed, paraffin-embedded tissue specimens were cut into 5μm thick sections using the microtome and left to dry overnight on a SuperFrost plus® slide (Thermo Scientific). Slides were placed in a metal rack and successively transferred through three Xylene solutions for 2 minutes each. The sections were re-hydrated by transferring down through graded alcohol solutions (100%, 90%, 80%, 70% and 50%). Finally the slides were washed in dH_2O.

One percent citrate-based antigen retrieval solution (H-3300, Vector Labs) was made to 300mL volume and the solution heated to 100^{o}C in a conventional microwave oven. The slides were immersed in antigen retrieval solution at 100^{o}C for 15 minutes and left to cool to room temperature for 30 minutes before being washed twice in PBS for 5 minutes.

The slides were transferred to an incubation chamber containing PBS-soaked tissue paper. Around the tissue specimen a square was drawn using a wax pencil. Specimens were subject to three blocking steps. Firstly, the tissue specimens were incubated in neat avidin-blocking solution (SP-2001, Vector Labs) for 30 minutes at room temperature and washed in PBS for 5 minutes. The slides were then incubated in neat biotin-blocking solution (SP-2001, Vector Labs) for 30 minutes at room temperature and washed in PBS for 5 minutes. Finally slides were incubated in 5% horse serum in PBS for 30 minutes at room temperature to block non-specific antibody binding.

Thereafter, the slides were washed twice in PBS twice for 5 minutes and incubated with the primary antibody in a solution of 5% horse serum in PBS for 1 hour at room temperature as shown in table 5.2.

Table 5.2 Working concentrations of primary antibodies used for immunofluorescent staining

Primary antibody	Dilution of stock antibody
Cytokeratin	1:400
α-smooth muscle actin	1:500*
TLR2 (eBioscience)	1:50
TLR4 (eBioscience)	1:50

PBS Phosphate buffered saline; TLR, Toll-like receptor
* Initially stock antibody was diluted to 1:5 with PBS and 1% BSA before storage at -80^{o}C

The slides were returned to the metal rack and washed three times in PBS for 5 minutes each. The secondary anti-mouse/anti-rabbit biotinylated antibody was prepared to a 1:400 dilution using 5% horse serum in PBS. The slides were returned to the incubation chamber and 200μL secondary antibody solution applied to each slide for 30 minutes at room temperature.

The slides were washed in three times in PBS and returned to the incubation chamber. Secondary antibody detection was undertaken using the Fluorescent Avidin kit (A-1100, Vector Labs). To each slide 100μL of 5% solution of fluorescein avidin DCS (anti-mouse IgG) in 0.5M sodium chloride was added and incubated in the dark for 10 minutes at room temperature. Thereafter, the slides were washed twice in PBS for 1 minute only in the dark.

Fluorescent detection was undertaken by adding 25μL of Vectashield Mounting Medium with 4',6-diamidino-2-phenylindole (DAPI) (H-1200, Vector Labs) to the section, applying a 22x22mm cover slip and leaving for 1 minute in position. The cover slip was then firmly positioned over the section to exclude any underlying bubbles.

Fluorescently labelled, DAPI counter-stained slides were left in the dark for one hour before viewing. Images were generated in the Leica fluorescent microscope (Leica Microsystems) using Leica software (LAS AF v2.5.0). Slides were scanned with an exposure of 90ms for DAPI and 248ms for FITC. To reduce the initial background signal, the images were set to a

+10 background adjustment. No colour or contrast adjustments were made. Finally, images were saved and exported as JPEG files.

5.2.4 Flow cytometry

Crypt intestinal epithelial cells were isolated and disaggregated using EDTA/DTT and pancreatin (section 3.2.4), and peripheral blood mononuclear cells were isolated from whole blood using Histopaque and Ficoll density gradient centrifugation (section 3.2.10). Cell concentration was calculated using trypan blue exclusion. Five hundred thousand ($0.5x10^6$) cells were transferred to each flow cytometry tube and the volume made up to 0.5mL with flow cytometry medium (2% foetal calf serum in HBSS without calcium or magnesium). Tubes were centrifuged at x300g for 10 minutes at room temperature to pellet the cells before removal of the supernatant by pipette.

Five microlitres of normal mouse serum was added to the tube and the tube flicked several times to loosen the pellet. Tubes were left for 15 minutes sitting over ice (approximately 4^oC). Thereafter no antibody, isotype antibody or primary antibody was added and incubated for 1 hour in the dark on ice at 4^oC, as follows:

1. No primary antibody
2. Anti-BerEP4-FITC 5µL (F0860, Dako)
3. Anti-BerEP4-FITC 5µL + IgG2aκ isotype control-APC 10µL (17-4724, eBioscience)
4. Anti-BerEP4-FITC 5µL + anti-TLR2-APC 10µL (17-9922, eBioscience)
5. Anti-BerEP4-FITC 5µL + anti-TLR4-APC 10µL (17-9917, eBioscience)
6. Anti-CD45-AF488 1µL (304019, BioLegend)

Next the cells were washed twice by adding 0.5mL of flow cytometry medium to the tube, re-suspending the cells by flicking the tube and centrifugation at 300g for 10 minutes at room temperature. After decanting the supernatant, the cells were re-suspended in 0.5mL of

fixative solution (0.5% formaldehyde in PBS), wrapped in foil to protect from the light and stored at 4^{o}C until analysis.

A sub-group of isolated crypt cells (n=6, two colonic healthy controls, four Crohn's colitis) were analysed immediately following antibody-stained on the Beckman Coulter MoFlo cell sorter, without being fixed in formaldehyde. Unfixed BerEP4-positive cells were positively sorted into a FACS tube containing 200µL of FACS medium (HBSS with calcium, magnesium and 10% FCS) on ice. Following sorting, the cells in suspension were transferred to an Eppendorf tube and centrifuged for 5 minutes at 1,000g using a microcentrifuge. Following removal of the supernatant, the cell pellet was resuspended and lysed in 600µl of Buffer RLT with 1% 2-mercaptoethanol. RNA was subsequently isolated using the Qiagen RNeasy Plus Mini Kit as per the manufacturer's instructions (section 2.2). RNA was stored at -80^{o}C until analysis.

A minimum of 20,000 total events per sample tube were collected for each subject undergoing flow cytometric analysis. Samples were initially analysed by forward and side scatter (which are measurements of cell size and density, respectively) to exclude dead cells (events adjacent to the zero points of both axes) and to exclude events considered to be clumped cells (events of large deflection on forward and/or side scatter).

To identify positive events, samples were run both without primary antibodies (to assess cellular auto-fluorescence) and with relevant isotype control antibodies. All events in the isotype control antibody samples were gated into the lower left quadrant of the dot plot and these quadrants were applied to analyses of the primary antibody samples. Positive events in primary antibody samples were those lying in any of the other three quadrants. All flow cytometric data were analysed using Weasel v3 software.

The patient demographics for the subjects included in the flow cytometry analyses are shown in table 5.3.

Table 5.3 Demographic data for flow cytometry study subjects

Demographic variable	Large intestine		
	Healthy control	Ulcerative colitis	Crohn's colitis
Number	7	4	8
Age mean (SEM) years	73.4 (3.52)	50.5 (8.37)*	41.3 (5.63)***
Sex male/female (% male)	3/4 (43)	0/4 (0)	1/7 (13)
Medications			
• 5ASA	0	0	1
• Thiopurine	0	0	1
• Anti-TNFα	0	0	2
Medical History			
• Venous thromboembolism	1	0	0
• Diabetes mellitus	1	2	0
• Osteoporosis	0	0	1
• Ischaemic heart disease	0	2	0
• MGUS	0	0	1
• Hypercholesterolaemia	0	2	0
• Hypertension	0	2	1
• Chronic kidney disease	0	0	1
• Prostate cancer	1	0	0

5ASA, 5-aminosalicylic acid; MGUS, monoclonal gammopathy of uncertain significance; TNFα, tumour necrosis factor-α

* P<0.05 ** p<0.01 *** p<0.001 versus healthy controls

5.3 Results

5.3.1 Isolated intestinal crypt cells express TLR2 and TLR4 protein

To investigate the expression of TLR2 and TLR4 protein by intestinal epithelial cells, suitable positive controls cells were required. Peripheral blood mononuclear cells (PBMC) are reported to express TLR2 and TLR4 mRNA and protein. Furthermore, in this study PBMC were demonstrated to express TLR2 and TLR4 mRNA using RT-PCR (section 4.3.2). To investigate the functionality of commercial antibodies against human TLR2 and TLR4, protein lysates from PBMC were used as positive controls.

PBMC were isolated and the total protein concentration of the cell lysate was calculated using the Bradford protein assay. Thereafter, 20μg of total protein was loaded to each SDS PAGE well and electrophoresis undertaken. Protein was blotted onto a PVDF membrane and incubated with a polyclonal anti-β-actin antibody or a purified anti-TLR2 or anti-TLR4 monoclonal antibody. PBMC lysates were shown to express TLR2 and TLR4 proteins (figure 5.3).

Next, primary intestinal epithelial cells were isolated and protein lysates collected from the large intestine of healthy controls and patients with Crohn's disease and ulcerative colitis. Thereafter, 40μg of total protein was loaded to each SDS PAGE well and examined using electrophoresis and Western blotting. Primary IEC samples from the large intestine of healthy controls and patients with active UC or Crohn's disease were shown to express TLR2 and TLR4 proteins (figure 5.4).

5.3.2 Pancreatin treatment does not affect expression of surface TLR2 or TLR4 protein

To investigate the functionality of monoclonal antibodies to human TLR2, TLR4 and CD45 using flow cytometry, PBMC were again chosen to act as positive control cells. Initially PBMC were incubated with either no antibody (control), allophycocyanin (APC)-conjugated

isotype control antibody or APC-conjugated anti-TLR2 primary antibody, without a preceding normal mouse serum blocking step. Importantly, cells were not permeabilised during this protocol. Therefore any primary antigen binding was due to surface protein expression and not intracellular protein binding.

PBMC were shown to express surface TLR2 protein, confirming the functionality of the anti-TLR2 antibody (figure 5.5A, C and D). Of note, the median fluorescent intensity (MFI) of the isotype antibody was greater than the no-antibody control, indicating non-specific isotype antibody binding by the PBMC (figure 5.5A, B and D). To address this issue, the protocol was modified to include a blocking step using normal mouse serum prior to the primary antibody incubation step. As a result of the addition of the serum blocking step, isotype antibody binding by PBMC was ameliorated (figure 5.6A-D). Therefore, all subsequent analyses were undertaken with a normal mouse serum blocking step prior to primary antibody incubation.

Peripheral blood mononuclear cells were shown to express surface TLR4 protein, confirming the functionality of the anti-TLR4 antibody (figure 5.7). Furthermore PBMC express surface CD45 (figure 5.8) but not the epithelial-specific surface antigen BerEP4 (figure 5.9). These data are consistent with the cell surface marker expression profile characterised in PBMC using immunocytochemical staining (section 3.3.2).

Pancreatin is a porcine-derived mixture of pancreatic enzymes and includes proteases, lipases and amylase. To investigate whether the pancreatin treatment step in the crypt cell isolation protocol resulted in either a reduction in the expression of surface TLR2 and TLR4 protein expression or an alteration in the antibody-antigen binding affinity, isolated PBMC were either suspended in medium for 90 minutes at room temperature or treated with 0.25% pancreatin for 90 minutes before being re-suspended in medium. Thereafter PBMC were

incubated with an anti-TLR2-APC primary antibody, isotype-APC control antibody or no-antibody control.

Peripheral blood mononuclear cells treated in medium (figure 5.10A-C) or pancreatin (figure 5.10D-F) demonstrated similar expression of surface TLR2 protein. The distribution of TLR2 protein expression was similar in both medium-treated (figure 5.10G) and pancreatin-treated (figure 5.10H) cells. Median fluorescent intensity of TLR2 expression was 197.2 units in medium-treated cells and 236.1 in pancreatin-treated cells, suggesting there was no loss of surface TLR2 protein expression with pancreatin treatment (figure 5.10I). A similar result was observed with TLR4 expression (data not shown).

5.3.3 Isolated intestinal crypt cells express BerEP4, but not CD45 protein

BerEP4 is a surface antigen expressed on cells of epithelial origin. BerEP4 expression is used clinically to confirm the epithelial origin of malignant cells using a monoclonal mouse antibody raised in the MCF-7 cell line and directed against human BerEP4 (281). To characterise their BerEP4 expression, EDTA-isolated crypt cells were disaggregated using pancreatin and incubated with a FITC-conjugated anti-human BerEP4 antibody and examined using flow cytometry.

Isolated crypt cells were shown to highly express BerEP4 (figure 5.11). The mean (SEM) number of BerEP4-positive events was 91.5$\pm$1.1%. To investigate the number of BerEP4-positive events in cells isolated from tissue of varying degrees of inflammation, colonic crypt cells were isolated from healthy controls and patients with UC and Crohn's colitis. The number of BerEP4-positive cells was similar in healthy controls (90.7$\pm$2.1%) compared to patients suffering Crohn's disease (90.0$\pm$2.1%, p=0.81) or UC (92.4$\pm$3.0%, p=0.66), figure 5.12A.

Similarly, the expression of surface CD45 protein was investigated in isolated crypt cells. Isolated crypt cells were shown to be almost exclusively CD45-negative (figure 5.13). The overall number of CD45-positive cells was 2.2±0.4%. The number of CD45-positive isolated crypt cells was similar in healthy controls (1.5±0.4%) compared to patients suffering Crohn's disease (2.5±0.7%, p=0.26) or UC (2.4±1.3%, p=0.44), figure 5.12B.

These observations were similar to the proportion of BerEP4-positive and CD45-positive cells calculated using immunocytochemical staining of cytospin preparations from healthy controls and patients with either Crohn's disease or UC (section 3.3.2).

5.3.4 BerEP4-positive crypt intestinal epithelial cells from patients with inflammatory bowel disease up-regulate TLR2 and TLR4 surface protein expression

To characterise the surface expression of TLR2 and TLR4 protein in patients with inflammatory bowel disease, intestinal crypt cells were isolated from patients with Crohn's disease and ulcerative colitis, and these were compared to isolated cells from healthy control subjects. To ensure only epithelial cells were analysed, all isolated cells were labelled with anti-human BerEP4. During analysis, median fluorescent intensity of TLR2 and TLR4 antibody signal was measured on BerEP4-positive events only. By undertaking this gating step, all non-epithelial cells were excluded from the analysis, allowing a pure epithelial cell population to be characterised. Colonic BerEP4-positive IEC isolated from patients with UC demonstrated expression of surface TLR2 and TLR4 protein (figure 5.14). Similar results were seen with isolated BerEP4-positive IEC from the large bowel of patients with CD.

The expression of TLR2 and TLR4 surface protein on BerEP4-positive IEC isolated from patients with IBD was compared to expression on cells isolated from healthy controls. BerEP4-positive colonic intestinal crypt epithelial cells from patients with histologically inflamed UC mucosa expressed greater surface TLR2 (median fluorescent intensity [inter-quartile range] 89.1 [39.0-146.1]) than healthy controls (10.1 [2.4-29.0], p=0.006, figure

5.15A). Similarly, BerEP4-positive crypt IEC from patients with histologically inflamed UC mucosa expressed greater TLR4 surface protein (73.0 [31.1-179.4]) compared to healthy controls (12.1 [4.9-25.3], p=0.024, figure 5.15B).

BerEP4-positive colonic crypt intestinal epithelial cells from the mucosa of patients with histologically inflamed Crohn's colitis expressed greater surface TLR2 protein than healthy controls (65.8 [19.3-126.3] versus 10.1 [2.4-29.0] respectively, p=0.029, figure 5.16A) and greater surface TLR4 protein than healthy controls (69.7 [26.4-115.1] versus 12.1 [4.9-25.3] respectively, p=0.021, figure 5.16B). These data are summarised in table 5.4.

Table 5.4 Expression of surface TLR2 and TLR4 protein in patients with inflammatory bowel disease relative and in healthy control subjects

Site	Group	N	TLR2 protein expression		TLR4 protein expression	
			Median [IQR]	p-value #	Median [IQR]	p-value #
Large bowel	Healthy control	7	10.1 [2.4-29.0]	-	12.1 [4.9-25.3]	-
	Ulcerative colitis (inflamed)	4	89.1 [39.0-146.1]	0.006	73.0 [31.1-179.4]	0.024
	Crohn's disease (inflamed)	8	65.8 [19.3-126.3]	0.029	69.7 [26.4-115.1]	0.021

Mann-Whitney Test versus healthy controls
IQR, inter-quartile range; N, number of cases

There appeared to be a polarity of TLR2 and TLR4 protein expression within the group of patients with Crohn's colitis (n=8). Although IEC from cases expressing higher surface TLR2 and TLR4 protein were more likely to not be receiving immunosuppressive treatment at the time of surgery (none of four cases receiving immunosuppressive treatment) compared to those cases with low surface TLR2 and TLR4 expression (three of four cases receiving immunosuppressive treatment), this difference was not significant (Fisher's exact test p=0.143).

5.3.5 Sorted BerEP4-positive intestinal epithelial cells express mRNA for TLR2 and TLR4

In a sub-group of isolated crypt cell samples, BerEP4-positive cells were sorted using a fluorescence-activated cell sorting (FACS) cytometer (MoFlo cytometer, Beckman Coulter). After the crypt cell isolation, primary antibody staining and surface protein expression analysis steps, cells from six cases (two large intestine samples from healthy controls and four large intestine samples patients with Crohn's colitis) were positively sorted for their BerEP4 expression and total RNA was subsequently isolated. RNA assessment using the Nanodrop® spectrophotometer revealed low concentrations of RNA (figure 5.17).

Despite the low mRNA concentration and poor RNA quality, conventional RT-PCR from these BerEP4-positive sorted cell samples demonstrated expression of HPRT mRNA in all samples (figure 5.18). Furthermore, conventional RT-PCT analysis demonstrated expression of TLR4 transcripts in all healthy control and Crohn's disease large intestine samples. TLR2 transcripts were demonstrated in all samples except one cDNA sample (from a patient with Crohn's colitis, figure 5.19).

5.3.6 Intestinal epithelial cells express TLR2 and TLR4 protein along the crypt-villus axis, with greatest expression in the basal crypt cells of inflamed Crohn's ileitis

To investigate by anatomical location the expression TLR2 and TLR4 protein, full-thickness whole bowel from operation resection specimens were collected from healthy controls and patients with inflammatory bowel disease (n=15). Specimens were formalin-fixed and paraffin-embedded before 5μm sections were mounted on glass sides, stained with anti-TLR2 or anti-TLR4 primary antibodies, followed by sequential incubation with a biotinylated secondary antibody, an avidin-FITC complex and a DAPI counter-stain (section 5.2.3). In addition control slides were also made, omitting the primary antibody step, to investigate for non-specific staining by the biotinylated secondary antibody or the avidin-FITC complex.

Weak TLR2 and TLR4 protein expression was demonstrated by intestinal epithelial cells of the colonic mucosa in healthy controls (figure 5.20). Patients with active ulcerative colitis (figure 5.21) and Crohn's colitis (figure 5.22) demonstrated stronger TLR2 and TLR4 expression by crypt epithelial cells. Within the lamina propria, mononuclear cells were also observed to stain brightly for TLR2 and TLR4 both in the peri-cryptal region and also in extending into the upper third of the lamina propria. This was in contrast to the LP cell staining pattern in healthy controls which was less intense and less extensive within the LP.

Examination of the small intestine demonstrated weak TLR2 and TLR4 protein staining by epithelial cells of healthy controls (figure 5.23), with more intense staining by epithelial cells from inflamed Crohn's ileitis (figure 5.24). Higher power images demonstrated that crypt base cells stained TLR2, and to a lesser extent TLR4 protein, more intensely than epithelial cells of the upper crypt (transit amplifying zone) or the villi (figure 5.25). Control slides demonstrated minimal fluorescent staining.

5.4 Figures

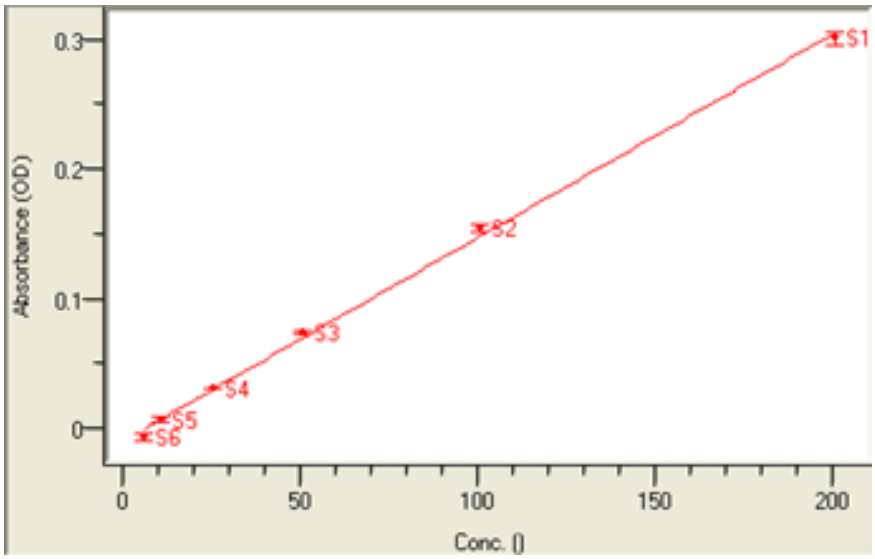

Figure 5.1 Linear relationship between absorbance of light at 595nm and total protein concentration in solution using the Bradford assay. The absorbance of light (Y-axis) at 595nm is directly proportional to the total protein concentration (X-axis, within the range ≤200µg/mL) using standard dilutions of bovine serum albumin and the Coomassie Blue reagent. The total protein concentration of an unknown sample can be extrapolating using the standard line shown above if it lies within the linear part of the standard curve.

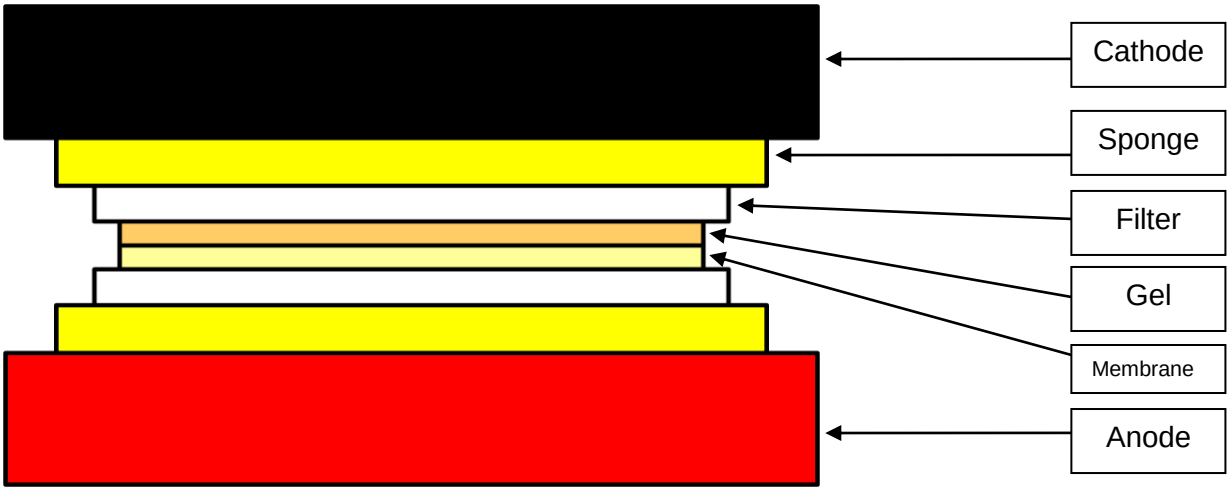

Figure 5.2 Assembly of experimental components for Western blotting. To perform the Western blot, two 100% methanol-soaked filters and two 100% methanol-soaked sponged were positioned either side of the protein-containined polyacrylamide gel and the polyvinylidene difluoride (PVDF) membrane. The application of a current across this arrangement resulted in blotting of the protein bands onto the membrane for subsequent detection using colorimetric methods.

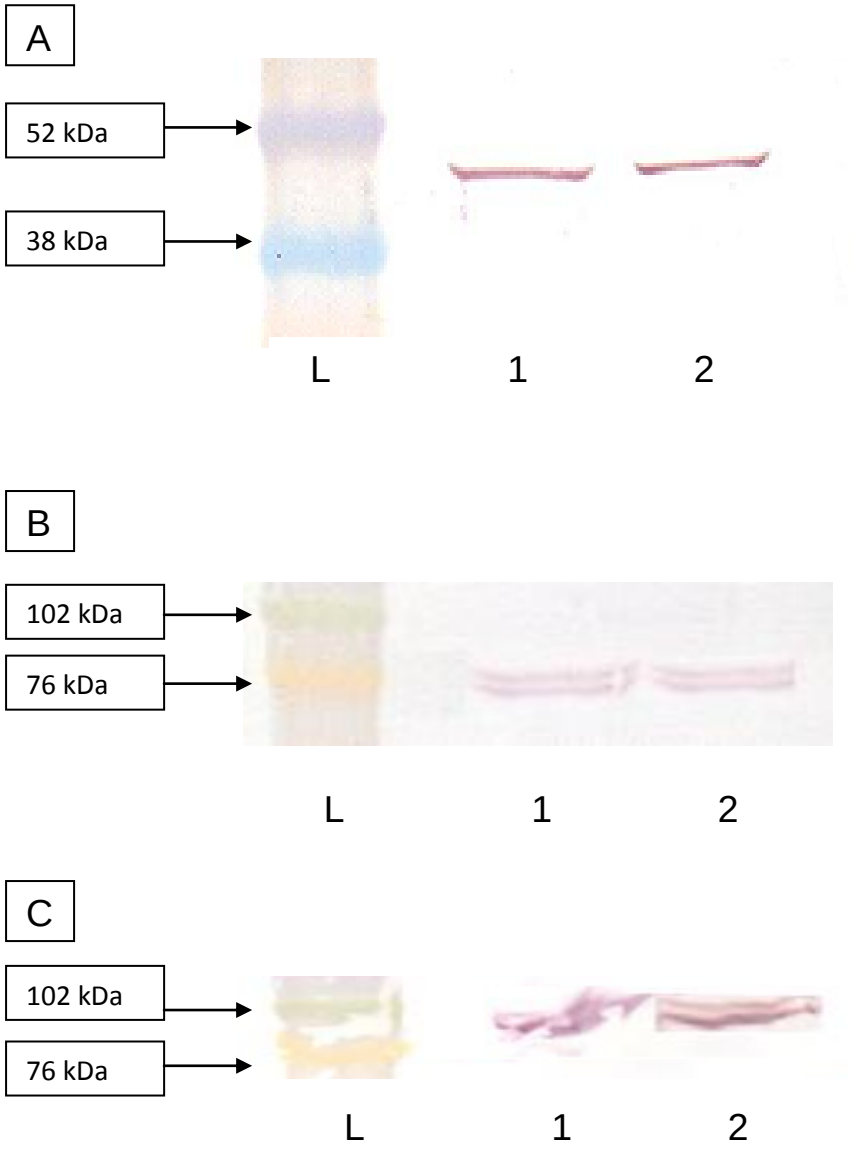

Figure 5.3 Primary peripheral blood mononuclear cells express TLR2 and TLR4 protein. Peripheral blood mononuclear cells (PBMC) were isolated using Ficoll gradient centrifugation for total protein lysate collection. 20µg of total protein was loaded into each SDS PAGE well prior to blotting onto a PVDF membrane. Protein expression was detected using membrane incubation with primary antibodies to (A) β-actin, (B) TLR2 or (C) TLR4 proteins and developing using Vector VIP peroxidase substrate. Bands were noted at the expected protein molecular weights for β-actin (42 kDa), TLR2 (90kDa) and TLR4 (93kDa). Samples were run in duplicate (lanes 1 and 2).

Da, Dalton; L, size ladder; PVDF, polyvinylidene difluoride; SDS PAGE, sodium dodecyl sulphate polyacrylamide gel electrophoresis; TLR, Toll-like receptor

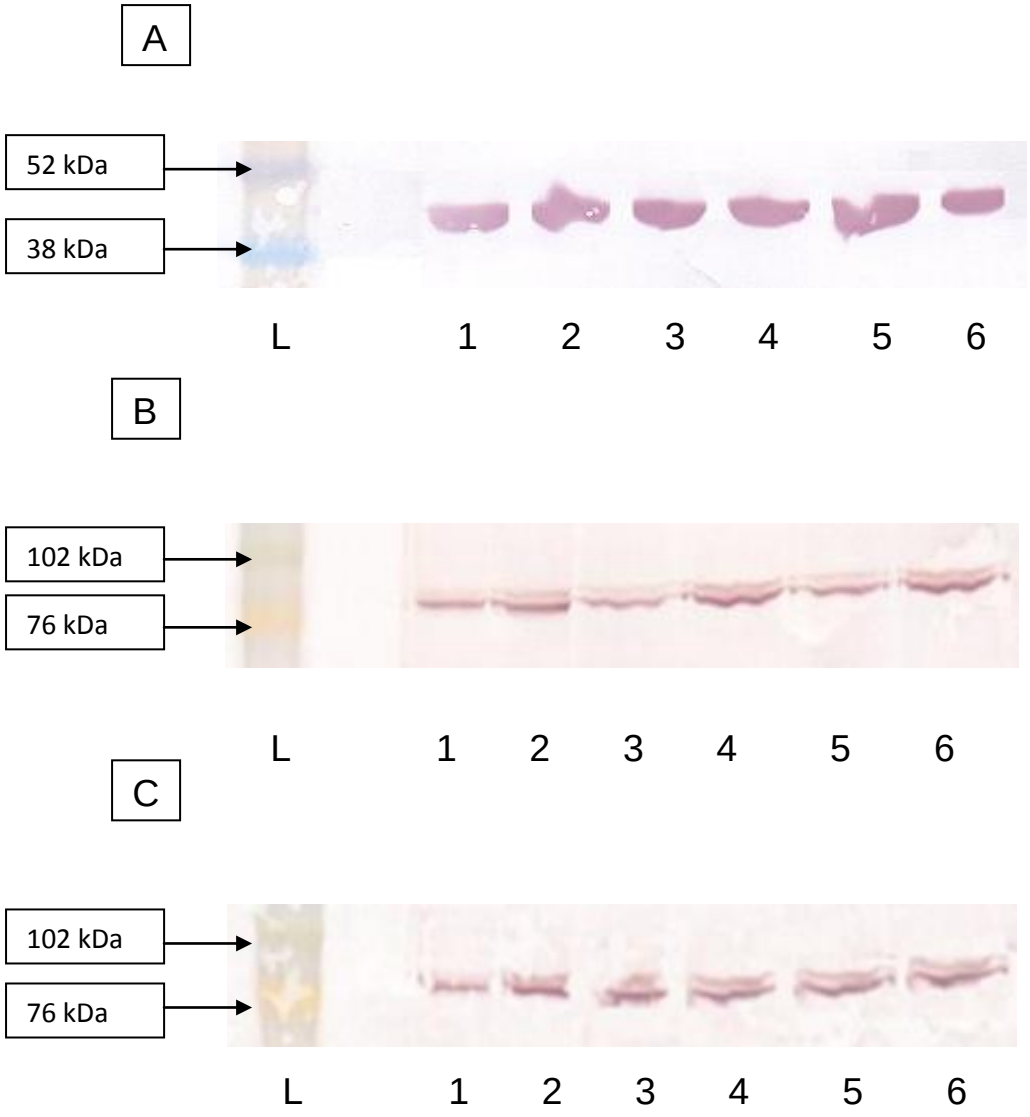

Figure 5.4 Primary intestinal crypt cells express TLR2 and TLR4 protein. Primary intestinal crypt cells were isolated for total protein lysate collection. 40µg of total protein was loaded into each SDS PAGE well prior to blotting onto a PVDF membrane. Protein expression was detected using membrane incubation with primary antibodies to (A) β-actin, (B) TLR2 or (C) TLR4 proteins and developing using Vector VIP peroxidase substrate. Bands were noted at the expected protein molecular weights for β-actin (42 kDa), TLR2 (90kDa) and TLR4 (93kDa).

Lanes 1 and 2: Healthy large bowel
Lanes 3 and 4: Inflamed Crohn's large bowel
Lanes 5 and 6: Inflamed ulcerative colitis large bowel

Da, Dalton; L size ladder; PVDF, polyvinylidene difluoride; SDS PAGE, sodium dodecyl sulphate polyacrylamide gel electrophoresis; TLR, Toll-like receptor

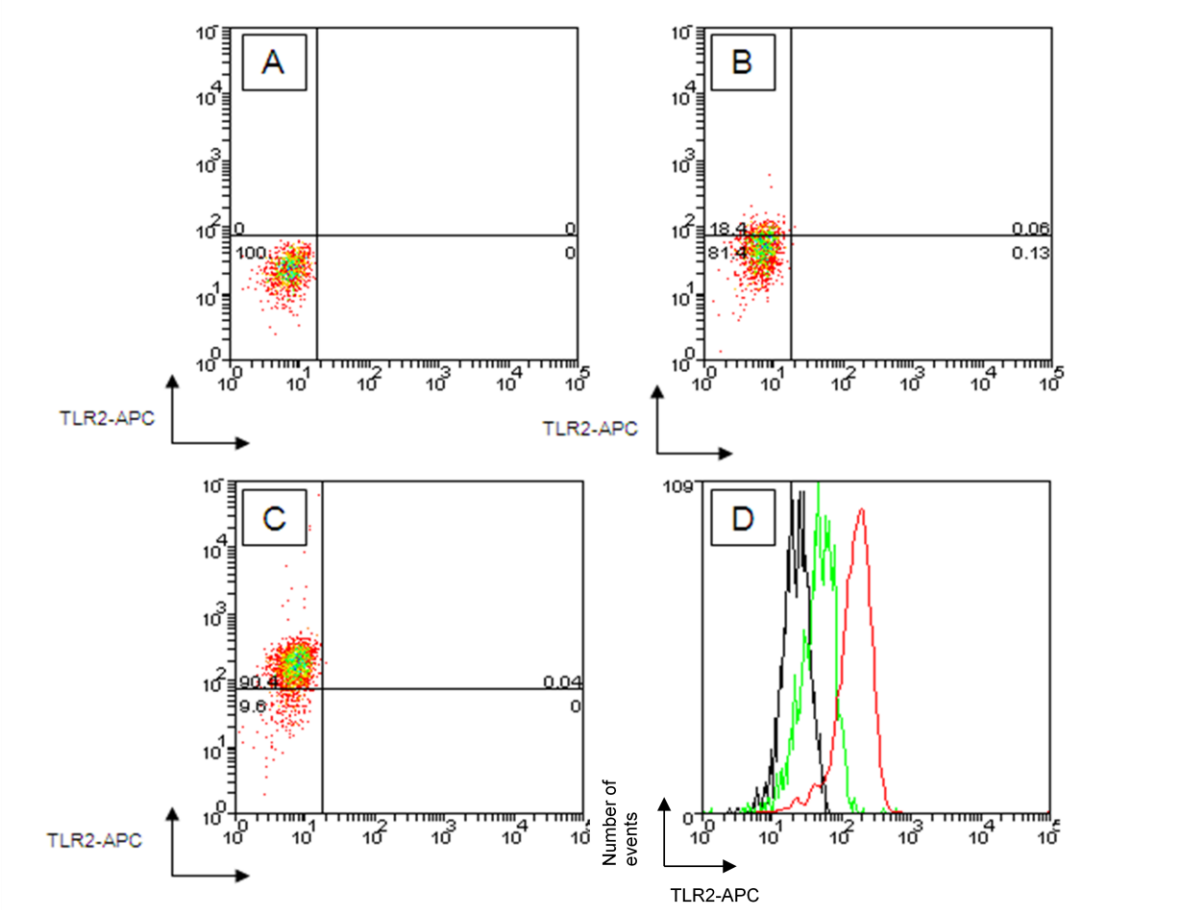

Figure 5.5 Peripheral blood mononuclear cells express surface TLR2 protein. Following Ficoll-gradient acquisition, PBMC were centrifuged to form a pellet in cytometry tubes, re-suspended in 20µL of medium and incubated with (A) no primary antibody, (B) isotype-APC control antibody or (C) primary anti-TLR2-APC antibody, prior to analysis on a flow cytometer. The overlay histogram (D) illustrated the expression of surface TLR2 expression by PBMC and non-specific isotype antibody binding. The X-axes of panels A-C represent unused gates.

Black: No antibody control
Green: Isotype-APC antibody
Red: TLR2-APC primary antibody

APC, Allophycocyanin; PBMC, peripheral blood mononuclear cells; TLR, Toll-like receptor

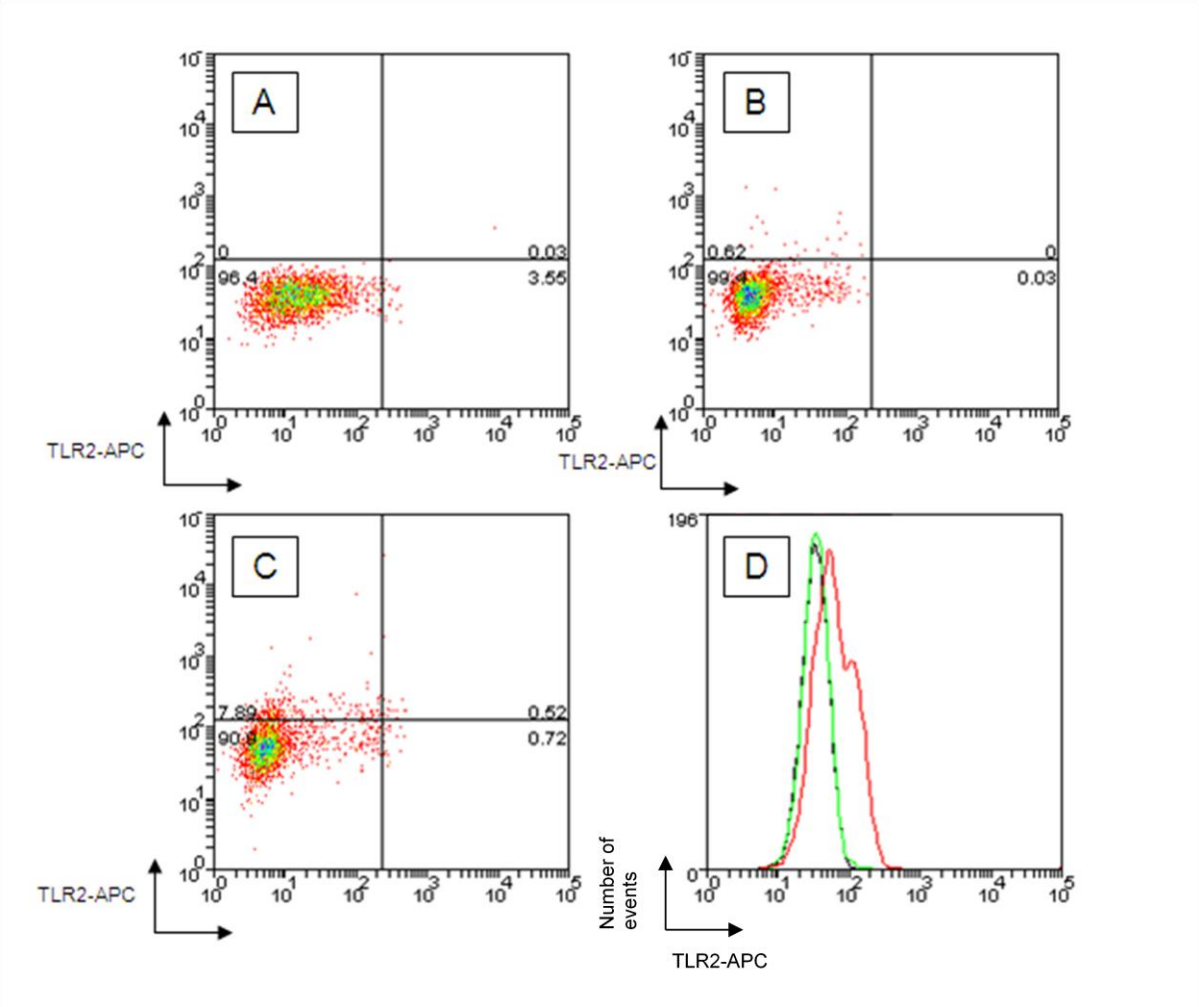

Figure 5.6 Incubation with normal mouse serum ameliorates isotype control antibody binding. Following Ficoll-gradient acquisition and centrifugation, PBMC were exposed to a normal mouse serum block step prior to incubation with (A) no primary antibody, (B) isotype-APC control antibody or (C) primary anti-TLR2-APC antibody, and subsequently analysed using flow cytometry. Dot plots (A-C) illustrate fluorescence. The overlay histogram (D) illustrated the surface binding of anti-TLR2 and isotype antibodies on PBMC following mouse serum blockade. The X-axes of panels A-C represent unused gates.

Black: No antibody control
Green: Isotype-APC antibody
Red: TLR2-APC primary antibody

APC, Allophycocyanin; PBMC, peripheral blood mononuclear cells; TLR, Toll-like receptor

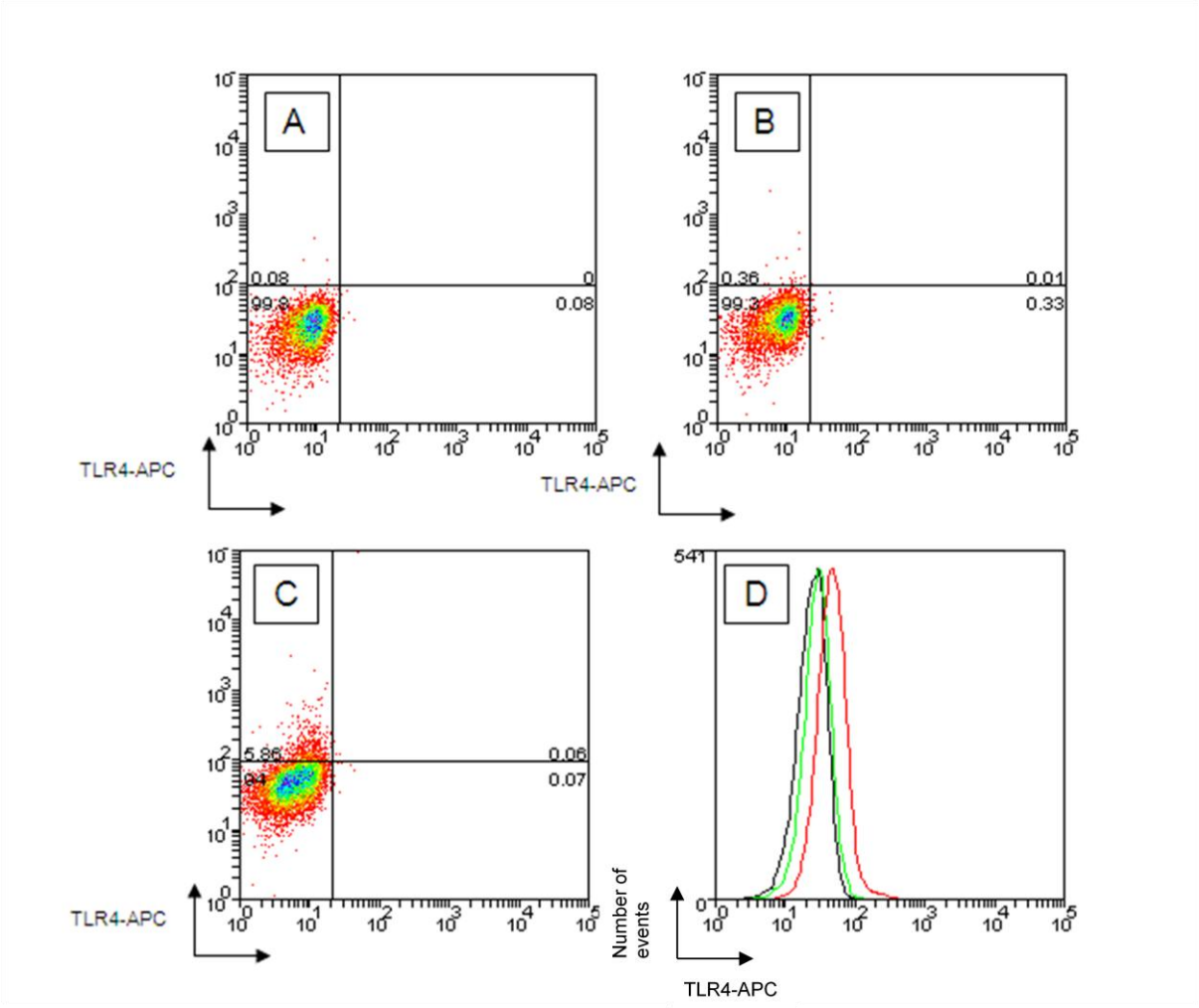

Figure 5.7 Peripheral blood mononuclear cells express surface TLR4 protein. Following Ficoll-gradient acquisition and subsequent blocking with normal mouse serum, isolated PBMC were incubated with (A) no primary antibody, (B) isotype-APC control antibody or (C) primary anti-TLR4-APC antibody, and analysed using flow cytometry. The overlay histogram (D) illustrated the surface TLR4 expression by PBMC. The X-axes of panels A-C represent unused gates.

Black: No antibody control
Green: Isotype-APC antibody
Red: TLR2-APC primary antibody

APC, Allophycocyanin; PBMC, peripheral blood mononuclear cells; TLR, Toll-like receptor

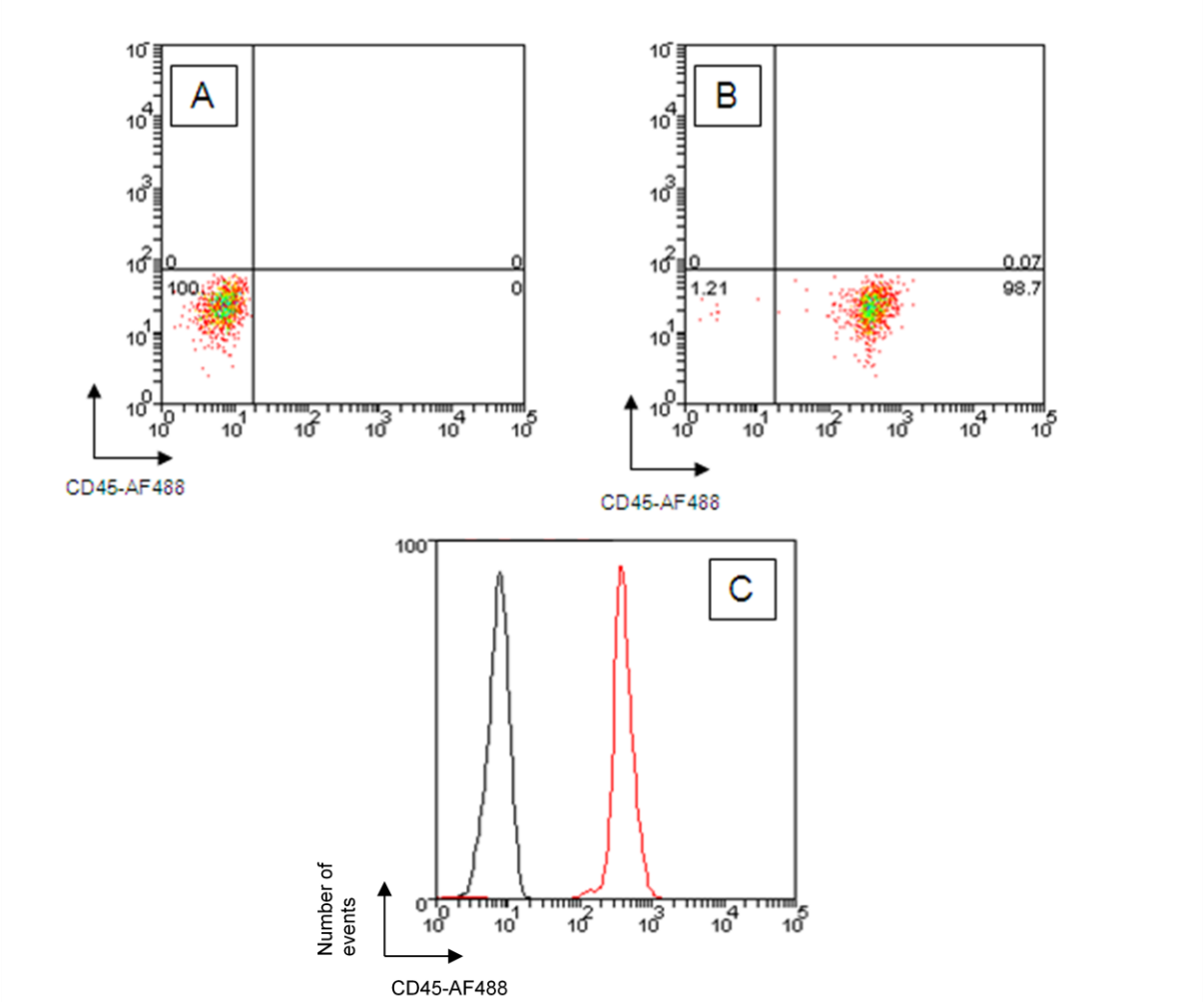

Figure 5.8 Human peripheral blood mononuclear cells express surface CD45 protein. Following Ficoll-gradient acquisition and subsequent blocking with normal mouse serum, isolated PBMC were incubated with (A) no primary antibody or (B) primary anti-CD45-AF488 antibody, and analysed using flow cytometry. The overlay histogram (C) illustrated the surface CD45 expression by PBMC. The Y-axes of panels A and B represent unused gates.

Black: No antibody control
Red: CD45-AF488

AF488, Alexa Fluor-488; PBMC, peripheral blood mononuclear cells

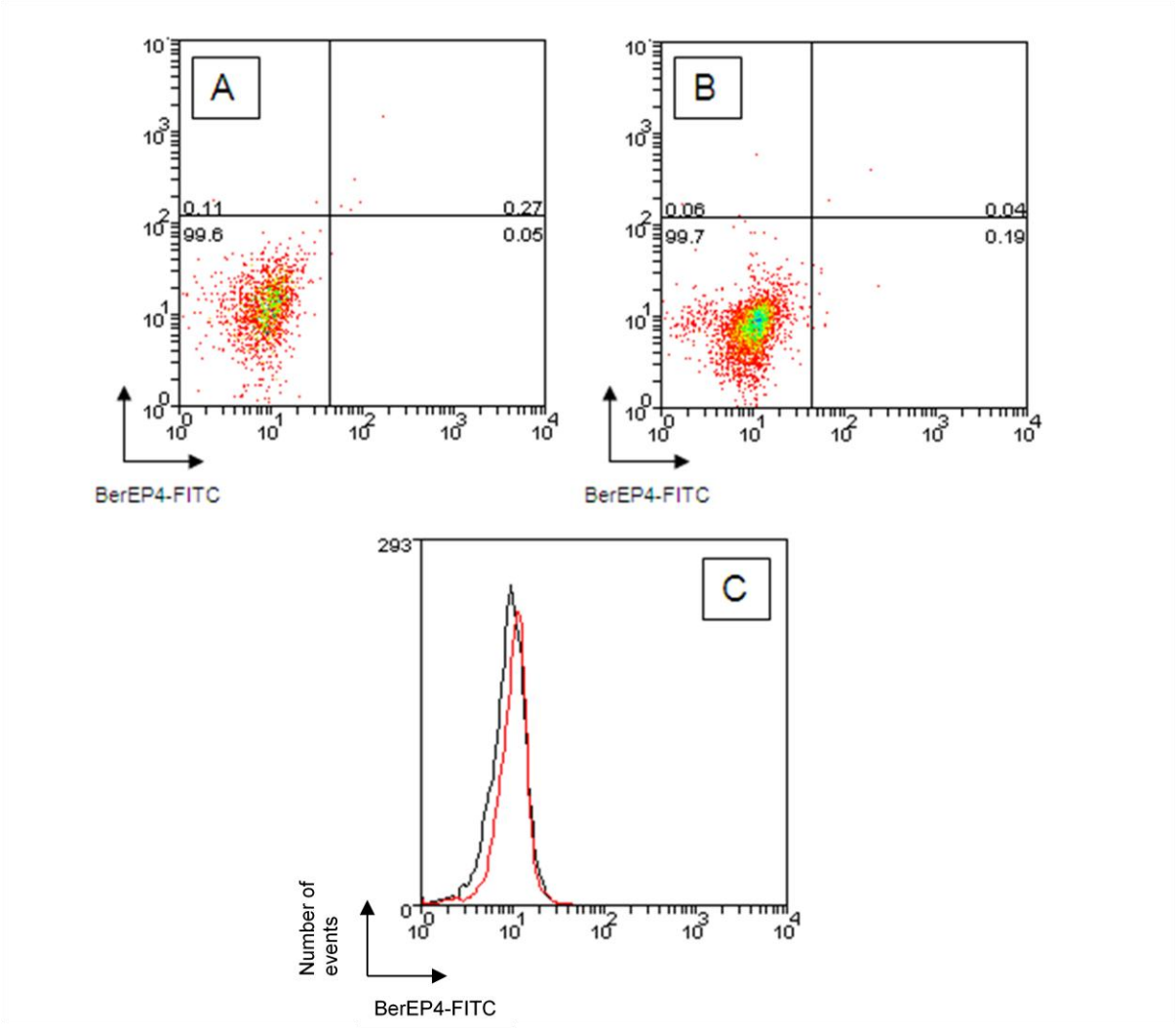

Figure 5.9 Peripheral blood mononuclear cells do not express surface BerEP4 protein. Following Ficoll-gradient acquisition and subsequent blocking with normal mouse serum, isolated PBMC were incubated with (A) no primary antibody or (B) primary anti-BerEP4-FITC antibody, and analysed using flow cytometry. The overlay histogram (C) illustrated the surface BerEP4 expression by PBMC. The Y-axes of panels A and B represent unused gates.

Black: No antibody control
Red: BerEP4-FITC

FITC, Fluorescein isothiocyanate; PBMC, peripheral blood mononuclear cells

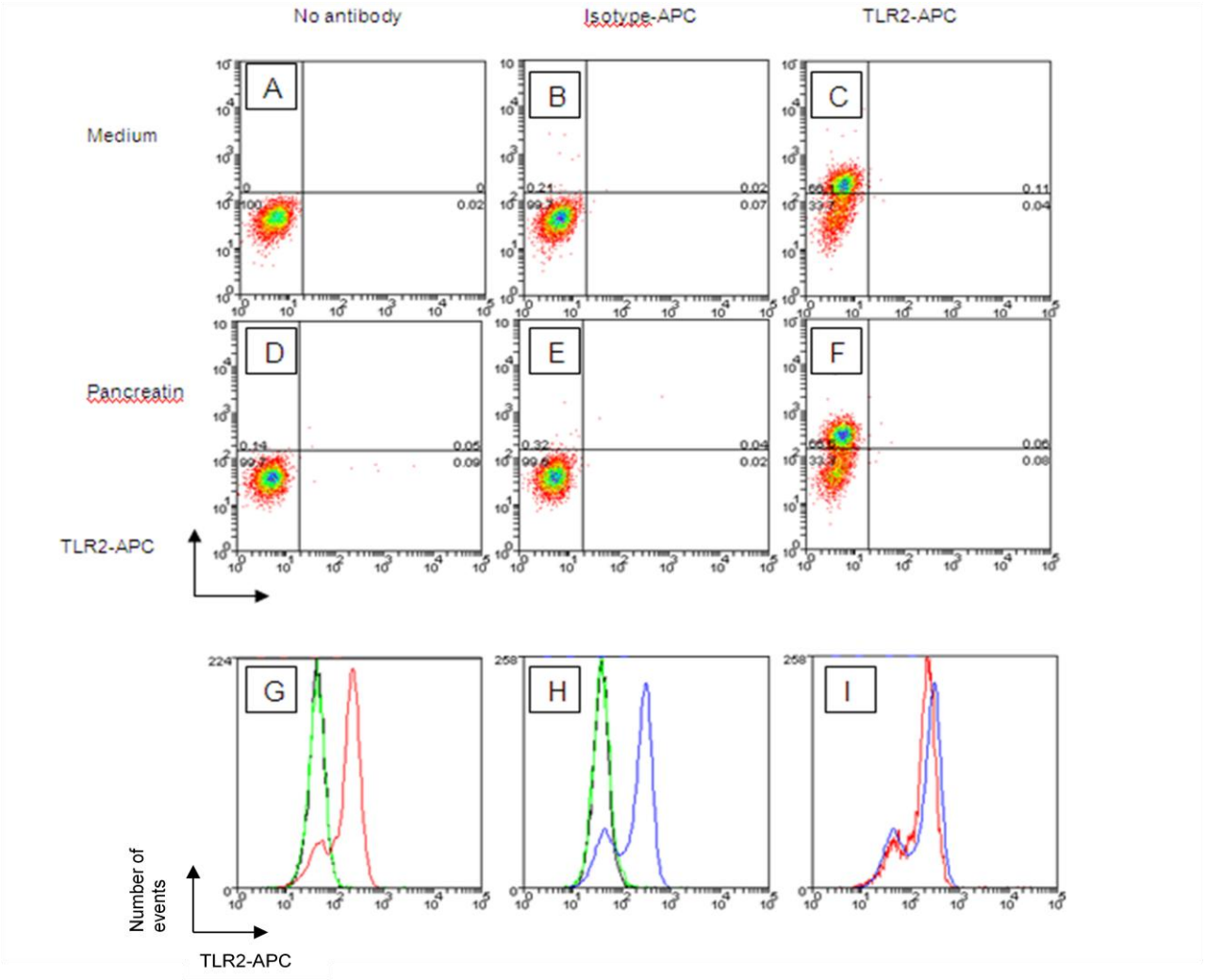

Figure 5.10 Expression of surface TLR2 protein on human peripheral blood mononuclear cells is unaffected by pancreatin treatment. Following Ficoll-gradient acquisition, isolated PBMC were either suspended in medium for 90 minutes followed by incubation with (A) no primary antibody, (B) isotype-APC control antibody or (C) primary anti-TLR2-APC antibody; or treated with pancreatin for 90 minutes followed by incubation with (D) no primary antibody, (E) isotype-APC control antibody or (F) primary anti-TLR2-APC antibody. Subsequently cells were analysed on a flow cytometer. The overlay histograms illustrated the expression of surface TLR2 protein both after suspension in medium (G) or following pancreatin treatment (H). The comparative expression of surface TLR2 protein between medium- or pancreatin-treated PBMC was illustrated in histogram I. The X-axes of panels A-F represent unused gates.

Black: No antibody control
Green: Isotype-APC antibody
Red: TLR2-APC primary antibody in medium-treated PBMC
Blue: TLR2-APC primary antibody in pancreatin-treated PBMC

APC, Allophycocyanin; PBMC, peripheral blood mononuclear cells; TLR, Toll-like receptor

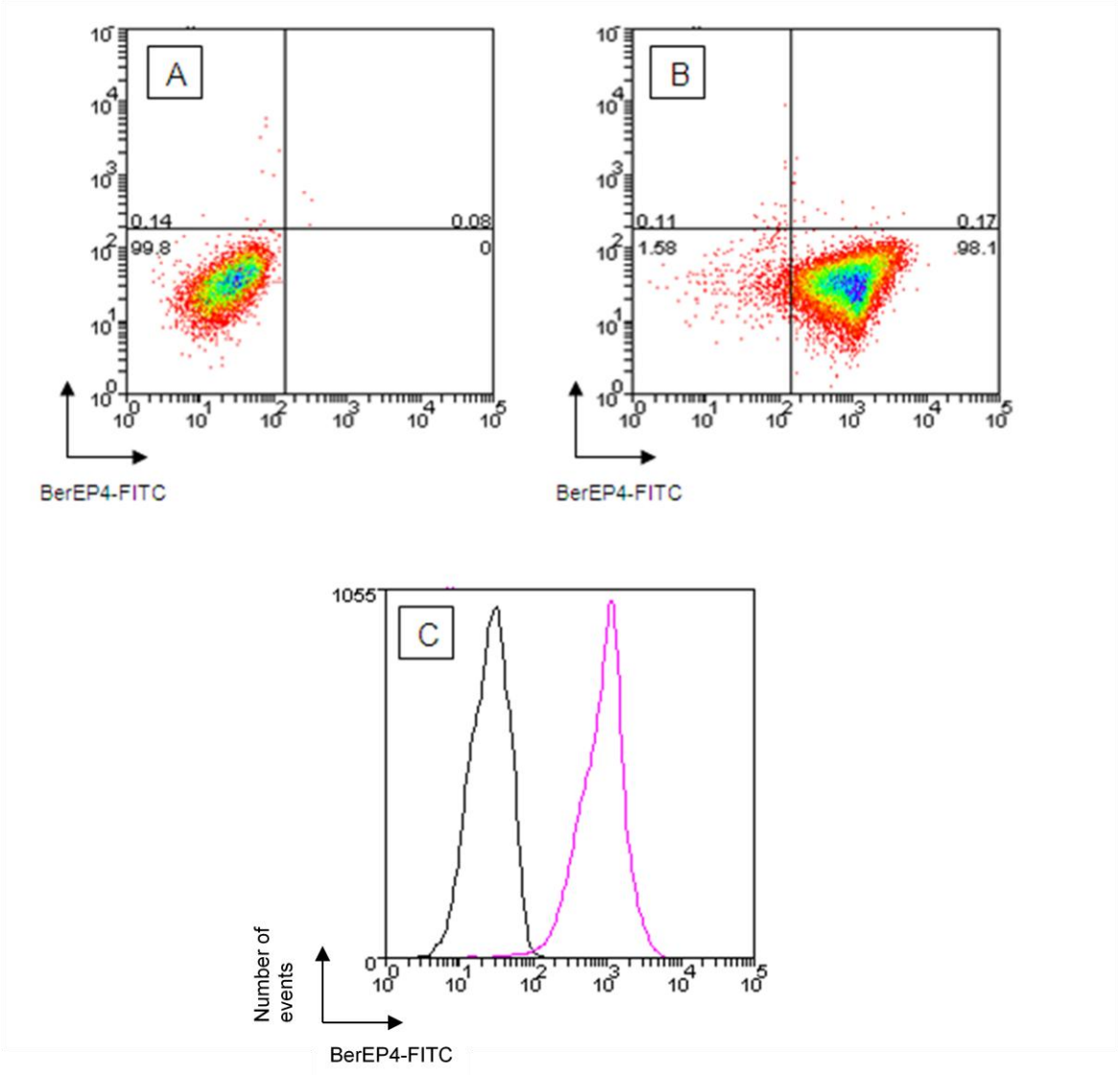

Figure 5.11 Isolated primary crypt cells express surface BerEP4 protein. Isolated intestinal crypt cells were incubated with normal mouse serum followed by either (A) isotype-FITC control or (B) primary anti-BerEP4-FITC antibody and analysed using flow cytometry. The overlay histogram illustrated the expression of BerEP4 on intestinal crypt cells (C). The Y-axes of panels A and B represent unused gates.

Black: Isotype-FITC control
Purple: BerEP4-FITC

FITC, Fluorescein isothiocyanate

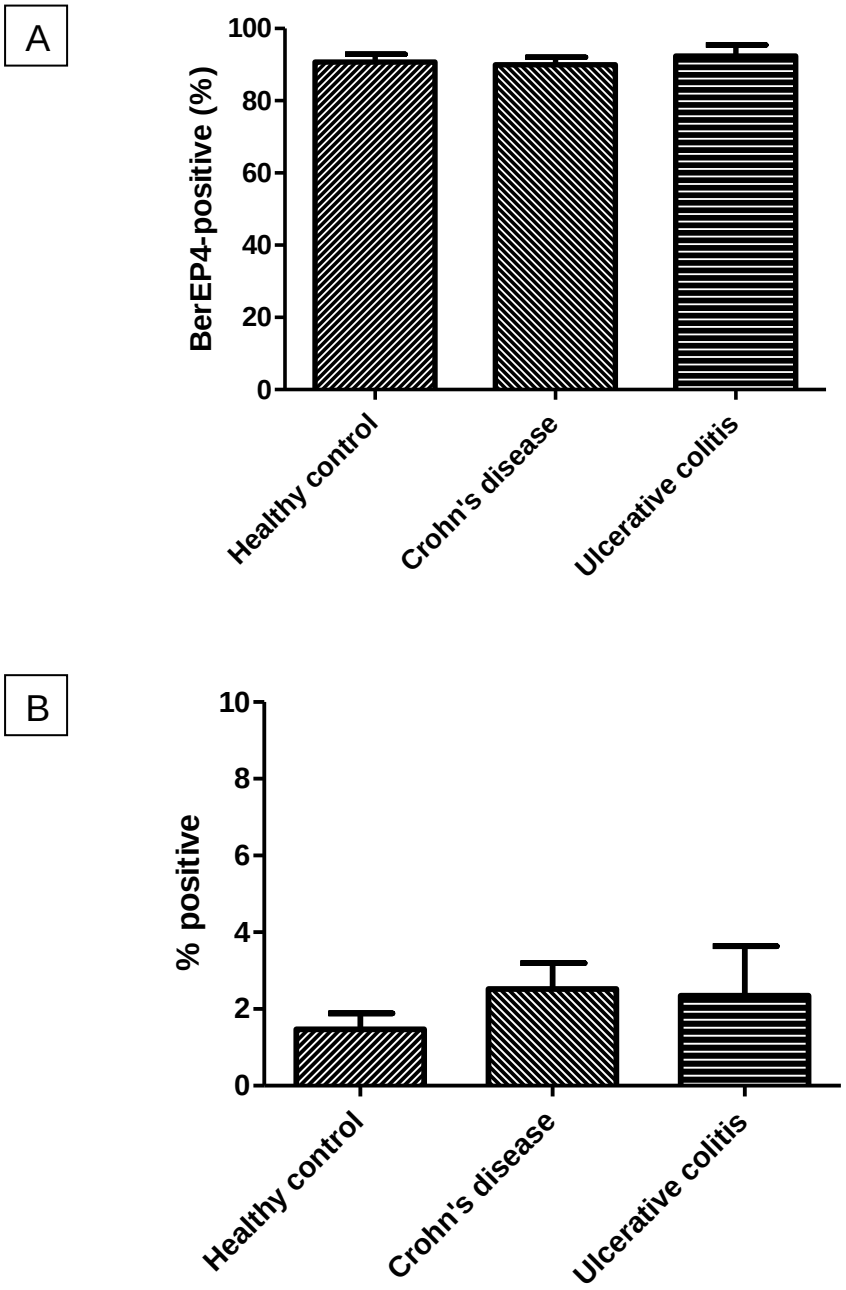

Figure 5.12 Primary crypt cells show similar proportions of BerEP4-positive and CD45-positive cells when isolated from healthy controls or patients with inflammatory bowel disease. Isolated intestinal crypt cells from healthy controls (n=7) or patients with inflammatory bowel disease (Crohn's disease n=14 or ulcerative colitis n=4) were incubated with anti-BerEP4-FITC conjugated or anti-CD45-AF488 conjugated monoclonal antibodies and analysed using flow cytometry. The proportion of antibody-positive cells was calculated by comparing median fluorescent intensity of the primary antibody corrected by the respective isotype control antibody. There was no significant difference in the percentage of (A) BerEP4-positive or (B) CD45-positive cells amongst the groups.

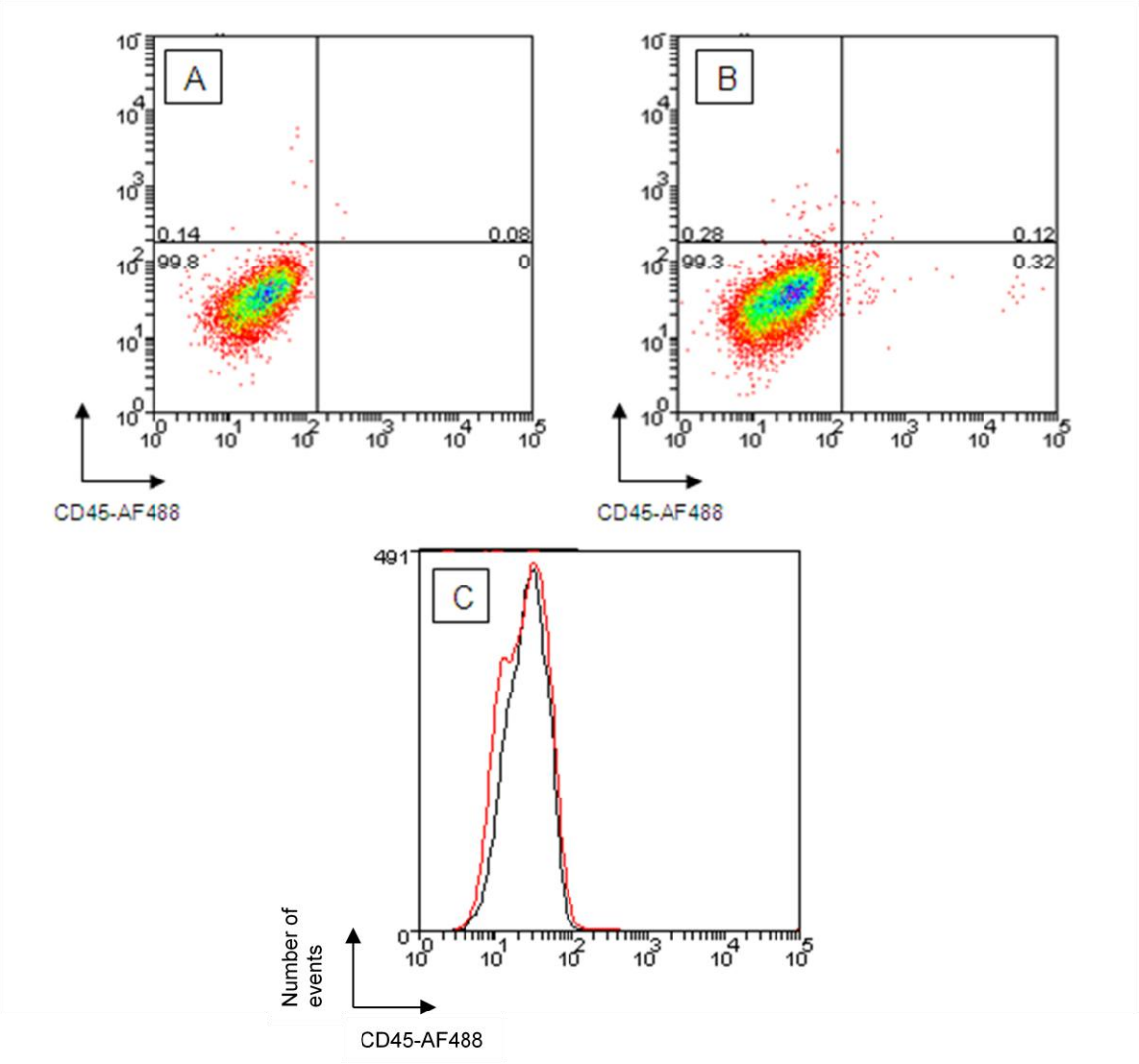

Figure 5.13 The majority of isolated primary intestinal crypt cells do not express surface CD45 protein. Isolated intestinal crypt cells were incubated with normal mouse serum followed by either (A) isotype-AF488 control or (B) primary anti-CD45-AF488 antibody and assessed by flow cytometry. The overlay histogram illustrated the difference fluorescence between the anti-CD45 and the isotype control antibodies on isolated crypt cells (C). The Y-axes of panels A and B represent unused gates.

Black: Isotype-AF488
Red: CD45-AF488

AF488, Alexa Fluor-488

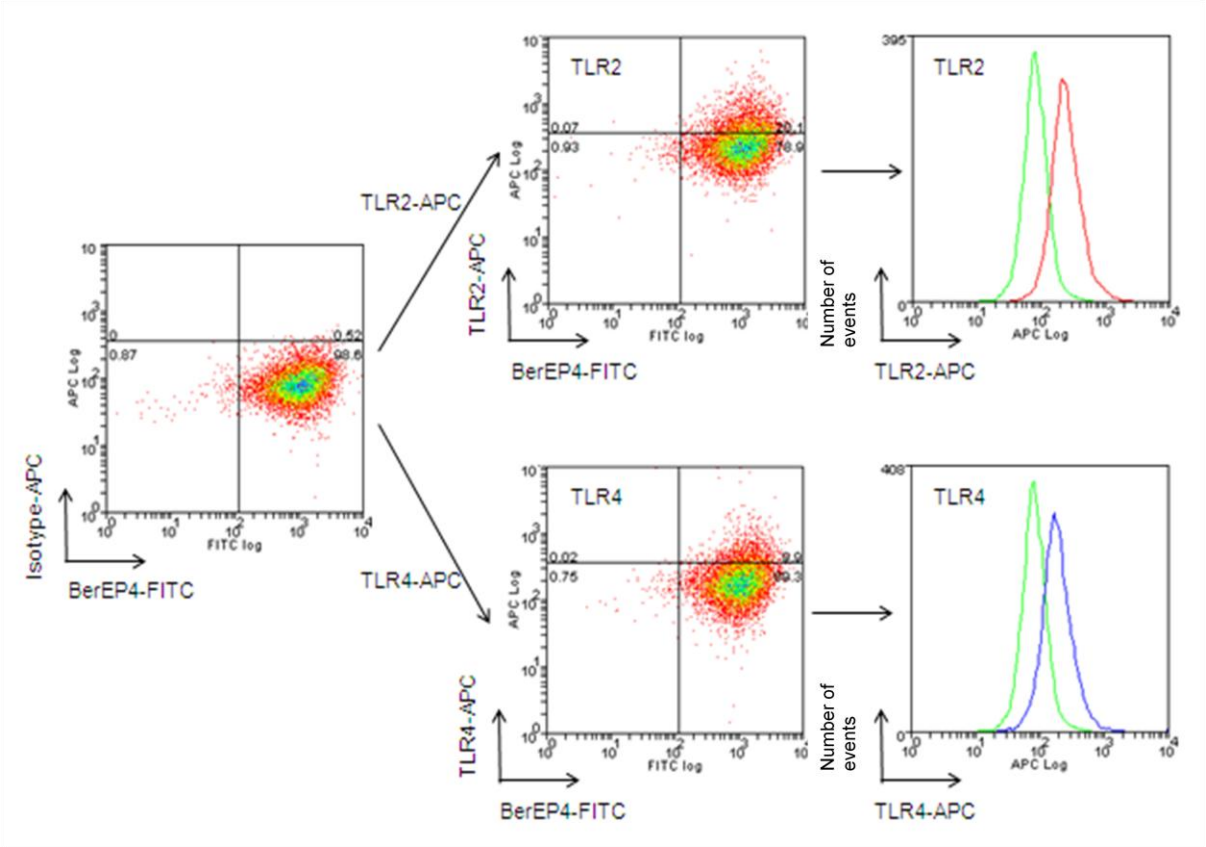

Figure 5.14 Isolated BerEP4-positive primary intestinal crypt cells express surface TLR2 and TLR4 protein. Isolated intestinal crypt cells from a patient with UC were incubated with anti-BerEP4-FITC antibody followed by either anti-TLR2-APC or anti-TLR4-APC monoclonal antibodies and assessed by flow cytometry. BerEP4-positive events (left panel) represent intestinal epithelial cells. BerEP4-positive intestinal epithelial cells express both TLR2 (upper middle panel) and TLR4 (lower middle panel). Median TLR2 (upper right panel) and TLR4 (lower right panel) surface protein expressions were calculated as the difference between the MFI of the primary antibody and the MFI of the isotype control antibody.

Green: Isotype-APC
Red: TLR2-APC
Blue: TLR4-APC

APC, allophycocyanin; MFI, median fluorescent intensity; TLR, Toll-like receptor; UC, ulcerative colitis

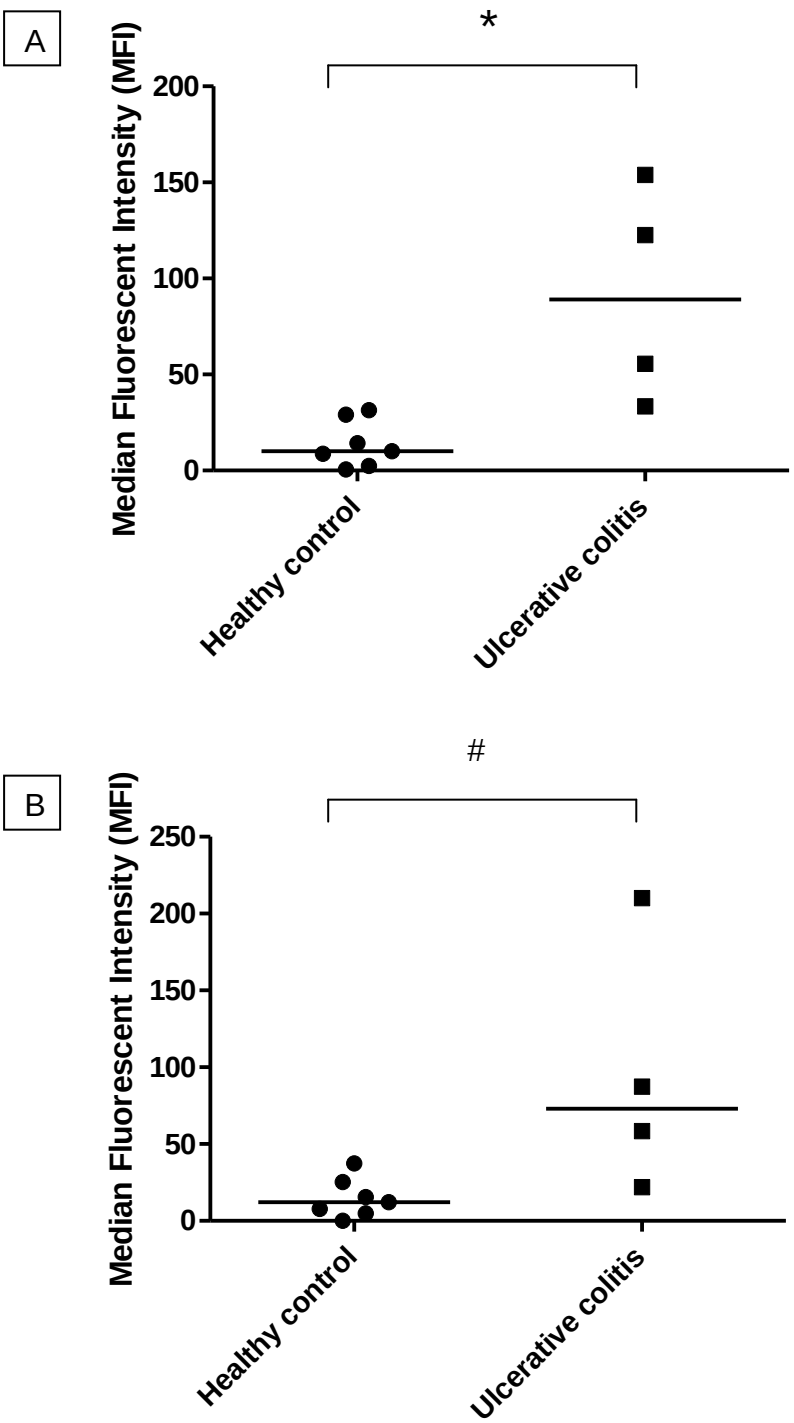

Figure 5.15 BerEP4-positive colonic intestinal epithelial cells from patients with ulcerative colitis up-regulate surface TLR2 and TLR4 protein expression. Isolated large intestinal crypt cells were stained with anti-BerEP4-FITC and either (A) anti-TLR2-APC or (B) anti-TLR4-APC monoclonal antibodies, and analysed on a flow cytometer. Analysis was undertaken after positively gating on BerEP4-expressing epithelial cells and excluding BerEP4-negative cells. Each data point represents the difference in median fluorescent intensity (MFI) between the primary and isotype control antibodies. Horizontal bars represent median values for the group.
* p=0.006; # p=0.024

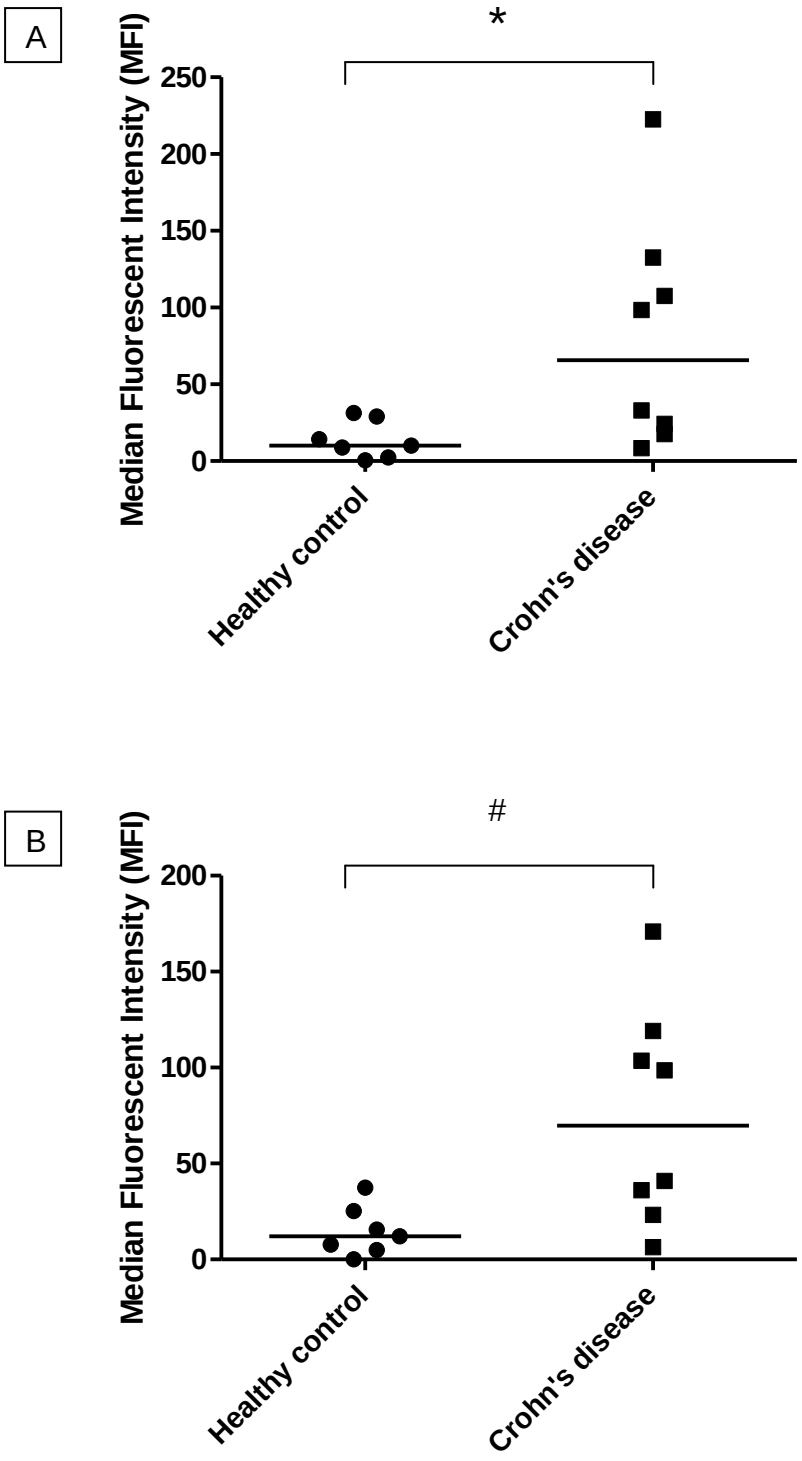

Figure 5.16 BerEP4-positive colonic intestinal epithelial cells from patients with Crohn's colitis up-regulate surface TLR2 and TLR4 protein expression. Isolated large intestinal crypt cells were stained with anti-BerEP4-FITC and either (A) anti-TLR2-APC or (B) anti-TLR4-APC monoclonal antibodies, and analysed on a flow cytometer. Analysis was undertaken after positively gating on BerEP4-expressing epithelial cells and excluding BerEP4-negative cells. Each data point represents the difference in median fluorescent intensity (MFI) between the primary and isotype control antibodies. Horizontal bars represent median values for the group.
* p=0.029; # p=0.021

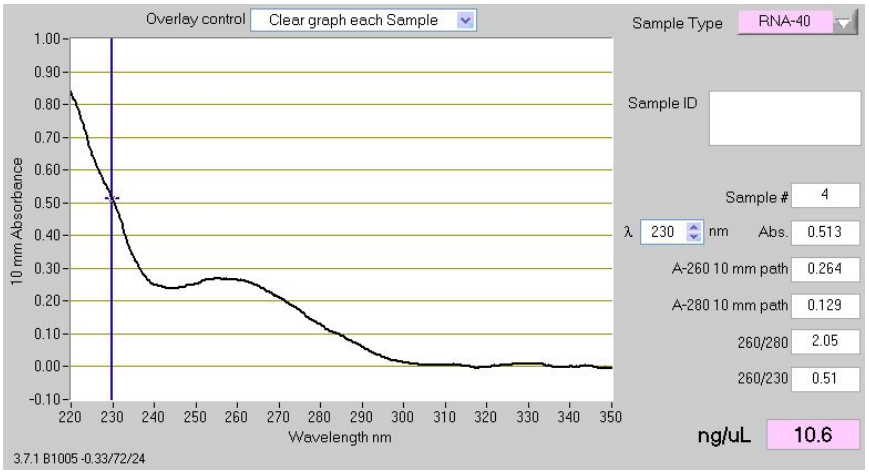

Figure 5.17 Spectrophotometric trace of sorted BerEP4-positive cells using the Nanodrop® spectrophotometer. Intestinal epithelial crypt cells were isolated using EDTA/DTT and labelled with an epithelial-specific monoclonal antibody against BerEP4. Total RNA was isolated from sorted BerEP4-positive crypt cells using the Qiagen RNeasy Plus Mini Kit. Subsequently, the quality and quantity of RNA was assessed using the Nanodrop® spectrophotometer.

DTT, Dithiothreitol; EDTA, Ethylenediaminetetraacetic acid

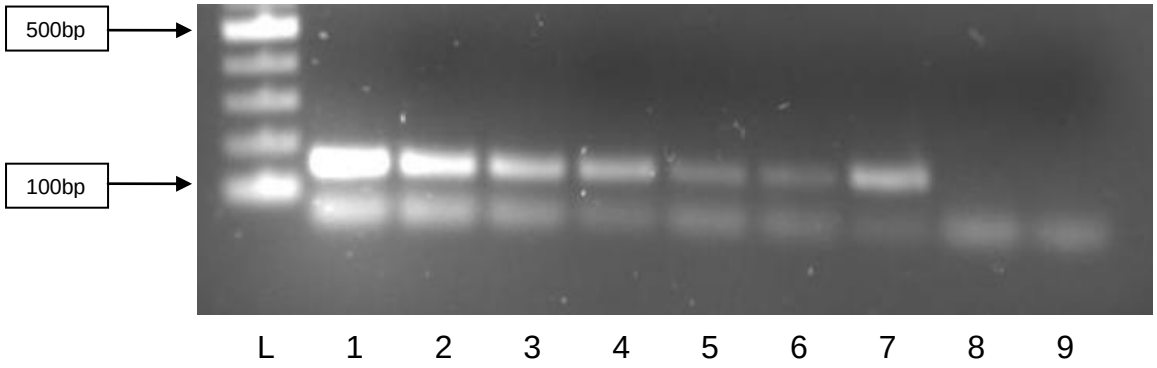

Figure 5.18 Sorted BerEP4-positive intestinal epithelial cells express HPRT mRNA. Isolated BerEP4-expressing intestinal crypt epithelial cells were sorted using FACS. Message RNA expression was analysed using conventional RT-PCR with agarose gel electrophoresis.

Lanes 1-2: Healthy control colon
Lanes 3-6: Crohn's disease colon
Lane 7: THP-1 monocyte cell line positive control
Lane 8: No RT negative control
Lane 9: No template negative control

FACS, fluorescence-activated cell sorting; HPRT, hypoxanthine guanine phosphoribosyltransferase; L, 100 base pair ladder; RT-PCR, reverse transcriptase polymerase chain reaction

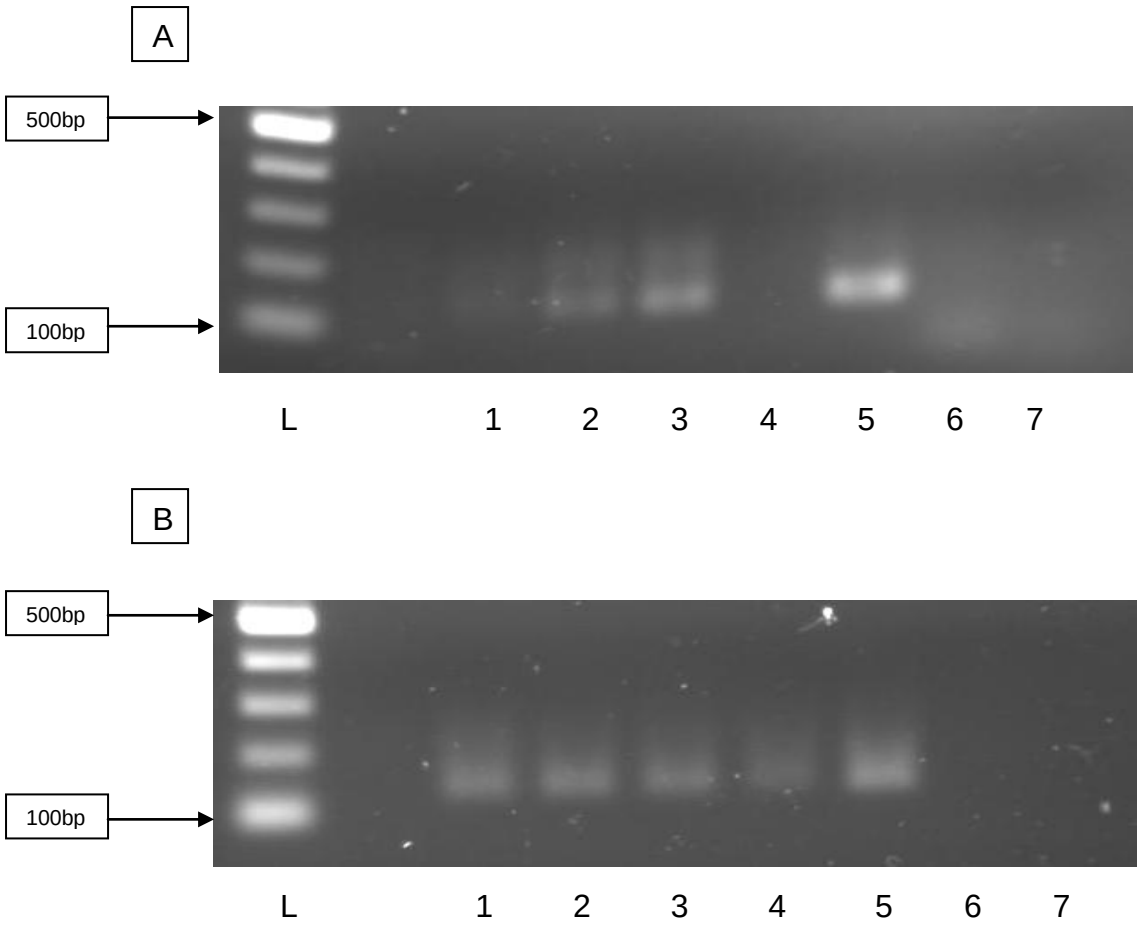

Figure 5.19 Sorted BerEP4-positive intestinal epithelial cells express TLR2 and TLR4 mRNA. Isolated BerEP4-expressing intestinal crypt epithelial cells were sorted using FACS. Message RNA expression was analysed using conventional RT-PCR with agarose gel electrophoresis. PCR was undertaken using real-time RT-PCR primers for (A) TLR2 (expected size 134bp) and (B) TLR4 (expected size 141bp).

Lanes 1, 3 and 4: Crohn's colitis
Lane 2: Healthy control colon
Lane 5: THP-1 monocyte cell line positive control
Lane 6: No RT negative control
Lane 7: No template negative control

BP, base pair; FACS, fluorescence-activated cell sorting; L, 100 base pair ladder; RT-PCR, reverse transcriptase polymerase chain reaction; TLR, Toll-like receptor

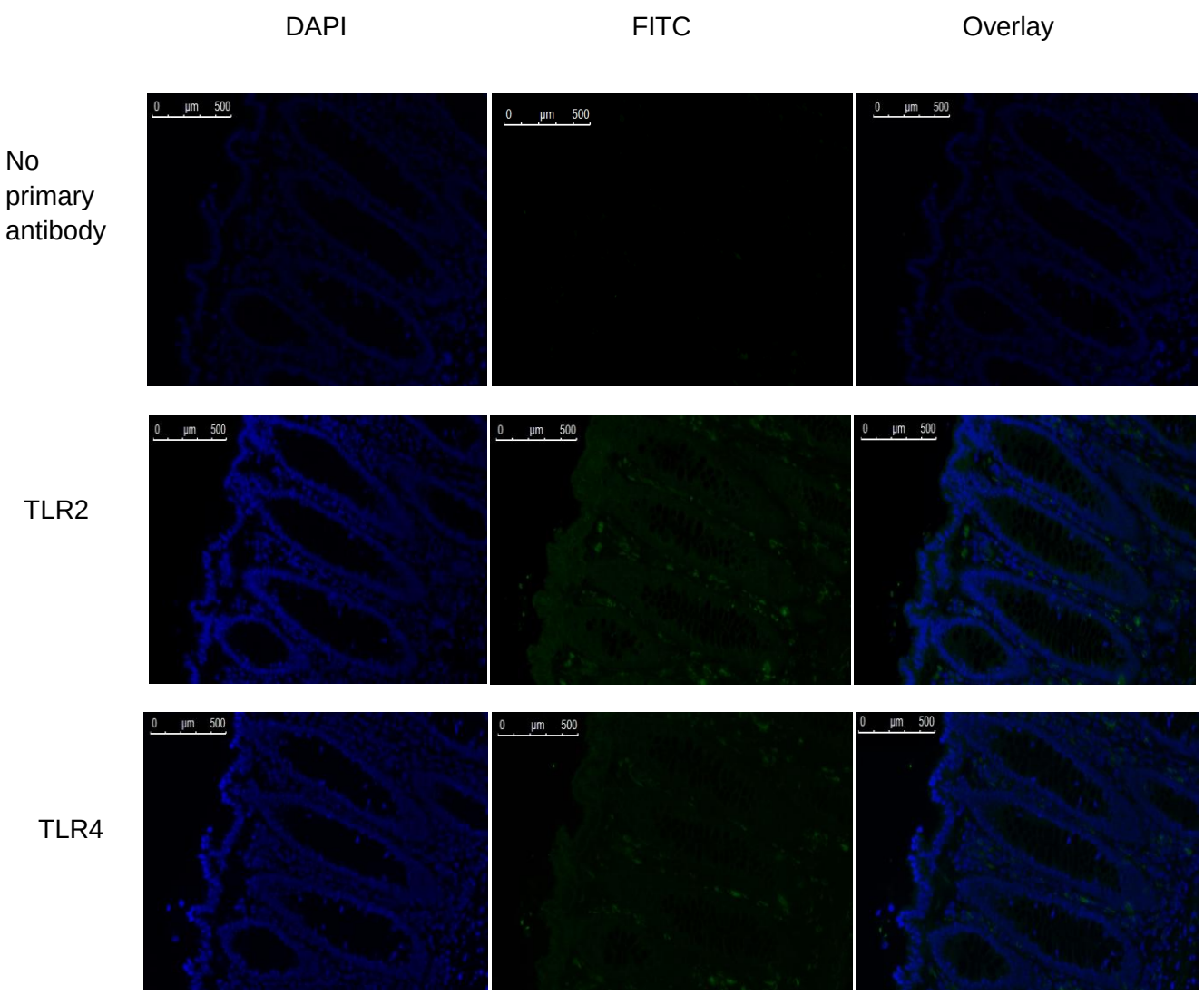

Figure 5.20 Intestinal epithelial cells from healthy control colon weakly express TLR2 and TLR4 protein. Full-thickness whole bowel was obtained from operation resection specimens of the colon before being formalin-fixed and paraffin-embedded. 5µm sections were mounted on glass slides and stained with (top row) no primary antibody control, (middle row) anti-TLR2 monoclonal antibody or (bottom row) anti-TLR4 monoclonal antibody. Slides were incubated with a biotinylated secondary antibody followed by an avidin-FITC conjugate and a DAPI counter-stain. Slides were viewed on a Leica fluorescent microscope (background adjustment: +10, colour adjustment: nil, exposure: 248ms).

DAPI, 4',6-diamidino-2-phenylindole; FITC, Fluorescein isothiocyanate; TLR, Toll-like receptor

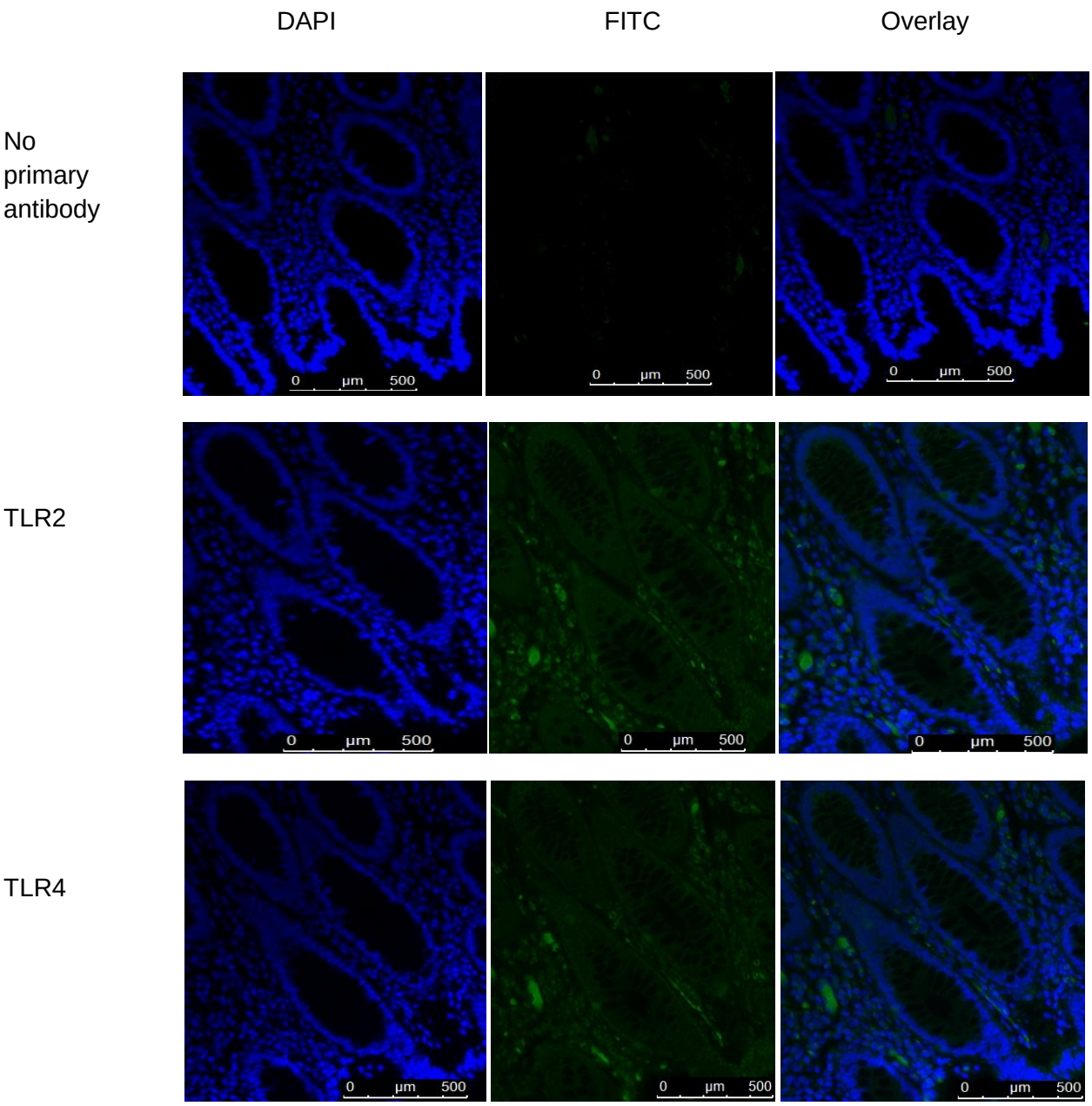

Figure 5.21 Intestinal epithelial cells from patients with ulcerative colitis express TLR2 and TLR4 protein. Full-thickness whole bowel was obtained from operation resection specimens of the colon before being formalin-fixed and paraffin-embedded. 5µm sections were mounted on glass slides and stained with (top row) no primary antibody control, (middle row) anti-TLR2 monoclonal antibody or (bottom row) anti-TLR4 monoclonal antibody. Slides were incubated with a biotinylated secondary antibody followed by an avidin-FITC conjugate and a DAPI counter-stain. Slides were viewed on a Leica fluorescent microscope (background adjustment: +10, colour adjustment: nil, exposure: 248ms).

DAPI, 4',6-diamidino-2-phenylindole; FITC, Fluorescein isothiocyanate; TLR, Toll-like receptor

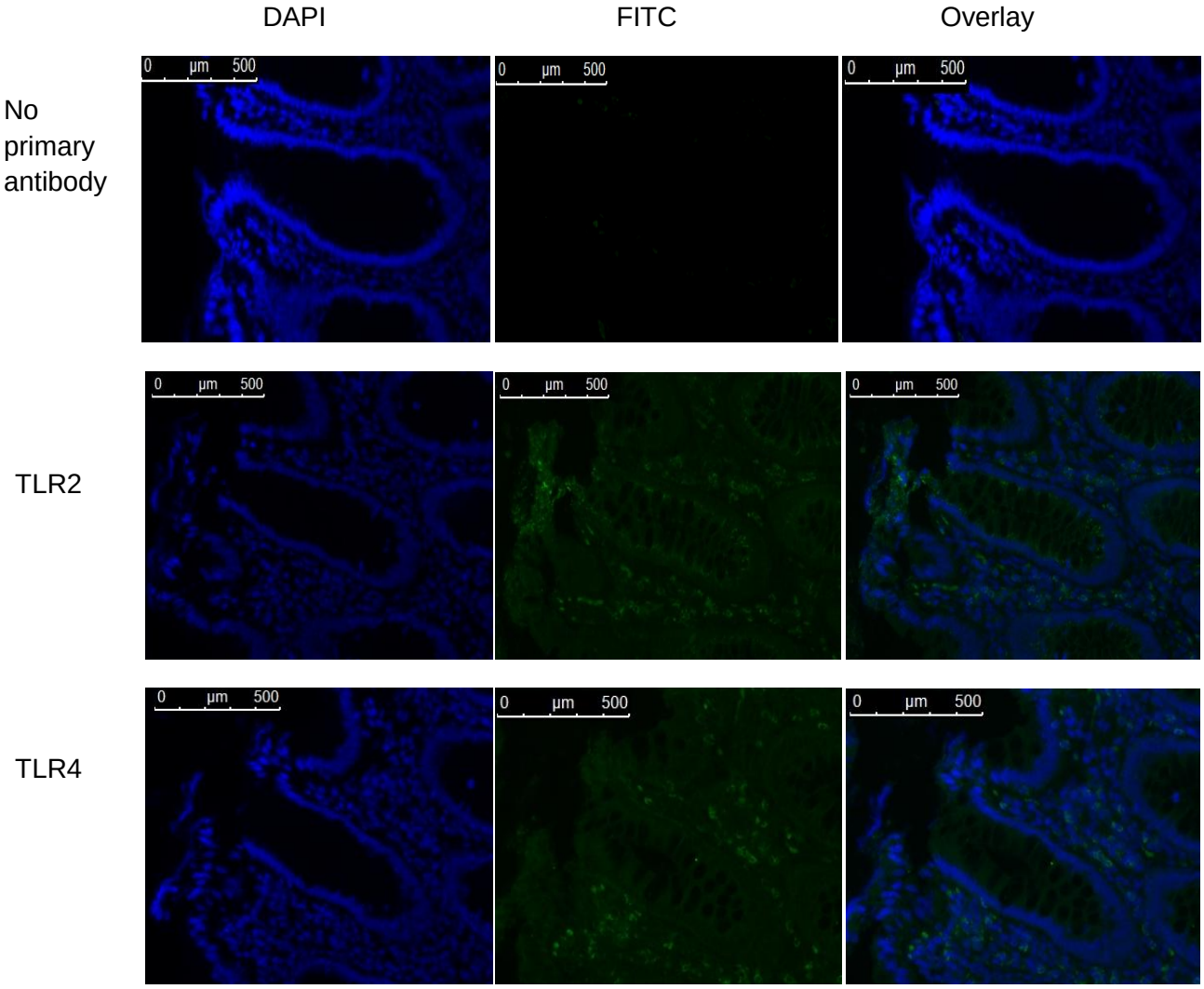

Figure 5.22 Intestinal epithelial cells from patients with Crohn's colitis express TLR2 and TLR4 protein. Full-thickness whole bowel was obtained from operation resection specimens of the colon before being formalin-fixed and paraffin-embedded. 5µm sections were mounted on glass slides and stained with (top row) no primary antibody control, (middle row) anti-TLR2 monoclonal antibody or (bottom row) anti-TLR4 monoclonal antibody. Slides were incubated with a biotinylated secondary antibody followed by an avidin-FITC conjugate and a DAPI counter-stain. Slides were viewed on a Leica fluorescent microscope (background adjustment: +10, colour adjustment: nil, exposure: 248ms).

DAPI, 4',6-diamidino-2-phenylindole; FITC, Fluorescein isothiocyanate; TLR, Toll-like receptor

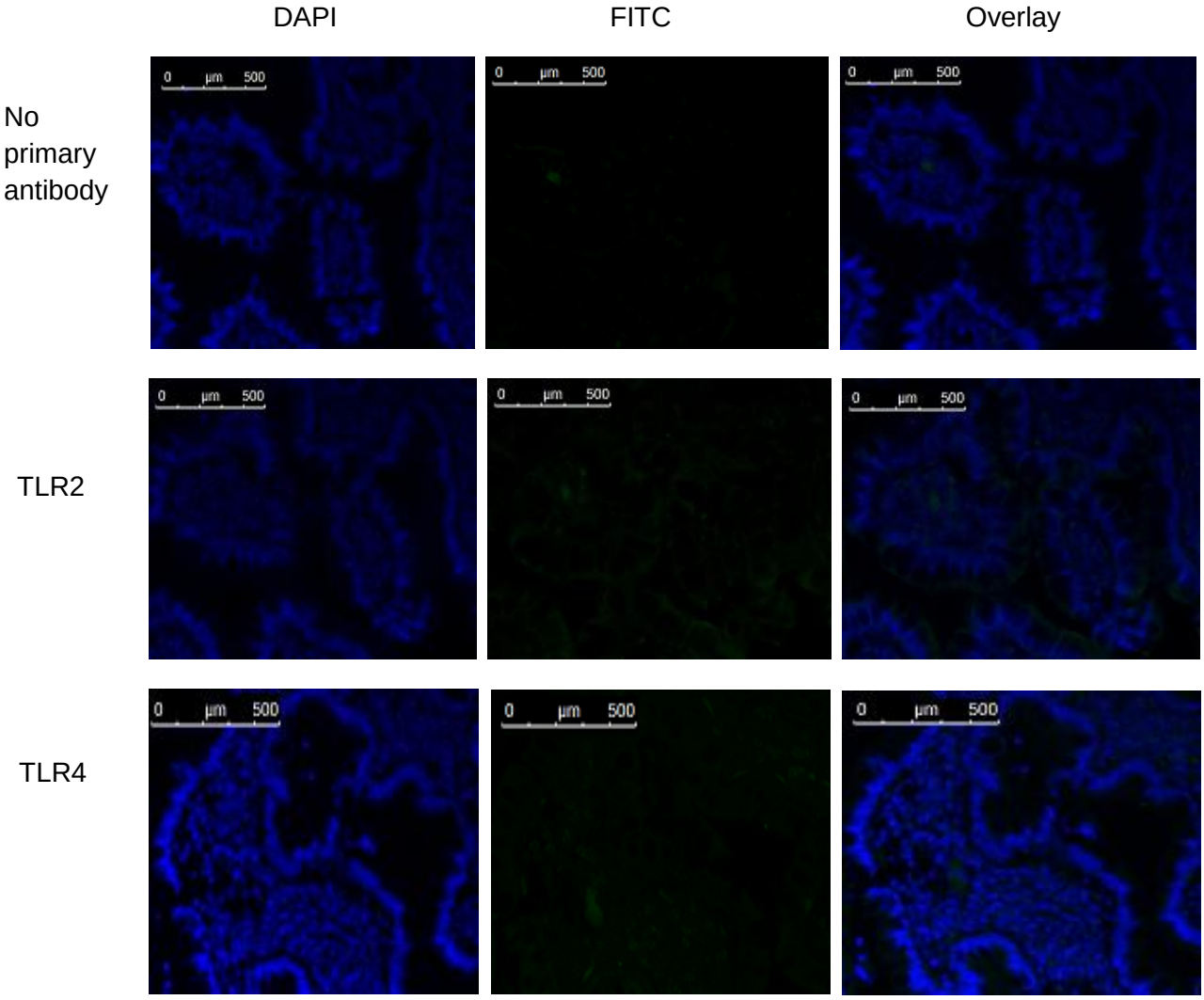

Figure 5.23 Intestinal epithelial cells from healthy control small intestine weakly express TLR2 and TLR4 protein. Full-thickness whole bowel was obtained from operation resection specimens of the small intestine before being formalin-fixed and paraffin-embedded. 5µm sections were mounted on glass slides and stained with (top row) no primary antibody control, (middle row) anti-TLR2 monoclonal antibody or (bottom row) anti-TLR4 monoclonal antibody. Slides were incubated with a biotinylated secondary antibody followed by an avidin-FITC conjugate and a DAPI counter-stain. Slides were viewed on a Leica fluorescent microscope (background adjustment: +10, colour adjustment: nil, exposure: 248ms).

DAPI, 4',6-diamidino-2-phenylindole; FITC, Fluorescein isothiocyanate; TLR, Toll-like receptor

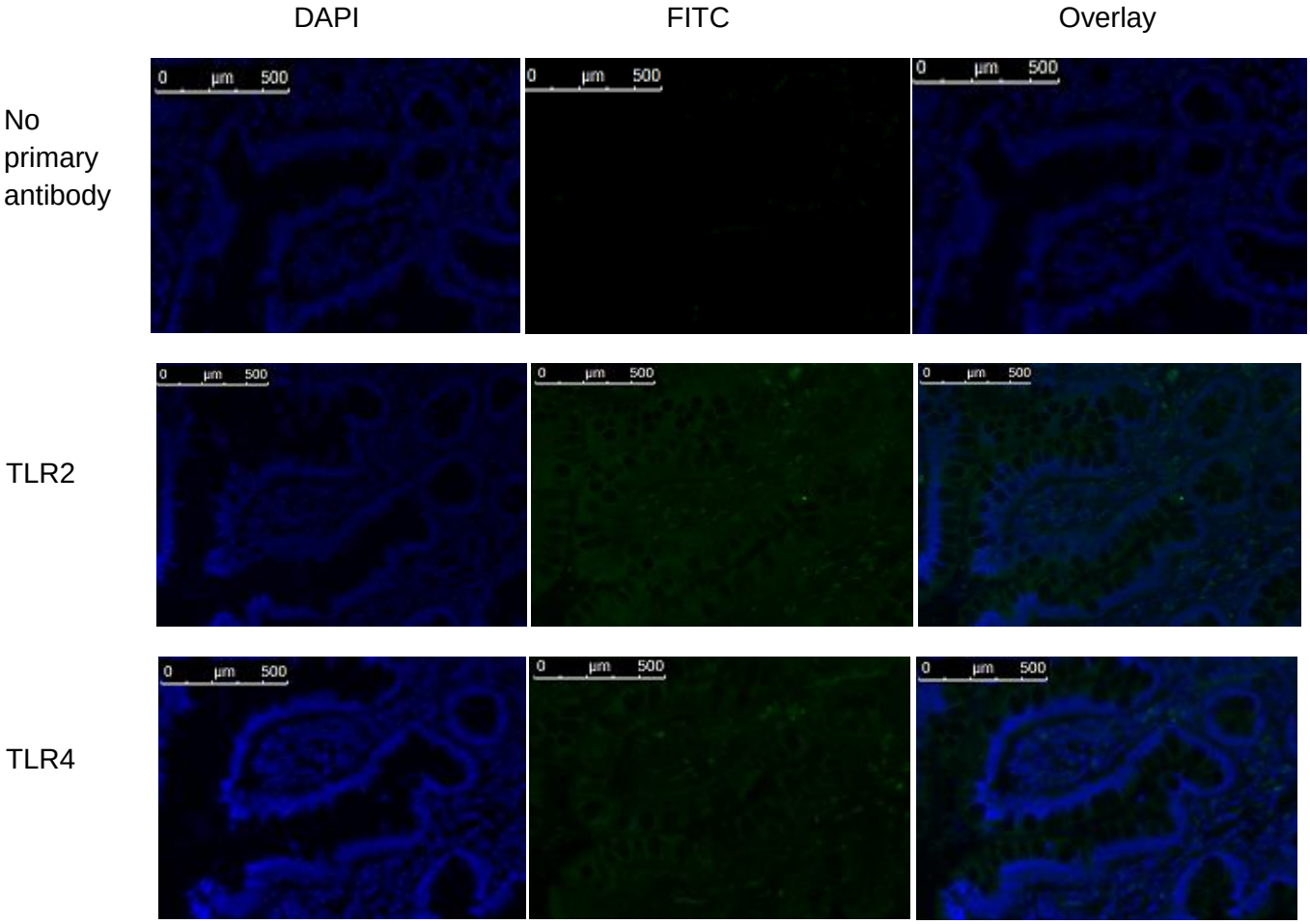

Figure 5.24 Intestinal epithelial cells from small intestinal Crohn's disease express TLR2 and TLR4 protein. Full-thickness whole bowel was obtained from operation resection specimens of the small intestine before being formalin-fixed and paraffin-embedded. 5µm sections were mounted on glass slides and stained with (top row) no primary antibody control, (middle row) anti-TLR2 monoclonal antibody or (bottom row) anti-TLR4 monoclonal antibody. Slides were incubated with a biotinylated secondary antibody followed by an avidin-FITC conjugate and a DAPI counter-stain. Slides were viewed on a Leica fluorescent microscope (background adjustment: +10, colour adjustment: nil, exposure: 248ms).

DAPI, 4',6-diamidino-2-phenylindole; FITC, Fluorescein isothiocyanate; TLR, Toll-like receptor

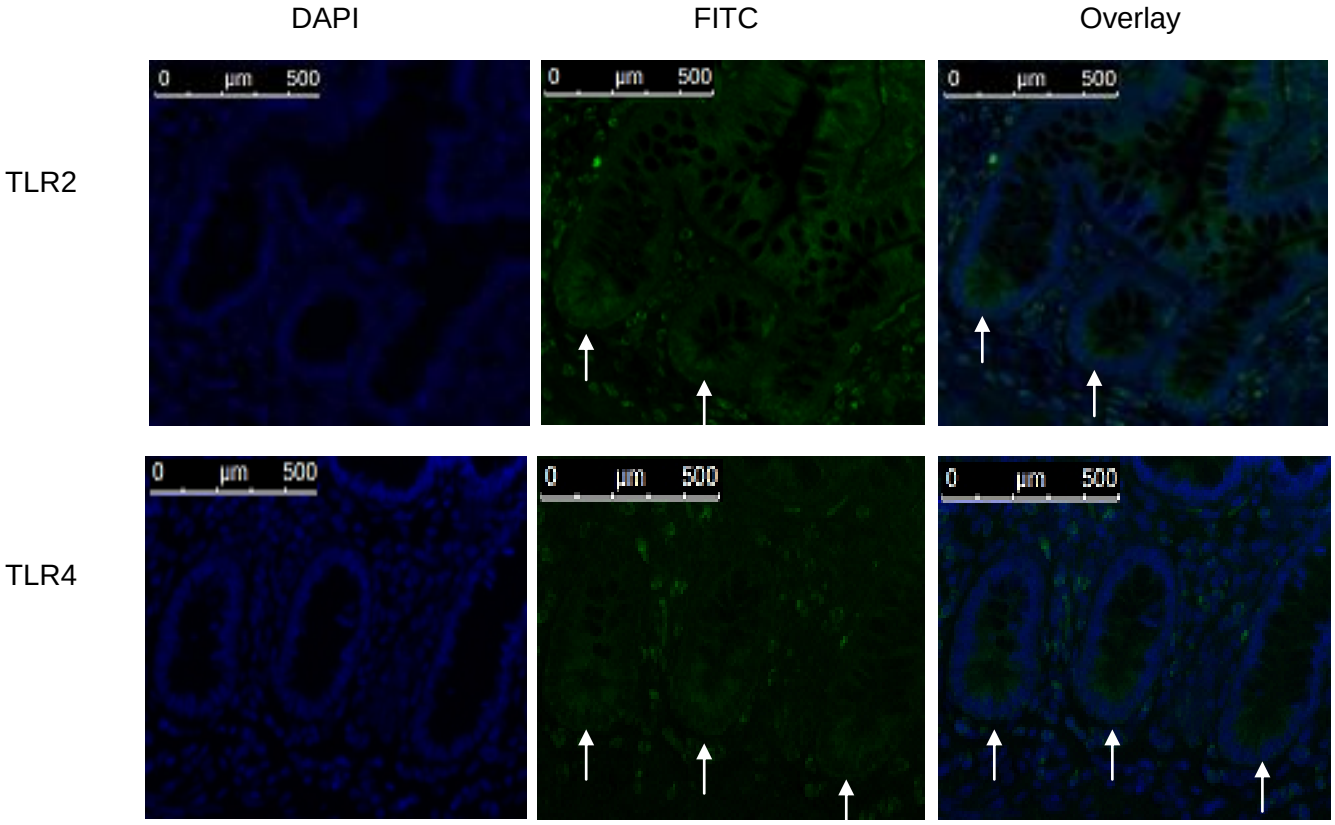

Figure 5.25 TLR2 and TLR4 protein expression is greatest in the basal crypt epithelial cells in small intestinal Crohn's disease. Full-thickness whole bowel was obtained from operation resection specimens of the small intestine before being formalin-fixed and paraffin-embedded. 5µm sections were mounted on glass slides and stained with (top row) anti-TLR2 monoclonal antibody or (bottom row) anti-TLR4 monoclonal antibody. Slides were incubated with a biotinylated secondary antibody followed by an avidin-FITC conjugate and a DAPI counter-stain. Slides were viewed on a Leica fluorescent microscope (background adjustment: +10, colour adjustment: nil, exposure: 248ms).The expression of TLR2 and TLR4 protein was examined by comparing intestinal epithelial cells in the crypt base to epithelial cells further along the crypt-villus axis. Crypt base epithelial cells demonstrate greater TLR2 and, to a lesser extend TLR4 protein, than non-basal epithelial cells (white arrows).

DAPI, 4',6-diamidino-2-phenylindole; FITC, Fluorescein isothiocyanate; TLR, Toll-like receptor

5.5 Discussion

The demonstration of the up-regulation of TLR2 and TLR4 mRNA in crypt IEC of the large bowel in UC and Crohn's disease (chapter 4) gives insight into the pathogenesis of IBD in relation to TLR expression. However it was important to characterise TLR2 and TLR4 expression at the protein level before more definitive conclusions can be drawn. To investigate the expression of TLR2 and TLR4 protein in crypt IEC Western blotting of whole cell lysate, single cell flow cytometry and full-thickness bowel section immunofluorescent staining were undertaken.

Following the acquisition of monoclonal antibodies directed against extracellular epitopes of the TLR2 and TLR4 proteins, the function of these antibodies was tested. Peripheral blood mononuclear cells are commonly used as TLR2- and TLR4-expressing positive controls, and this study has demonstrated expression of TLR2 and TLR4 transcript in these cells (section 4.3.2). Western blotting of whole cell lysate confirmed TLR2 and TLR4 protein expression in PBMC. Subsequently, TLR2 and TLR4 protein expression was demonstrated in whole cell lysate samples from primary colonic crypt cells derived from healthy controls and patients with UC and Crohn's colitis.

Demonstration of surface TLR2 and TLR4 protein expression using flow cytometry has not been reported in primary IEC. Melmed *et al.* used flow cytometry to analyse TLR4 surface protein expression in T84 and Caco-2 human intestinal cancer cells lines and reported low level expression in both cell lines (231). Otte *et al.* reported surface TLR2 and TLR4 protein expression on the SW480 intestinal cancer cell line, and demonstrated a reduction in expression following overnight incubation in the relevant receptor ligand (243). Surface TLR4 expression using flow cytometry in a variety of cell lines has been reported by other groups (155, 233, 246).

Following acquisition using EDTA/DTT, crypt cells were disaggregated using pancreatin, a mixture of porcine pancreas-derived proteolytic enzymes, lipases and amylase. This enzyme mixture is used to break down the intercellular bonds between cells which release individual cells suitable for single cell analysis. However, it was important to investigate whether pancreatin treatment could result in either loss of surface TLR protein or could damage the extracellular antibody-specific epitope such that primary antibody binding would be impaired. Pancreatin- and medium-treated PBMC were shown to express similar levels of surface TLR2 and TLR4 protein, suggesting pancreatin treatment did not alter primary antibody binding.

The BerEP4 surface protein is an epithelial antigen used in clinical laboratory practise to determine the epithelial origin of tumour cells (281). Crypt cells were shown to be 90-92.4% BerEP4-positive, confirming their phenotype as being epithelial-derived. This was consistent with the immunocytochemical data showing that approximately 97% of freshly isolated crypt cells stained positively for BerEP4 (section 3.3.2). The slightly lower BerEP4-positive rate may be a consequence of greater cell death during the flow cytometry protocol compared to the cytospin slide preparation undertaken for immunocytochemical staining. Of importance, the proportion of BerEP4-positive cells in cellular preparations was statistically similar in healthy controls compared to cell isolated form patients with UC or Crohn's colitis. This suggests that the crypt cell isolation preparation yielded a similar proportion of epithelial cells in all groups and therefore these groups are comparable.

In chapter 3 immunocytochemical studies were undertaken on isolated crypt cells to determine the number of CD45-positive cells. These experiments showed that between 1.9% and 2.2% of all crypt cells were CD45-positive, with the numbers of CD45-positive crypt cells being statistically similar when comparing healthy controls to patients with IBD (section 3.3.2). To further quantify the number of CD45-positive cells present in preparations following EDTA/DTT and pancreatin treatment, isolated cells were labelled with a fluorescent

anti-CD45 antibody and examined by flow cytometry. The number of CD45-positive crypt cells ranged from 1.5% to 2.5%. There was no significant difference in the number of CD45-positive cells in crypt cell preparations from healthy controls compared to patients with IBD. From these results it was concluded that crypt cells were predominantly of epithelial origin and that crypt cells isolated from the mucosa of patients with IBD did not yield greater numbers of haematopoietic cells. Therefore, EDTA and pancreatin treatment is a reliable method for isolating IEC. Furthermore, these isolated crypt cells are comparable between the different disease groups.

To quantitatively analyse the surface expression of TLR2 and TLR4 protein on crypt IEC from patients with IBD, isolated crypt cells were dual labelled with fluorescent antibodies to the epithelial-specific marker BerEP4 and TLR2 or TLR4 proteins. The strength of this technique is that only crypt cells staining positively for BerEP4 were included in the analysis. This allowed all non-epithelial cellular events to be removed from the analysis of surface TLR2 and TLR4 protein expression.

BerEP4-positive crypt IEC from patients with UC demonstrated greater expression of surface TLR2 and TLR4 proteins (8-fold and 6-fold, respectively) compared to healthy controls. Likewise, BerEP4-positive crypt cells from patients with Crohn's colitis demonstrated greater expression of surface TLR2 and TLR4 proteins (6-fold and 5-fold, respectively) compared to healthy controls.

These data supports the results from section 4.3.5, showing significant up-regulation of TLR2 and TLR4 mRNA transcripts in crypt cells from patients with UC and Crohn's colitis. Interestingly, the relative up-regulation of TLR2 and TLR4 mRNA transcripts in crypt cells from IBD patients was in the order of 2-fold to 3.5-fold, which is less than the relative up-regulation at the protein level. It is possible that degradation of mRNA during the cell isolation protocol occurred at a more rapid rate than protein degradation, resulting in a

greater loss of transcripts during cell isolation and, therefore, a lesser observed difference between controls and patients with IBD. On the other hand, the samples for the transcript analysis and the surface protein analysis were collected at different times during the study period. Therefore, the observed differences in relative expression at the transcript and protein levels may simply reflect the fact that the samples were obtained from different groups of subjects.

Following the labelling with anti-BerEP4 antibody and the analysis of surface TLR2 and TLR4 protein expression, isolated BerEP4-positive IEC were sorted using FACS. Subsequently, mRNA was isolated from these cells and TLR2 and TLR4 mRNA expression analysed by conventional RT-PCR. BerEP4-positive crypt IECs derived from healthy controls and patients with Crohn's colitis were shown to express both TLR2 and TLR4 transcripts. These data confirm TLR2 and TLR4 mRNA expression in BerEP4-positive colonic crypt intestinal epithelial cells of healthy controls and patients with IBD.

This is the first study to report up-regulated surface TLR2 and TLR4 protein expression on crypt IEC of patients with IBD using flow cytometry. Qualitative expression of TLR2 and TLR4 protein by crypt IEC has been reported using immunohistochemistry in the adult small and large intestine (252, 254) and on the basolateral surface of foetal ileal epithelial cells (240). In IBD, Cario and Podolsky reported up-regulation of TLR4, but not TLR2, protein using immunohistochemistry by IEC of the small and large intestine of patients with UC and Crohn's disease, regardless of disease activity (260), though this is not a universal finding (262). Therefore reported data on the expression of TLR2 and TLR4 in IBD is limited.

This study supports the report by Cario and Podolsky in suggesting up-regulation of TLR4, but conflicts with their report regarding TLR2 expression (260). Flow cytometry is a more accurate, quantitative method of assessing TLR2 and TLR4 protein expression and this may explain the observed conflicting expression of the former receptor. Interestingly, in mice

DSS-induced colitis resulted in IEC up-regulation of both TLR2 and TLR4 protein, as assessed by using Western blotting, and TLR4 protein was shown to be expressed further up the crypt with increasing disease severity using immunohistochemical staining (250).

In this study, crypt epithelial cells were isolated at the time of surgical intestinal resection. Patients were therefore those with chronic IBD symptoms that required surgical resection due to either persisting disease activity despite maximal medical therapy or due to non-response to medical therapy. This explains why some patients were taking several immunosuppressive medications at the time of surgery and why others were not. This is a reasonable group of patients with IBD to study because these patients usually have active disease and are therefore likely to show the biological changes associated with IBD.

The number of isolated epithelial cells required to perform immunohistochemical staining, RNA isolation for transcript analysis and analysis of protein expression using western blotting and flow cytometry precluded using endoscopically-obtained biopsy specimens. There were no samples of crypt epithelial cells isolated from resected colectomy specimens undertaken for acute severe ulcerative colitis. This group would likely express the highest level of TLR2 and TLR4 and would be an interesting group to study. However, patients with acute severe colitis often have severe mucosal ulceration with extensive epithelial cell loss. Obtaining adequate numbers of crypt cells from such cases is challenging. Furthermore, patients with chronically active IBD rather than acute severe colitis are likely to represent a cohort of patients in which modulation of the inflammatory response through the use of novel agents (such as TLR-blocking agents) may be most suited.

The functionality of TLR2 and TLR4 protein has not been reported in human primary IEC, though response to a TLR8 ligand is reported (256) and primary mucosal specimens are reported to respond to the TLR5 ligand flagellin following its application to the basolateral, but not the apical cell surface (255). Human intestinal epithelial cancer cell lines have been

shown to respond to TLR2 and TLR4 ligands (154, 231, 232, 242, 243, 246). Despite the micro array data in this study demonstrating up-regulation of the TLR-associated signalling molecule ECSIT mRNA in crypt cells from patients with UC, future work is required to investigate the functionality of these receptors in primary intestinal epithelial cells.

Despite the quantitative flow cytometry data reported here demonstrating up-regulation of surface TLR2 and TLR4 protein on colonic crypt IECs in patients with IBD, the western blot protein bands of whole cell lysates from patients with UC and Crohn's colitis appeared to be a similar size when compared to the protein bands from healthy controls. This may suggest that the total protein was similar in whole cell lysates isolated from healthy controls and patients with IBD, but surface protein expression was significantly greater in the latter. However, western blotting is a qualitative method of measuring total protein expression whereas flow cytometry is fully quantitative. Therefore, these discrepancies may be the result of the inherent differences of the two techniques.

Trafficking of TLR4 protein from the cell membrane to the Golgi complex has been reported in TLR4-transfected HEK293 cells (247) and it has been shown that surface TLR protein, rather than cytoplasmic protein, is functionally active in SW480 and TLR4-transfected HEK293 cell lines (246, 247). Furthermore, Otte *et al.* demonstrated that although total TLR2 and TLR4 protein levels were unchanged (using western blotting), surface TLR2 and TLR4 protein expression was reduced (using flow cytometry) when SW480 cells were pre-exposed to TLR2 and TLR4 receptor ligands, suggesting that loss of surface protein is an IEC mechanism for acquiring tolerance to TLR2 and TLR4 ligands (243). Therefore, the up-regulation of surface TLR2 and TLR4 protein in crypt IECs from patients with IBD demonstrated in this study may result from trafficking of protein from the cytoplasm to the (functionally relevant) cell surface and it suggests that this increased TLR2 and TLR4 protein expression occurs in the functionally relevant cellular compartment.

To further investigate the location of TLR2 and TLR4 protein expression within the crypt, immunofluorescent staining of whole bowel sections was undertaken. Intestinal epithelial cells were shown to express TLR2 and TLR4 protein throughout the crypt and this expression appeared to be localised to the cell membrane. Moreover, the intensity of staining appeared to be greater by colonic crypt IEC from patients with UC, and by both small and large intestine crypt IEC from patients with Crohn's disease, than in healthy controls. These data are consistent with the flow cytometry data, suggesting TLR2 and TLR4 protein expression appears to be on the plasma membrane and are up-regulated in active IBD.

TLR2 and TLR4 immunofluorescent staining by crypt epithelial cells is visible on both the apical and basolateral cell membrane, though it was not possible to determine if expression was greater in one of these two compartments. Predominantly basolateral TLR5 protein expression has been reported in confluent T84 cell monolayers (241) and primary mucosal samples (255). Apical to basolateral scattering of TLR2 and TLR4 protein following receptor ligation has been demonstrated in confluent monolayers of T84 (242) and SW480 cells (243) which may represent a mechanism of tolerance to luminal antigen in these IEC models. This study has demonstrated persisting apical TLR2 and TLR4 protein expression in active small and large intestinal IBD.

An interesting observation from the IF images is that crypt based epithelial cells in Crohn's ileitis appeared to stain TLR2 and TLR4 protein at a greater intensity than the remaining epithelial cells of the crypts. This region of the crypt is the location of both the putative intestinal stem cell (173) and the Paneth cell (108). Although Paneth cells are reported to demonstrate TLR-associated signalling (238), the expression of TLR2 and TLR4 by intestinal stem cells is unreported. This issue is addressed further in chapters 6 and 7.

In summary, intestinal mucosal treatment with EDTA/DTT and pancreatin results in the isolation of crypt intestinal epithelial cells with few contaminating non-epithelial cells. Staining with the epithelial-specific antibody BerEP4 allows the identification and sorting of a homogenous group of pure intestinal epithelial cells. Primary BerEP4-positive crypt intestinal epithelial cells demonstrate expression of TLR2 and TLR4 protein, which is in part expressed in the functionally active location of the cell membrane surface. Crypt IEC derived from patients with Crohn's colitis and UC express significantly more surface TLR2 and TLR4 protein than IEC derived from healthy controls, and this may be important in the pathogenesis of colonic IBD. In the small intestinal crypts there is a population of crypt base cells which express greater TLR2 and TLR4 protein than the other crypt IEC and the nature of these cells requires further investigation. These data provide further insight into the pathogenesis of inflammatory bowel disease.

Chapter 6: Expression of toll-like receptors-2 and -4 by intestinal myofibroblasts and their interaction with intestinal crypt cells

6.1 Introduction

In section 1.7, the structure and function of the intestinal myofibroblast (MF) was introduced. Furthermore, the role of the intestinal MF in modulating the immune response and in the formation of fibrosis during inflammatory conditions of the intestine was discussed. Intestinal wall fibrosis is a recognised feature of chronic inflammatory bowel diseases. In UC fibrosis is limited to the mucosa and sub-mucosa, resulting in thickening of the muscularis mucosa with stiffening and shortening of the colon; whereas in Crohn's disease the expansion of the ECM is trans-mural, resulting clinically in stricturing or penetrating (fistulating) disease (2). While most patients initially present with inflammatory Crohn's disease, almost all patients progress to a penetrating or stricturing phenotype over the course of the disease (181). While there have been significant advances in the treatment of inflammatory and penetrating IBD in recent years, particularly with the introduction of biological therapies (282), there has been little development in the prevention or treatment of stricturing disease. Therefore, better understandings of the mechanisms which lead to MF-induced fibrosis are urgently required.

Alpha-smooth muscle actin- and vimentin-positive MF have been identified in increased numbers in the mucosa of patients with both UC and Crohn's disease (283). It has also been demonstrated that MF isolated from patients with Crohn's disease proliferate at a greater rate than MF isolated from normal subjects or patients with UC (284). Furthermore, isolated MF from patients with IBD express higher levels of mRNA for MMP-1, MMP-3 and TIMP-1 than do MF isolated from normal mucosa (285-287). These studies suggest that MF may play a role in the pathogenesis of stricturing and fibrosis in IBD.

There is evidence to suggest intestinal MF play a role in both intestinal mucosal homeostasis and in the regulation of the immune response (section 1.7). Indeed, MF may play a role in retaining inflammatory molecules and leukocytes within inflamed tissue, resulting in the transition from acute to chronic inflammation as is seen in IBD and the subsequent development of intestinal fibrosis.

Recent work has investigated the interaction between isolated crypt epithelial cells and cultured MF monolayers *in vitro*. The IEC adhere to MF monolayers in a β1-integrin-independent manner and remain viable for a number of days (210). Interestingly epithelial cells expressing the putative intestinal stem cell marker musashi-1 are over-represented in the adherent cell population, suggesting that stem cells may preferentially bind to MF layers. Furthermore, isolated cells with side population characteristics (a group of cells enriched with intestinal stem cells, chapter 7) were shown to adhere to MF layers (210). This suggests that IEC-MF co-cultures are a useful way of isolating an epithelial cell population enriched with putative stem cells from isolated crypt epithelial cells.

The purpose of this chapter was to culture primary human MF from healthy controls and patients with active IBD. Given that MF appear to play a number of roles in shaping the immune response, such as recruiting and retaining immune cells in the sub-epithelial layer of the intestinal mucosa, producing pro-inflammatory and chemotactic cytokines and expressing innate immune system pattern recognition receptors, the differential expression of TLR2 and TLR4 mRNA and protein by MF was investigated in healthy controls and patients with IBD. Furthermore, the reported preferential interaction between cultured MF layers and ISC was used to investigate the expression of TLR2 and TLR4 in MF-adherent, stem cell-enriched intestinal crypt cells.

6.2 Methods

6.2.1 Myofibroblast isolation

The isolation of myofibroblasts from the lamina propria was originally described by Mahida *et al* (167). Mucosal strips were treated with EDTA/DTT to remove the overlying epithelium. Following the collection of the E3 crypt IEC by shaking (section 3.2.4), the remaining mucosal strips were washed a further five times in HBSS (with Mg/Ca). At this stage mucosal strips are completely depleted of the epithelial cell lining. The strips were cut into smaller (2-3mm) pieces and plated out into 60mm culture dishes in 7ml of medium (500mL RPMI 1640 containing filter-sterilised 10% FCS, 5mL of 200mM glutamine and 50,000 units of penicillin G, 50mg streptomycin sulphate and 24mg gentamicin).

This medium was changed twice weekly until at least three colonies of MF had formed on the base of the dish, which usually required 4-6 weeks culture. At this stage the mucosal strips were removed (and discarded) and the medium was replaced with complete MF medium (section 6.2.2). The medium was changed 3 times weekly until a confluent layer of MF was observed, usually requiring a further 4 weeks. At this stage, the cells were washed with 1mL of 0.1% trypsin and incubated with a further fresh 1.5mL of 0.1% trypsin for 15mins until cell detachment occurred.

Following cell detachment, 2mL of MF medium was added to neutralise the trypsin and the cells were collected and transferred to a T75 flask pre-filled with 11mL of MF medium. Medium was changed three times weekly and cells cultured again until confluent over 1-2 weeks in preparation for further splitting, freezing or transfer to cover slips for use in experimentation.

6.2.2 Myofibroblast culture

Complete MF medium was prepared as follows: 500mL RPMI 1640 (52400-041, Gibco, Invitrogen) with 0.2µm filter-sterilised 10% FCS, 5mL of 200mM glutamine, 50,000 units of penicillin G (Britannia Pharmaceuticals), 50mg streptomycin sulphate (Sigma-Aldrich) and 24mg gentamicin (Roussel Laboratories) (P/S/G) and 5ml of non-essential amino acid (NEAA) mix (Gibco, Invitrogen).

Prior to medium changes, MF cultures were examined under the light microscope to assess growth. Cells were split when 85-90% confluent, which was usually within 14 days. Medium was removed and cells briefly washed with 2mL 0.1% trypsin (Sigma-Aldrich) in Versine (0.02% ethylenediaminetetraacetic acid, EDTA, in phosphate buffered saline, PBS, pH7.2). This was removed and replaced with a further 3mL of fresh 0.1% trypsin and incubated for 10 minutes at 37^{o}C. Light microscopy was used to confirm cell detachment and 3mL of medium added to neutralise the trypsin, making total volume of 6mL. This fluid was split equally (3mL) into two new T75 flasks each containing 13mL of fresh medium.

For RNA transcript expression analysis, cultured MF were isolated for total RNA isolation (section 2.2) at passage 3. For flow cytometric analysis of surface TLR2 and TLR4 protein analysis, cultured MF were isolated at passage 4 or 5. For crypt cell-MF co-culture experiments, isolated MF were transferred onto glass cover slips in 24-well plates at passage 2. Following cell detachment using trypsin, the 6mL volume of suspended cells was made up to 25mL with MF media and mixed thoroughly. For each plate, 12 cover slips were sterilised in 100% ethanol and dried at room temperature before being placed individually into wells. Into each cover slip-containing well, 2mL of suspended MF were added. Cells were left to adhere to the cover slip over night. The medium was replaced with fresh medium 24 hours later. Thereafter media was replaced every 2-3 days.

6.2.3 Intestinal epithelial cell-myofibroblast co-culture experiments

Myofibroblasts were grown until confluent on cover slips and cultured for a further minimum period of 7 days before being considered suitable for use in co-culture experimentation. IEC were isolated from the mucosa of large bowel tissue resections. IEC were counted using trypan blue exclusion and suspended in complete MF medium at a concentration of $0.25x10^6$ viable cells/mL.

To each cover slip-containing well, 1mL of suspended IEC was added and incubated for 30 minutes at 37^{o}C. The medium was then replaced three times to remove non-adherent epithelial cells. Finally, the cover slips were fixed in cold acetone for at least 1 minute and stored at -20^{o}C until required.

6.2.4 Immunocytochemical staining of myofibroblasts and intestinal epithelial cell-myofibroblast co-culture experiments

Cover slips stored at -20^{o}C were thawed for 30 minutes at room temperature and hydrated in PBS for 20 minutes. Non-specific blocking was undertaken with 5% serum (S-2000, Vector Labs), 25% avidin block and 25% biotin block (SP-2001, Vector Labs). The cover slips were then incubated with the primary antibody for 1 hour at room temperature at the following dilutions:

Cytokeratin	1:400
BerEP4 (Epithelial antigen)	1:400
α-smooth muscle actin	1:500
Vimentin	1:40
Desmin	1:20
CD45	1:400
TLR2	1:250
TLR4	1:250

Following a 0.3% hydrogen peroxide in methanol peroxidase blocking step, the biotinylated secondary antibody was applied for 30 minutes. Following incubation with the avidin/biotin mixture (PK-6200, Vector labs) for 30 minutes, the cover slips were developed using the DAB substrate (SK-4100, Vector labs) for 2-4 minutes, all at room temperature.

Cover slips were counter stained in haematoxylin for 2 minutes, in 1% acid alcohol for 10 seconds and in ammoniated water for 60 seconds. The cover slips were dehydrated in graded alcohol solution and three xylene solutions before being mounted on a new slide with DPX and dried overnight in a fume hood.

6.2.5 Flow cytometric analysis of myofibroblasts

Confluent myofibroblasts layers were cultured in T75 flasks. The medium was removed and the cells washed briefly in 0.1% trypsin. Cells were then incubated in 3mL fresh 0.1% trypsin for 10 minutes at 37^{o}C. Once cell detachment was confirmed with light microscopy, 3mL medium was added to neutralise the trypsin and cell concentration calculated by trypan blue exclusion. 50x10^{3} cells were added to each FACS tube and centrifuged for 5 minutes at 300g. The supernatant was removed and 5µL mouse serum added for 15 minutes at 4^{o}C. Thereafter, isotype or primary antibodies were added to the tubes as follows:

Tube 1: No primary antibody

Tube 2: BerEP4-FITC 5µL

Tube 3: IgG2a,κ-APC isotype 10µL

Tube 4: Anti-TLR2-APC 20µL

Tube 5: Anti-TLR4-APC 10µL

Tube 6: Anti-CD45-AF488 1µL

Cells were incubated for 1 hour at 4^{o}C in the dark. The cells were washed twice in 0.5mL of cold HBSS (FACS) medium (2% foetal calf serum in HBSS without calcium or magnesium)

followed by centrifugation for 5 minutes at 300g. Finally the cells were re-suspended in 0.5mL FACS fixative (0.5% formaldehyde in HBSS (without Ca/Mg) with 2% FCS) and stored at 4^{o}C in the dark until analysis.

6.3 Results

6.3.1 Primary isolated myofibroblasts in long-term culture show typical morphological features and express typical markers of intestinal myofibroblasts

Mucosal tissue from healthy controls and patients with inflammatory bowel disease were treated with EDTA/DTT to remove the epithelial cell layer and expose the microscopic channels in the underlying basement membrane and lamina propria. Following a period of tissue culture, colonies of intestinal myofibroblasts were isolated and cultured in T75 flasks over a period of several weeks until fully confluent.

Prior to fully confluent growth, myofibroblast cells could be seen under light microscopy to form the characteristic spindle shapes described during myofibroblast isolation from various tissues (figure 6.1A). As cultured cells approached confluent growth, myofibroblasts were observed to form complex colonies of spindle-shaped cells (figure 6.1B).

Primary cultured intestinal myofibroblasts were demonstrated to positively stain for the MF-associated markers α-smooth muscle actin, vimentin and desmin (figure 6.2). Moreover, cultured MF did not stain for the epithelial cell marker BerEP4 (figure 6.3).

6.3.2 Intestinal myofibroblasts in long term culture express TLR2 and TLR4 protein

To investigate the reported expression of TLR2 and TLR4 in intestinal myofibroblasts, primary isolated colonic myofibroblasts from healthy controls were initially cultured until confluent in T75 flasks. The myofibroblasts were trypsinised and the cells collected. Protein lysates were obtained and the total protein concentration measured using the Bradford assay. Duplicate total protein samples of 40μg and 80μg were loaded into wells and analysed using SDS-PAGE and Western blotting, using anti-β-actin, anti-TLR2 and anti-TLR4 antibodies.

Intestinal myofibroblast samples were shown to express TLR2 and TLR4 protein by western blotting (figure 6.4). It was noted that TLR2 and TLR4 protein expression was lower than in intestinal crypt cells (Chapter 5, figure 5.2). Protein bands were visible using 80µg of total protein, but barely visible using 40µg of total protein.

To further examine the expression of TLR2 and TLR4 protein, intestinal myofibroblasts from the small and large bowel of healthy controls were cultured on coverslips until the observed growth was confluent by light microscopy. Following acetone fixation, the coverslips were stained with monoclonal antibodies to TLR2 and TLR4. Colonic intestinal MF expressed both TLR2 and TLR4 protein immunocytochemically (figure 6.5). Similar results were seen with intestinal MF derived from healthy small intestine.

6.3.3 Patients with inflammatory bowel disease differentially express TLR2 and TLR4 mRNA, but not protein in intestinal myofibroblasts

To investigate whether intestinal myofibroblasts from patients with active inflammatory bowel disease differentially express TLR2 and TLR4, myofibroblasts from patient with Crohn's disease and ulcerative colitis were isolated and cultured in T75 flasks. Following the establishment of long term cultures, myofibroblasts were isolated for RNA isolation at passage 3 and for flow cytometric analysis at passages 4-6. Long term cultures were established from at least three subjects for each group.

Following RNA isolation using the RNeasy Plus Mini kit, samples were reverse transcribed into cDNA and analysed using SYBR Green real-time RT-PCR to calculate the mRNA expression in IBD patients relative to a pooled sample of healthy control myofibroblasts. To analyse differential protein expression, cells were collected and stained with monoclonal APC-conjugated antibodies to TLR2 and TLR4 before being analysed on a flow cytometer. The measured median fluorescent intensity (MFI) for the isotype control antibody was subtracted from the MFI of the primary antibody to correct for non-specific antibody binding.

Compared to healthy controls, small intestinal myofibroblasts isolated from patients with Crohn's ileitis showed a trend towards up-regulated expression of TLR2 mRNA (relative expression median [range] 4.80 [4.32-7.02] versus 1.0 [0.89-1.12], p=0.100) and TLR4 mRNA (2.95 [2.52-3.41] versus 1.0 [0.64-1.54], p=0.100), figure 6.6. At the protein level using flow cytometry, a similar trend was observed in small intestine MF from patients with Crohn's ileitis, but this did not reach statistical significance for either TLR2 (MFI [range] 31.1 [17.7-48.0] versus 21.4 [1.7-24.8], p=0.400) or TLR4 (35.2 [19.8-55.1] versus 29.7 [0.0-34.1], p=0.400), figure 6.7.

Regarding myofibroblasts from the large intestine, samples from patients with ulcerative colitis significantly down-regulated TLR2 mRNA (relative expression 0.32 [0.30-0.33] versus 1.0 [0.43-1.41, p=0.009) but not TLR4 mRNA (0.47 [0.36-0.77] versus 1.0 [0.14-3.39, p=0.776). There was no differential expression of TLR2 mRNA (0.62 [0.49-0.64] versus 1.0 [0.43-1.41, p=0.282) or TLR4 mRNA (2.06 [1.67-5.65] versus 1.0 [0.14-3.39, p=0.085) in colonic myofibroblasts from patients with Crohn's colitis compared to healthy controls (figure 6.8).

The patterns of TLR2 and TLR4 protein expression by flow cytometry in colonic myofibroblasts from patients with IBD were similar to the patterns of mRNA expression (figure 6.9). There was no significant difference in TLR2 or TLR4 expression in myofibroblasts from either Crohn's colitis or ulcerative colitis compared to MF from healthy controls (p>0.05 for all analyses). There data are summarised in tables 6.1 and 6.2.

Table 6.1 Expression of TLR2 and TLR4 mRNA by intestinal myofibroblasts isolated from patients with inflammatory bowel disease relative to expression in healthy controls

Relative mRNA expression		TLR2			TLR4		
Sample site	Disease group	N	Median [range]	P-value *	N	Median [range]	P-value *
Small bowel	Healthy control	3	1.0 [0.89-1.12]	-	3	1.0 [0.0.64-1.54]	-
	Crohn's ileitis	3	4.80 [4.32-7.02]	0.100	3	2.95 [2.52-3.41]	0.100
Large bowel	Healthy control	9	1.0 [0.43-1.41]	-	8	1.0 [0.14-3.39]	-
	Crohn's colitis	3	0.62 [0.49-0.64]	0.282	3	2.06 [1.67-5.65]	0.085
	Ulcerative colitis	3	0.32 [0.30-0.33]	0.009	3	0.47 [0.36-0.77]	0.776

* versus healthy control; N, number of samples

Table 6.2 Expression of surface TLR2 and TLR4 protein on intestinal myofibroblasts isolated from patients with inflammatory bowel disease and healthy controls subjects

Median fluorescent intensity		TLR2			TLR4		
Sample site	Disease group	N	Median [range]	P-value *	N	Median [range]	P-value *
Small bowel	Healthy control	3	21.4 [1.7-24.8]	-	3	29.7 [0.0-34.1]	-
	Crohn's ileitis	3	31.1 [17.7-48.0]	0.400	3	35.2 [19.8-55.1]	0.400
Large bowel	Healthy control	5	12.8 [4.3-25.4]	-	5	9.5 [4.7-28.2]	-
	Crohn's colitis	3	28.2 [0.0-31.4]	0.571	3	26.7 [0.0-38.8]	0.786
	Ulcerative colitis	3	7.3 [0.0-23.7]	0.786	3	3.9 [0.0-33.6]	0.571

* versus healthy control; N, number of samples

6.3.4 BerEP4-positive intestinal crypt cells adhere to intestinal myofibroblast layers

To investigate their interaction with isolated intestinal epithelial crypt cells, primary normal colonic myofibroblasts were cultured until confluent on glass coverslips. Intestinal crypt epithelial cells (n=16 [normal colon 3, Crohn's ileitis 1, Crohn's colitis 5, UC 7]) were isolated using EDTA/DTT and disaggregated into individual cells using pancreatin (section 3.2.4). Isolated crypt cells were suspended in myofibroblast medium and co-cultured on myofibroblast monolayers for 30 minutes, before non-adherent cells were removed by washing. Coverslips were then fixed in acetone and labelled with a monoclonal antibody to

BerEP4, before development using the DAB substrate and counter-staining with haematoxylin.

Prior to acetone fixation coverslips were examined by light microscopy. Small intestinal epithelial cells were seen to adhere to the underlying myofibroblast monolayer (figure 6.10). Intestinal cells were noticeably smaller than the underlying intestinal myofibroblasts.

Following acetone fixation, coverslips were stained with the epithelial-specific monoclonal antibody to BerEP4. Intestinal crypt cells stained positively for BerEP4 (n=16), but myofibroblasts were BerEP4-negative (figure 6.11A and B). Examination of adherent BerEP4-positive cells under high power magnification (x40) demonstrated occasion spur-like processes extending out from the membrane of the adherent epithelial cell (figure 6.11C and D).

6.3.5 Adherent intestinal crypt cells and intestinal myofibroblasts express TLR2 and TLR4 protein

Epithelial cells adhering to myofibroblast monolayers have been reported to represent a population of epithelial cells enriched for the expression of the intestinal stem cell marker musashi-1 (210). To investigate if these adherent epithelial cells expressed TLR2 and TLR4 protein, coverslips containing co-cultured intestinal myofibroblast and intestinal epithelial cells (n=20 [normal colon 5, Crohn's ileitis 1, Crohn's colitis 7, UC 7]) were stained with monoclonal antibodies to TLR2 and TLR4 and acetone-fixation. Coverslips were developed using DAB substrate and counter-stained with haematoxylin.

Adherent epithelial crypt cells were shown to stain positively for TLR2 and TLR4 protein (n=20). The underlying myofibroblasts were also positive-staining for TLR2 and TLR4 protein, but the staining of the MF was less intense than the staining of the adherent epithelial crypt cells (figure 6.12).

6.4 Figures

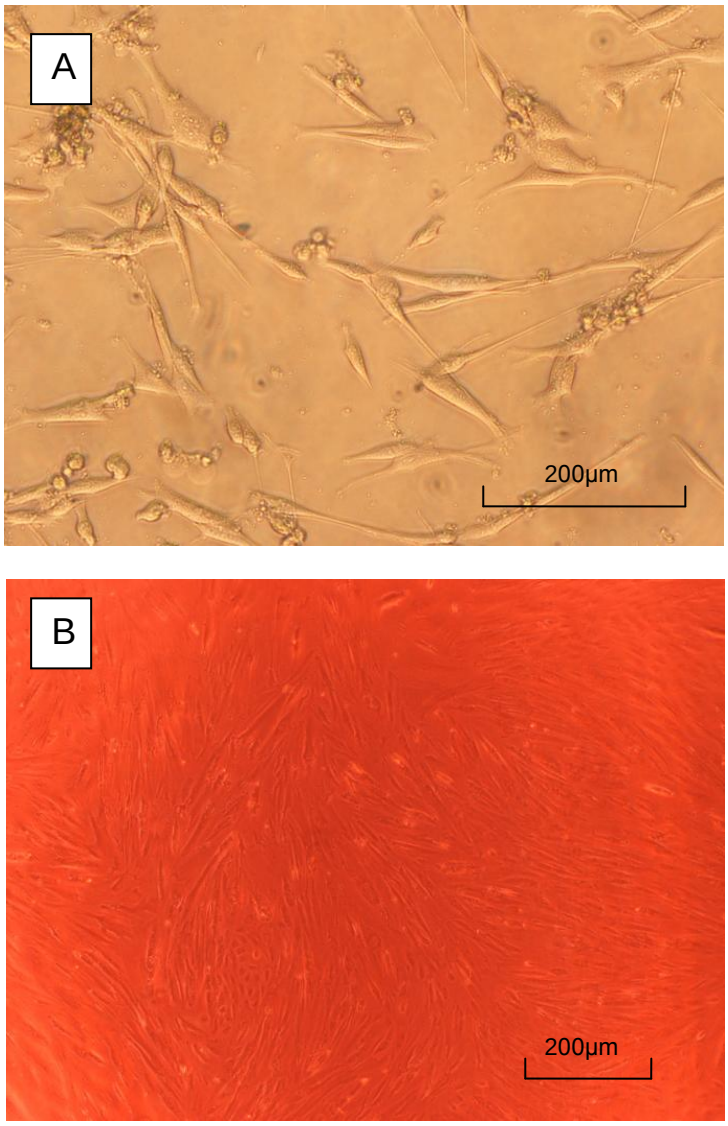

Figure 6.1 Cultured primary colonic myofibroblasts display a spindle-shaped morphology. Primary human mucosal samples were treated with EDTA/DTT to remove the overlying epithelial cell layer. The residual mucosa was cultured until migrating MF formed colonies on the growth plate. The mucosal tissue samples were discarded at this stage and the MF colonies were further cultured until fully confluent, before being transferred to T75 flasks for long term culture. MF cultures display a typical spindle shape (A) when examined by light microscopy and form complex colonies in long term culture (B).

DTT, dithiothreitol; EDTA, ethylenediaminetetraacetic acid; MF, myofibroblast

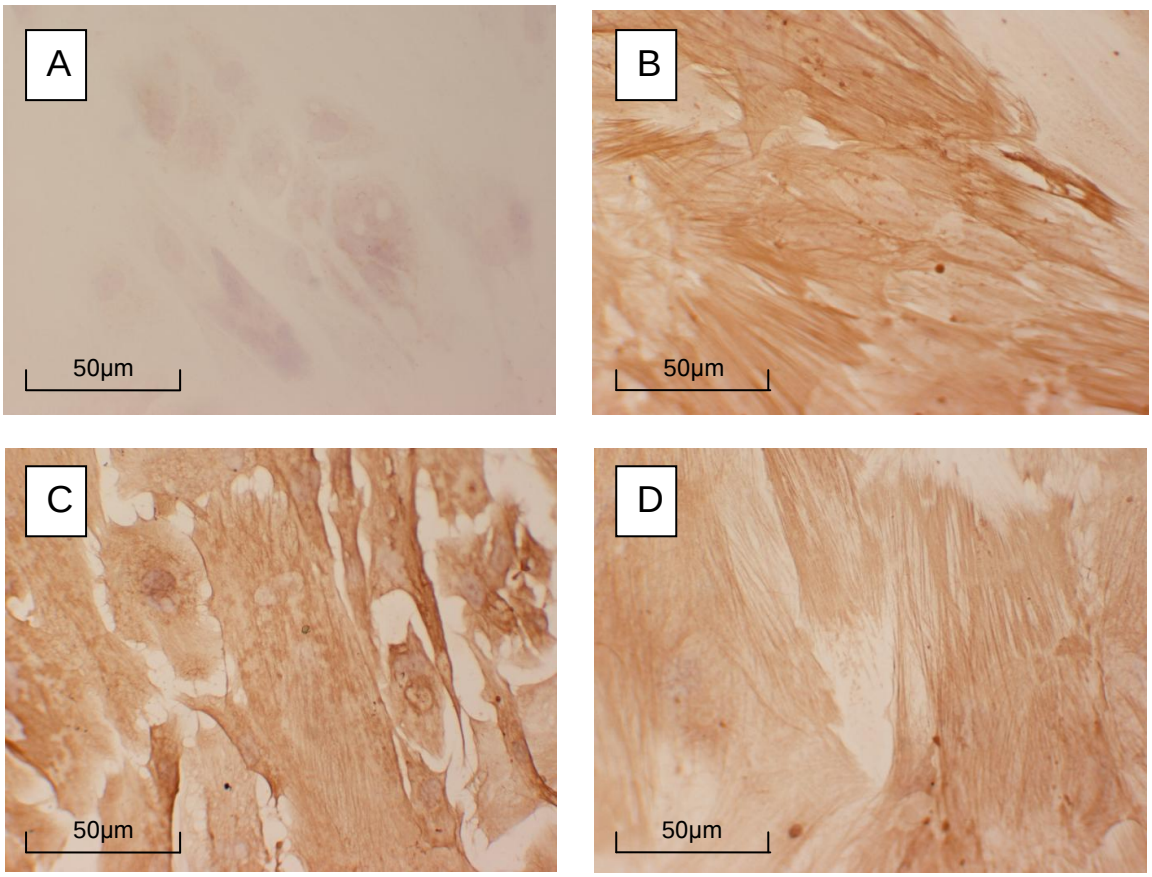

Figure 6.2 Cultured primary colonic myofibroblasts express α-smooth muscle actin, vimentin and desmin. Primary human intestinal MF colonies (n=5) were cultured on glass coverslips until fully confluent, before being acetone-fixed. Coverslips were stained with (A) no primary antibody, (B) anti-α-smooth muscle actin, (C) anti-vimentin, or (D) anti-desmin antibodies and developed using DAB substrate. Cultured primary human MF stained positively for α-smooth muscle actin (A), vimentin (B) and desmin (C).

DAB, 3,3'-diaminobenzidine; MF, myofibroblast

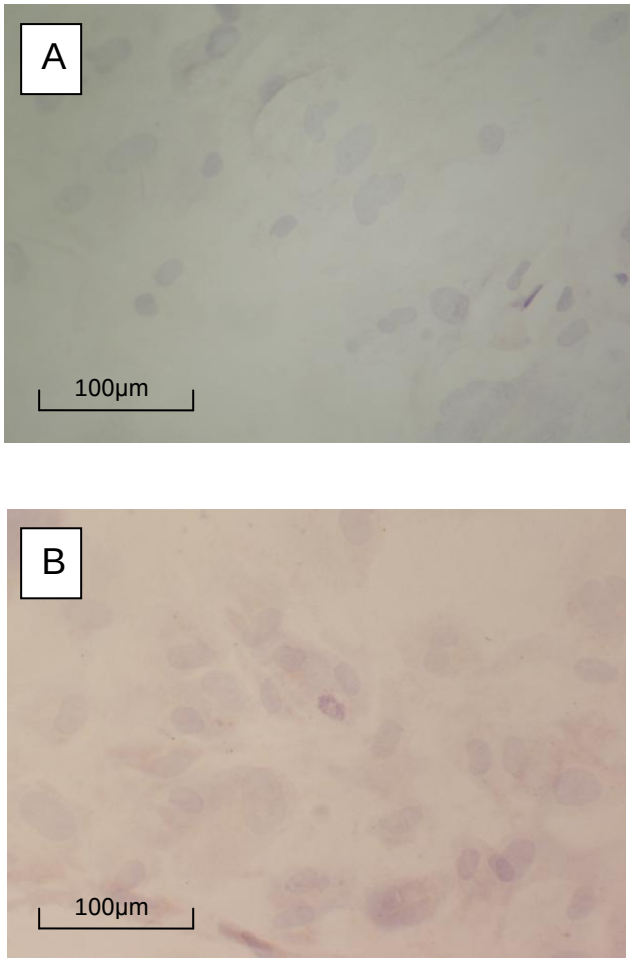

Figure 6.3 Cultured primary colonic myofibroblasts do not express BerEP4. Primary human intestinal MF (n=5) were cultured until fully confluent on glass coverslips and fixed in acetone. Coverslips were stained with (A) no primary antibody or (B) anti-BerEP4 monoclonal antibody, and developed using DAB substrate before counter-staining with haematoxylin. Cultured primary human MF did not express BerEP4.

DAB, 3,3'-diaminobenzidine; MF, myofibroblast

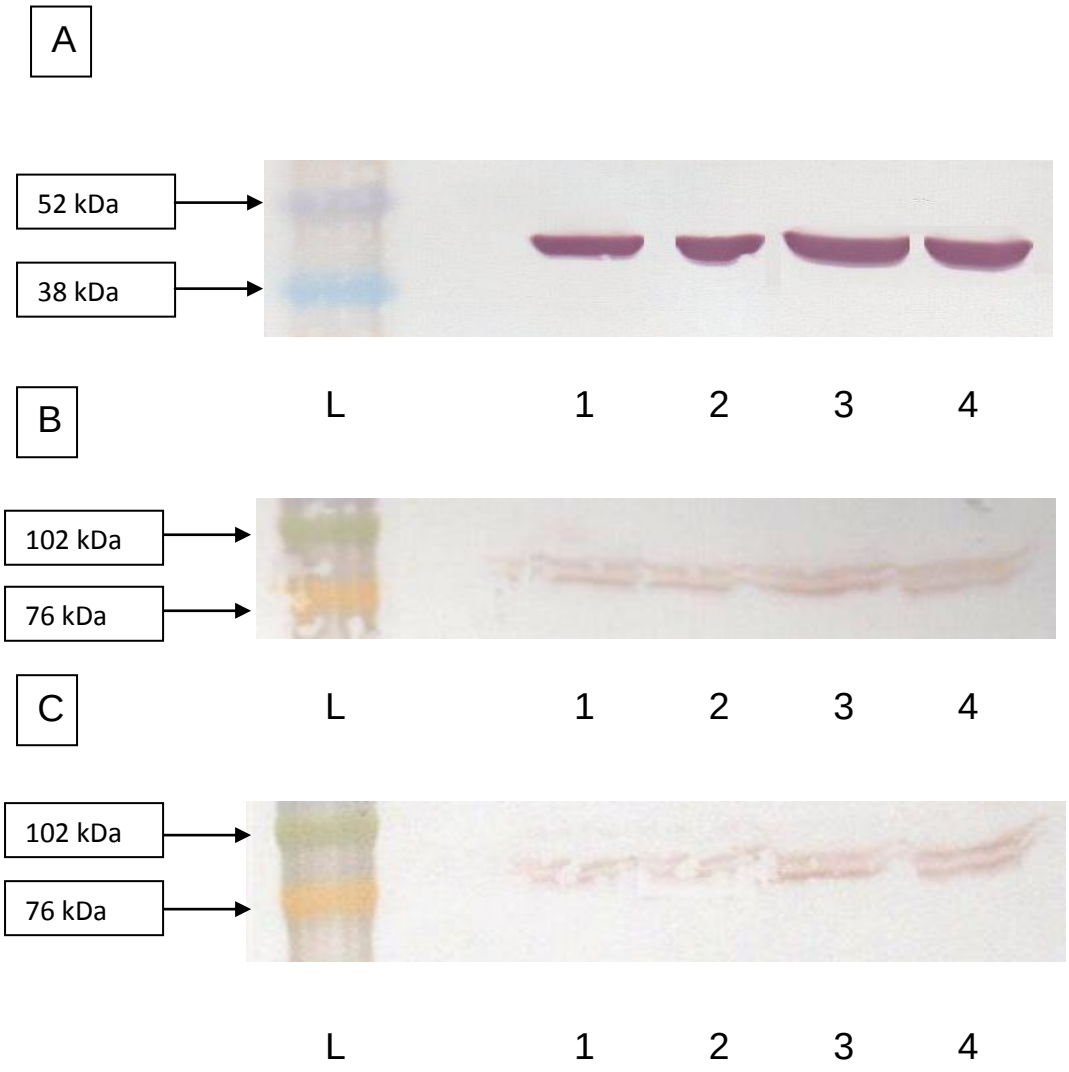

Figure 6.4 Cultured primary colonic myofibroblasts express TLR2 and TLR4 protein. Primary intestinal myofibroblasts were cultured until fully confluent in T75 flasks. Cells were collected and lysed for total protein quantification using the Bradford assay. The expression of (A) β-actin, (B) TLR2 and (C) TLR4 protein was examined using SDS PAGE and Western blotting. Duplicate samples of 40µg (lanes 1 and 2) or 80µg (lanes 3 and 4) of total protein were loaded into adjacent wells. Bands were noted at the expected protein molecular weights for β-actin (42 kDa), TLR2 (90kDa) and TLR4 (93kDa). TLR2 and TLR4 expression was shown to be expressed at low levels, particularly in the 40µg lanes.

Da, Dalton; L, size ladder; SDS PAGE, sodium dodecyl sulphate polyacrylamide gel electrophoresis; TLR, Toll-like receptor

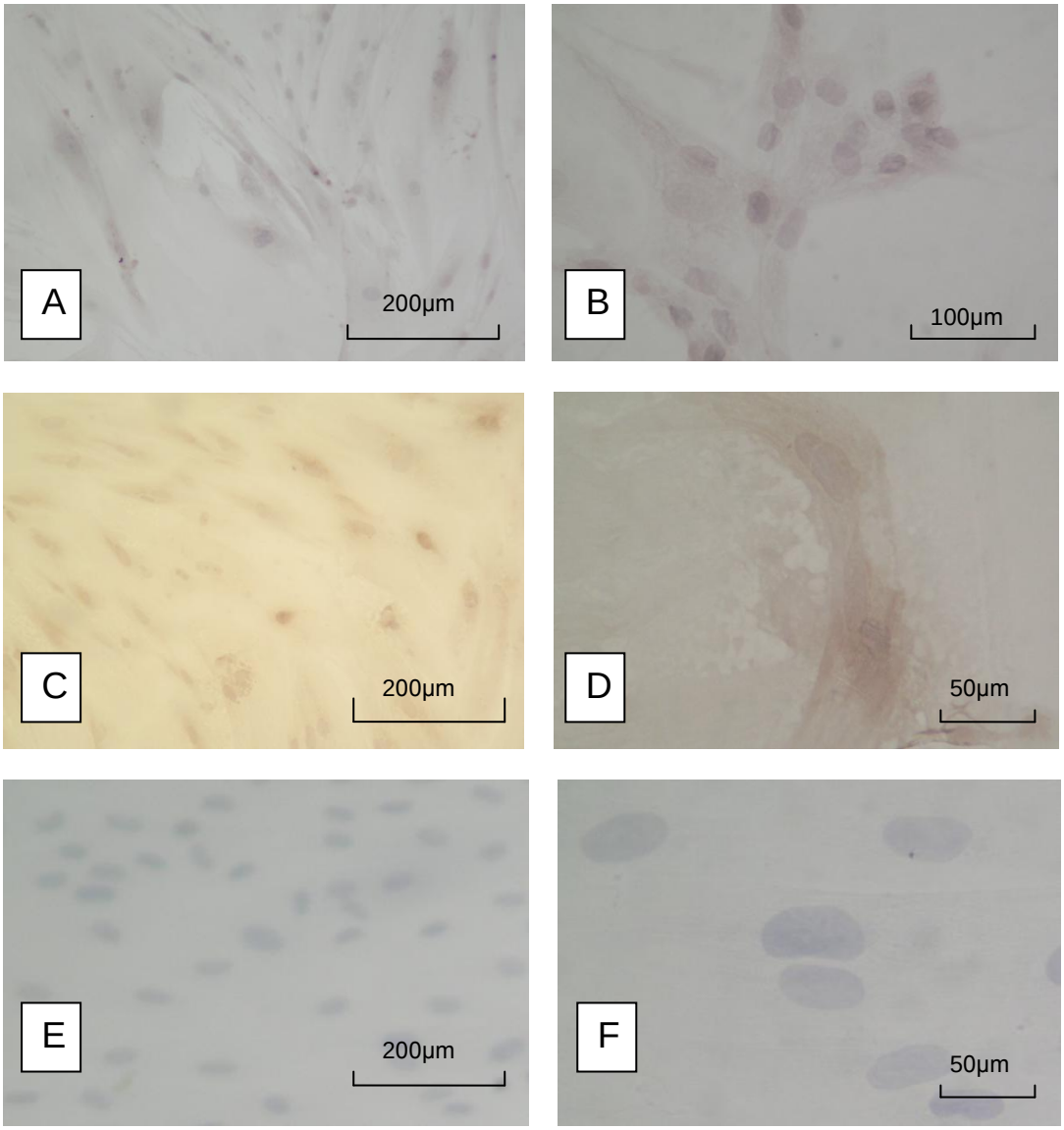

Figure 6.5 Cultured primary normal colonic myofibroblasts express TLR2 and TLR4 protein. Primary human intestinal MF isolated from healthy control large bowel mucosa (n=3) were cultured until fully confluent on glass coverslips and fixed in acetone. Coverslips were stained with anti-TLR2 or anti-TLR4 monoclonal antibodies, developed using DAB substrate, counter-stained with haematoxylin and viewed by light microscopy. Cultured primary MF expressed both TLR2 at low (X10) and high (x40) power (A and B, respectively) and TLR4 at low and high power (C and D, respectively). Low and high power no-antibody control slides are also shown (E and F, respectively).

DAB, 3,3'-diaminobenzidine; MF, myofibroblast, TLR, Toll-like receptor

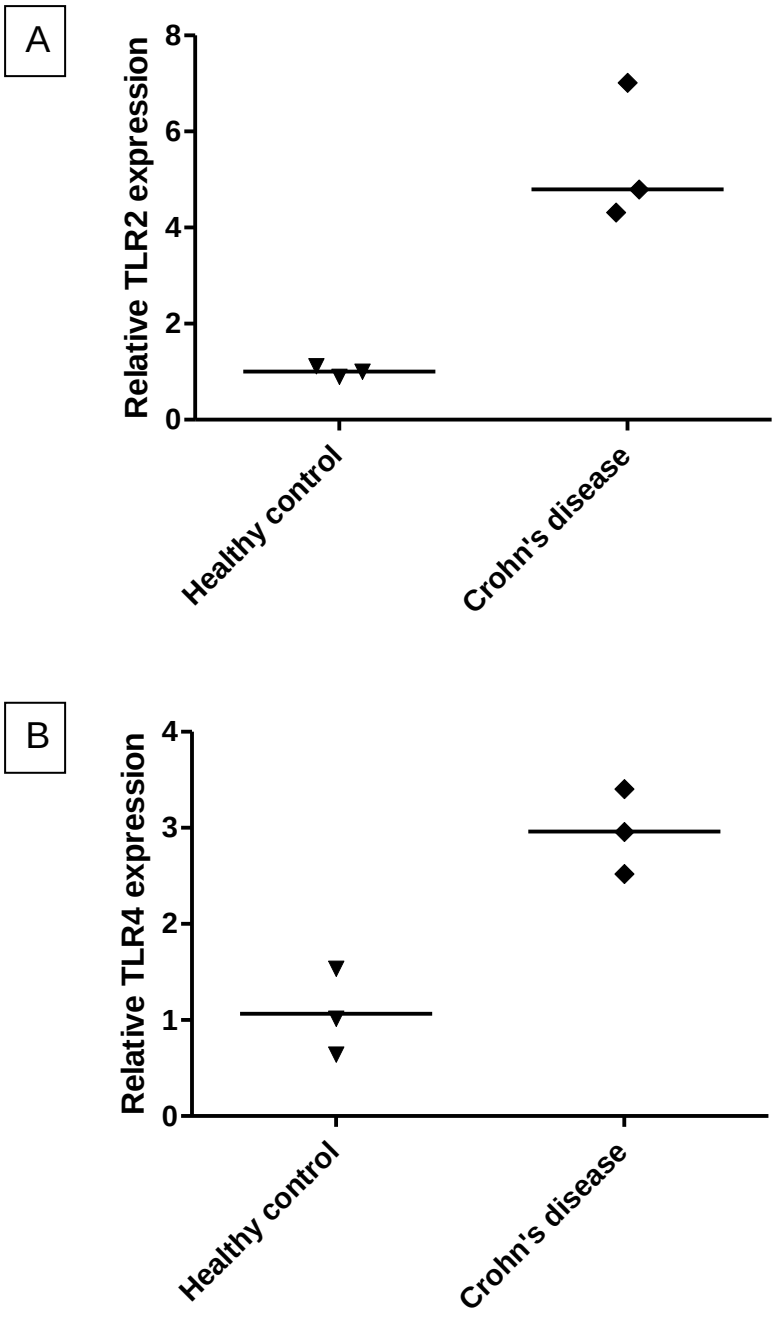

Figure 6.6 Small intestinal myofibroblasts from patients with Crohn's ileitis trend towards up-regulation of TLR2 and TLR4 mRNA expression. Primary small intestinal myofibroblasts from healthy controls and patients with CD were cultured in T75 flasks until cell monolayers were fully confluent. At this stage MF were collected for mRNA isolation, cDNA synthesis and subsequent analysis of (A) TLR2 and (B) TLR4 expression relative to HPRT using real-time RT-PCR. Each data point represents the mean TLR2 or TLR4 mRNA expression of three triplicate runs per sample, expressed relative to the pooled healthy control small bowel samples. Horizontal bars represent median expression for the group.

CD, Crohn's disease; HPRT, Hypoxanthine guanine phosphoribosyltransferase; RT-PCR, reverse transcriptase polymerase chain reaction; TLR, Toll-like receptor

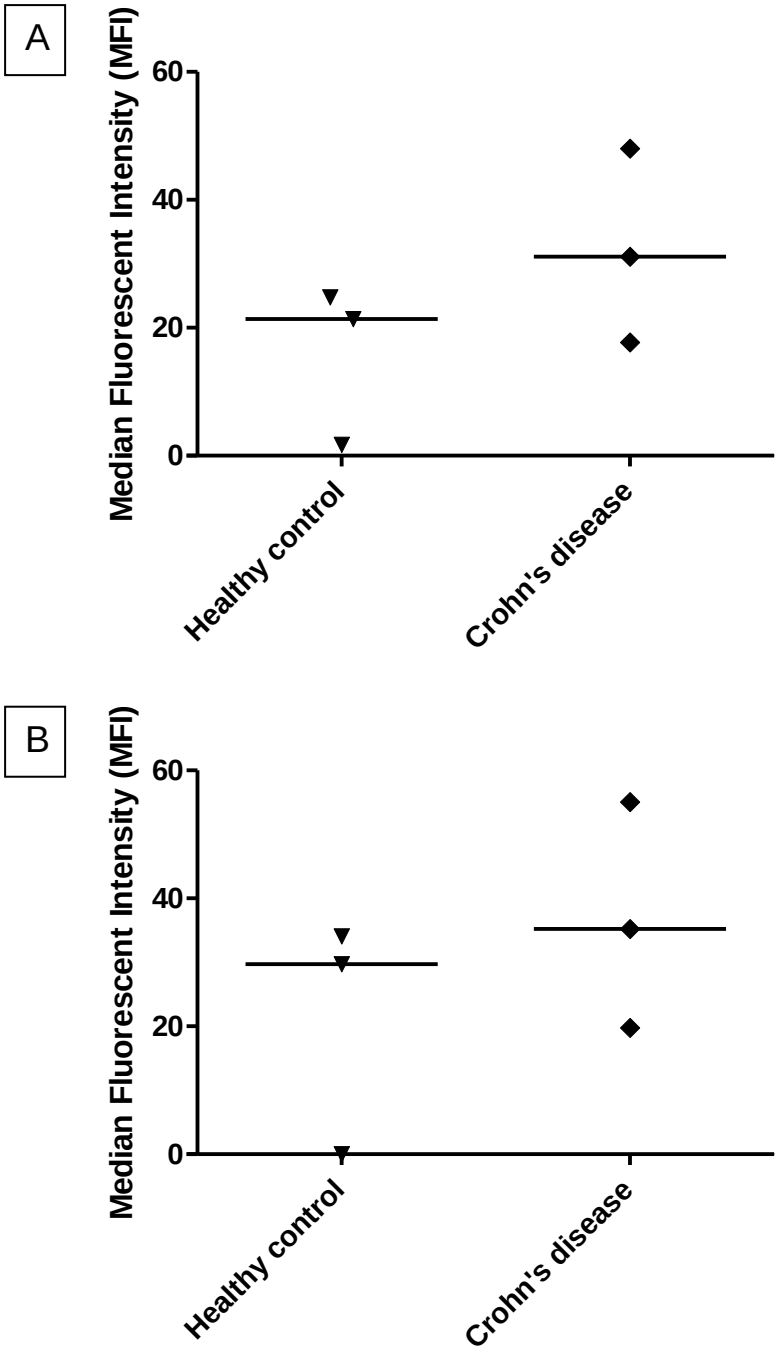

Figure 6.7 Small intestinal myofibroblasts from healthy controls and patients with Crohn's ileitis express similar levels of surface TLR2 and TLR4 proteins. Primary small intestinal myofibroblasts from healthy controls and patients with CD were cultured until cell monolayers were fully confluent. At this stage MF were collected, stained with either (A) anti-TLR2 or (B) anti-TLR4 APC-conjugated monoclonal antibodies and subsequently examined by flow cytometry. Each data point represents the difference in median fluorescent intensity between the primary and isotype control antibodies. Horizontal bars represent median expression for the group.

APC, allophycocyanin; CD, Crohn's disease; MF, myofibroblasts; TLR, Toll-like receptor

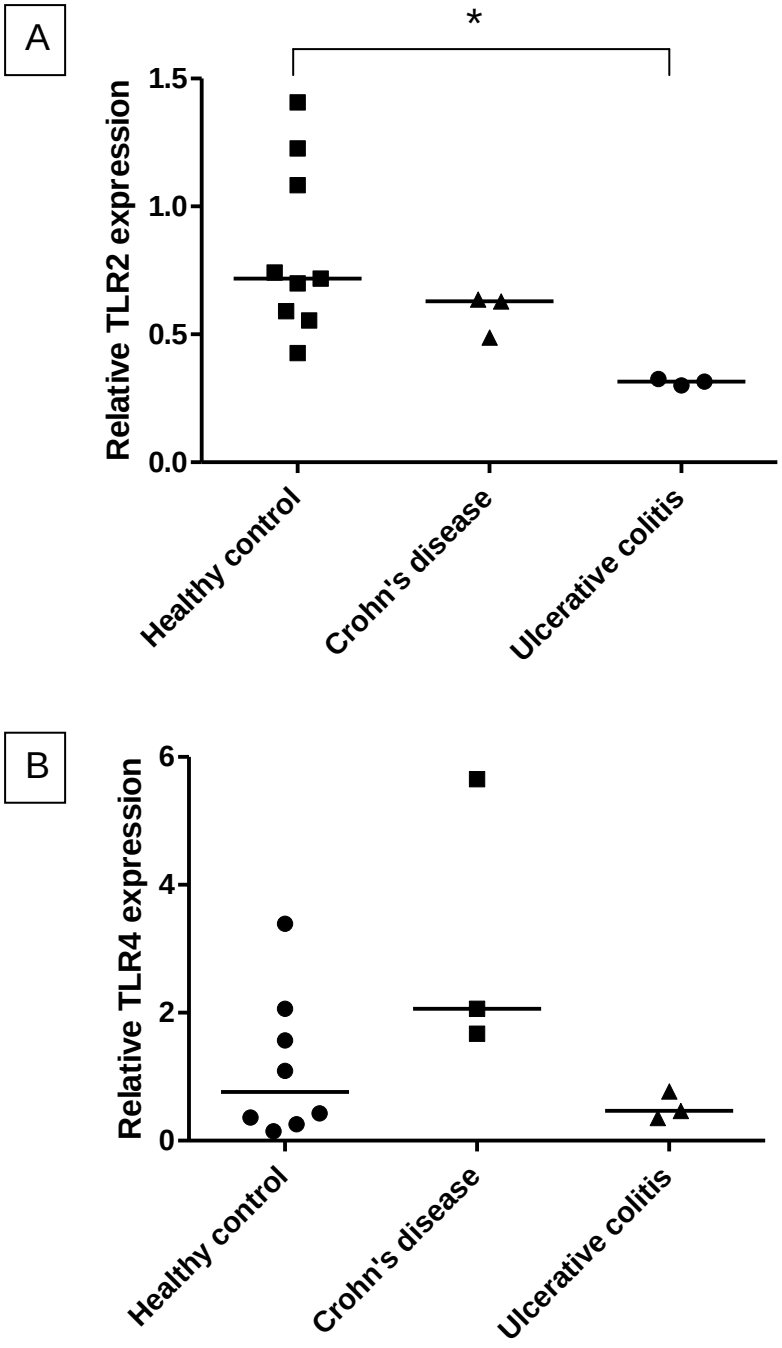

Figure 6.8 Colonic myofibroblasts from patients with ulcerative colitis down-regulate TLR2 mRNA expression. Primary colonic myofibroblasts from healthy controls and patients with IBD were cultured until cell monolayers were fully confluent. At this stage MF were collected for mRNA isolation, cDNA synthesis and subsequent analysis of (A) TLR2 and (B) TLR4 expression relative to HPRT using real-time RT-PCR. Each data point represents the mean TLR2 or TLR4 mRNA expression of three triplicate runs per sample, expressed relative to the pooled healthy control large bowel samples. Horizontal bars represent median expression for the group.
* p=0.009

HPRT, hypoxanthine guanine phosphoribosyltransferase; IBD, inflammatory bowel disease; RT-PCR, reverse transcriptase polymerase chain reaction; TLR, Toll-like receptor

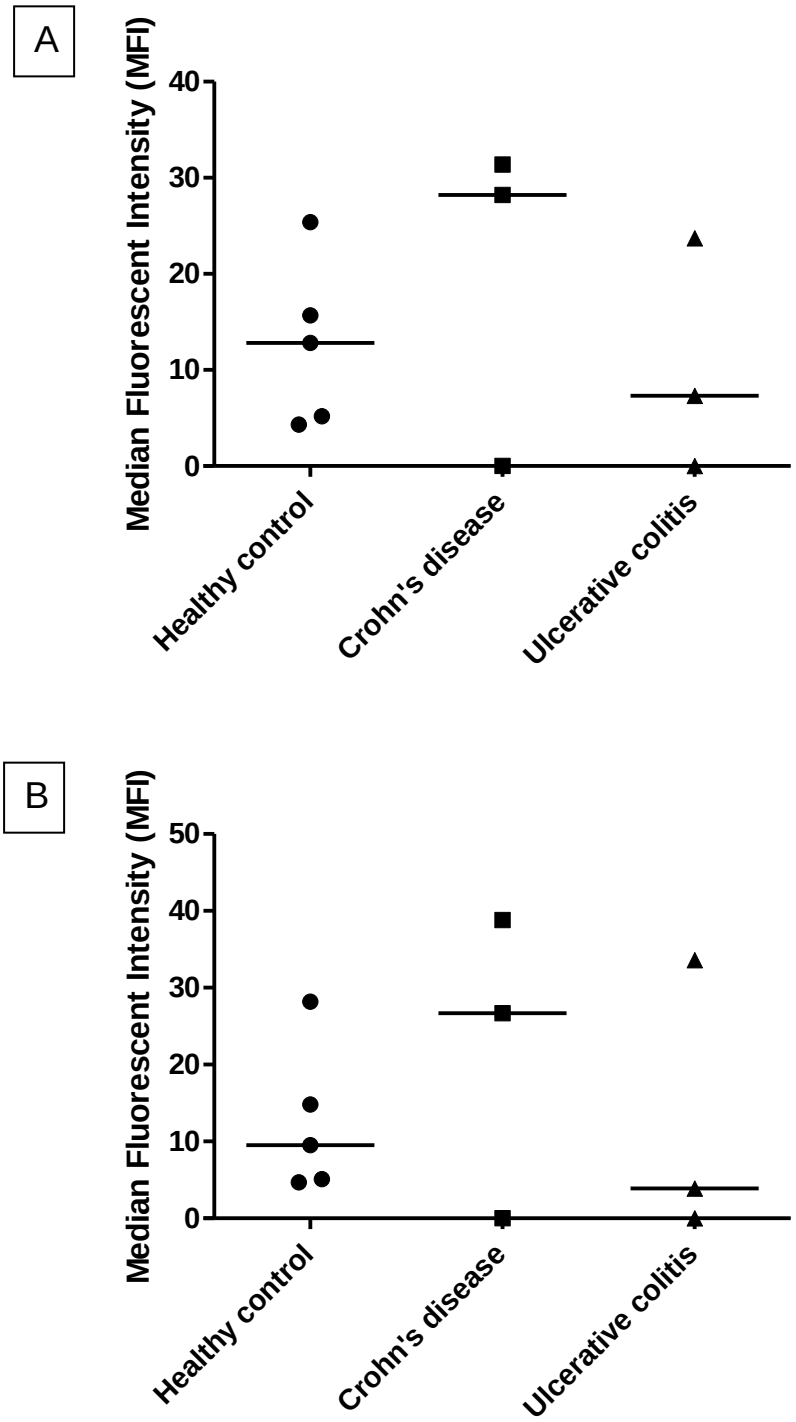

Figure 6.9 Colonic myofibroblasts from patients with inflammatory bowel disease express similar surface TLR2 and TLR4 proteins compared to healthy controls. Primary colonic myofibroblasts from healthy controls and patients with IBD were cultured until cell monolayers were fully confluent. At this stage MF were collected, stained with either (A) anti-TLR2 or (B) anti-TLR4 APC-conjugated monoclonal antibodies and subsequently examined by flow cytometry. Each data point represents the difference in median fluorescent intensity between the primary and isotype control antibodies. Horizontal bars represent median expression for the group.

APC, allophycocyanin; IBD, inflammatory bowel disease; MF, myofibroblasts; TLR, Toll-like receptor

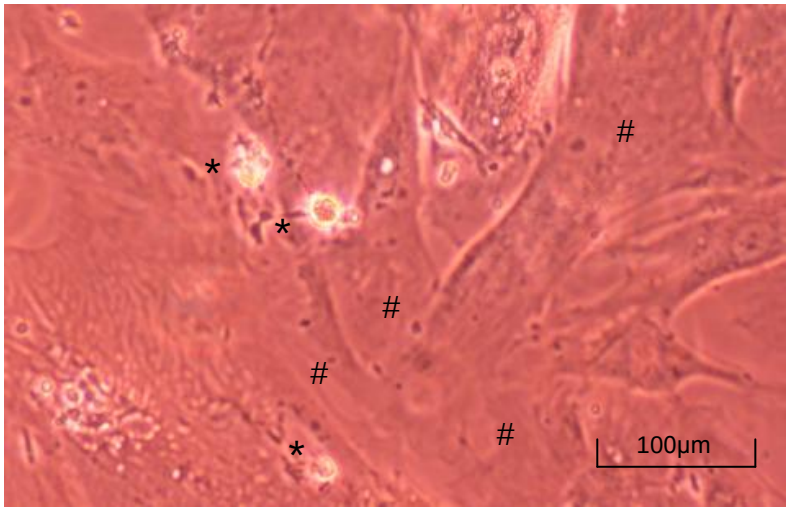

Figure 6.10 Isolated colonic crypt cells adhere to cultured intestinal myofibroblast layers. Primary normal colonic myofibroblasts were cultured on glass coverslips until fully confluent. Primary normal small intestine crypt cells were isolated from mucosal samples using EDTA/DTT and disaggregated using pancreatin, before being added onto the confluent myofibroblast monolayer. After a 30 minutes period of co-culture, non-adherent intestinal crypt cells were removed by washing and the coverslip viewed with the light microscope at high power (x40). Intestinal crypt cells (*) were seen to adhere to the underlying myofibroblast monolayer (#). Notably, the myofibroblasts were much larger in size than the adherent intestinal crypt cells.

DTT, dithiothreitol; EDTA, ethylenediaminetetraacetic acid

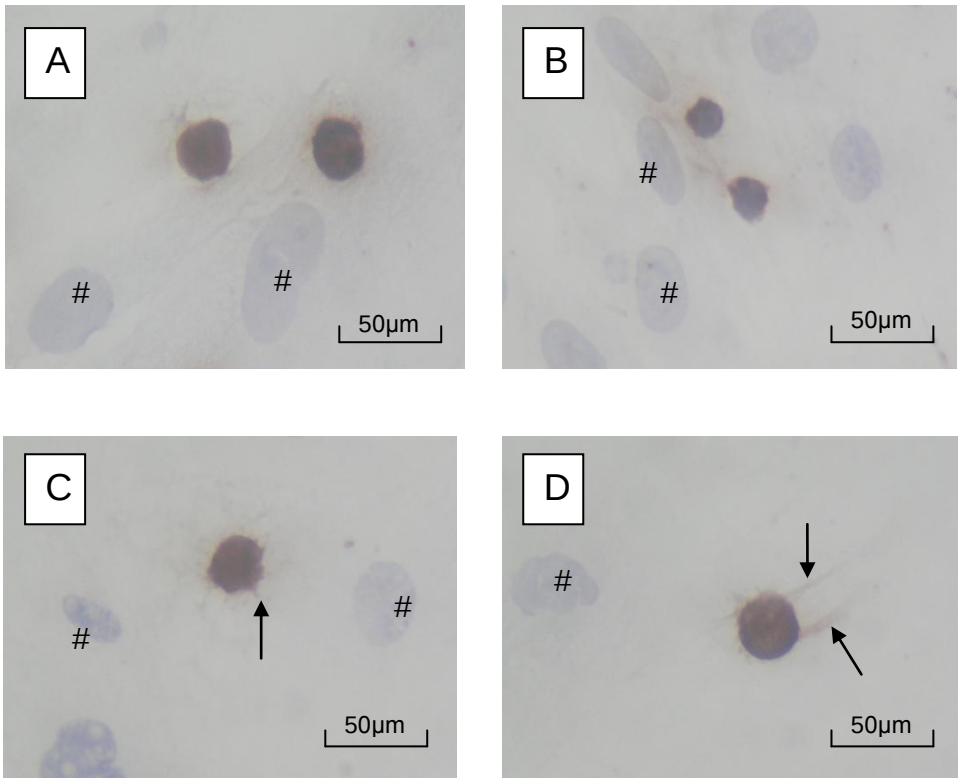

Figure 6.11 Colonic crypt cells adherent to myofibroblast monolayers are BerEP4-positive and demonstrate spur-like cytoplasmic projections. Primary normal colonic myofibroblasts were cultured until fully confluent on glass coverslips. Isolated and disaggregated normal colonic crypt cells were co-cultured on myofibroblast monolayers for 30 minutes and subsequently the non-adherent cells removed by washing (n=10). Coverslips were fixed in acetone, incubated with an anti-BerEP4 monoclonal antibody, developed using DAB substrate and finally counter-stained with haematoxylin. Brown-staining BerEP4-positive intestinal epithelial cells were seen to adhere to the much larger underlying myofibroblasts (A and B). Haematoxylin-staining myofibroblast nuclei were marked (#). In some cases, spur-like projections were seen extending from the epithelial cell cytoplasm (C and D, arrows).

DAB, 3,3'-diaminobenzidine substrate

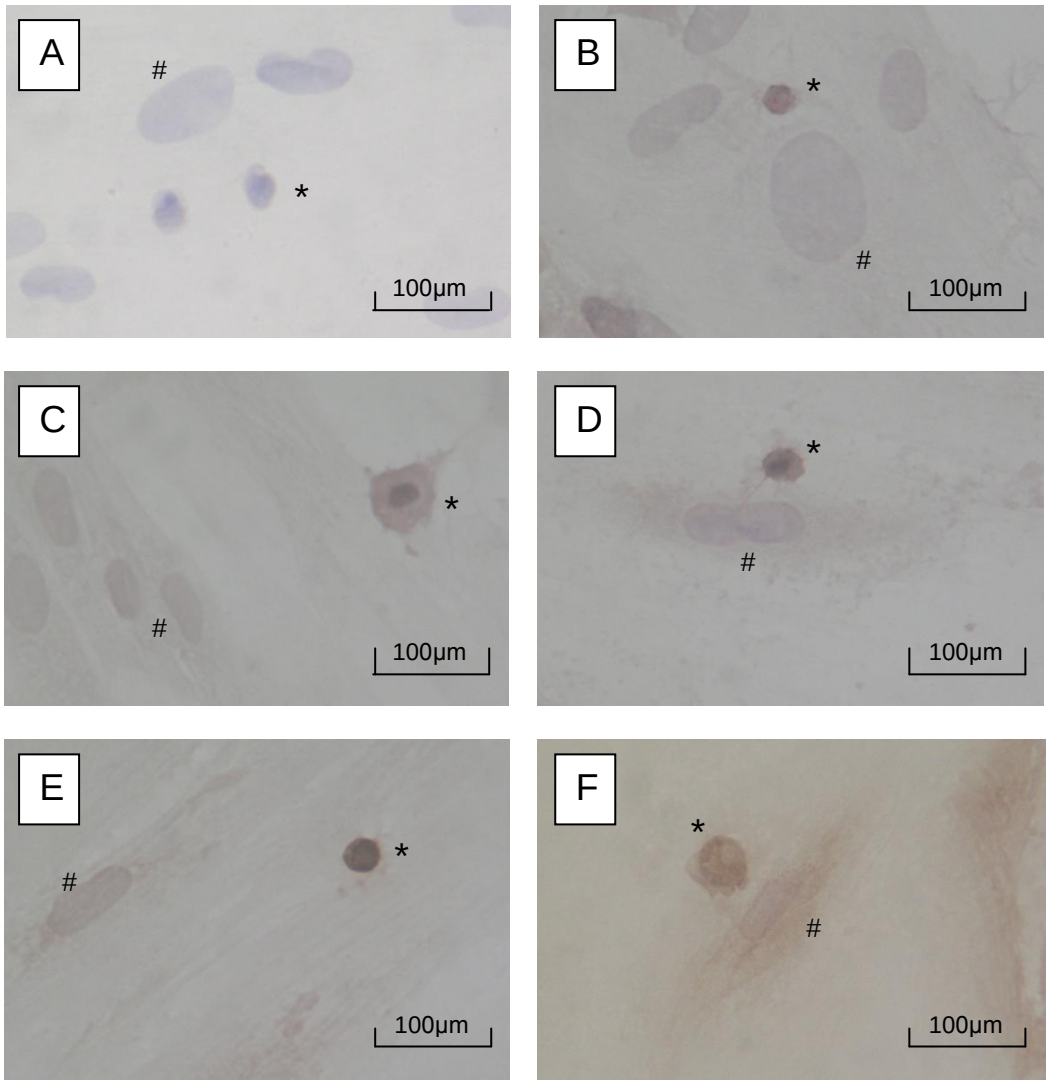

Figure 6.12 Co-cultured colonic crypt cells and colonic myofibroblasts express TLR2 and TLR4 protein. Primary normal colonic myofibroblasts were cultured until fully confluent on glass cover slips. Isolated and disaggregated colonic crypt cells from a patient with Crohn's colitis were co-cultured on myofibroblast monolayers and subsequently the non-adherent cells removed by washing (n=10). The cover slips were fixed in acetone and stained with either (A) no primary antibody, (B-D) anti-TLR2 antibody or (E and F) anti-TLR4 antibody. Cover slips were developed using DAB substrate and counter-stained with haematoxylin. TLR2- and TLR4-positive intestinal crypt cells (*) were seen to adhere to myofibroblasts (#), which were also TLR2- and TLR4-positive. Adherent intestinal crypt cells demonstrated stronger staining for TLR2 (B-D) and TLR4 (E and F) than the underlying myofibroblasts.

DAB, 3,3'-diaminobenzidine substrate; TLR, Toll-like receptor

6.5 Discussion

Primary intestinal myofibroblasts were successfully cultured from the small and large intestine of healthy controls and patients with inflammatory bowel disease, and maintained in culture for a period of several months. The cultured MF demonstrated typical spindle-shaped morphology and expressed the MF-associated intracellular markers α-smooth muscle actin, vimentin and desmin, but not the epithelial-specific marker BerEP4.

Primary MF monolayer cultures from the normal small and large intestine were shown to express TLR2 and TLR4 protein using whole cell lysate Western blotting, immunocytochemical staining of cultured MF colonies on coverslips and flow cytometric analysis of individual intestinal MF, supporting the report by Otte *et al.* that primary cultured intestinal MF express TLR2 and TLR4 transcripts (182). This suggests that primary human intestinal MF have the ability to sense bacterial ligands in the lamina propria via TLR2 and TLR4, and therefore may play a role in mediating the mucosal inflammatory response through TLR signalling. Indeed primary cultured large intestinal MF cells have been reported to respond to the TLR4 ligand LPS by expressing COX-2 (183).

Notably, primary cultured MF expressed less total TLR2 and TLR4 protein than isolated intestinal crypt cells, as assessed by Western blotting. Protein bands of the expected size were easily identified on western blots using primary intestinal crypt cell lysates after loading 20μg of total protein, whereas protein bands from MF lysates using 40μg of total protein were barely visible and 80μg of total protein was required from MF whole cell lysates to demonstrate bands of similar width. Moreover, when normal colonic crypt cells were co-cultured on normal colonic MF monolayers, immunohistochemical analysis of TLR2 and TLR4 protein expression showed that crypt cells stained more intensely than the underlying MF cells. Conversely, median fluorescent intensity of surface TLR2 and TLR4 protein

expressions using flow cytometry were statistically similar between normal colonic crypt cells and normal colonic MF ($p=1.0$ and $p=0.876$, respectively).

The intestinal epithelial cell-myofibroblast co-culture experiments demonstrated that adherent crypt cells are markedly smaller than the underlying MF cells. Conversely, when MF were harvested using trypsin and analysed by flow cytometry they were smaller (as assessed by forward scatter on the flow cytometer) than isolated crypt cells, suggesting that harvested MF round up and significantly reduce in size following trypsinisation. This could result in increased density of surface TLR2 and TLR4 expression following MF harvest. Myofibroblasts in culture took on a classical spindle-shaped appearance and were much larger in size than isolated crypt cells. Therefore, the observations that total TLR2 and TLR4 protein is less in MF than IEC (as assessed by western blotting) and that cultured MF cells are larger than isolated crypt IEC suggests that surface TLR2 and TLR4 expression is less dense in MF. This is supported by the IEC-MF co-culture immunostaining experiments which demonstrated more intense staining of the adherent crypt cells compared to the underlying MF monolayer cells.

When primary ileal MF cultures from patients with Crohn's ileitis were compared to small intestine MF cultures from healthy controls, there was a trend towards up-regulation of TLR2 and TLR4 transcripts and, to a lesser extent, up-regulation of surface TLR2 and TLR4 proteins. However, there was no differential expression of TLR2 or TLR4 between intestinal MF derived from patients with Crohn's colitis compared to healthy control colonic MF at either the transcript or protein level. There was a statistically significant down-regulation of TLR2 mRNA transcript in intestinal MF from patients with UC compared to healthy controls. However TLR4 mRNA expression was similar between the two groups and there was no significant difference in the expression of surface TLR2 or TLR4 protein on intestinal MF from patients with UC compared to healthy control colonic MF.

There are several explanations for these data. Firstly it is possible that, while intestinal MF certainly demonstrated both TLR2 and TLR4 transcript and protein expression, they do not differentially express these receptors during states of mucosal inflammation. However, trends in expression between groups were observed, and it is possible that the small number of specimens in each disease group (n=3 for IBD groups) may have contributed to a lack of statistically significant differences.

It is important to note that the MF isolated for TLR2 and TLR4 transcripts and protein expression analyses were collected following a prolonged period of cell culture in an *ex vivo* environment (several weeks or months). This *ex vivo* culture period may have a significant bearing on the expression of TLR2 and TLR4. Therefore, any differential expression amongst the groups may have been diminished as a result of long term cell culture. However, primary cultured intestinal MF from healthy controls and patients with UC and Crohn's disease were reported to demonstrate distinct patterns of TGFβ isoform expression which were sustained through several MF passages (284). Whether sustained expression is also true of TLR2 and TLR4 remains unknown.

However, looking more generally at the trends in TLR2 and TLR4 expression, it is interesting than small and large intestinal MF derived from patients with Crohn's disease tended to up-regulate TLR2 and TLR4 expression, whereas colonic intestinal MF derived from patients with UC tended to down-regulate TLR2 and TLR4 expression. Intestinal MF are associated with the formation of intestinal fibrosis and are reported to be expressed in greater numbers (283) and with greater proliferative capacity (284) in the mucosa in IBD, particularly in Crohn's disease which is associated with intestinal strictures (2). It is possible that TLR2 and TLR4 signalling plays a role in regulating intestinal MF function and the burden of mucosal antigens in inflamed mucosa may play a role in mediating the innate and adaptive immune responses through direct bacterial sensing. The observation that TLR2 and TLR4 may be

up-regulated in intestinal MF of patients with Crohn's disease requires further investigation before their role in mediating intestinal fibrosis can be more fully understood.

On the contrary, intestinal fibrosis in UC is unusual and generally limited to the mucosa and sub-mucosa. The down-regulation of TLR2 mRNA by intestinal MF in this study may occur as a tolerogenic response to increased bacterial antigenic exposure in the lamina propria following loss of the overlying epithelium. The relative hypo-responsiveness of mucosal MF to bacterial antigens may explain why colonic stricturing is less common in patients with UC compared to Crohn's disease (2).

It has previously been shown in this laboratory that intestinal crypt cells expressing the intestinal stem cell marker musashi-1 (Msi-1) represent less than 1% of the total isolated crypt cell population. However, co-culturing isolated and disaggregated intestinal crypt cells with confluent intestinal MF monolayers results in the adherence of a population of crypt cells to the MF monolayer which express Msi-1 in approximately 60% of cells (210). This suggests that intestinal stem cells preferentially adhere to MF monolayers. This technique provides a convenient way of isolating a sub-population of crypt cells enriched with stem cells for subsequent analysis.

This study demonstrated adherence of BerEP4-positive crypt intestinal epithelial cells to primary colonic MF monolayers. These adherent IEC are much smaller than the underlying intestinal MF and display slender processes which extend towards the MF monolayer, as previously observed using electron microscopy (210). Myofibroblast-adherent crypt cells expressed TLR2 and TLR4 protein, suggesting that the sub-population enriched for intestinal stem cells also expressed TLR2 and TLR4 protein. Moreover, TLR2 and TLR4 staining was more intense in the adherent crypt cells compared to the underlying MF, suggesting greater TLR2 and TLR4 expression by the adherent stem cell-enriched population than by the

underlying MF monolayer, though this may reflect down-regulation of TLR2 and TLR4 by MF following a relatively prolonged period of cell culture, as previously discussed.

To further isolate a population of cells enriched with an intestinal stem cell phenotype and to discuss the implications of TLR2 and TLR4 expression by intestinal stem cells, further studies were undertaken on isolated intestinal crypt cells. Intestinal stem cells were identified by their ability to efflux the fluorescent DNA-binding dye Hoechst 33342, identifying a stem cell-enriched group of cells known as the side population. This work is discussed in detail in chapter 7.

In summary, primary intestinal myofibroblast cultures were successfully maintained over a period of several months. These cultured cells demonstrated the typical morphology and expressed typical MF-associated intracellular markers. Primary cultured intestinal myofibroblasts expressed TLR2 and TLR4 transcript and surface protein, suggesting that they may play a role mediating mucosal inflammation by sensing bacteria that penetrate the epithelial barrier via TLR2 and TLR4 signalling. In a subsequent small study, intestinal myofibroblasts isolated from patients with UC down-regulated TLR2 mRNA expression. There was a trend towards up-regulation of TLR2 and TLR4 in intestinal MF from patients with Crohn's ileitis. This may be an important mechanism in the pathogenesis of myofibroblast-mediated fibrosis and stricturing in distal ileum of patients with Crohn's disease. Finally, co-culturing intestinal crypt cells onto MF monolayers is known to result in the adherence of a sub-population of IEC enriched for intestinal stem cells. These adherent cells were shown to express TLR2 and TLR4 protein, suggesting intestinal stem cells are also TLR2- and TLR4-expressing cells.

Chapter 7: Isolation and characterisation of putative stem cells in the human large bowel and their expression of Toll-like receptors

7.1 Introduction

The location, function and regulation of the intestinal stem cell (ISC) were introduced in section 1.8. The ISC is responsible for the repletion of the epithelial layer every five days and play a key role in the mucosal response to epithelial injury (187). Identification of ISC has relied on the retention of tritiated thymidine (^{3}HTdR) labelled DNA (193) and immunohistochemically staining a number of intracellular protein ISC markers (174). This has precluded the isolation and sorting of ISC to allow their better characterisation.

The identification of a side population of cells, initially in murine bone marrow (202) and subsequently in the small intestine of mice (208) and the human colon (210), has enabled researchers to sort a population of cells highly enriched with stem cell properties. This technique relies on the observation that side population cells, but not other non-stem cells, efflux the DNA-binding fluorescent dye Hoechst 33342, a process which is ameliorated by the ABCG2 pump-blocking agents, verapamil and fumitremorgin C (212).

Current evidence suggests that host-microbial interactions are important in the pathogenesis of IBD (13). Importantly, intra-epithelial neutrophil infiltration (cryptitis) and neutrophil crypt abscess formation are key histological features in IBD which result in epithelial cell loss and subsequent exposure of the underlying lamina propria to bacterial antigens (215). Regeneration of the epithelial barrier requires expansion and differentiation of the intestinal stem cell population. Therefore it is possible that the stem cell population, located in the base of the crypt, plays an important role in the pathogenesis of IBD through innate immune receptor-mediated bacterial sensing.

To date there is no published data describing the expression of toll-like receptors in this stem cell-enriched side population of cells. This study has demonstrated that unselected intestinal crypt epithelial cells express TLR2 and TLR4 transcripts and protein (chapters 4 and 5), but it is unclear if these TLR-expressing IEC are derived from intestinal crypt cells with stem cell properties. The aim of this chapter was to isolate normal colonic intestinal side population cells and to investigate their expression of TLR2 and TLR4 mRNA and protein.

7.2 Methods

7.2.1 Isolation of side population cells by Hoechst 33342 dye efflux

Stock solutions of the key reagents were made and stored at 4^{o}C in the dark. A stock solution of x100 (5mmol/L) verapamil (V4629, Sigma-Aldrich) was made by adding 49.1mg verapamil hydrochloride to 20mL 95% ethanol. A stock solution of x100 (1mmol/L) fumitremorgin C (ALX-350-127, Alexis Biochemicals) was made by adding 0.25mg of FTC to 658.8µL dimethyl sulfoxide (DMSO). Finally, a stock solution of x200 (0.5mg/mL) Hoechst 33342 was made by adding 2.5mg Hoechst 33342 (bisBenzimide H 33342, B2261-25MG, Sigma) to 5mL of distilled water.

Disaggregated IEC were isolated using EDTA/DTT and pancreatin. The cells were counted using trypan blue exclusion and 10^6 cells transferred to each of a dozen clean 15mL BD Falcon^{TM} tubes. The cell suspension volume was made up to 2mL/tube with pre-warmed (37^{o}C) DMEM (FACS) medium (500mL DMEM with 0.2µm filter-sterilised 2% FCS and 10mM (1.19g) HEPES) to give a cell concentration of 0.5x10^6 cells/mL.

To identify the SP, one of two ABCG2-blocking agents was added to a tube of isolated crypt cells. The cells in this tube were used only to demonstrate the presence of the ABCG2 pump (by demonstrating its blockade resulted in loss of its dye efflux properties using the blocking agent), but these cells were not used for either cell surface TLR2 or TLR4 expression analyses or for RNA isolation. Either 20µL of stock verapamil or 20µL of stock fumitremorgin C was added to these tubes and incubated in a shaking water bath at 37^{o}C for 15 minutes, with manual inversion twice during this incubation. During this period the remaining cell-containing tubes (unexposed to verapamil or fumitremorgin C) were kept at 37^{o}C in a water bath. Following the verapamil/FTC incubation step, 10µL of the stock solution of Hoechst 33342 was added to all tubes, giving a working concentration of Hoechst 33342 of 2.5µg/mL.

Initially, preliminary experiments were undertaken to identify the optimal conditions for Hoechst 33342 staining of isolated IEC. Hoechst 33342 concentrations of 2.5-5μg/mL were incubated with IEC for 30, 60 and 90 minutes in a shaking water bath at 37^{o}C. Hoechst 33342 concentration of 5μg/mL reduced IEC viability, as did incubation times beyond 30 minutes. Therefore all subsequent experiments were run with Hoechst 33342 incubation at 2.5μg/mL for 30 minutes. Tubes were mixed by inversion twice during this 30 minutes incubation.

Following the Hoechst 33342 incubation step, all tubes were placed on ice for 30 minutes and kept at below 4^{o}C thereafter. Following cooling, the tubes were centrifuged at 800rpm (300g) for 5 minutes at 4^{o}C and the supernatant removed. Cell pellets were re-suspended in 0.5mL of HBSS (FACS) (500mL HBSS with Ca/Mg with 0.2μm filter sterilised 2% FCS and 10mM HEPES (1.19g) at pH 7) and maintained at 4^{o}C until analysis. Immediately prior to cytological analysis 1μL of propidium iodide (PI) was added to the cell suspension to allow exclusion of non-viable cells.

Using a Beckman Coulter MoFlo cell sorter, Hoechst 33342 dye excitation at wavelength 405nm using violet light (405nm) was undertaken, followed by measurement of fluorescent emission at two wavelengths using a 450/50nm Band Pass (BP) blue optical filter and 620nm Long Pass (LP) red optical filter. For subsequent RNA isolation or assessment of cell surface marker expression, cells from both the side population (SP) and epithelial cells from outside the side population region (non-side population cells, NSP) were sorted into individual FACS tubes containing 200μL of chilled HBSS (FACS) medium on ice until required.

Viable crypt cells were initially identified using forward and side scatter analyses. Non-viable cells (adjacent to the intersection of the X- and Y-axes) and clumped cells (with large deflection on forward and/or side scatter) were excluded from analysis and cell sorting.

Viable cells were further analysed for clumping by viewing gated cells simultaneously in the blue linear (FL7-Height) and blue area (FL7-Area) channels. Single cells were those with equal signal in both FL7-Height and FL7-Area channels, whereas clumped cells demonstrated higher signal in the FL7-Area channel than the FL7-Height channel and were therefore excluded. Cell viability was further analysed by PI uptake. PI is a non-membrane permeable fluorophore and is only up-taken by non-viable cells with permeable cell membranes. Cells demonstrating high PI fluorescence in the FL2 channel were therefore excluded as non-viable.

Finally cells were analysed in the red (FL10 log) and blue (FL7 log) channels for Hoechst 33342 fluorescence. Two tubes were analysed to demonstrate ABCG2 blockade, indicating cells with a stem cell phenotype. The first contained Hoechst 33342-stained crypt cells and the second tube contained Hoechst 33342-stained crypt cells pre-incubated with verapamil/fumitremorgin C. If the former tube demonstrated a proportion of cells with low signal in both the blue and red channels (known as the Hoechst 33342-low region, indicating Hoechst 33342 efflux) and the latter tube demonstrated amelioration of events in this Hoechst 33342-low region (indicating loss of Hoechst 33342 efflux), this suggested that cells in the Hoechst 33342-low region expressed functional ABCG2 pumps (i.e. demonstrating these cells to have side population characteristics, figure 7.1).

In this case, a gate was drawn around the Hoechst 33342-low region to identify the stem cell-enriched side population of cells. Subsequently, tubes incubated with Hoechst 33342 (but not verapamil/fumitremorgin C) were analysed in an identical manner, and cells falling inside the Hoechst 33342-low (side population) region were positively sorted for further analysis. At least $5x10^3$ cells in the side population gated region were analysed per tube. Analysis was undertaken using Weasel v3 software.

7.2.2 RNA isolation from sorted cell populations and conventional RT-PCR analysis

Isolated epithelial cells characterised as cytometrically from both side population and non-side population regions were transferred to Eppendorf tubes and centrifuged at 13,000rpm (>10,000g) for 5 minutes followed by removal of the supernatant. Total RNA was isolated using the Qiagen RNeasy Plus Mini Kit (product 74134, Qiagen) as per the manufacturer's instructions (section 2.2). Samples of total RNA were labelled and stored at -80^{o}C in 20µL aliquots. RNA samples were assessed using a Nanodrop® spectrophotometer (Thermo Scientific) (section 2.3.1).

Side population cells were analysed for the expression of HPRT, TLR2 and TLR4 mRNA using the conventional RT-PCR primers and protocol described in section 2.4.3.2. However, 45 PCR cycles were used in the protocol for TLR2 and TLR4 cDNA amplification, whereas the standard 40 cycles was used for HPRT cDNA PCR. In addition SP cells were analysed for the expression of TLR3, TLR5 and TLR9 mRNA transcripts using commercial primers (QuantiTect Primer Assay primers, Qiagen). Details of these commercial primers are shown in table 7.1.

Table 7.1 Exon amplification and amplicon length for commercial TLR3, TLR5 and TLR9 real-time RT-PCR primers

Gene	Qiagen product code	Amplified exons	Amplicon length (bp)
TLR3	QT00007714	2/3	90bp
TLR5	QT01682079	2/3	147bp
TLR9	QT00015183	1/2	146bp

Bp, base pairs; TLR, Toll-like receptor

The PCR master mix was made as follows (total 25µL): 2x QuantiTect SYBR Green PCR Mastermix 12.5µL, 10x QuantiTect Primer Assay (for TLR3, TLR5 or TLR9) 2.5µL, nuclease-free water 7.5µL and cDNA 2.5µL. The samples were thoroughly mixed before being amplified on a Veriti rapid cycler (Applied Biosystems) using the following protocol: 95^{o}C for

15 minutes (hot start); 45 cycles of 94^{o}C for 15 seconds (denaturation), 55^{o}C for 30 seconds (annealing) and 72^{o}C for 30 seconds (elongation); and finally 72^{o}C for 10 minutes to complete synthesis. Samples were then separated using 1% agarose gel electrophoresis and visualised using an ultraviolet (UV) trans-illuminator (section 2.4.3.3).

7.2.3 Flow cytometric analysis of surface marker expression of sorted cell populations

In some cases, to allow for sorting of SP/NSP cell populations (for subsequent RNA isolation) and to allow simultaneous measurement of surface marker expression, disaggregated crypt IEC were labelled with monoclonal antibodies to various cell surface markers following the Hoechst 33342 dye incubation step, but prior to cytometric sorting. In such cases, dye efflux properties were investigated using a modified protocol from that detailed in section 7.2.1. Following incubation in Hoechst 33342, cells were centrifuged at 800rpm (300g) for 5 minutes at 4^{o}C. The supernatants were removed and 5µL mouse serum added for 15 minutes to block potential non-specific or FcR-binding. Thereafter, primary or isotype antibodies were added to the tubes in the following order:

Tube 1: No primary antibody
Tube 2: BerEP4-FITC 5µL (Dako F-0860)
Tube 3: BerEP4-FITC 5µL + IgG2a,κ-APC isotype 10µL (eBioscience 17-4724)
Tube 4: BerEP4-FITC 5µL + Anti-TLR2-APC 20µL (eBioscience 17-9922)
Tube 5: BerEP4-FITC 5µL + Anti-TLR4-APC 10µL (eBioscience 17-9917)
Tube 6: Anti-CD45-AF488 1µL (BioLegend 304019)

These cells were incubated for 1 hour at 4^{o}C in the dark. Next 0.5mL of cold HBSS (FACS) was added to each tube and the cells re-suspended. The tubes were centrifuged for 5 minutes at 800rpm (300g) at 4^{o}C and the supernatant removed. Finally the cells were re-suspended in 0.5mL HBSS (FACS) and kept on ice in the dark until analysis.

During the analysis process, in addition to the identification of cells with SP/NSP characteristics (section 7.2.1), these cell populations were gated upon to allow simultaneous characterisation of the expression of surface BerEP4, TLR2, TLR4 and CD45 proteins by measuring fluorescent signal in the FITC, APC and AF488 channels, respectively. Expression of surface protein was expressed as the median fluorescent intensity difference between the primary antibody sample and either the isotype-control or the no-antibody control sample. At least $5x10^3$ cells in the side population gated region were analysed and sorted per tube. All analyses were undertaken using Weasel v3 software.

7.3 Results

7.3.1 Isolated colonic crypt cells treated with Hoechst 33342 demonstrate a sub-population of cells with side population characteristics

The defining feature of side population (SP) cells is the ability to efflux the fluorescent nuclear dye Hoechst 33342 via the ABCG2 pump. SP cells derived from bone marrow and intestine are enriched with stem cells as demonstrated by their ability to save mice from lethal irradiation and to express markers of haematopoietic and intestinal stem cells, respectively. To define the SP required the blockage of the ABCG2 pump using an agent such as verapamil or fumitremorgin C.

Intestinal crypt cells from healthy controls were isolated using EDTA/DTT and disaggregated using pancreatin (section 3.2.4). Cells were then incubated with Hoechst 33342 before being kept at 4^{o}C until analysis on a MoFlo cytometer. Immediately prior to analysis on the flow cytometer, isolated cells were incubated with propidium iodide (PI) to assess cell viability.

Hoechst 33342 efflux was assessed on the red and blue lasers. Abolition of Hoechst 33342 efflux was assessed on samples containing isolated crypt cells pre-incubated with an ABCG2-blocking agent. A side population was considered present if pre-incubation with an ABCG2-blocking agent resulted in a reduction in cells numbers within the SP region of at least 75% (230).

Within these criteria, a side population of cells was demonstrated in isolated intestinal epithelial cells from healthy subjects (n=6, figure 7.1). Although it was possible to resolve the SP using fumitremorgin C as the ABCG2-blocking agent, verapamil was observed to be a more efficient ABCG2-blocking agent. Of note, compared to Hoechst 33342-treated crypt cells, verapamil treatment resulted in a significant reduction in cell viability as assessed by PI staining (54.3% $\pm$ 2.9 versus 36.8% $\pm$ 2.4, respectively, $p<0.001$). On occasion, verapamil

treatment resulted in the total loss of all viable cells and in such cases resolution of the SP was not possible. Fumitremorgin C was observed to reduce cell viability noticeably less than verapamil (41.4% ± 1.7, p=0.003 versus Hoechst 33342-treated cells), but was less effective at blocking the ABCG2 pump, as measured by a less than 75% reduction in SP region cell numbers following ABCG2-blockade (region 4, figure 7.1). Verapamil was therefore chosen as the ABCG2 pump-blocking agent of choice in subsequent experiments.

7.3.2 DyeCycle Violet is an alternative fluorescent molecule capable of discriminating side population cells with ABCG2-mediated efflux properties

Flow cytometric cell sorters with ultraviolet (UV) lasers (wavelength 350nm) are readily able to resolve a side population of cells from a variety of primary tissue types. However, such equipment is expensive and often unavailable to many laboratories. More commonly, flow cytometers are equipped with near-UV lasers (wavelength 370nm) or violet laser diodes (VLD, wavelength 408-401nm) which are smaller, less expensive and do not contain maintenance-intensive argon- or krypton-ion gas lasers. Near-UV lasers have been shown to resolve mouse bone marrow SP cells with excellent resolution, whereas VLD cytometers demonstrate poorer resolution and reduced ability to accurately discriminate the SP (288).

DyeCycle Violet (DCV) is an alternative DNA-binding fluorescent molecule with similar emission characteristics to Hoechst 33342 but with a longer wavelength excitation maxima (369nm) (289). On isolated murine bone marrow cells, DCV has been shown to discriminate an equally precise SP of cells using a violet laser diode compared to that resolved using a traditional UV gas laser. Moreover, immunophenotyping of sorted cells from either the violet laser-resolved DCV SP or the UV laser-resolved Hoechst 33342 SP were identical in their stem cell lineage surface marker expression phenotypes (289).

The ability of DCV to discriminate a SP of intestinal crypt epithelial cells using a violet laser diode was investigated using the Beckman Coulter MoFlo cell sorter. A protocol similar that

described in section 7.2.1 was used, but the addition of Hoechst 33342 was replaced by the addition of 2µL DCV to a cell suspension of $0.5x10^6$ IEC in 1mL. Using this modified protocol, a SP of intestinal crypt epithelial cells was discriminated (n=3, figure 7.2). The addition of either verapamil or fumitremorgin C (10µL to 1mL cell suspension for both) resulted in a greater than four-fold reduction in cell numbers in the SP region (region 5, figure 7.2).

7.3.3 Sorted side population and non-side population cells express BerEP4 but not CD45

To investigate the expression of the epithelial marker BerEP4 and the haematopoietic marker CD45 on side population cells, healthy intestinal crypt cells were isolated and stained with Hoechst 33342 or DCV. Side population wells were resolved using verapamil ABCG2-blockade and sorted into tubes containing FACS medium. Cells were collected following centrifugation and labelled with either anti-BerEP4-FITC or anti-CD45-AF488 monoclonal antibodies. Thereafter, cells were fixed in 0.5% formaldehyde until analysis.

Side population cells were demonstrated to be BerEP4-positive (mean ± SEM 97.9±2.1%, n=3, figure 7.3) but CD45-negative (0.35±0.35%, n=3, figure 7.4). Non-side population cells were immunophenotypically similar (BerEP4-positive 92.6±7.2%, n=3, and CD45-positive 0.15±0.1%, n=3).

7.3.4 Side population and non-side population cells express similar levels of surface TLR2 and TLR4 protein

To investigate the expression of TLR2 and TLR4 on side population cells from healthy controls, large intestinal crypt cells were isolated and incubated with either Hoechst 33342 or DCV. Following fluorescent dye incubation, cells were chilled and centrifuged before staining with either anti-TLR2 or anti-TLR4 APC-conjugated monoclonal antibodies. Side population cells were resolved using verapamil-induced ABCG2-blockade.

At the time of SP discrimination using the MoFlo cytometer, cell events in the SP-gated sub-population were simultaneously analysed for TLR2 and TLR4 expression by measuring APC median fluorescent intensity within the gated region. In addition, a sub-population of non-side population of cells were also analysed for TLR2 and TLR4 expression and to act as a paired comparison group.

Side population intestinal epithelial cells were observed to express both surface TLR2 and TLR4 protein (n=3, figure 7.5). Both TLR2 and TLR4 showed a trend towards higher expression in side population compared to non-side population sub-groups, but the differences were not statistically significant using a paired Wilcoxon test (TLR2: SP median [range] 7.1 [2.4-24] versus NSP 2.3 [1.3-3.9], p=0.25, n=3; TLR4: SP 7.7 [1.1-12.2] versus NSP 5.6 [3.2-6.8], p=0.59, n=3), figure 7.6.

7.3.5 Sorted side population cells express TLR2, TLR3, TLR4 and TLR5 mRNA

To investigate whether RNA could be isolated following their analysis and sorting by flow cytometry, side population and non-side population cells were demonstrated using the Hoechst 33342 fluorescent dye incubation and verapamil-mediated ABCG2-blockage of healthy control intestinal crypt cells. SP and NSP cells were sorted into cytometry tubes containing 200μL of FACS medium on ice. Following collection, cells were centrifuged and the supernatant discarded. RNA was isolated using the RNeasy Plus Mini kit and reverse-transcribed into cDNA. The expression of HPRT, TLR2 and TLR4 mRNA was then investigated using conventional polymerase chain reaction.

Three samples from healthy colon crypt epithelial cells were sorted into SP and NSP samples. Analysis of the quality of isolated RNA using the Nanodrop® spectrophotometer was not possible due to low RNA concentration (<10ng/μL). Nonetheless, all three samples expressed HPRT transcript, though expression appeared weaker in sample 3 than in samples 1 and 2 (figure 7.7A). Samples 1 and 2 also demonstrated mRNA expression for

TLR2 and TLR4 in both the SP and NSP isolates. However, there was no detectable expression of TLR2 or TLR4 mRNA in sample 3 (figure 7.7B and C).

Side population samples were also analysed for expression of TLR5, TLR3 and TLR9 mRNA expression. Two of the three SP samples were shown to express TLR5 mRNA transcript, as did pooled mRNA samples from unsorted crypt intestinal epithelial cells from the small and large intestine, primary PBMC and T84 and THP-1 cell lines (figure 7.8A). All three SP samples expressed TLR3 mRNA, as did human primary PBMC and the T84 epithelial cell line, but not the THP-1 monocyte cell line (figure 7.8B). TLR3 RT-PCR amplification product bands were weaker than those of TLR5 RT-PCR amplification. Side population cells did not express transcripts for TLR9 mRNA (figure 7.8C). There was weak expression of TLR9 mRNA by PBMC and the T84 epithelial cell line, but the THP-1 cell line did not express TLR9 mRNA (figure 7.8C).

7.4 Figures

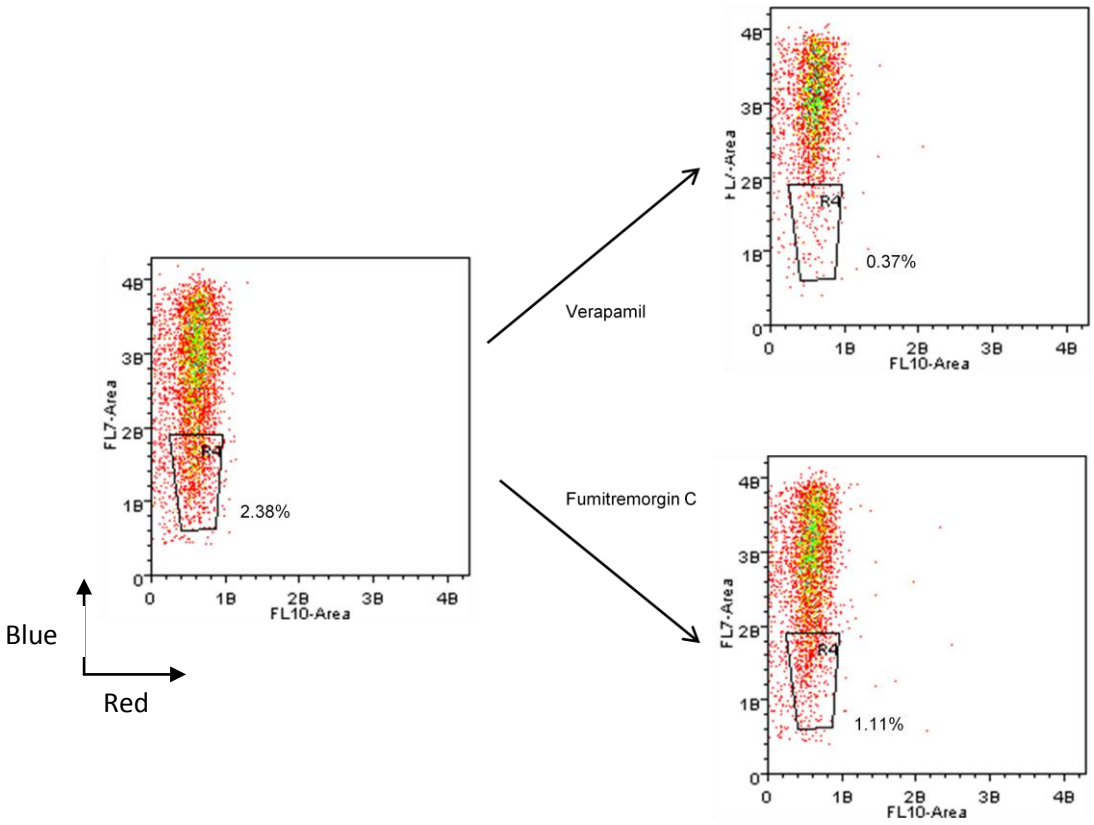

Figure 7.1 Isolated colonic intestinal crypt cells demonstrate a population of cells with side population characteristics. Isolated colonic crypt cells were incubated with the fluorescent dye Hoechst 33348 alone (left side) or following incubation with an ABDG2-blocking agent, either verapamil (right, top) or fumitremorgin C (right, bottom). The proportion of cells with low fluorescence in both the red (FL10) and blue (FL7) channels (region 4, R4) reduced from 2.38% in unblocked cells to 0.37% or 1.11% with verapamil and fumitremorgin C, respectively. This region represents a population of cells which have the phenotype of Hoechst 33342 dye exclusion via the ABCG2 efflux pump and are known as side population cells.

ABCG2, ATP binding cassette (ABC) transporter Bcrp1

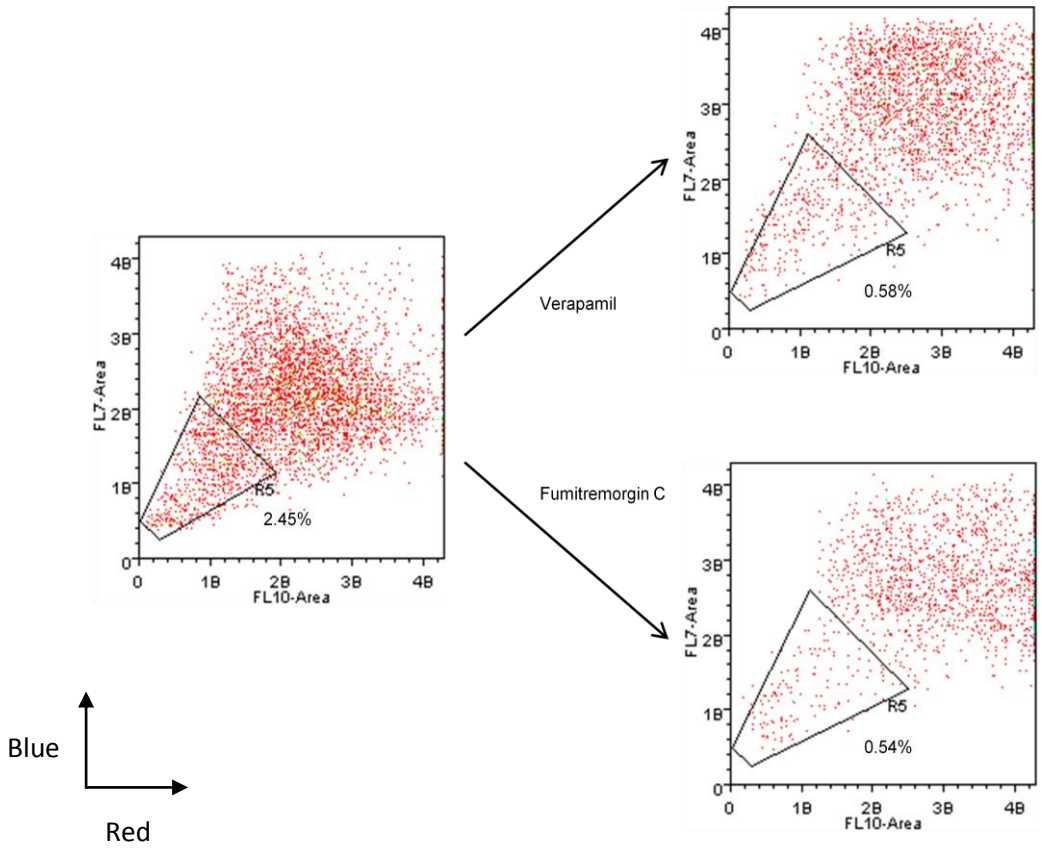

Figure 7.2 Isolated colonic intestinal crypt cells demonstrate a population of cells with side population characteristics using DyeCycle Violet. Isolated colonic crypt cells were incubated with the fluorescent molecule DyeCycle Violet alone (left side) or following incubation with an ABDG2-blocking agent, either verapamil (right, top) or fumitremorgin C (right, bottom). The proportion of cells with low fluorescence in both the red (FL10) and blue (FL7) channels (region 5, R5) reduced from 2.45% in unblocked cells to 0.58% or 0.54% with verapamil and fumitremorgin C, respectively. This region represents a population of cells which have the phenotype of ABCG2 efflux pump expression and are known as side population cells.

ABCG2, ATP binding cassette (ABC) transporter Bcrp1

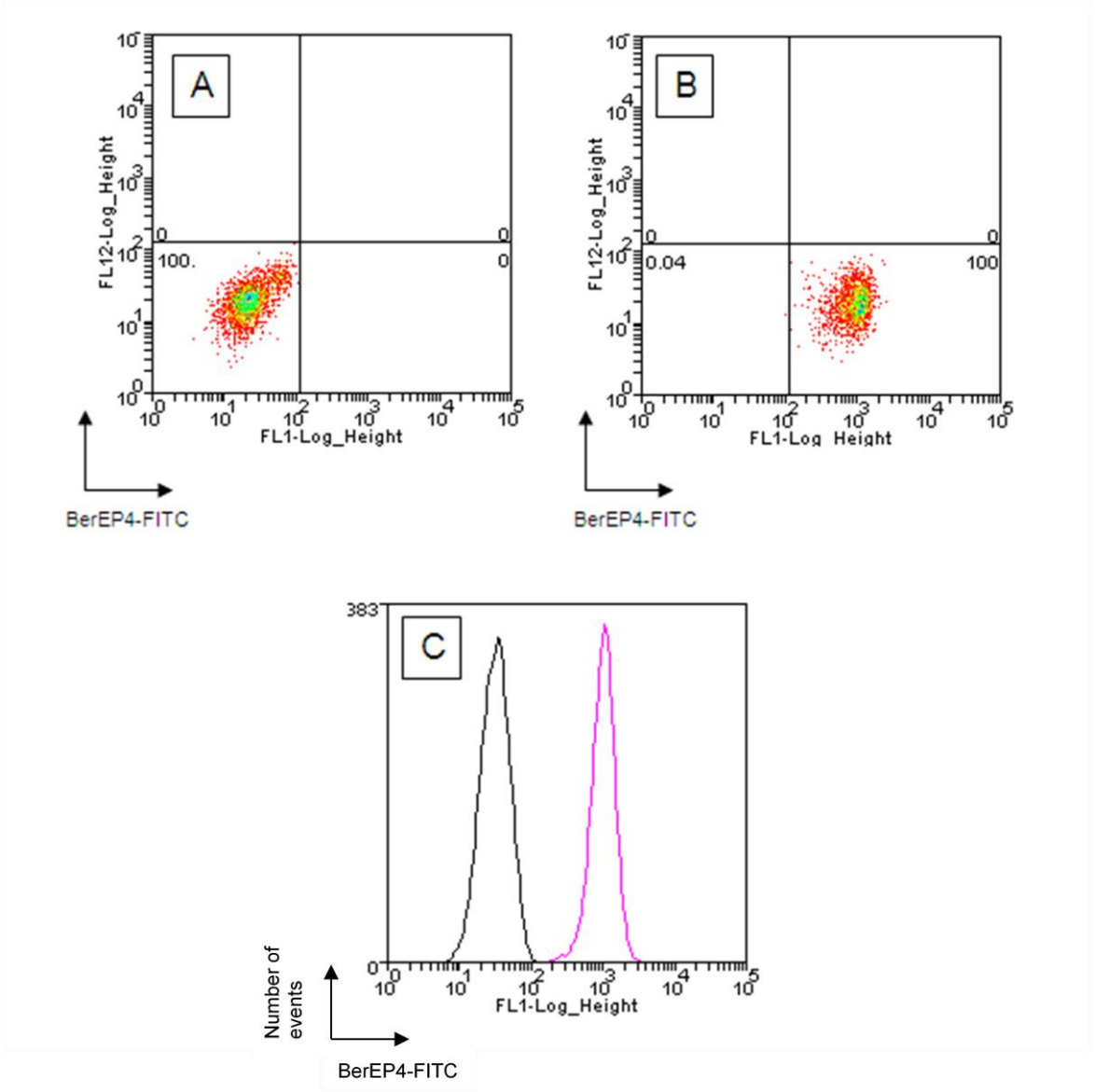

Figure 7.3 Sorted side population cells express surface BerEP4 protein. Intestinal crypt epithelial cells were isolated and incubated with the fluorescent dye Hoechst 33342 or DCV. Side population cells were identified by demonstrating that their efflux of the fluorescent dye was ameliorated using the ABCG2-blocking agent verapamil. Side population cells were sorted and subsequently stained with (A) isotype control FITC-conjugated or (B) anti-BerEP4 FITC-conjugated monoclonal antibodies, followed by analysis on a flow cytometer. Data were overlaid on a histogram (C) to illustrate comparative distribution of antibody fluorescence in each tube. The Y-axes in panels A and B represent unused gates.

Black: Isotype-FITC control
Purple: BerEP4-FITC

ABCG2, ATP binding cassette (ABC) transporter Bcrp1; DCV, DyeCycle Violet; FITC, Fluorescein isothiocyanate

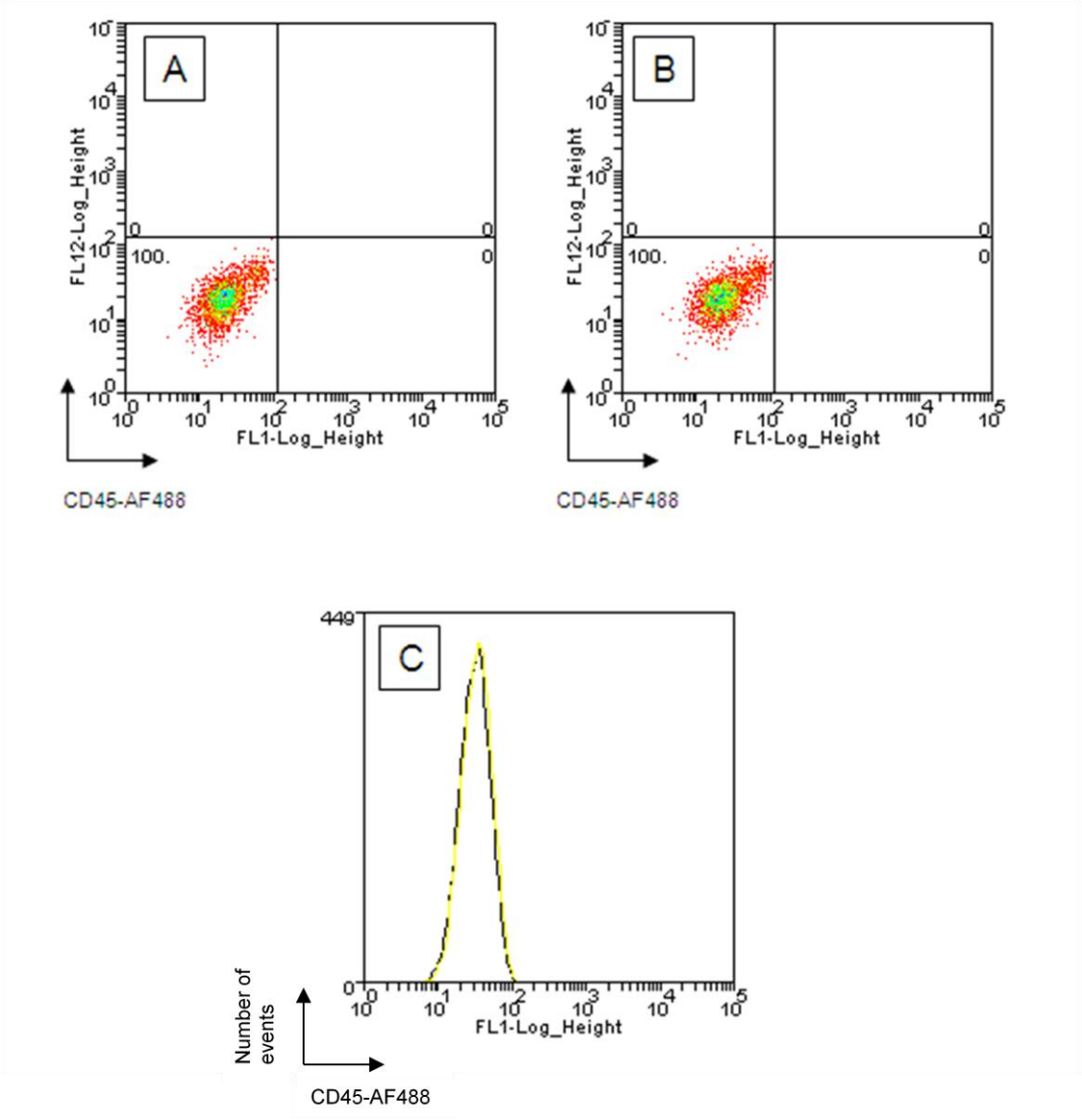

Figure 7.4 Sorted side population cells do not express CD45 protein. Intestinal crypt epithelial cells were isolated and incubated with the fluorescent dye Hoechst 33342 or DCV. Side population cells were identified by demonstrating that their efflux of the fluorescent dye was ameliorated using the ABCG2-blocking agent verapamil. Side population cells were sorted and subsequently stained with (A) isotype control AF488-conjugated or (B) anti-CD45 AF488-conjugated monoclonal antibodies, followed by analysis on a flow cytometer. Data were overlaid on a histogram (C) to illustrate comparative distribution of antibody fluorescence in each tube. The Y-axes in panels A and B represent unused gates.

Black: Isotype-AF488 control
Yellow: CD45-AF488

ABCG2, ATP binding cassette (ABC) transporter Bcrp1; AF488, Alexa Fluor-488; DCV, DyeCycle Violet

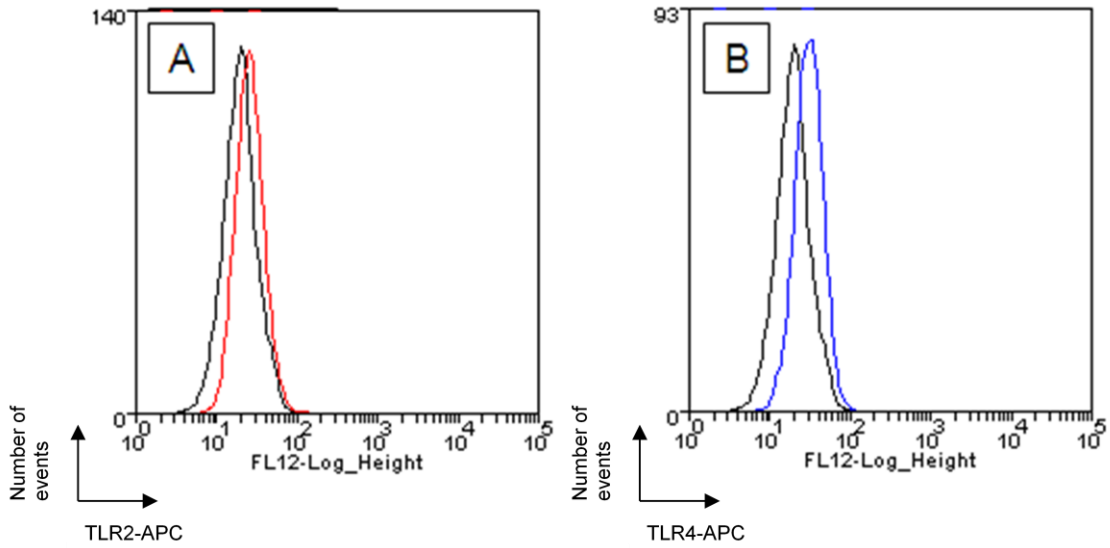

Figure 7.5 Side population cells express surface TLR2 andTLR4 protein. Isolated crypt intestinal cells were incubated with the fluorescent dye Hoechst 33342 or DCV followed by staining with either (A) anti-TLR2 APC-conjugated or (B) anti-TLR4 APC-conjugated monoclonal antibodies. Side population cells were identified by demonstrating that their efflux of the fluorescent dye was ameliorated using the ABCG2-blocking agent verapamil. Subsequently, cells with side population characteristics were gated, and the expression of TLR2 and TLR4 surface protein was characterised by measuring fluorescence in the APC channel at the time of cell sorting.

Black: Isotype-APC control
Red: TLR2-APC
Blue: TLR4-APC

ABCG2, ATP binding cassette (ABC) transporter Bcrp1; APC, Allophycocyanin; DCV, DyeCycle Violet

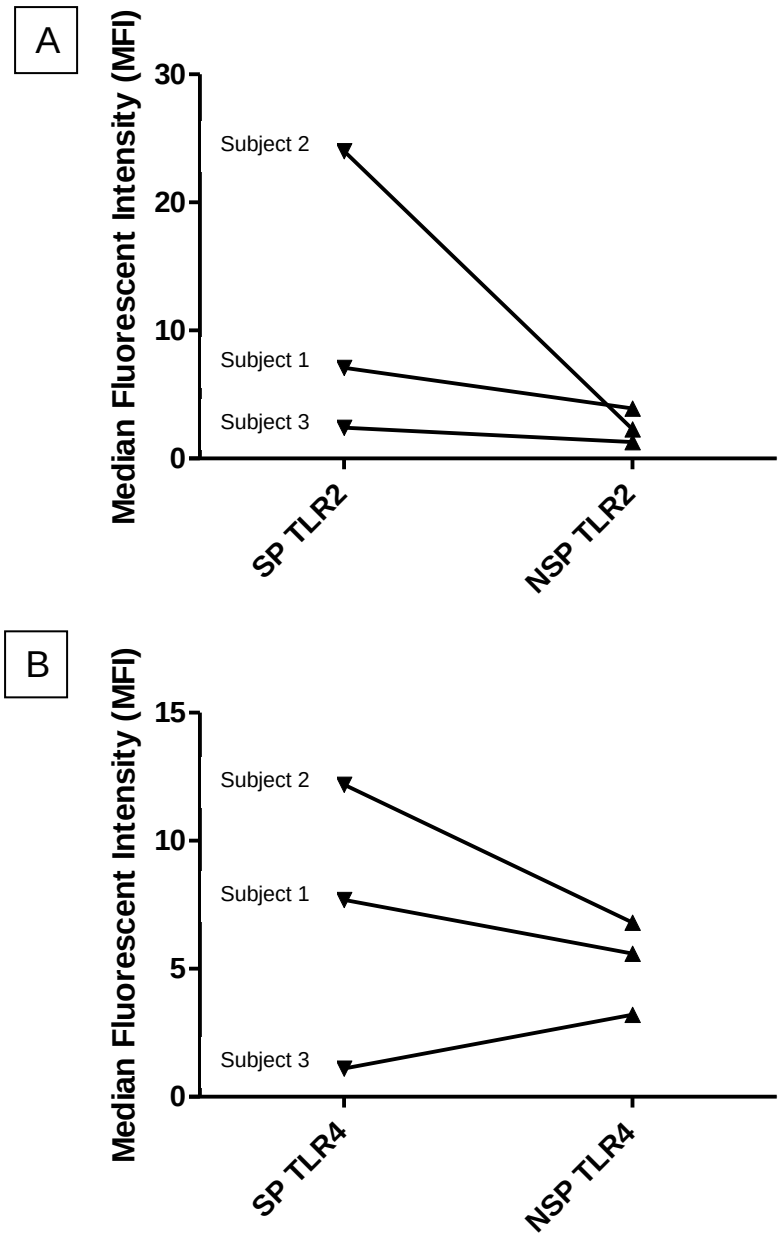

Figure 7.6 Side population cells express similar levels of TLR2 and TLR4 protein compared to non-side population cells. Isolated intestinal crypt cells were incubated with the fluorescent dye Hoechst 33342 or DCV, followed by staining with either (A) anti-TLR2 APC-conjugated or (B) anti-TLR4 APC-conjugated monoclonal antibodies. Side population cells (SP) were identified by demonstrating that their efflux of the fluorescent dye was ameliorated using the ABCG2-blocking agent verapamil. In contrast, cells demonstrating no dye efflux properties in the red (FL10) and blue (FL7) channels following ABCG2-blockade were termed non-side population cells (NSP). Subsequently, cells with SP and NSP characteristics were gated, and the expression of TLR2 and TLR4 surface protein was calculated as the difference between the median fluorescence intensities of the primary and isotype antibodies in the APC channel. Subject numbers correspond to the subjects in figures 7.7 and 7.8.

ABCG2, ATP binding cassette (ABC) transporter Bcrp1; APC, allophycocyanin; DCV, DyeCycle Violet; NSP, non-side population; SP, side population; TLR, Toll-like receptor

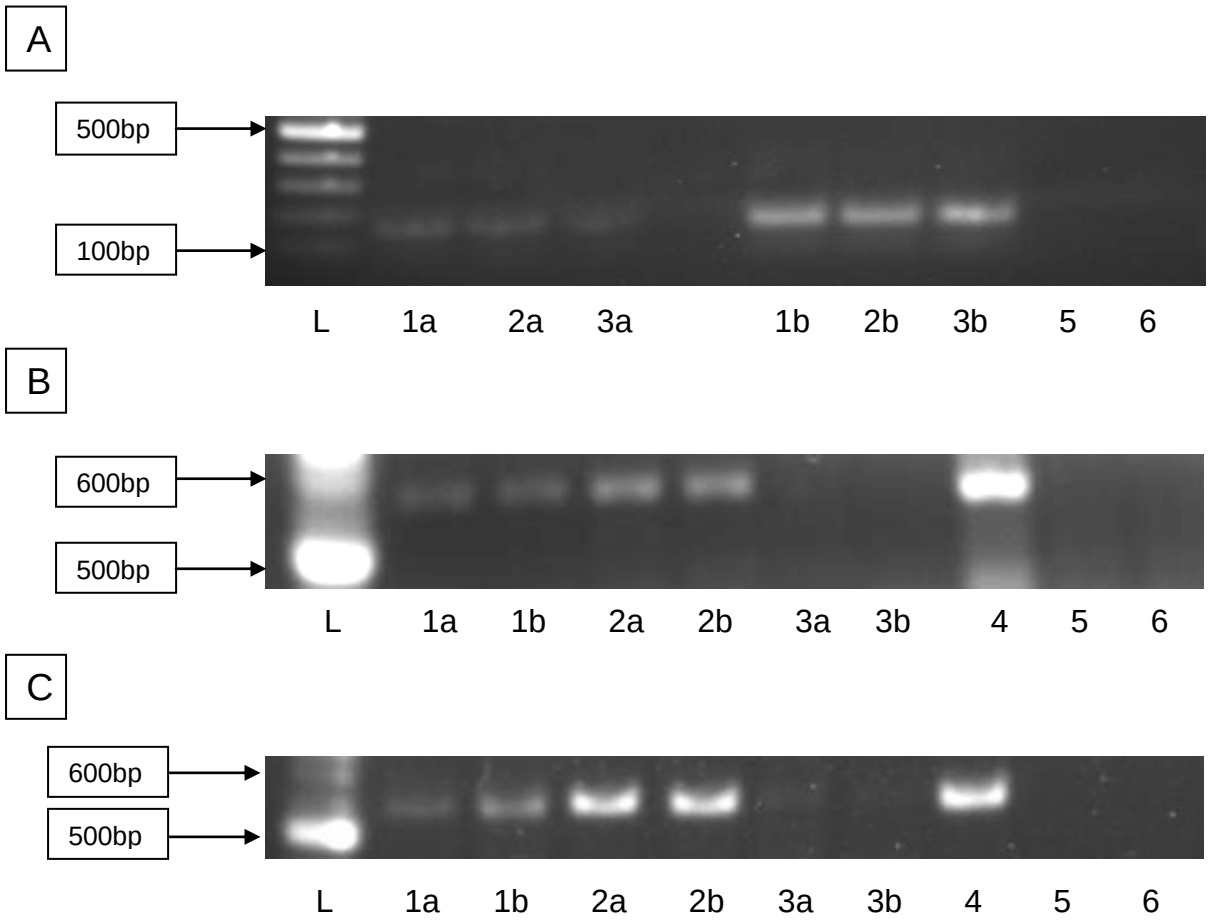

Figure 7.7 Sorted side population cells express TLR2 and TLR4 mRNA. Side population cells (SP) were identified from isolated intestinal crypt cells (n=3) by demonstrating that their efflux of a fluorescent dye (Hoechst 33342 or DCV) was ameliorated using the ABCG2-blocking agent verapamil. Cells demonstrating no dye efflux properties were termed non-side population cells (NSP). Subsequently, SP and NSP cells were cytometrically sorted and RNA isolated before conventional RT-PCR was undertaken. The mRNA expression of (A) HPRT (160bp), (B) TLR2 (599bp) and (C) TLR4 (507bp) was investigated using agarose gel electrophoresis and UV transillumination.

Lanes 1-3: Side population cells (a) and non-side population cells (b) from subjects 1-3
Lane 4: PBMC positive control
Lane 5: No reverse transcriptase (negative) control
Lane 6: No cDNA template (negative) control

DCV, DyeCycle Violet; HPRT, Hypoxanthine guanine phosphoribosyltransferase; L 100 base pair ladder; PBMC, peripheral blood mononuclear cell; RT-PCR, reverse transcriptase polymerase chain reaction; TLR, Toll-like receptor; UV, ultra-violet light

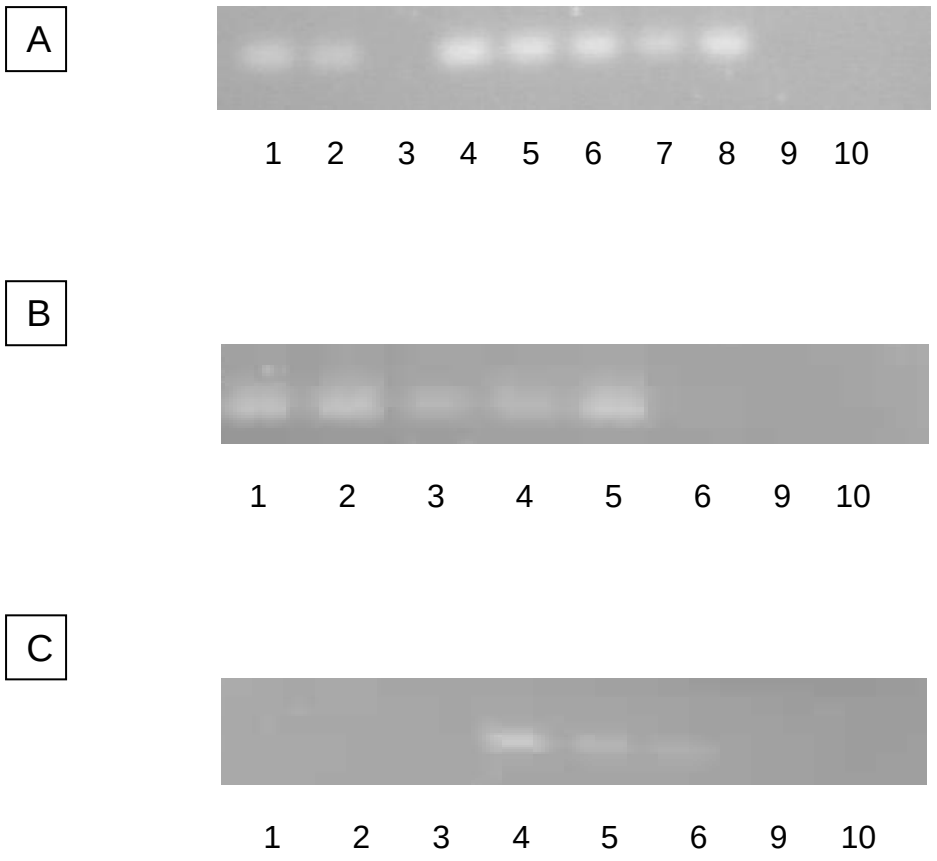

Figure 7.8 Sorted side population cells express transcripts for TLR5 and TLR3, but not TLR9 mRNA. Side population cells (SP) were identified from isolated intestinal crypt cells (n=3) by demonstrating that their efflux of a fluorescent dye (Hoechst 33342 or DCV) was ameliorated using the ABCG2-blocking agent verapamil. Cells demonstrating no dye efflux properties were termed non-side population cells (NSP). Subsequently, SP and NSP cells were cytometrically sorted and RNA isolated before conventional RT-PCR was undertaken. The mRNA expression of (A) TLR5 (147bp), (B) TLR3 (90bp) and (C) TLR9 (146bp) was investigated using agarose gel electrophoresis and UV transillumination.

Lanes 1-3: Side population cell from subjects 1-3
Lane 4: PBMC
Lane 5: T84 human epithelial cell line
Lane 6: THP-1 human monocyte cell line
Lane 7: Pooled healthy control small intestine unsorted crypt intestinal epithelial cells (n=7)
Lane 8: Pooled healthy control colon unsorted crypt intestinal epithelial cells (n=13)
Lane 9: No reverse transcriptase (negative) control
Lane 10: No cDNA template (negative) control

DCV, DyeCycle Violet; HPRT, Hypoxanthine guanine phosphoribosyltransferase; PBMC, peripheral blood mononuclear cell; RT-PCR, reverse transcriptase polymerase chain reaction; TLR, Toll-like receptor; UV, ultra-violet light

7.5 Discussion

The demonstration of a side population of cells by their ability to efflux the DNA-binding fluorescent dye Hoechst 33342, which is ameliorated by pre-incubation of cells with an ABCG2-blocking agent such as verapamil or FTC, has allowed investigators to cytometrically sort a sub-population of cells enriched for stem cells. This technique was originally described using murine haematopoietic stem cells (202), and subsequently side population cells have been described in murine liver (205) and skeletal muscle (206, 207) and in human breast (203) and prostate (204). Prior to this discovery, intestinal stem cells were identifiable only by their label-retaining properties (193) or via immunohistochemical staining of a number of intracellular markers (174), and could not be sorted for down-stream analysis. SP cells expressing intestinal stem cell markers have been reported in the mouse jejunum (208) and more recently in the human colon (210).

Traditionally, to be able to identify the SP cells it has been a requirement of flow cytometers that a UV laser is used at a wavelength of approximately 350nm for Hoechst 33342 dye excitation. The Beckman Coulter MoFlo cytometer contains a violet laser diode (VLD, wavelength 401-408nm) which is smaller, less expensive and does not contain a maintenance-intensive argon- or krypton-ion gas laser. It has been reported that VLD laser-containing flow cytometers are still able to resolve the murine bone marrow SP cells using Hoechst 33342 dye, although discrimination of the target SP is poorer than with the use of near-UV (wavelength 370nm) and UV lasers (wavelength 350nm) (288).

This study set out to investigate if a SP of colonic epithelial cells could be resolved using the Beckman Coulter MoFlo VLD laser cytometer. Indeed it was possible to discriminate a SP of intestinal crypt epithelial cells isolated from healthy colonic mucosa and it was also possible to selectively sort these cells directly into culture medium for down-stream analysis. Although both verapamil and FTC were shown to block the ABCG2 efflux pump and facilitate in the

identification of the SP cells, verapamil was consistently the more effective blocking agent. However, verapamil treatment was associated with a reduction in total isolated cell viability and, on occasion, verapamil incubation resulted in complete loss of all viable cells with failure to resolve the side population.

To attempt to improve the discrimination of the SP cells using the VLD laser, an alternative DNA-binding fluorescent dye to replace Hoechst 33342 was sought. DyeCycle Violet (DCV) is reported to demonstrate similar emission characteristics to Hoechst 33342 under both UV and violet light, but has longer wavelength excitation maxima (369 nm), and allowed accurate identification of a SP of murine bone marrow cells which expressed the predicted haematopoietic stem cell markers Sca-1 and c-kit (289). Subsequently, DCV has been reported to discriminate the SP of an enriched stem cell population in benign and malignant primary prostate tissue and several prostate cancer cell lines (CWR-R1, DU-145 and RWPE-1 cells) (290) and in a human bladder cancer cell line (SW780) (291). There is therefore good data to suggest that DCV dye exclusion is a valid reagent for identifying stem cell-enriched SP cells.

This study demonstrated that when using DCV dye it was possible to discriminate a side population of crypt intestinal epithelial cells from primary human colon, using both verapamil and FTC as ABCG2-blocking agents and using the VLD laser of the MoFlo cytometer. However, resolution of the SP of cells did not appear to be superior to the resolution of the SP using Hoechst 33342. Since DCV is significantly more expensive than Hoechst 33342 and offered no improvement in SP cell resolution, Hoechst 33342 dye was used for all subsequent down-stream analyses of sorted SP cells.

To allow further characterisation, SP cells isolated using Hoechst 33342 were sorted and stained with antibodies to the epithelial specific marker BerEP4 and the haematopoietic marker CD45. Isolated SP cells were shown to be exclusively BerEP4-positive and CD45-

negative, suggesting that these isolated SP cells were epithelial and not haematopoietic in origin. Previous work in this laboratory has demonstrated that SP cells isolated by Hoechst 33342 dye efflux express the putative ISC marker CD133 and over-express β1-integrin, but do not express the haematopoietic stem cell marker CD34 using flow cytometry. Furthermore, isolated SP cells express the ISC marker Msi-1 using immunocytochemical staining (210). Therefore, SP cells sorted by Hoechst 33342 express epithelial cell and intestinal stem cell markers, but not markers of haematopoietic stem cells, and are a suitable population of cells on which to further analyse ISC characteristics.

Interestingly, sorted SP and NSP cells expressed surface TLR2 and TLR4 protein in all samples using flow cytometry. Moreover, when these SP cells were sorted and collected, transcripts for TLR2 and TLR4 mRNA were identified in two of the three samples. The third sample demonstrated mRNA of poor quality and low concentration, which may have been a contributing factor the lack of visible bands following conventional RT-PCR amplification.

Myofibroblast-adherent epithelial cells are predominantly Msi-1-positive intestinal stem cells (210). Earlier in this study, un-sorted intestinal crypt cells were co-cultured with myofibroblast monolayers (section 6.2.3). Staining of these co-cultured cells demonstrated TLR2 and TLR4 expression by both MF and adherent cells, however the adherent IEC demonstrated more intense staining than the underlying MF cells (section 6.3.5).

These data suggest that putative intestinal stem cells isolated by SP cell sorting or through their interaction with cultured intestinal myofibroblasts express TLR2 and TLR4 transcripts and protein, as identified using a variety of laboratory techniques. When the expression of surface TLR2 and TLR4 protein on SP cells was compared to expression on NSP (non-stem) cells, there was no significant difference in absolute expression levels, though a trend towards higher expression was noted for both TLR2 and TLR4 in SP cells.

Side population cells also expressed transcripts for TLR5 and TLR3 mRNA. Agonists for TLR5 have been shown to protect against the induction of radiation-induced enteritis if given prior to radiation treatment (161). Furthermore, parenteral TLR3 ligands protect against the development of murine experimental colitis (159). These data further implicate the intestinal stem cell in directly sensing microbial ligands through the recognition of flagellated bacteria and microbial dsRNA, respectively.

This is the first report to demonstrate TLR2, TLR3, TLR4 and TLR5 expression in a human ISC-enriched population. A recent abstract reported the epithelial-specific over-expression of TLR4 in mice expressing the green fluorescent protein-labelled ISC marker Lgr5 (292). Over-expression of epithelial TLR4 in mice resulted both in the expansion of the Lgr5-positive stem cell population and in nuclear accumulation of β-catenin, two events which are associated with tumorigenesis. Moreover, villin-TLR4 mice with DSS-induced colitis are highly susceptible to azoxymethane-induced neoplasia, which was inhibited using a TLR4/MD-2 antagonist (273) and which may signal through epidermal growth factor receptor ligands (293). This provides evidence that TLR4 signalling is directly important in ISC function and may play a role in neoplastic transformation.

Interestingly, this group have also demonstrated increased immunostaining of TLR4 in human ulcerative colitis-associated dysplasia and cancer (273). To the contrary, the TLR4 Asp299Gly gene polymorphism (which interrupts TLR4 signalling) is reported to confer a greater risk of advanced stage in sporadic human colonic adenocarcinoma, suggesting loss of TLR4 signalling may convey a worse prognosis in this setting (294).

Stem cells are vital for replenishing the epithelial cell surface of the intestine, which turns over every five days in the healthy state (187). Following epithelial injury stem cell expansion is a key step in epithelial restitution and mucosal healing (295). Exposure to ligands for TLR2, TLR3, TLR4 and TLR9 are protective against various models of experimental colitis in

mice (159). Exposure to the TLR4 ligand LPS prior to radiation injury protects mice form radiation enteritis (160) and the TLR5 ligand flagellin has similar radio-protective effects on intestine and bone marrow in mice and primates (161). It was unclear from these publications if these ligands acted directly or indirectly on the intestinal stem cell population.

My studies suggest that ISC may be able to directly sense intestinal Gram-positive, Gram-negative and flagellated bacteria via their expression of TLR2, TLR3, TLR4 and TLR5, and imply that the protective effects of prior exposure to these ligands in experimental models of colitis and radiation enteritis may act via direct ligand interaction with these receptors on the stem cells themselves. Moreover, TLR4 signalling in intestinal stem cells may be an important pathway in colitis-associated tumorigenesis. It would be interesting to investigate if there is differential expression of TLR2, TLR4 and TLR5 by intestinal stem cells in patients with active IBD and in patients with IBD-associated dysplasia and cancer.

Intestinal stem cells may therefore play a role in bacterial sensing, which is known to be important in maintaining intestinal homeostasis. These data also suggest that TLR-directed therapeutic interventions in inflammatory colonic diseases may act directly on the stem cells themselves, providing a possible future mechanism for influencing intestinal stem cell function.

Chapter 8: Discussion and conclusions

The inflammatory bowel diseases ulcerative colitis and Crohn's disease are incurable, chronic inflammatory conditions which primarily affect the distal ileum and colon. IBD is associated with significant morbidity. Current medical treatments are successful at inducing and maintaining disease remission in a proportion of patients, but many patients inevitably require surgical intervention. Although there have been significant advances in the treatment of IBD with the introduction of anti-tumour necrosis factor-alpha therapy, a significant number of patients either fail to respond or lose response to this treatment. A better understanding of the underlying pathogenesis of IBD may lead to more effective treatments in the future.

Pathologically IBD results in a dense inflammatory cell infiltrate into the intestinal mucosa, resulting in the histopathological features of epithelial cell loss, crypt architectural distortion and dense peri- and intra-crypt inflammation, causing cryptitis and crypt abscesses. At the base of the crypts reside intestinal stem cells surrounded by the stromal cells, forming the stem cell niche. Interaction between the cells of the niche is important to the regulation of stem cell proliferation and differentiation, a vital process in restitution following epithelial injury.

Toll-like receptors are innate immune system pattern recognition receptors expressed by a variety of cells, including intestinal epithelial cells. These receptors bind to highly conserved cellular molecules expressed by a number of micro-organisms, including commensal and pathogenic bacteria. The role of toll-like receptor signalling in the intestinal mucosa is complex. While toll-like receptor signalling is indispensable in the formation of a healthy mucosal immune system and in maintaining homeostasis, excessive receptor signalling results in and perpetuates intestinal inflammation and may play a role in carcinogenesis.

With this in mind, this study set out to characterise the expression of Toll-like receptors 2 and 4 by crypt intestinal epithelial cells in patients with inflammatory bowel disease. The crypt epithelial cells were chosen specifically for a number of reasons. Firstly, the crypt lumen does not normally contain bacteria and it is only during intestinal inflammation that bacteria are present in the crypt. Secondly, cryptitis and crypt abscesses are pathological features of inflammatory bowel disease, implicating the crypt epithelium as a focal region of mucosal inflammation in inflammatory bowel disease. Thirdly, it is reported that the expression of Toll-like receptor 2 and 4 is greatest in the crypt epithelial cells, with down-regulation of expression demonstrated as epithelial cells migrate to the intestinal luminal surface. Finally, the crypt is the location of the intestinal stem cells which are vital in responding to mucosal injury by replenishing the epithelium.

Initially this study demonstrated that ethylenediaminetetraacetic acid (for the isolation of intestinal crypts) and pancreatin treatment (for the disaggregation of crypt epithelial cells) resulted in the isolation of a population of individual crypt epithelial cells. These crypt cells contained few non-epithelial cells. Moreover, isolated crypt cells from patients with inflammatory bowel disease did not result in haematopoietic cell contamination. This technique also isolated Paneth cells from mucosal samples of the small intestine.

Quantitative analysis demonstrated up-regulation of Toll-like receptors 2 and 4 transcripts and cell surface proteins by crypt intestinal epithelial cells from patients with ulcerative colitis and Crohn's colitis. Toll-like receptor 4 transcript was also up-regulated in crypt cells from patients with Crohn's ileitis. This data suggests that Toll-like receptors 2 and 4 play a role in the pathogenesis of inflammatory bowel disease and may offer a future therapeutic target for active disease. This is the first study to report surface toll-like receptor expression by primary intestinal epithelial cells using flow cytometry.

This study also demonstrated an up-regulation of the expression of Toll-like receptor 4 transcript in histologically normal, un-inflamed crypt cells from patients with ulcerative colitis. Moreover, both Toll-like receptors 2 and 4 transcripts were similarly expressed in paired normal and inflamed specimens from patients with left-sided ulcerative colitis. These data suggest that Toll-like receptor 2 and 4 expression is constitutive in the crypt epithelial cells of patients with ulcerative colitis. This may indicate a primary predisposition to ulcerative colitis in these individuals and suggests up-regulated Toll-like receptor expression by intestinal epithelial cells is not purely a secondary phenomenon.

Intestinal myofibroblasts are important mucosal cells which play a significant role in the regulation of intestinal stem cells in the stem cell niche. Myofibroblasts regulate the mucosal immune response by secreting a number of inflammatory mediators and sensing bacterial ligands. Myofibroblasts are also responsible for the formation of the intestinal fibrosis observed in inflammatory bowel disease, particularly Crohn's ileitis. This study has demonstrated expression of Toll-like receptors 2 and 4 by primary cultured intestinal myofibroblasts, which may be up-regulated in Crohn's ileitis and may play a role in the pathogenesis of intestinal fibrosis. Moreover, Toll-like receptor 2 transcript is down-regulated in ulcerative colitis, a condition where intestinal fibrosis is less common.

Isolated crypt cells adhere to cultured primary intestinal myofibroblasts and these adherent cells are highly enriched for intestinal stem cells. This study reports that adherent crypt cells express Toll-like receptors 2 and 4 proteins, suggesting intestinal stem cells express these receptors.

Efflux of the fluorescent dye Hoechst 33342 via the ATP binding cassette transporter Bcrp1 allows identification of a group of cells referred to as side population cells. These cells are highly enriched for epithelial and intestinal stem cells markers. This study has demonstrated that side population cells expressed the epithelial-specific marker BerEP4 but not the

haematopoietic marker CD45. Furthermore side population cells expressed Toll-like receptors 2 and 4 transcripts and protein, and expressed TLR3 and TLR5 transcripts.

Together with the observations from the myofibroblast-adherent crypt cell experiments, these data suggest intestinal stem cells are able to directly sense microbial products through Toll-like receptors 2, 3, 4 and 5. Signalling through toll-like receptors has been reported to protect mice from experimental colitis and radiation-induced enteritis. The demonstration of Toll-like receptors 2, 3, 4 and 5 expression by intestinal stem cells suggests this protective effect may act directly on intestinal stem cells and provides a mechanism through which intestinal stem cell function may be manipulated in health and during mucosal inflammation. This may have wider reaching implications given the observation that Toll-like receptor 4 signalling is implicated in experimental colitis-induced colonic cancer and manipulation of Toll-like receptor 4 signalling may become an important future cancer chemo-protective therapy in inflammatory bowel disease.

There are limitations to the current study which warrant discussion. The histological assessment of the activity of mucosal inflammation was undertaken by a Clinical Histopathologist blinded to the underlying diagnosis and disease activity of each study participant. In all cases, the mucosal samples from which the intestinal crypt cells were isolated, and from which the histological assessment was made, were taken from immediately adjacent regions of the bowel (with macroscopically similar degrees of inflammation), but not from the exact same site. It is likely Toll-like receptors expression data from the isolated crypt cells were representative of those from adjacent tissue (on which the histological activity of severity was assessed). However this may not always have been the case, particularly in subjects with Crohn's disease which is characterised by skip lesions in disease extent.

The magnitude of the differences in the differential expression of Toll-like receptors 2 and 4 at the transcript levels and the protein level were dissimilar. Surface protein expression was several-fold greater than the corresponding mRNA expression when comparing subjects with IBD and healthy controls. One explanation for this observation is that the rate of degradation of cellular mRNA was more rapid than that of surface protein, resulting in a reduction in the observed differential expression in the former. It is also possible that, because the subjects contributing to the real-time RT-PCR and flow cytometry data were not taken from the same cohort of individuals, there may have been differences amongst these groups which explain the differences in Toll-like receptor 2 and 4 expression rather than mRNA degradation. Ideally, analysis of transcript and surface protein expression would have been undertaken on the same group of subjects to allow a more meaningful discussion on the magnitude of Toll-like receptor expression.

Investigation of the expression of Toll-like receptors 2 and 4 in crypt cells from patients with Crohn's ileitis was limited to the mRNA level. Similarly, specimens from subjects with acute severe colitis were also limited to the mRNA level. It would have been desirable to have been able to investigate the expression of Toll-like receptors 2 and 4 at the surface protein level in these groups for completeness. Likewise, the observed greater expression of Toll-like receptors 2 and 4 transcripts in crypt cells from histologically normal regions of mucosa in patients with left-sided UC compared to healthy controls was only investigated at the transcript level. Analysis of surface expression at the protein level in this unique group of patients would be very interesting.

In chapter 6, the expression of Toll-like receptors 2 and 4 was investigated in cultured myofibroblasts from healthy control and patients with IBD. The sample sizes for IBD subjects were limited to three cases in each group. This was in part due to the lengthy and complex myofibroblast acquisition and culture protocol, which limited the number of specimens which could be cultured over several months, and partly due to tissue availability in the latter period

of the study. Therefore, while there appeared to be trends in the differential expression of Toll-like receptors in myofibroblasts from patients with Crohn's ileitis and ulcerative colitis, larger sample groups are required to definitively answer this issue. The data reported in his chapter should be regarded as preliminary data.

A significant number of samples were required to optimise the protocol for identifying side population cells using both Hoechst 33342 and DyeCycle Violet fluorescent dyes. However, the expression of Toll-like receptors in the side population cells were reported in a group of three healthy large intestine control specimens. Further investigation using a larger sample size, including healthy samples from the small intestine, would be required to more definitively address the issue of Toll-like receptor expression in the intestinal stem cells population.

All crypt cell samples were isolated the day following acquisition of the mucosal tissue from the study participant. In many cases, primary tissue was not available for collection until late in the working day. It was not possible to isolate crypt cells and undertake flow cytometric analysis on live cells the same day due to time constraints. Therefore, all acquired tissue was maintained in tissue culture medium overnight and the cell isolation protocol undertaken at the beginning of the following day. This allowed continuity in the handling of all specimens and allowed the acquisition of live cells for flow cytometric analysis and sorting. However, there was a risk that cell viability, mRNA quality and protein quality would decline during the overnight storage step. Therefore interpretation of the Toll-like receptor mRNA and protein expression data should be undertaken with this born in mind.

This study had a number of strengths. Care was taken to phenotypically characterise the isolated crypt cell population, ensuring that only epithelial cells and intestinal myofibroblasts, but not haematopoietic cells were included in the Toll-like receptor expression data analysis. CD45-positive cells were excluded from all flow cytometric analyses, allowing only BerEP4-

positive (i.e. epithelial) cells to be analysed. This is the first study to positively gate for epithelial cells in this way using flow cytometry.

Extensive demographic data was obtained for each subject enabling the investigation of factors which may have explained the observed differences between groups. Apart from age and immunosuppressant drug therapies, all groups were well matched. Moreover, an age-related decline in Toll-like receptor expression was excluded as an explanation for the differential expression between the younger IBD groups and the older healthy control groups using a sub-group analysis of the healthy control subjects.

The study included subjects with IBD of varying degrees of histological disease activity, as assessed by a blinded Clinical Histopathologist using a published and well-reported method. This allowed assessment of the effect of disease activity and local mucosal inflammation on Toll-like receptor expression, a novel aspect of this study. Moreover, the inclusion of a sub-group of patients with left-sided colitis allowed assessment of the expression of Toll-like receptors in histologically normal mucosal from patients with UC. This data has provided insights into the primary expression of Toll-like receptors in this unique group.

The assessments of both mRNA and protein expression were undertaken using more than one technique for each molecule, providing greater confidence in the observed differences amongst IBD and healthy control groups. Transcript and protein assays were undertaken using well established and widely reported techniques. These techniques were highly reproducible and provided mRNA of high quality, as assessed by spectrophotometry and micro-fluid capillary electrophoresis. All primers and antibodies used in the analyses were extensively tested for functionality using established control templates.

The analyses of primary crypt intestinal cells from human samples of patients with IBD using quantitative methods, including real-time RT-PCR and flow cytometry, were both novel to

this study and allowed accurate quantification of Toll-like receptor expression. This is the first study to quantitatively demonstrate up-regulation of Toll-like receptors 2 and 4 in crypt intestinal epithelial cells in human IBD.

Future studies in this field should aim to determine if the Toll-like receptors expressed by primary human intestinal epithelial cells are functional when exposed to their respective ligands. Although this has been demonstrated in human epithelial cancer cell lines, primary intestinal epithelial Toll-like receptor function has not been reported. Demonstration of their functionality would strengthen the evidence suggesting that Toll-like receptors play important roles in maintaining intestinal homeostasis in humans and in the pathogenesis of human inflammatory bowel disease.

The role of Toll-like receptor expression and signalling in intestinal myofibroblasts, particularly in myofibroblasts derived from patients with stricturing Crohn's ileitis, also warrants further investigation in a larger cohort of patients, particularly as a stricturing phenotype is common to Crohn's disease. Investigation of sustained or diminished Toll-like receptor expression with successive primary cell culture passage would be interesting to undertake. It has been demonstrated that transforming growth factor-β isoforms are consistently expressed during successive passages during myofibroblast culture, but this has not been reported for Toll-like receptors.

Finally, the role of Toll-like receptor signalling in intestinal stem cell regulation is likely to be of great scientific interest over the next few years. Toll-like receptor-mediated regulation of intestinal stem cell function may have implications beyond mucosal inflammation to that of preventing radiation-induced enteritis and to a better understanding of colitis-associated cancer in the future.

References

1. Bray J, Cragg P, Macknight A, Mills R. Lecture notes on human physiology. 4 ed: Blackwell Science Ltd; 1999. 610 p.
2. Podolsky DK. Inflammatory bowel disease. N Engl J Med. 2002;347(6):417-29. Epub 2002/08/09.
3. Loftus EV, Jr. Clinical epidemiology of inflammatory bowel disease: Incidence, prevalence, and environmental influences. Gastroenterology. 2004;126(6):1504-17. Epub 2004/05/29.
4. Probert CS, Brown M. Are there any ethnic groups that are more likely to develop IBD? Inflamm Bowel Dis. 2008;14 Suppl 2:S24-5. Epub 2008/09/26.
5. Hunter MM, McKay DM. Review article: helminths as therapeutic agents for inflammatory bowel disease. Alimentary Pharmacology and Thererapy. 2004;19(2):167-77.
6. Abraham C, Cho JH. Inflammatory bowel disease. N Engl J Med. 2009;361(21):2066-78. Epub 2009/11/20.
7. Bernstein CN, Wajda A, Blanchard JF. The clustering of other chronic inflammatory diseases in inflammatory bowel disease: a population-based study. Gastroenterology. 2005;129(3):827-36. Epub 2005/09/07.
8. Singh S, Graff LA, Bernstein CN. Do NSAIDs, antibiotics, infections, or stress trigger flares in IBD? Am J Gastroenterol. 2009;104(5):1298-313; quiz 314. Epub 2009/04/02.
9. Silverberg MS, Satsangi J, Ahmad T, Arnott ID, Bernstein CN, Brant SR, et al. Toward an integrated clinical, molecular and serological classification of inflammatory bowel disease: Report of a Working Party of the 2005 Montreal World Congress of Gastroenterology. Can J Gastroenterol. 2005;19 Suppl A:5-36. Epub 2005/09/10.
10. Geboes K, van den Oord J, De Wolf-Peeters C, Desmet V, Rutgeerts P, Janssens J, et al. The cellular composition of granulomas in mesenteric lymph nodes from patients with Crohn's disease. Virchows Arch A Pathol Anat Histopathol. 1986;409(5):679-92. Epub 1986/01/01.
11. Quie PG, White JG, Holmes B, Good RA. In vitro bactericidal capacity of human polymorphonuclear leukocytes: diminished activity in chronic granulomatous disease of childhood. J Clin Invest. 1967;46(4):668-79. Epub 1967/04/01.
12. Marks DJ, Harbord MW, MacAllister R, Rahman FZ, Young J, Al-Lazikani B, et al. Defective acute inflammation in Crohn's disease: a clinical investigation. Lancet. 2006;367(9511):668-78. Epub 2006/03/01.
13. Sartor RB. Microbial influences in inflammatory bowel diseases. Gastroenterology. 2008;134(2):577-94. Epub 2008/02/05.
14. Arnott ID, Landers CJ, Nimmo EJ, Drummond HE, Smith BK, Targan SR, et al. Sero-reactivity to microbial components in Crohn's disease is associated with disease severity and progression, but not NOD2/CARD15 genotype. Am J Gastroenterol. 2004;99(12):2376-84. Epub 2004/12/02.
15. Ferrante M, Henckaerts L, Joossens M, Pierik M, Joossens S, Dotan N, et al. New serological markers in inflammatory bowel disease are associated with complicated disease behaviour. Gut. 2007;56(10):1394-403. Epub 2007/04/26.
16. Bossuyt X. Serologic markers in inflammatory bowel disease. Clin Chem. 2006;52(2):171-81. Epub 2005/12/13.
17. Vermeire S, Rutgeerts P. Antibody responses in Crohn's disease. Gastroenterology. 2004;126(2):601-4. Epub 2004/02/06.
18. Targan SR, Landers CJ, Yang H, Lodes MJ, Cong Y, Papadakis KA, et al. Antibodies to CBir1 flagellin define a unique response that is associated independently with complicated Crohn's disease. Gastroenterology. 2005;128(7):2020-8. Epub 2005/06/09.

19. Henckaerts L, Pierik M, Joossens M, Ferrante M, Rutgeerts P, Vermeire S. Mutations in pattern recognition receptor genes modulate seroreactivity to microbial antigens in patients with inflammatory bowel disease. Gut. 2007;56(11):1536-42. Epub 2007/06/28.
20. Seibold F, Brandwein S, Simpson S, Terhorst C, Elson CO. pANCA represents a cross-reactivity to enteric bacterial antigens. J Clin Immunol. 1998;18(2):153-60. Epub 1998/04/09.
21. Terjung B, Soehne J, Lechtenberg B, Gottwein J, Muennich M, Herzog V, et al. p-ANCA in Autoimmune Liver Disorders Recognize Human Beta-Tubulin Isotype 5 and Cross-react with Microbial Protein FtsZ. Gut. 2009. Epub 2009/12/03.
22. Marks DJ, Segal AW. Innate immunity in inflammatory bowel disease: a disease hypothesis. J Pathol. 2008;214(2):260-6. Epub 2007/12/29.
23. Harper PH, Lee EC, Kettlewell MG, Bennett MK, Jewell DP. Role of the faecal stream in the maintenance of Crohn's colitis. Gut. 1985;26(3):279-84. Epub 1985/03/01.
24. Tysk C, Lindberg E, Jarnerot G, Floderus-Myrhed B. Ulcerative colitis and Crohn's disease in an unselected population of monozygotic and dizygotic twins. A study of heritability and the influence of smoking. Gut. 1988;29(7):990-6. Epub 1988/07/01.
25. Cho JH. The genetics and immunopathogenesis of inflammatory bowel disease. Nat Rev Immunol. 2008;8(6):458-66. Epub 2008/05/27.
26. Hugot JP, Chamaillard M, Zouali H, Lesage S, Cezard JP, Belaiche J, et al. Association of NOD2 leucine-rich repeat variants with susceptibility to Crohn's disease. Nature. 2001;411(6837):599-603. Epub 2001/06/01.
27. Ogura Y, Bonen DK, Inohara N, Nicolae DL, Chen FF, Ramos R, et al. A frameshift mutation in NOD2 associated with susceptibility to Crohn's disease. Nature. 2001;411(6837):603-6. Epub 2001/06/01.
28. Economou M, Trikalinos TA, Loizou KT, Tsianos EV, Ioannidis JP. Differential effects of NOD2 variants on Crohn's disease risk and phenotype in diverse populations: a metaanalysis. Am J Gastroenterol. 2004;99(12):2393-404. Epub 2004/12/02.
29. Lesage S, Zouali H, Cezard JP, Colombel JF, Belaiche J, Almer S, et al. CARD15/NOD2 mutational analysis and genotype-phenotype correlation in 612 patients with inflammatory bowel disease. Am J Hum Genet. 2002;70(4):845-57. Epub 2002/03/05.
30. Genome-wide association study of 14,000 cases of seven common diseases and 3,000 shared controls. Nature. 2007;447(7145):661-78. Epub 2007/06/08.
31. Rioux JD, Xavier RJ, Taylor KD, Silverberg MS, Goyette P, Huett A, et al. Genome-wide association study identifies new susceptibility loci for Crohn disease and implicates autophagy in disease pathogenesis. Nat Genet. 2007;39(5):596-604. Epub 2007/04/17.
32. Hampe J, Franke A, Rosenstiel P, Till A, Teuber M, Huse K, et al. A genome-wide association scan of nonsynonymous SNPs identifies a susceptibility variant for Crohn disease in ATG16L1. Nat Genet. 2007;39(2):207-11. Epub 2007/01/04.
33. Xavier RJ, Huett A, Rioux JD. Autophagy as an important process in gut homeostasis and Crohn's disease pathogenesis. Gut. 2008;57(6):717-20. Epub 2008/02/15.
34. Huett A, Xavier RJ. Autophagy at the gut interface: mucosal responses to stress and the consequences for inflammatory bowel diseases. Inflamm Bowel Dis. 2010;16(1):152-74. Epub 2009/07/04.
35. Arbour NC, Lorenz E, Schutte BC, Zabner J, Kline JN, Jones M, et al. TLR4 mutations are associated with endotoxin hyporesponsiveness in humans. Nat Genet. 2000;25(2):187-91. Epub 2000/06/03.
36. Brand S, Staudinger T, Schnitzler F, Pfennig S, Hofbauer K, Dambacher J, et al. The role of Toll-like receptor 4 Asp299Gly and Thr399Ile polymorphisms and CARD15/NOD2 mutations in the susceptibility and phenotype of Crohn's disease. Inflamm Bowel Dis. 2005;11(7):645-52. Epub 2005/06/24.
37. Franchimont D, Vermeire S, El Housni H, Pierik M, Van Steen K, Gustot T, et al. Deficient host-bacteria interactions in inflammatory bowel disease? The toll-like receptor (TLR)-4 Asp299gly

polymorphism is associated with Crohn's disease and ulcerative colitis. Gut. 2004;53(7):987-92. Epub 2004/06/15.
38. Gazouli M, Mantzaris G, Kotsinas A, Zacharatos P, Papalambros E, Archimandritis A, et al. Association between polymorphisms in the Toll-like receptor 4, CD14, and CARD15/NOD2 and inflammatory bowel disease in the Greek population. World J Gastroenterol. 2005;11(5):681-5. Epub 2005/01/19.
39. De Jager PL, Franchimont D, Waliszewska A, Bitton A, Cohen A, Langelier D, et al. The role of the Toll receptor pathway in susceptibility to inflammatory bowel diseases. Genes Immun. 2007;8(5):387-97. Epub 2007/06/01.
40. Gewirtz AT, Vijay-Kumar M, Brant SR, Duerr RH, Nicolae DL, Cho JH. Dominant-negative TLR5 polymorphism reduces adaptive immune response to flagellin and negatively associates with Crohn's disease. Am J Physiol Gastrointest Liver Physiol. 2006;290(6):G1157-63. Epub 2006/01/28.
41. Torok HP, Glas J, Tonenchi L, Bruennler G, Folwaczny M, Folwaczny C. Crohn's disease is associated with a toll-like receptor-9 polymorphism. Gastroenterology. 2004;127(1):365-6. Epub 2004/07/06.
42. Yamazaki K, McGovern D, Ragoussis J, Paolucci M, Butler H, Jewell D, et al. Single nucleotide polymorphisms in TNFSF15 confer susceptibility to Crohn's disease. Hum Mol Genet. 2005;14(22):3499-506. Epub 2005/10/14.
43. McGovern DP, Butler H, Ahmad T, Paolucci M, van Heel DA, Negoro K, et al. TUCAN (CARD8) genetic variants and inflammatory bowel disease. Gastroenterology. 2006;131(4):1190-6. Epub 2006/10/13.
44. Muise AM, Walters TD, Glowacka WK, Griffiths AM, Ngan BY, Lan H, et al. Polymorphisms in E-cadherin (CDH1) result in a mis-localised cytoplasmic protein that is associated with Crohn's disease. Gut. 2009;58(8):1121-7. Epub 2009/04/29.
45. Delves PJ, Roitt IM. The immune system. Second of two parts. N Engl J Med. 2000;343(2):108-17. Epub 2000/07/13.
46. Brand S. Crohn's disease: Th1, Th17 or both? The change of a paradigm: new immunological and genetic insights implicate Th17 cells in the pathogenesis of Crohn's disease. Gut. 2009;58(8):1152-67. Epub 2009/07/14.
47. Iwakura Y, Ishigame H. The IL-23/IL-17 axis in inflammation. J Clin Invest. 2006;116(5):1218-22. Epub 2006/05/04.
48. Fujino S, Andoh A, Bamba S, Ogawa A, Hata K, Araki Y, et al. Increased expression of interleukin 17 in inflammatory bowel disease. Gut. 2003;52(1):65-70. Epub 2002/12/13.
49. Duerr RH, Taylor KD, Brant SR, Rioux JD, Silverberg MS, Daly MJ, et al. A genome-wide association study identifies IL23R as an inflammatory bowel disease gene. Science. 2006;314(5804):1461-3. Epub 2006/10/28.
50. Tremelling M, Cummings F, Fisher SA, Mansfield J, Gwilliam R, Keniry A, et al. IL23R variation determines susceptibility but not disease phenotype in inflammatory bowel disease. Gastroenterology. 2007;132(5):1657-64. Epub 2007/05/09.
51. Barrett JC, Hansoul S, Nicolae DL, Cho JH, Duerr RH, Rioux JD, et al. Genome-wide association defines more than 30 distinct susceptibility loci for Crohn's disease. Nat Genet. 2008;40(8):955-62. Epub 2008/07/01.
52. Fisher SA, Tremelling M, Anderson CA, Gwilliam R, Bumpstead S, Prescott NJ, et al. Genetic determinants of ulcerative colitis include the ECM1 locus and five loci implicated in Crohn's disease. Nat Genet. 2008;40(6):710-2. Epub 2008/04/29.
53. Franke A, Balschun T, Karlsen TH, Hedderich J, May S, Lu T, et al. Replication of signals from recent studies of Crohn's disease identifies previously unknown disease loci for ulcerative colitis. Nat Genet. 2008;40(6):713-5. Epub 2008/04/29.
54. Mannon PJ, Fuss IJ, Mayer L, Elson CO, Sandborn WJ, Present D, et al. Anti-interleukin-12 antibody for active Crohn's disease. N Engl J Med. 2004;351(20):2069-79. Epub 2004/11/13.

55. Elson CO, Cong Y, Weaver CT, Schoeb TR, McClanahan TK, Fick RB, et al. Monoclonal anti-interleukin 23 reverses active colitis in a T cell-mediated model in mice. Gastroenterology. 2007;132(7):2359-70. Epub 2007/06/16.
56. Fellermann K, Stange DE, Schaeffeler E, Schmalzl H, Wehkamp J, Bevins CL, et al. A chromosome 8 gene-cluster polymorphism with low human beta-defensin 2 gene copy number predisposes to Crohn disease of the colon. Am J Hum Genet. 2006;79(3):439-48. Epub 2006/08/16.
57. Griga T, Wilkens C, Schmiegel W, Folwaczny C, Hagedorn M, Duerig N, et al. Association between the promoter polymorphism T/C at position -159 of the CD14 gene and anti-inflammatory therapy in patients with inflammatory bowel disease. Eur J Med Res. 2005;10(5):183-6. Epub 2005/06/11.
58. Klein W, Tromm A, Griga T, Folwaczny C, Hocke M, Eitner K, et al. Interaction of polymorphisms in the CARD15 and CD14 genes in patients with Crohn disease. Scand J Gastroenterol. 2003;38(8):834-6. Epub 2003/08/28.
59. McGovern DP, Hysi P, Ahmad T, van Heel DA, Moffatt MF, Carey A, et al. Association between a complex insertion/deletion polymorphism in NOD1 (CARD4) and susceptibility to inflammatory bowel disease. Hum Mol Genet. 2005;14(10):1245-50. Epub 2005/03/26.
60. Ho GT, Soranzo N, Nimmo ER, Tenesa A, Goldstein DB, Satsangi J. ABCB1/MDR1 gene determines susceptibility and phenotype in ulcerative colitis: discrimination of critical variants using a gene-wide haplotype tagging approach. Hum Mol Genet. 2006;15(5):797-805. Epub 2006/01/26.
61. Pierik M, Joossens S, Van Steen K, Van Schuerbeek N, Vlietinck R, Rutgeerts P, et al. Toll-like receptor-1, -2, and -6 polymorphisms influence disease extension in inflammatory bowel diseases. Inflamm Bowel Dis. 2006;12(1):1-8. Epub 2005/12/24.
62. Rioux JD, Daly MJ, Silverberg MS, Lindblad K, Steinhart H, Cohen Z, et al. Genetic variation in the 5q31 cytokine gene cluster confers susceptibility to Crohn disease. Nat Genet. 2001;29(2):223-8. Epub 2001/10/05.
63. Peltekova VD, Wintle RF, Rubin LA, Amos CI, Huang Q, Gu X, et al. Functional variants of OCTN cation transporter genes are associated with Crohn disease. Nat Genet. 2004;36(5):471-5. Epub 2004/04/27.
64. Waller S, Tremelling M, Bredin F, Godfrey L, Howson J, Parkes M. Evidence for association of OCTN genes and IBD5 with ulcerative colitis. Gut. 2006;55(6):809-14. Epub 2005/12/20.
65. Russell RK, Drummond HE, Nimmo ER, Anderson NH, Noble CL, Wilson DC, et al. Analysis of the influence of OCTN1/2 variants within the IBD5 locus on disease susceptibility and growth indices in early onset inflammatory bowel disease. Gut. 2006;55(8):1114-23. Epub 2006/02/14.
66. Libioulle C, Louis E, Hansoul S, Sandor C, Farnir F, Franchimont D, et al. Novel Crohn disease locus identified by genome-wide association maps to a gene desert on 5p13.1 and modulates expression of PTGER4. PLoS Genet. 2007;3(4):e58. Epub 2007/04/24.
67. Louis E, Libioulle C, Reenaers C, Belaiche J, Georges M. Genetics of ulcerative colitis: the come-back of interleukin 10. Gut. 2009;58(9):1173-6. Epub 2009/08/13.
68. Kuhn R, Lohler J, Rennick D, Rajewsky K, Muller W. Interleukin-10-deficient mice develop chronic enterocolitis. Cell. 1993;75(2):263-74. Epub 1993/10/22.
69. Sellon RK, Tonkonogy S, Schultz M, Dieleman LA, Grenther W, Balish E, et al. Resident enteric bacteria are necessary for development of spontaneous colitis and immune system activation in interleukin-10-deficient mice. Infect Immun. 1998;66(11):5224-31. Epub 1998/10/24.
70. Ruiz PA, Shkoda A, Kim SC, Sartor RB, Haller D. IL-10 gene-deficient mice lack TGF-beta/Smad signaling and fail to inhibit proinflammatory gene expression in intestinal epithelial cells after the colonization with colitogenic Enterococcus faecalis. J Immunol. 2005;174(5):2990-9. Epub 2005/02/25.
71. Matsuda R, Koide T, Tokoro C, Yamamoto T, Godai T, Morohashi T, et al. Quantitive cytokine mRNA expression profiles in the colonic mucosa of patients with steroid naive ulcerative colitis during active and quiescent disease. Inflamm Bowel Dis. 2009;15(3):328-34. Epub 2008/10/24.

72. Colombel JF, Rutgeerts P, Malchow H, Jacyna M, Nielsen OH, Rask-Madsen J, et al. Interleukin 10 (Tenovil) in the prevention of postoperative recurrence of Crohn's disease. Gut. 2001;49(1):42-6. Epub 2001/06/20.
73. Schreiber S, Fedorak RN, Nielsen OH, Wild G, Williams CN, Nikolaus S, et al. Safety and efficacy of recombinant human interleukin 10 in chronic active Crohn's disease. Crohn's Disease IL-10 Cooperative Study Group. Gastroenterology. 2000;119(6):1461-72. Epub 2000/12/13.
74. Murphy KT, Paul; Walport, Mark. Janeway's Immunobiology. 7th ed: Garland Science; 2008. 887 p.
75. Turner JR. Intestinal mucosal barrier function in health and disease. Nat Rev Immunol. 2009;9(11):799-809. Epub 2009/10/27.
76. Delves PJ, Roitt IM. The immune system. First of two parts. N Engl J Med. 2000;343(1):37-49. Epub 2000/07/07.
77. Spits H, Di Santo JP. The expanding family of innate lymphoid cells: regulators and effectors of immunity and tissue remodeling. Nature Immunology. 2011;12(1):21-7.
78. Mowat AM. Anatomical basis of tolerance and immunity to intestinal antigens. Nat Rev Immunol. 2003;3(4):331-41. Epub 2003/04/02.
79. Sun JB, Czerkinsky C, Holmgren J. Mucosally induced immunological tolerance, regulatory T cells and the adjuvant effect by cholera toxin B subunit. Scand J Immunol. 2010;71(1):1-11. Epub 2009/12/19.
80. Iwasaki A, Medzhitov R. Regulation of adaptive immunity by the innate immune system. Science. 2010;327(5963):291-5. Epub 2010/01/16.
81. Gay NJ, Keith FJ. Drosophila Toll and IL-1 receptor. Nature. 1991;351(6325):355-6. Epub 1991/05/30.
82. Testro AG, Visvanathan K. Toll-like receptors and their role in gastrointestinal disease. J Gastroenterol Hepatol. 2009;24(6):943-54. Epub 2009/07/30.
83. Fukata M, Vamadevan AS, Abreu MT. Toll-like receptors (TLRs) and Nod-like receptors (NLRs) in inflammatory disorders. Semin Immunol. 2009;21(4):242-53. Epub 2009/09/15.
84. Kopp E, Medzhitov R, Carothers J, Xiao C, Douglas I, Janeway CA, et al. ECSIT is an evolutionarily conserved intermediate in the Toll/IL-1 signal transduction pathway. Genes Dev. 1999;13(16):2059-71. Epub 1999/08/31.
85. O'Neill LA, Bowie AG. The family of five: TIR-domain-containing adaptors in Toll-like receptor signalling. Nat Rev Immunol. 2007;7(5):353-64. Epub 2007/04/26.
86. Cell Signaling Technology. Toll-like receptor pathway. Cell Signaling Technology; 2009 [cited 2010 20th July]; Available from: http://www.cellsignal.com/reference/pathway/Toll_Like.html.
87. Liew FY, Xu D, Brint EK, O'Neill LA. Negative regulation of toll-like receptor-mediated immune responses. Nat Rev Immunol. 2005;5(6):446-58. Epub 2005/06/02.
88. Wald D, Qin J, Zhao Z, Qian Y, Naramura M, Tian L, et al. SIGIRR, a negative regulator of Toll-like receptor-interleukin 1 receptor signaling. Nat Immunol. 2003;4(9):920-7. Epub 2003/08/20.
89. Abreu MT, Vora P, Faure E, Thomas LS, Arnold ET, Arditi M. Decreased expression of Toll-like receptor-4 and MD-2 correlates with intestinal epithelial cell protection against dysregulated proinflammatory gene expression in response to bacterial lipopolysaccharide. J Immunol. 2001;167(3):1609-16. Epub 2001/07/24.
90. Ley RE, Peterson DA, Gordon JI. Ecological and evolutionary forces shaping microbial diversity in the human intestine. Cell. 2006;124(4):837-48. Epub 2006/02/25.
91. Gill SR, Pop M, Deboy RT, Eckburg PB, Turnbaugh PJ, Samuel BS, et al. Metagenomic analysis of the human distal gut microbiome. Science. 2006;312(5778):1355-9. Epub 2006/06/03.
92. Van der Sluis M, De Koning BA, De Bruijn AC, Velcich A, Meijerink JP, Van Goudoever JB, et al. Muc2-deficient mice spontaneously develop colitis, indicating that MUC2 is critical for colonic protection. Gastroenterology. 2006;131(1):117-29. Epub 2006/07/13.

93. Suenaert P, Bulteel V, Lemmens L, Noman M, Geypens B, Van Assche G, et al. Anti-tumor necrosis factor treatment restores the gut barrier in Crohn's disease. Am J Gastroenterol. 2002;97(8):2000-4. Epub 2002/08/23.
94. Blair SA, Kane SV, Clayburgh DR, Turner JR. Epithelial myosin light chain kinase expression and activity are upregulated in inflammatory bowel disease. Lab Invest. 2006;86(2):191-201. Epub 2006/01/13.
95. Hollander D, Vadheim CM, Brettholz E, Petersen GM, Delahunty T, Rotter JI. Increased intestinal permeability in patients with Crohn's disease and their relatives. A possible etiologic factor. Ann Intern Med. 1986;105(6):883-5. Epub 1986/12/01.
96. Buhner S, Buning C, Genschel J, Kling K, Herrmann D, Dignass A, et al. Genetic basis for increased intestinal permeability in families with Crohn's disease: role of CARD15 3020insC mutation? Gut. 2006;55(3):342-7. Epub 2005/07/08.
97. Wyatt J, Vogelsang H, Hubl W, Waldhoer T, Lochs H. Intestinal permeability and the prediction of relapse in Crohn's disease. Lancet. 1993;341(8858):1437-9. Epub 1993/06/05.
98. Artis D. Epithelial-cell recognition of commensal bacteria and maintenance of immune homeostasis in the gut. Nat Rev Immunol. 2008;8(6):411-20. Epub 2008/05/13.
99. Cebra JJ. Influences of microbiota on intestinal immune system development. Am J Clin Nutr. 1999;69(5):1046S-51S. Epub 1999/05/08.
100. Mazmanian SK, Liu CH, Tzianabos AO, Kasper DL. An immunomodulatory molecule of symbiotic bacteria directs maturation of the host immune system. Cell. 2005;122(1):107-18. Epub 2005/07/13.
101. Egan LJ, Eckmann L, Greten FR, Chae S, Li ZW, Myhre GM, et al. IkappaB-kinasebeta-dependent NF-kappaB activation provides radioprotection to the intestinal epithelium. Proc Natl Acad Sci U S A. 2004;101(8):2452-7. Epub 2004/02/26.
102. Chen LW, Egan L, Li ZW, Greten FR, Kagnoff MF, Karin M. The two faces of IKK and NF-kappaB inhibition: prevention of systemic inflammation but increased local injury following intestinal ischemia-reperfusion. Nat Med. 2003;9(5):575-81. Epub 2003/04/15.
103. Nenci A, Becker C, Wullaert A, Gareus R, van Loo G, Danese S, et al. Epithelial NEMO links innate immunity to chronic intestinal inflammation. Nature. 2007;446(7135):557-61. Epub 2007/03/16.
104. Kullberg BJ, Ferwerda G, de Jong DJ, Drenth JP, Joosten LA, Van der Meer JW, et al. Crohn's disease patients homozygous for the 3020insC NOD2 mutation have a defective NOD2/TLR4 cross-tolerance to intestinal stimuli. Immunology. 2008;123(4):600-5. Epub 2007/11/22.
105. Hedl M, Li J, Cho JH, Abraham C. Chronic stimulation of Nod2 mediates tolerance to bacterial products. Proc Natl Acad Sci U S A. 2007;104(49):19440-5. Epub 2007/11/23.
106. Yang Z, Fuss IJ, Watanabe T, Asano N, Davey MP, Rosenbaum JT, et al. NOD2 transgenic mice exhibit enhanced MDP-mediated down-regulation of TLR2 responses and resistance to colitis induction. Gastroenterology. 2007;133(5):1510-21. Epub 2007/10/05.
107. Cunliffe RN, Mahida YR. Expression and regulation of antimicrobial peptides in the gastrointestinal tract. J Leukoc Biol. 2004;75(1):49-58. Epub 2003/10/04.
108. Elphick DA, Mahida YR. Paneth cells: their role in innate immunity and inflammatory disease. Gut. 2005;54(12):1802-9. Epub 2005/11/15.
109. Nuding S, Fellermann K, Wehkamp J, Stange EF. Reduced mucosal antimicrobial activity in Crohn's disease of the colon. Gut. 2007;56(9):1240-7. Epub 2007/04/26.
110. Elphick D, Liddell S, Mahida YR. Impaired luminal processing of human defensin-5 in Crohn's disease: persistence in a complex with chymotrypsinogen and trypsin. Am J Pathol. 2008;172(3):702-13. Epub 2008/02/09.
111. Wehkamp J, Salzman NH, Porter E, Nuding S, Weichenthal M, Petras RE, et al. Reduced Paneth cell alpha-defensins in ileal Crohn's disease. Proc Natl Acad Sci U S A. 2005;102(50):18129-34. Epub 2005/12/07.

112. Wehkamp J, Harder J, Weichenthal M, Schwab M, Schaffeler E, Schlee M, et al. NOD2 (CARD15) mutations in Crohn's disease are associated with diminished mucosal alpha-defensin expression. Gut. 2004;53(11):1658-64. Epub 2004/10/14.
113. Simms LA, Doecke JD, Walsh MD, Huang N, Fowler EV, Radford-Smith GL. Reduced alpha-defensin expression is associated with inflammation and not NOD2 mutation status in ileal Crohn's disease. Gut. 2008;57(7):903-10. Epub 2008/02/29.
114. Corr SC, Gahan CC, Hill C. M-cells: origin, morphology and role in mucosal immunity and microbial pathogenesis. FEMS Immunol Med Microbiol. 2008;52(1):2-12. Epub 2007/12/18.
115. Chabot S, Wagner JS, Farrant S, Neutra MR. TLRs regulate the gatekeeping functions of the intestinal follicle-associated epithelium. J Immunol. 2006;176(7):4275-83. Epub 2006/03/21.
116. Neal MD, Leaphart C, Levy R, Prince J, Billiar TR, Watkins S, et al. Enterocyte TLR4 mediates phagocytosis and translocation of bacteria across the intestinal barrier. J Immunol. 2006;176(5):3070-9. Epub 2006/02/24.
117. Mayer L, Eisenhardt D, Salomon P, Bauer W, Plous R, Piccinini L. Expression of class II molecules on intestinal epithelial cells in humans. Differences between normal and inflammatory bowel disease. Gastroenterology. 1991;100(1):3-12. Epub 1991/01/01.
118. Bloom S, Simmons D, Jewell DP. Adhesion molecules intercellular adhesion molecule-1 (ICAM-1), ICAM-3 and B7 are not expressed by epithelium in normal or inflamed colon. Clin Exp Immunol. 1995;101(1):157-63. Epub 1995/07/01.
119. Nakazawa A, Dotan I, Brimnes J, Allez M, Shao L, Tsushima F, et al. The expression and function of costimulatory molecules B7H and B7-H1 on colonic epithelial cells. Gastroenterology. 2004;126(5):1347-57. Epub 2004/05/08.
120. Dotan I, Allez M, Nakazawa A, Brimnes J, Schulder-Katz M, Mayer L. Intestinal epithelial cells from inflammatory bowel disease patients preferentially stimulate CD4+ T cells to proliferate and secrete interferon-gamma. Am J Physiol Gastrointest Liver Physiol. 2007;292(6):G1630-40. Epub 2007/03/10.
121. Saemann MD, Bohmig GA, Osterreicher CH, Burtscher H, Parolini O, Diakos C, et al. Anti-inflammatory effects of sodium butyrate on human monocytes: potent inhibition of IL-12 and up-regulation of IL-10 production. FASEB J. 2000;14(15):2380-2. Epub 2000/10/12.
122. Bocker U, Yezerskyy O, Feick P, Manigold T, Panja A, Kalina U, et al. Responsiveness of intestinal epithelial cell lines to lipopolysaccharide is correlated with Toll-like receptor 4 but not Toll-like receptor 2 or CD14 expression. Int J Colorectal Dis. 2003;18(1):25-32. Epub 2002/11/30.
123. Macpherson AJ, Uhr T. Induction of protective IgA by intestinal dendritic cells carrying commensal bacteria. Science. 2004;303(5664):1662-5. Epub 2004/03/16.
124. Rescigno M, Di Sabatino A. Dendritic cells in intestinal homeostasis and disease. J Clin Invest. 2009;119(9):2441-50. Epub 2009/09/05.
125. Coombes JL, Powrie F. Dendritic cells in intestinal immune regulation. Nat Rev Immunol. 2008;8(6):435-46. Epub 2008/05/27.
126. Zaph C, Troy AE, Taylor BC, Berman-Booty LD, Guild KJ, Du Y, et al. Epithelial-cell-intrinsic IKK-beta expression regulates intestinal immune homeostasis. Nature. 2007;446(7135):552-6. Epub 2007/02/27.
127. Watanabe N, Hanabuchi S, Soumelis V, Yuan W, Ho S, de Waal Malefyt R, et al. Human thymic stromal lymphopoietin promotes dendritic cell-mediated CD4+ T cell homeostatic expansion. Nat Immunol. 2004;5(4):426-34. Epub 2004/03/03.
128. Watanabe N, Wang YH, Lee HK, Ito T, Cao W, Liu YJ. Hassall's corpuscles instruct dendritic cells to induce CD4+CD25+ regulatory T cells in human thymus. Nature. 2005;436(7054):1181-5. Epub 2005/08/27.
129. Taylor BC, Zaph C, Troy AE, Du Y, Guild KJ, Comeau MR, et al. TSLP regulates intestinal immunity and inflammation in mouse models of helminth infection and colitis. J Exp Med. 2009;206(3):655-67. Epub 2009/03/11.

130. Tanaka J, Saga K, Kido M, Nishiura H, Akamatsu T, Chiba T, et al. Proinflammatory Th2 Cytokines Induce Production of Thymic Stromal Lymphopoietin in Human Colonic Epithelial Cells. Dig Dis Sci. 2009. Epub 2009/09/17.
131. Rimoldi M, Chieppa M, Salucci V, Avogadri F, Sonzogni A, Sampietro GM, et al. Intestinal immune homeostasis is regulated by the crosstalk between epithelial cells and dendritic cells. Nat Immunol. 2005;6(5):507-14. Epub 2005/04/12.
132. Iliev ID, Spadoni I, Mileti E, Matteoli G, Sonzogni A, Sampietro GM, et al. Human intestinal epithelial cells promote the differentiation of tolerogenic dendritic cells. Gut. 2009;58(11):1481-9. Epub 2009/07/03.
133. Hart AL, Al-Hassi HO, Rigby RJ, Bell SJ, Emmanuel AV, Knight SC, et al. Characteristics of intestinal dendritic cells in inflammatory bowel diseases. Gastroenterology. 2005;129(1):50-65. Epub 2005/07/14.
134. Smythies LE, Sellers M, Clements RH, Mosteller-Barnum M, Meng G, Benjamin WH, et al. Human intestinal macrophages display profound inflammatory anergy despite avid phagocytic and bacteriocidal activity. J Clin Invest. 2005;115(1):66-75. Epub 2005/01/05.
135. Fujita S, Seino K, Sato K, Sato Y, Eizumi K, Yamashita N, et al. Regulatory dendritic cells act as regulators of acute lethal systemic inflammatory response. Blood. 2006;107(9):3656-64. Epub 2006/01/18.
136. Iliev ID, Mileti E, Matteoli G, Chieppa M, Rescigno M. Intestinal epithelial cells promote colitis-protective regulatory T-cell differentiation through dendritic cell conditioning. Mucosal Immunol. 2009;2(4):340-50. Epub 2009/04/24.
137. Matteoli G, Mazzini E, Iliev ID, Mileti E, Fallarino F, Puccetti P, et al. Gut CD103+ dendritic cells express indoleamine 2,3-dioxygenase which influences T regulatory/T effector cell balance and oral tolerance induction. Gut. 2010;59(5):595-604. Epub 2010/04/30.
138. Iwata M, Hirakiyama A, Eshima Y, Kagechika H, Kato C, Song SY. Retinoic acid imprints gut-homing specificity on T cells. Immunity. 2004;21(4):527-38. Epub 2004/10/16.
139. Kang SG, Lim HW, Andrisani OM, Broxmeyer HE, Kim CH. Vitamin A metabolites induce gut-homing FoxP3+ regulatory T cells. J Immunol. 2007;179(6):3724-33. Epub 2007/09/06.
140. Coombes JL, Siddiqui KR, Arancibia-Carcamo CV, Hall J, Sun CM, Belkaid Y, et al. A functionally specialized population of mucosal CD103+ DCs induces Foxp3+ regulatory T cells via a TGF-beta and retinoic acid-dependent mechanism. J Exp Med. 2007;204(8):1757-64. Epub 2007/07/11.
141. Sun CM, Hall JA, Blank RB, Bouladoux N, Oukka M, Mora JR, et al. Small intestine lamina propria dendritic cells promote de novo generation of Foxp3 T reg cells via retinoic acid. J Exp Med. 2007;204(8):1775-85. Epub 2007/07/11.
142. Mileti E, Matteoli G, Iliev ID, Rescigno M. Comparison of the immunomodulatory properties of three probiotic strains of Lactobacilli using complex culture systems: prediction for in vivo efficacy. PLoS One. 2009;4(9):e7056. Epub 2009/09/17.
143. te Velde AA, van Kooyk Y, Braat H, Hommes DW, Dellemijn TA, Slors JF, et al. Increased expression of DC-SIGN+IL-12+IL-18+ and CD83+IL-12-IL-18- dendritic cell populations in the colonic mucosa of patients with Crohn's disease. Eur J Immunol. 2003;33(1):143-51. Epub 2003/02/21.
144. de Baey A, Mende I, Baretton G, Greiner A, Hartl WH, Baeuerle PA, et al. A subset of human dendritic cells in the T cell area of mucosa-associated lymphoid tissue with a high potential to produce TNF-alpha. J Immunol. 2003;170(10):5089-94. Epub 2003/05/08.
145. van Beelen AJ, Zelinkova Z, Taanman-Kueter EW, Muller FJ, Hommes DW, Zaat SA, et al. Stimulation of the intracellular bacterial sensor NOD2 programs dendritic cells to promote interleukin-17 production in human memory T cells. Immunity. 2007;27(4):660-9. Epub 2007/10/09.
146. Yeung MM, Melgar S, Baranov V, Oberg A, Danielsson A, Hammarstrom S, et al. Characterisation of mucosal lymphoid aggregates in ulcerative colitis: immune cell phenotype and TcR-gammadelta expression. Gut. 2000;47(2):215-27. Epub 2000/07/18.

147. Ikeda Y, Akbar F, Matsui H, Onji M. Characterization of antigen-presenting dendritic cells in the peripheral blood and colonic mucosa of patients with ulcerative colitis. Eur J Gastroenterol Hepatol. 2001;13(7):841-50. Epub 2001/07/28.
148. Mahida YR, Wu KC, Jewell DP. Characterization of antigen-presenting activity of intestinal mononuclear cells isolated from normal and inflammatory bowel disease colon and ileum. Immunology. 1988;65(4):543-9. Epub 1988/12/01.
149. Foligne B, Zoumpopoulou G, Dewulf J, Ben Younes A, Chareyre F, Sirard JC, et al. A key role of dendritic cells in probiotic functionality. PLoS One. 2007;2(3):e313. Epub 2007/03/22.
150. Hershberg RM, Cho DH, Youakim A, Bradley MB, Lee JS, Framson PE, et al. Highly polarized HLA class II antigen processing and presentation by human intestinal epithelial cells. J Clin Invest. 1998;102(4):792-803. Epub 1998/08/26.
151. Buning J, Hundorfean G, Schmitz M, Zimmer KP, Strobel S, Gebert A, et al. Antigen targeting to MHC class II-enriched late endosomes in colonic epithelial cells: trafficking of luminal antigens studied in vivo in Crohn's colitis patients. FASEB J. 2006;20(2):359-61. Epub 2005/12/24.
152. Allez M, Brimnes J, Dotan I, Mayer L. Expansion of CD8+ T cells with regulatory function after interaction with intestinal epithelial cells. Gastroenterology. 2002;123(5):1516-26. Epub 2002/10/31.
153. Brimnes J, Allez M, Dotan I, Shao L, Nakazawa A, Mayer L. Defects in CD8+ regulatory T cells in the lamina propria of patients with inflammatory bowel disease. J Immunol. 2005;174(9):5814-22. Epub 2005/04/22.
154. Abreu MT, Arnold ET, Thomas LS, Gonsky R, Zhou Y, Hu B, et al. TLR4 and MD-2 expression is regulated by immune-mediated signals in human intestinal epithelial cells. J Biol Chem. 2002;277(23):20431-7. Epub 2002/03/30.
155. Mueller T, Terada T, Rosenberg IM, Shibolet O, Podolsky DK. Th2 cytokines down-regulate TLR expression and function in human intestinal epithelial cells. J Immunol. 2006;176(10):5805-14. Epub 2006/05/04.
156. Strober W, Fuss IJ, Blumberg RS. The immunology of mucosal models of inflammation. Annu Rev Immunol. 2002;20:495-549. Epub 2002/02/28.
157. Xavier RJ, Podolsky DK. Unravelling the pathogenesis of inflammatory bowel disease. Nature. 2007;448(7152):427-34. Epub 2007/07/27.
158. Rakoff-Nahoum S, Paglino J, Eslami-Varzaneh F, Edberg S, Medzhitov R. Recognition of commensal microflora by toll-like receptors is required for intestinal homeostasis. Cell. 2004;118(2):229-41. Epub 2004/07/21.
159. Cario E. Therapeutic impact of toll-like receptors on inflammatory bowel diseases: a multiple-edged sword. Inflamm Bowel Dis. 2008;14(3):411-21. Epub 2007/10/18.
160. Riehl T, Cohn S, Tessner T, Schloemann S, Stenson WF. Lipopolysaccharide is radioprotective in the mouse intestine through a prostaglandin-mediated mechanism. Gastroenterology. 2000;118(6):1106-16. Epub 2000/06/02.
161. Burdelya LG, Krivokrysenko VI, Tallant TC, Strom E, Gleiberman AS, Gupta D, et al. An agonist of toll-like receptor 5 has radioprotective activity in mouse and primate models. Science. 2008;320(5873):226-30. Epub 2008/04/12.
162. Cario E, Gerken G, Podolsky DK. Toll-like receptor 2 enhances ZO-1-associated intestinal epithelial barrier integrity via protein kinase C. Gastroenterology. 2004;127(1):224-38. Epub 2004/07/06.
163. Cario E, Gerken G, Podolsky DK. Toll-like receptor 2 controls mucosal inflammation by regulating epithelial barrier function. Gastroenterology. 2007;132(4):1359-74. Epub 2007/04/06.
164. Fort MM, Mozaffarian A, Stover AG, Correia Jda S, Johnson DA, Crane RT, et al. A synthetic TLR4 antagonist has anti-inflammatory effects in two murine models of inflammatory bowel disease. J Immunol. 2005;174(10):6416-23. Epub 2005/05/10.
165. Ungaro R, Fukata M, Hsu D, Hernandez Y, Breglio K, Chen A, et al. A novel Toll-like receptor 4 antagonist antibody ameliorates inflammation but impairs mucosal healing in murine colitis. Am J Physiol Gastrointest Liver Physiol. 2009;296(6):G1167-79. Epub 2009/04/11.

166. Andoh A, Bamba S, Brittan M, Fujiyama Y, Wright NA. Role of intestinal subepithelial myofibroblasts in inflammation and regenerative response in the gut. Pharmacol Ther. 2007;114(1):94-106. Epub 2007/03/03.
167. Mahida YR, Beltinger J, Makh S, Goke M, Gray T, Podolsky DK, et al. Adult human colonic subepithelial myofibroblasts express extracellular matrix proteins and cyclooxygenase-1 and -2. Am J Physiol. 1997;273(6 Pt 1):G1341-8. Epub 1998/01/22.
168. Kohnen G, Kertschanska S, Demir R, Kaufmann P. Placental villous stroma as a model system for myofibroblast differentiation. Histochemistry and cell biology. 1996;105(6):415-29. Epub 1996/06/01.
169. Valentich JD, Popov V, Saada JI, Powell DW. Phenotypic characterization of an intestinal subepithelial myofibroblast cell line. Am J Physiol. 1997;272(5 Pt 1):C1513-24. Epub 1997/05/01.
170. Hynes RO. The extracellular matrix: not just pretty fibrils. Science. 2009;326(5957):1216-9. Epub 2009/12/08.
171. Mahida YR, Galvin AM, Gray T, Makh S, McAlindon ME, Sewell HF, et al. Migration of human intestinal lamina propria lymphocytes, macrophages and eosinophils following the loss of surface epithelial cells. Clin Exp Immunol. 1997;109(2):377-86. Epub 1997/08/01.
172. Strater J, Wedding U, Barth TF, Koretz K, Elsing C, Moller P. Rapid onset of apoptosis in vitro follows disruption of beta 1-integrin/matrix interactions in human colonic crypt cells. Gastroenterology. 1996;110(6):1776-84. Epub 1996/06/01.
173. Scoville DH, Sato T, He XC, Li L. Current view: intestinal stem cells and signaling. Gastroenterology. 2008;134(3):849-64. Epub 2008/03/08.
174. Wang P, Hou SX. Regulation of intestinal stem cells in mammals and Drosophila. J Cell Physiol. 2010;222(1):33-7. Epub 2009/09/10.
175. He XC, Zhang J, Tong WG, Tawfik O, Ross J, Scoville DH, et al. BMP signaling inhibits intestinal stem cell self-renewal through suppression of Wnt-beta-catenin signaling. Nat Genet. 2004;36(10):1117-21. Epub 2004/09/21.
176. Kosinski C, Li VS, Chan AS, Zhang J, Ho C, Tsui WY, et al. Gene expression patterns of human colon tops and basal crypts and BMP antagonists as intestinal stem cell niche factors. Proc Natl Acad Sci U S A. 2007;104(39):15418-23. Epub 2007/09/21.
177. Andoh A, Bamba S, Fujiyama Y, Brittan M, Wright NA. Colonic subepithelial myofibroblasts in mucosal inflammation and repair: contribution of bone marrow-derived stem cells to the gut regenerative response. J Gastroenterol. 2005;40(12):1089-99. Epub 2005/12/27.
178. Hughes KR, Sablitzky F, Mahida YR. Expression profiling of Wnt family of genes in normal and inflammatory bowel disease primary human intestinal myofibroblasts and normal human colonic crypt epithelial cells. Inflamm Bowel Dis. 2011;17(1):213-20. Epub 2010/09/18.
179. Rieder F, Fiocchi C. Intestinal fibrosis in inflammatory bowel disease - Current knowledge and future perspectives. J Crohns Colitis. 2008;2(4):279-90. Epub 2008/12/01.
180. Brittan M, Chance V, Elia G, Poulsom R, Alison MR, MacDonald TT, et al. A regenerative role for bone marrow following experimental colitis: contribution to neovasculogenesis and myofibroblasts. Gastroenterology. 2005;128(7):1984-95. Epub 2005/06/09.
181. Cosnes J, Cattan S, Blain A, Beaugerie L, Carbonnel F, Parc R, et al. Long-term evolution of disease behavior of Crohn's disease. Inflamm Bowel Dis. 2002;8(4):244-50. Epub 2002/07/20.
182. Otte JM, Rosenberg IM, Podolsky DK. Intestinal myofibroblasts in innate immune responses of the intestine. Gastroenterology. 2003;124(7):1866-78. Epub 2003/06/14.
183. Zhang Z, Andoh A, Inatomi O, Bamba S, Takayanagi A, Shimizu N, et al. Interleukin-17 and lipopolysaccharides synergistically induce cyclooxygenase-2 expression in human intestinal myofibroblasts. J Gastroenterol Hepatol. 2005;20(4):619-27. Epub 2005/04/20.
184. Kanazawa S, Tsunoda T, Onuma E, Majima T, Kagiyama M, Kikuchi K. VEGF, basic-FGF, and TGF-beta in Crohn's disease and ulcerative colitis: a novel mechanism of chronic intestinal inflammation. Am J Gastroenterol. 2001;96(3):822-8. Epub 2001/03/31.

185. Zhang Z, Andoh A, Yasui H, Inatomi O, Hata K, Tsujikawa T, et al. Interleukin-1beta and tumor necrosis factor-alpha upregulate interleukin-23 subunit p19 gene expression in human colonic subepithelial myofibroblasts. International journal of molecular medicine. 2005;15(1):79-83. Epub 2004/12/08.
186. Hata K, Andoh A, Shimada M, Fujino S, Bamba S, Araki Y, et al. IL-17 stimulates inflammatory responses via NF-kappaB and MAP kinase pathways in human colonic myofibroblasts. Am J Physiol Gastrointest Liver Physiol. 2002;282(6):G1035-44. Epub 2002/05/23.
187. Yen TH, Wright NA. The gastrointestinal tract stem cell niche. Stem Cell Rev. 2006;2(3):203-12. Epub 2007/07/13.
188. Schofield R. The relationship between the spleen colony-forming cell and the haemopoietic stem cell. Blood cells. 1978;4(1-2):7-25. Epub 1978/01/01.
189. Danese S. Nonimmune cells in inflammatory bowel disease: from victim to villain. Trends Immunol. 2008;29(11):555-64. Epub 2008/10/08.
190. Potten CS, Loeffler M. Stem cells: attributes, cycles, spirals, pitfalls and uncertainties. Lessons for and from the crypt. Development. 1990;110(4):1001-20. Epub 1990/12/01.
191. Bjerknes M, Cheng H. The stem-cell zone of the small intestinal epithelium. I. Evidence from Paneth cells in the adult mouse. The American journal of anatomy. 1981;160(1):51-63. Epub 1981/01/01.
192. Bjerknes M, Cheng H. The stem-cell zone of the small intestinal epithelium. III. Evidence from columnar, enteroendocrine, and mucous cells in the adult mouse. The American journal of anatomy. 1981;160(1):77-91. Epub 1981/01/01.
193. Potten CS, Owen G, Booth D. Intestinal stem cells protect their genome by selective segregation of template DNA strands. Journal of cell science. 2002;115(Pt 11):2381-8. Epub 2002/05/15.
194. Yatabe Y, Tavare S, Shibata D. Investigating stem cells in human colon by using methylation patterns. Proceedings of the National Academy of Sciences of the United States of America. 2001;98(19):10839-44. Epub 2001/08/23.
195. Cheng H, Leblond CP. Origin, differentiation and renewal of the four main epithelial cell types in the mouse small intestine. V. Unitarian Theory of the origin of the four epithelial cell types. The American journal of anatomy. 1974;141(4):537-61. Epub 1974/12/01.
196. Garrison AP, Helmrath MA, Dekaney CM. Intestinal stem cells. J Pediatr Gastroenterol Nutr. 2009;49(1):2-7. Epub 2009/06/09.
197. Sakakibara S, Imai T, Hamaguchi K, Okabe M, Aruga J, Nakajima K, et al. Mouse-Musashi-1, a neural RNA-binding protein highly enriched in the mammalian CNS stem cell. Developmental biology. 1996;176(2):230-42. Epub 1996/06/15.
198. Okano H, Kawahara H, Toriya M, Nakao K, Shibata S, Imai T. Function of RNA-binding protein Musashi-1 in stem cells. Experimental cell research. 2005;306(2):349-56. Epub 2005/06/01.
199. Potten CS, Booth C, Tudor GL, Booth D, Brady G, Hurley P, et al. Identification of a putative intestinal stem cell and early lineage marker; musashi-1. Differentiation; research in biological diversity. 2003;71(1):28-41. Epub 2003/02/01.
200. Fre S, Huyghe M, Mourikis P, Robine S, Louvard D, Artavanis-Tsakonas S. Notch signals control the fate of immature progenitor cells in the intestine. Nature. 2005;435(7044):964-8. Epub 2005/06/17.
201. von Furstenberg RJ, Gulati AS, Baxi A, Doherty JM, Stappenbeck TS, Gracz AD, et al. Sorting mouse jejunal epithelial cells with CD24 yields a population with characteristics of intestinal stem cells. Am J Physiol Gastrointest Liver Physiol. 2011;300(3):G409-17. Epub 2010/12/25.
202. Goodell MA, Brose K, Paradis G, Conner AS, Mulligan RC. Isolation and functional properties of murine hematopoietic stem cells that are replicating in vivo. J Exp Med. 1996;183(4):1797-806. Epub 1996/04/01.

203. Alvi AJ, Clayton H, Joshi C, Enver T, Ashworth A, Vivanco MM, et al. Functional and molecular characterisation of mammary side population cells. Breast cancer research : BCR. 2003;5(1):R1-8. Epub 2003/02/01.
204. Bhatt RI, Brown MD, Hart CA, Gilmore P, Ramani VA, George NJ, et al. Novel method for the isolation and characterisation of the putative prostatic stem cell. Cytometry A. 2003;54(2):89-99. Epub 2003/07/25.
205. Kotton DN, Fabian AJ, Mulligan RC. A novel stem-cell population in adult liver with potent hematopoietic-reconstitution activity. Blood. 2005;106(5):1574-80. Epub 2005/05/05.
206. Asakura A, Seale P, Girgis-Gabardo A, Rudnicki MA. Myogenic specification of side population cells in skeletal muscle. J Cell Biol. 2002;159(1):123-34. Epub 2002/10/16.
207. Jackson KA, Mi T, Goodell MA. Hematopoietic potential of stem cells isolated from murine skeletal muscle. Proc Natl Acad Sci U S A. 1999;96(25):14482-6. Epub 1999/12/10.
208. Dekaney CM, Rodriguez JM, Graul MC, Henning SJ. Isolation and characterization of a putative intestinal stem cell fraction from mouse jejunum. Gastroenterology. 2005;129(5):1567-80. Epub 2005/11/16.
209. Gulati AS, Ochsner SA, Henning SJ. Molecular properties of side population-sorted cells from mouse small intestine. Am J Physiol Gastrointest Liver Physiol. 2008;294(1):G286-94. Epub 2007/11/17.
210. Samuel S, Walsh R, Webb J, Robins A, Potten C, Mahida YR. Characterization of putative stem cells in isolated human colonic crypt epithelial cells and their interactions with myofibroblasts. Am J Physiol Cell Physiol. 2009;296(2):C296-305. Epub 2008/12/17.
211. Lalande ME, Miller RG. Fluorescence flow analysis of lymphocyte activation using Hoechst 33342 dye. The journal of histochemistry and cytochemistry : official journal of the Histochemistry Society. 1979;27(1):394-7. Epub 1979/01/01.
212. Zhou S, Schuetz JD, Bunting KD, Colapietro AM, Sampath J, Morris JJ, et al. The ABC transporter Bcrp1/ABCG2 is expressed in a wide variety of stem cells and is a molecular determinant of the side-population phenotype. Nat Med. 2001;7(9):1028-34. Epub 2001/09/05.
213. Ozvegy C, Litman T, Szakacs G, Nagy Z, Bates S, Varadi A, et al. Functional characterization of the human multidrug transporter, ABCG2, expressed in insect cells. Biochem Biophys Res Commun. 2001;285(1):111-7. Epub 2001/07/05.
214. Zhou S, Zong Y, Lu T, Sorrentino BP. Hematopoietic cells from mice that are deficient in both Bcrp1/Abcg2 and Mdr1a/1b develop normally but are sensitized to mitoxantrone. Biotechniques. 2003;35(6):1248-52. Epub 2003/12/20.
215. Jenkins D, Balsitis M, Gallivan S, Dixon MF, Gilmour HM, Shepherd NA, et al. Guidelines for the initial biopsy diagnosis of suspected chronic idiopathic inflammatory bowel disease. The British Society of Gastroenterology Initiative. J Clin Pathol. 1997;50(2):93-105. Epub 1997/02/01.
216. Reed RH, David; Weyers, Jonathan; Jones, Allan. Practical skills in biomolecular sciences. 2nd ed: Pearson education; 2003.
217. Imbeaud S, Graudens E, Boulanger V, Barlet X, Zaborski P, Eveno E, et al. Towards standardization of RNA quality assessment using user-independent classifiers of microcapillary electrophoresis traces. Nucleic Acids Res. 2005;33(6):e56. Epub 2005/04/01.
218. Mueller OL, S; Schroeder A. RNA Integrity Number (RIN) - Standardisation of RNA Quality Control. [Application note]: Agilent Technologies, Application note (Publication number 5989-1165EN); 2004; 1-8]. Available from: http://www.chem.agilent.com/en-us/Search/Library/_layouts/Agilent/PrimaryDocumentViewer.ashx?whid=37507.
219. Schroeder A, Mueller O, Stocker S, Salowsky R, Leiber M, Gassmann M, et al. The RIN: an RNA integrity number for assigning integrity values to RNA measurements. BMC Mol Biol. 2006;7:3. Epub 2006/02/02.
220. Rudloff U, Bhanot U, Gerald W, Klimstra DS, Jarnagin WR, Brennan MF, et al. Biobanking of Human Pancreas Cancer Tissue: Impact of Ex-Vivo Procurement Times on RNA Quality. Ann Surg Oncol. 2010. Epub 2010/02/18.

221. Qiagen. QuantiTect Reverse Transcription Handbook. 2009; Available from: http://www.qiagen.com/products/pcr/quantitectpcrsystems/quantitectrevtranscriptionkit.aspx.
222. Basic Local Alignment Search Tool. National Centre for Biotechnology Information; 2010; Available from: http://blast.ncbi.nlm.nih.gov/Blast.cgi.
223. Vector Laboratories. Enzyme Immunoassays, Hybridoma screening and Western blots. 2008; Available from: http://www.vectorlabs.com/Protocols/Supprotocols/ELISA.pdf.
224. Bjerknes M, Cheng H. Gastrointestinal stem cells. II. Intestinal stem cells. Am J Physiol Gastrointest Liver Physiol. 2005;289(3):G381-7. Epub 2005/08/12.
225. Evans GS, Flint N, Potten CS. Primary cultures for studies of cell regulation and physiology in intestinal epithelium. Annual review of physiology. 1994;56:399-417. Epub 1994/01/01.
226. Whitehead RH, Brown A, Bhathal PS. A method for the isolation and culture of human colonic crypts in collagen gels. In vitro cellular & developmental biology : journal of the Tissue Culture Association. 1987;23(6):436-42. Epub 1987/06/01.
227. Booth C, Patel S, Bennion GR, Potten CS. The isolation and culture of adult mouse colonic epithelium. Epithelial cell biology. 1995;4(2):76-86. Epub 1995/01/01.
228. Bjerknes M, Cheng H. Methods for the isolation of intact epithelium from the mouse intestine. The Anatomical record. 1981;199(4):565-74. Epub 1981/04/01.
229. Whitehead RH, Demmler K, Rockman SP, Watson NK. Clonogenic growth of epithelial cells from normal colonic mucosa from both mice and humans. Gastroenterology. 1999;117(4):858-65. Epub 1999/09/29.
230. Samuel S. Studies in human colonic epithelial and putative stem cells and their interaction with myofibroblasts. PhD Thesis: University of Nottingham; 2008.
231. Melmed G, Thomas LS, Lee N, Tesfay SY, Lukasek K, Michelsen KS, et al. Human intestinal epithelial cells are broadly unresponsive to Toll-like receptor 2-dependent bacterial ligands: implications for host-microbial interactions in the gut. J Immunol. 2003;170(3):1406-15. Epub 2003/01/23.
232. Cario E, Rosenberg IM, Brandwein SL, Beck PL, Reinecker HC, Podolsky DK. Lipopolysaccharide activates distinct signaling pathways in intestinal epithelial cell lines expressing Toll-like receptors. J Immunol. 2000;164(2):966-72. Epub 2000/01/07.
233. Takahashi K, Sugi Y, Hosono A, Kaminogawa S. Epigenetic regulation of TLR4 gene expression in intestinal epithelial cells for the maintenance of intestinal homeostasis. J Immunol. 2009;183(10):6522-9. Epub 2009/10/23.
234. Tsuchiya S, Yamabe M, Yamaguchi Y, Kobayashi Y, Konno T, Tada K. Establishment and characterization of a human acute monocytic leukemia cell line (THP-1). Int J Cancer 1980;26(2):171-6.
235. Riley SA, Mani V, Goodman MJ, Dutt S, Herd ME. Microscopic activity in ulcerative colitis: what does it mean? Gut. 1991;32(2):174-8. Epub 1991/02/01.
236. Ootani A, Li X, Sangiorgi E, Ho QT, Ueno H, Toda S, et al. Sustained in vitro intestinal epithelial culture within a Wnt-dependent stem cell niche. Nat Med. 2009;15(6):701-6. Epub 2009/04/29.
237. Sato T, Vries RG, Snippert HJ, van de Wetering M, Barker N, Stange DE, et al. Single Lgr5 stem cells build crypt-villus structures in vitro without a mesenchymal niche. Nature. 2009;459(7244):262-5. Epub 2009/03/31.
238. Vaishnava S, Behrendt CL, Ismail AS, Eckmann L, Hooper LV. Paneth cells directly sense gut commensals and maintain homeostasis at the intestinal host-microbial interface. Proc Natl Acad Sci U S A. 2008;105(52):20858-63. Epub 2008/12/17.
239. Thermo Scientific. Lysozyme/Muramidase antibody-1. 2012; Available from: http://www.thermoscientific.com/ecomm/servlet/productsdetail_11152___11955836_-1.
240. Fusunyan RD, Nanthakumar NN, Baldeon ME, Walker WA. Evidence for an innate immune response in the immature human intestine: toll-like receptors on fetal enterocytes. Pediatr Res. 2001;49(4):589-93. Epub 2001/03/27.

241. Gewirtz AT, Navas TA, Lyons S, Godowski PJ, Madara JL. Cutting edge: bacterial flagellin activates basolaterally expressed TLR5 to induce epithelial proinflammatory gene expression. J Immunol. 2001;167(4):1882-5. Epub 2001/08/08.
242. Cario E, Brown D, McKee M, Lynch-Devaney K, Gerken G, Podolsky DK. Commensal-associated molecular patterns induce selective toll-like receptor-trafficking from apical membrane to cytoplasmic compartments in polarized intestinal epithelium. Am J Pathol. 2002;160(1):165-73. Epub 2002/01/12.
243. Otte JM, Cario E, Podolsky DK. Mechanisms of cross hyporesponsiveness to Toll-like receptor bacterial ligands in intestinal epithelial cells. Gastroenterology. 2004;126(4):1054-70. Epub 2004/04/02.
244. Hornef MW, Frisan T, Vandewalle A, Normark S, Richter-Dahlfors A. Toll-like receptor 4 resides in the Golgi apparatus and colocalizes with internalized lipopolysaccharide in intestinal epithelial cells. J Exp Med. 2002;195(5):559-70. Epub 2002/03/06.
245. Hornef MW, Normark BH, Vandewalle A, Normark S. Intracellular recognition of lipopolysaccharide by toll-like receptor 4 in intestinal epithelial cells. J Exp Med. 2003;198(8):1225-35. Epub 2003/10/22.
246. Suzuki M, Hisamatsu T, Podolsky DK. Gamma interferon augments the intracellular pathway for lipopolysaccharide (LPS) recognition in human intestinal epithelial cells through coordinated up-regulation of LPS uptake and expression of the intracellular Toll-like receptor 4-MD-2 complex. Infect Immun. 2003;71(6):3503-11. Epub 2003/05/23.
247. Latz E, Visintin A, Lien E, Fitzgerald KA, Monks BG, Kurt-Jones EA, et al. Lipopolysaccharide rapidly traffics to and from the Golgi apparatus with the toll-like receptor 4-MD-2-CD14 complex in a process that is distinct from the initiation of signal transduction. J Biol Chem. 2002;277(49):47834-43. Epub 2002/09/27.
248. Lee SK, Il Kim T, Kim YK, Choi CH, Yang KM, Chae B, et al. Cellular differentiation-induced attenuation of LPS response in HT-29 cells is related to the down-regulation of TLR4 expression. Biochem Biophys Res Commun. 2005;337(2):457-63. Epub 2005/10/06.
249. Bu HF, Wang X, Tang Y, Koti V, Tan XD. Toll-like receptor 2-mediated peptidoglycan uptake by immature intestinal epithelial cells from apical side and exosome-associated transcellular transcytosis. J Cell Physiol. 2010;222(3):658-68. Epub 2009/12/19.
250. Ortega-Cava CF, Ishihara S, Rumi MA, Kawashima K, Ishimura N, Kazumori H, et al. Strategic compartmentalization of Toll-like receptor 4 in the mouse gut. J Immunol. 2003;170(8):3977-85. Epub 2003/04/12.
251. Lee J, Mo JH, Katakura K, Alkalay I, Rucker AN, Liu YT, et al. Maintenance of colonic homeostasis by distinctive apical TLR9 signalling in intestinal epithelial cells. Nat Cell Biol. 2006;8(12):1327-36. Epub 2006/11/28.
252. Furrie E, Macfarlane S, Thomson G, Macfarlane GT. Toll-like receptors-2, -3 and -4 expression patterns on human colon and their regulation by mucosal-associated bacteria. Immunology. 2005;115(4):565-74. Epub 2005/07/14.
253. Nandakumar NS, Pugazhendhi S, Ramakrishna BS. Effects of enteropathogenic bacteria & lactobacilli on chemokine secretion & Toll like receptor gene expression in two human colonic epithelial cell lines. Indian J Med Res. 2009;130(2):170-8. Epub 2009/10/03.
254. Bogunovic M, Dave SH, Tilstra JS, Chang DT, Harpaz N, Xiong H, et al. Enteroendocrine cells express functional Toll-like receptors. Am J Physiol Gastrointest Liver Physiol. 2007;292(6):G1770-83. Epub 2007/03/31.
255. Rhee SH, Im E, Riegler M, Kokkotou E, O'Brien M, Pothoulakis C. Pathophysiological role of Toll-like receptor 5 engagement by bacterial flagellin in colonic inflammation. Proc Natl Acad Sci U S A. 2005;102(38):13610-5. Epub 2005/09/15.
256. Steenholdt C, Andresen L, Pedersen G, Hansen A, Brynskov J. Expression and function of toll-like receptor 8 and Tollip in colonic epithelial cells from patients with inflammatory bowel disease. Scand J Gastroenterol. 2009;44(2):195-204. Epub 2008/11/06.

257. Pedersen G, Andresen L, Matthiessen MW, Rask-Madsen J, Brynskov J. Expression of Toll-like receptor 9 and response to bacterial CpG oligodeoxynucleotides in human intestinal epithelium. Clin Exp Immunol. 2005;141(2):298-306. Epub 2005/07/06.
258. Wolfs TG, Derikx JP, Hodin CM, Vanderlocht J, Driessen A, de Bruine AP, et al. Localization of the lipopolysaccharide recognition complex in the human healthy and inflamed premature and adult gut. Inflamm Bowel Dis. 2010;16(1):68-75. Epub 2009/12/17.
259. Gribar SC, Anand RJ, Sodhi CP, Hackam DJ. The role of epithelial Toll-like receptor signaling in the pathogenesis of intestinal inflammation. J Leukoc Biol. 2008;83(3):493-8. Epub 2007/12/28.
260. Cario E, Podolsky DK. Differential alteration in intestinal epithelial cell expression of toll-like receptor 3 (TLR3) and TLR4 in inflammatory bowel disease. Infect Immun. 2000;68(12):7010-7. Epub 2000/11/18.
261. Stanislawowski M, Wierzbicki PM, Golab A, Adrych K, Kartanowicz D, Wypych J, et al. Decreased Toll-like receptor-5 (TLR-5) expression in the mucosa of ulcerative colitis patients. Journal of physiology and pharmacology : an official journal of the Polish Physiological Society. 2009;60 Suppl 4:71-5. Epub 2010/01/30.
262. Hausmann M, Kiessling S, Mestermann S, Webb G, Spottl T, Andus T, et al. Toll-like receptors 2 and 4 are up-regulated during intestinal inflammation. Gastroenterology. 2002;122(7):1987-2000. Epub 2002/06/11.
263. Naik S, Kelly EJ, Meijer L, Pettersson S, Sanderson IR. Absence of Toll-like receptor 4 explains endotoxin hyporesponsiveness in human intestinal epithelium. J Pediatr Gastroenterol Nutr. 2001;32(4):449-53. Epub 2001/06/09.
264. Dale JW, von Schantz M. From genes to genomes: concepts and applications of DNA technology. 2nd ed: Wiley; 2007.
265. Ambion. MessageAmp™ II aRNA Amplification Kit: RNA Amplification for Array Analysis. 2010; 39]. Available from: http://products.invitrogen.com/ivgn/product/AM1751.
266. Van Gelder RN, von Zastrow ME, Yool A, Dement WC, Barchas JD, Eberwine JH. Amplified RNA synthesized from limited quantities of heterogeneous cDNA. Proc Natl Acad Sci U S A. 1990;87(5):1663-7. Epub 1990/03/01.
267. Mackay IM, Arden KE, Nitsche A. Real-time PCR in virology. Nucleic Acids Res. 2002;30(6):1292-305. Epub 2002/03/09.
268. Giulietti A, Overbergh L, Valckx D, Decallonne B, Bouillon R, Mathieu C. An overview of real-time quantitative PCR: applications to quantify cytokine gene expression. Methods. 2001;25(4):386-401. Epub 2002/02/16.
269. Bhatia P, Taylor WR, Greenberg AH, Wright JA. Comparison of glyceraldehyde-3-phosphate dehydrogenase and 28S-ribosomal RNA gene expression as RNA loading controls for northern blot analysis of cell lines of varying malignant potential. Anal Biochem. 1994;216(1):223-6. Epub 1994/01/01.
270. Bereta J, Bereta M. Stimulation of glyceraldehyde-3-phosphate dehydrogenase mRNA levels by endogenous nitric oxide in cytokine-activated endothelium. Biochem Biophys Res Commun. 1995;217(1):363-9. Epub 1995/12/05.
271. Lekanne Deprez RH, Fijnvandraat AC, Ruijter JM, Moorman AF. Sensitivity and accuracy of quantitative real-time polymerase chain reaction using SYBR green I depends on cDNA synthesis conditions. Anal Biochem. 2002;307(1):63-9. Epub 2002/07/26.
272. Pfaffl MW. A new mathematical model for relative quantification in real-time RT-PCR. Nucleic Acids Res. 2001;29(9):e45. Epub 2001/05/09.
273. Fukata M, Shang L, Santaolalla R, Sotolongo J, Pastorini C, Espana C, et al. Constitutive activation of epithelial TLR4 augments inflammatory responses to mucosal injury and drives colitis-associated tumorigenesis. Inflamm Bowel Dis. 2011;17(7):1464-73. Epub 2011/06/16.
274. Sanchez-Muñoz f, Dominguez-Lopez A, Yamamoto-Furusho JK. Role of cytokines in inflammatory bowel disease. World J Gastroenterol. 2008;14(27):4280-8.

275. Ortega-Cava CF, Ishihara S, Rumi MA, Aziz MM, Kazumori H, Yuki T, et al. Epithelial toll-like receptor 5 is constitutively localized in the mouse cecum and exhibits distinctive down-regulation during experimental colitis. Clin Vaccine Immunol. 2006;13(1):132-8. Epub 2006/01/24.
276. West AP, Brodsky IE, Rahner C, Woo DK, Erdjument-Bromage H, Tempst P, et al. TLR signalling augments macrophage bactericidal activity through mitochondrial ROS. Nature. 2011;472(7344):476-80. Epub 2011/04/29.
277. Knight P, Campbell BJ, Rhodes JM. Host-bacteria interaction in inflammatory bowel disease. Br Med Bull. 2008;88(1):95-113. Epub 2008/10/22.
278. Chichlowski M, Hale LP. Bacterial-mucosal interactions in inflammatory bowel disease: an alliance gone bad. Am J Physiol Gastrointest Liver Physiol. 2008;295(6):G1139-49. Epub 2008/10/18.
279. Rosenstiel P, Sina C, End C, Renner M, Lyer S, Till A, et al. Regulation of DMBT1 via NOD2 and TLR4 in intestinal epithelial cells modulates bacterial recognition and invasion. J Immunol. 2007;178(12):8203-11. Epub 2007/06/06.
280. Szebeni B, Veres G, Dezsofi A, Rusai K, Vannay A, Mraz M, et al. Increased expression of Toll-like receptor (TLR) 2 and TLR4 in the colonic mucosa of children with inflammatory bowel disease. Clin Exp Immunol. 2008;151(1):34-41. Epub 2007/11/10.
281. Dako. Data sheet: Epithelial Antigen Clone BerEP4-FITC. 2009 [cited 2012 04/04/2012]; Available from: http://www.dako.com/uk/download.pdf?objectid=117048003.
282. Rutgeerts P, Vermeire S, Van Assche G. Biological therapies for inflammatory bowel diseases. Gastroenterology. 2009;136(4):1182-97. Epub 2009/03/03.
283. Andoh A, Fujino S, Okuno T, Fujiyama Y, Bamba T. Intestinal subepithelial myofibroblasts in inflammatory bowel diseases. J Gastroenterol. 2002;37 Suppl 14:33-7. Epub 2003/02/08.
284. McKaig BC, Hughes K, Tighe PJ, Mahida YR. Differential expression of TGF-beta isoforms by normal and inflammatory bowel disease intestinal myofibroblasts. Am J Physiol Cell Physiol. 2002;282(1):C172-82. Epub 2001/12/18.
285. McKaig BC, McWilliams D, Watson SA, Mahida YR. Expression and regulation of tissue inhibitor of metalloproteinase-1 and matrix metalloproteinases by intestinal myofibroblasts in inflammatory bowel disease. Am J Pathol. 2003;162(4):1355-60. Epub 2003/03/26.
286. Louis E, Ribbens C, Godon A, Franchimont D, De Groote D, Hardy N, et al. Increased production of matrix metalloproteinase-3 and tissue inhibitor of metalloproteinase-1 by inflamed mucosa in inflammatory bowel disease. Clin Exp Immunol. 2000;120(2):241-6. Epub 2000/05/03.
287. von Lampe B, Barthel B, Coupland SE, Riecken EO, Rosewicz S. Differential expression of matrix metalloproteinases and their tissue inhibitors in colon mucosa of patients with inflammatory bowel disease. Gut. 2000;47(1):63-73. Epub 2000/06/22.
288. Telford WG, Frolova EG. Discrimination of the Hoechst side population in mouse bone marrow with violet and near-ultraviolet laser diodes. Cytometry A. 2004;57(1):45-52. Epub 2003/12/31.
289. Telford WG, Bradford J, Godfrey W, Robey RW, Bates SE. Side population analysis using a violet-excited cell-permeable DNA binding dye. Stem Cells. 2007;25(4):1029-36. Epub 2006/12/23.
290. Mathew G, Timm EA, Jr., Sotomayor P, Godoy A, Montecinos VP, Smith GJ, et al. ABCG2-mediated DyeCycle Violet efflux defined side population in benign and malignant prostate. Cell Cycle. 2009;8(7):1053-61. Epub 2009/03/10.
291. She JJ, Zhang PG, Wang ZM, Gan WM, Che XM. Identification of side population cells from bladder cancer cells by DyeCycle Violet staining. Cancer Biol Ther. 2008;7(10):1663-8. Epub 2008/09/13.
292. Santaolalla R, Davies JM, Ruiz J, Espana C, Fukata M, Abreu MT, editors. TLR4 activates LGR5 expression in the colon: a link between cancer stem cells and innate immune signals. Digestive Diseases Week: Session L3265, Presentation 175; 2012; San Diego, US.
293. Hsu D, Fukata M, Hernandez YG, Sotolongo JP, Goo T, Maki J, et al. Toll-like receptor 4 differentially regulates epidermal growth factor-related growth factors in response to intestinal mucosal injury. Lab Invest. 2010;90(9):1295-305. Epub 2010/05/26.

294. Eyking A, Ey B, Runzi M, Roig AI, Reis H, Schmid KW, et al. Toll-like receptor 4 variant D299G induces features of neoplastic progression in Caco-2 intestinal cells and is associated with advanced human colon cancer. Gastroenterology. 2011;141(6):2154-65. Epub 2011/09/17.
295. Dekaney CM, Gulati AS, Garrison AP, Helmrath MA, Henning SJ. Regeneration of intestinal stem/progenitor cells following doxorubicin treatment of mice. Am J Physiol Gastrointest Liver Physiol. 2009;297(3):G461-70. Epub 2009/07/11.